TECHNISCHE UNIVERSITÄT MÜNCHEN

TUM School of Life Sciences

Identification, Induction, and Characterisation of *Latilactobacillus sakei* and *Latilactobacillus curvatus* Prophages and Their Implications on Raw Meat Fermentation

Conrad Ludwig Ambros

Vollständiger Abdruck der von der TUM School of Life Sciences der Technischen Universität München zur Erlangung eines

Doktors der Naturwissenschaften (Dr. rer. nat.)

genehmigten Dissertation.

Vorsitz:		Prof. Dr.-Ing. Marius Henkel
Prüfende der Dissertation:	1.	apl. Prof. Dr. Matthias A. Ehrmann
	2.	Prof. Dr. Wilfried Schwab

Die Dissertation wurde am 02.01.2025 bei der Technischen Universität München eingereicht und durch die TUM School of Life Sciences am 03.04.2025 angenommen.

ACKNOWLEDGEMENTS

My first thanks go to you, the reader. Thank you for picking up this dissertation to gather more information about *Latilactobacillus* phages.

Figure 1. Dry-fermented salami next to *L. curvatus* TMW 1.2406 culture.

An enormous thanks to you, Matthias, for your expertise as a doctorate father, the time you invested in me and my research, for providing me with the most excellent topic, and the fantastic everyday lunch talks; I will surely miss these and our beloved “pampa alba multi obscura” (our favourite *pudding* provided by the canteen). Also, thank you for always lending me an ear and supporting me during publishing. I learned a metric ton from you (and still am). Many thanks to Prof. Dr Wilfried Schwab for the second examination of this dissertation and to Prof. Dr Rudi F. Vogel for the scientific feedback and mentorship. Thank you, Prof. Dr Wolfgang Liebl, for including our chair of technical microbiology in your own and giving us a new home to research. Thanks to our excellent technical assistants, Maggie and Moni, for always telling me where I can find stuff in the lab, ordering my lab consumables, and helping me when there is much work but no time. Thanks to our secretaries Angela, Annette, and Helga. Thank you so much for proofreading my publications, Frea and Angie. Thanks to all my colleagues for the joyful time and exciting talks. Thanks especially to Becky; our talks about anime and tabletop game sessions were excellent. Thanks to my office buddies, my first consultants for unexpected experimental data, Marion, Tobi, my project partner Max, Christina, Franzie, Marie-Luise, and Frea. Thank you for the fun and nerdy talks about coffee, Marius, Phillip, and Laurenz.

The biggest thanks must go to my family and my beautiful wife, Ines. The most significant achievement during my research time was marrying you! Thank you so, so much for all your support. I genuinely mean it. You are the refuge when I need it. Thank you for everything (including fantastic food), my wonderful family.

ABBREVIATIONS

Abbreviation	Meaning
A	Adenosine
AMR	Antimicrobial resistance
ANI(b)	Average nucleotide identity (based on BLAST+)
AP	Aligned percentage of nucleotides
ARG	Antibiotic resistance genes
ATP	Adenosine triphosphate
attB	Phage attachment site
attL	Left prophage attachment site
attP	Bacterial attachment site
attR	Right prophage attachment site
BaPI	Bacteriocin-phage interaction
BP	Baird-Parker
C	Cytidine
CARD	Comprehensive Antibiotic Resistance Database
CDS	Coding sequences
dH_2O	Demineralised water
DNA	Deoxyribonucleic acid
dsDNA	Double-stranded DNA
E.	*Escherichia*
EDTA	Ethylenediaminetetraacetic acid
G	Guanosine
GMP	Guanosine monophosphate
Gt C	Gigatons of carbon
ICTV	International Committee on Taxonomy of Viruses
IQR	Interquartile range
L.	*Latilactobacillus*
LAB	Lactic acid bacteria
Lc.	*Lacticaseibacillus*
Le.	*Levilactobacillus*
Lp.	*Lactiplantibacillus*
MALDI-TOF MS	Matrix-assisted laser desorption/ionisation time-of-flight mass spectrometry
MitC	Mitomycin C
MOI	Multiplicity of infection (Infecting phages per cell)
mMRS	Modified De Man, Rogosa, and Sharpe medium
mMRS(A)	Modified De Man, Rogosa, and Sharpe agar
MTase	Methyltransferase
OD_{600}	Optical density measured at a wavelength of 600 nm
P.	*Pediococcus*
PCR	Polymerase chain reaction
PEG	Polyethylene glycol
PGI	Glucose-6-phosphate isomerase
PHASTER	Phage Search Tool Enhanced Release
RBP	Receptor-binding protein
REase	Restriction endonuclease
RM system	Restriction-modification system
RT	Room/ambient temperature

Abbreviation	Meaning
S.	*Staphylococcus*
SD	Standard deviation
SDS	Sodium dodecyl sulfate
SNP	Single nucleotide polymorphism
SPI	Spontaneous phage induction
Ssp.	Subspecies
T	Thymidine
t_E	Elongation time per cycle
TEM	Transmission electron microscopy
TerL	Terminase (large subunit)
TerS	Terminase (small subunit)
TilS	$tRNA^{Ile}$-lysidine synthetase
TMP	Tape measure protein
t(m)RNA	Transfer(-messenger) ribonucleic acid
TSA	Tryptone soya broth agar
TSB	Tryptone soya broth
U	Uridine
UV	Ultraviolet
WT	Wild-type

LIST OF FIGURES

LIST OF TABLES

PUBLICATIONS, POSTERS, AND FUNDING

Ambros CL, Ehrmann MA. Fate, Inducibility, and Behavior of Latilactobacillus curvatus Temperate Phage TMW 1.591 P1 during Sausage Fermentation. *J Appl Microbiol* 2024. lxae175. https://doi.org/10.1093/jambio/lxae175

Ambros CL, Ehrmann MA. Distribution, inducibility, and characteristics of *Latilactobacillus curvatus* temperate phages. *Microbiome Res Rep* 2023. 2(4): 34. http://dx.doi.org/10.20517/mrr.2023.18

Ambros, CL, Ehrmann, MA. Distribution, inducibility, and characterisation of prophages in *Latilactobacillus sakei*. *BMC Microbiol* 2022. **22**, 267. https://doi.org/10.1186/s12866-022-02675-y

Ambros CL, Ehrmann MA. Prediction and Inducibility of prophages in the meat starter *Latilactobacillus sakei*; 23.08.2023-25.08.2023, 13th International Symposium on Lactic Acid Bacteria, Egmond aan Zee, online participation due to covid pandemic. Poster presentation.

This thesis contains data from the aforementioned peer-reviewed publications. The work of this thesis was part of and funded by an IGF Project of the FEI (Project 21093 N), supported within the program for promoting the Industrial Collective Research (IGF) of the German Ministry of Economics and Climate Action (BMWK), based on a resolution of the German Parliament. The funding party had no influence on the interpretation of the results.

TABLE OF CONTENTS

ABSTRACT

Bacteriophages (short: phages) are viruses that specifically infect bacteria. In contrast to virulent phages that always lyse their host after infection, temperate phages either lyse their host or integrate their genomes into the host genomes as prophages. In this state, prophages are dormant and replicate passively during cell division until reactivation (induction). While prophages were discussed as beneficial to their hosts, extensive host lysis during lytic propagation may negatively influence the fitness of a bacterial starter organism. Although phage research started over 100 years ago and more and more species were analysed for their prophages, *Latilactobacillus* (*L.*) *sakei* and *L. curvatus* remained on the bucket list. This is surprising considering their value for meat fermentation. Information regarding the influence of temperate phages on meat fermentation also remained scarce. This thesis addresses both issues as it describes the prophage content of those species and analyses the impact of an intact prophage on its host during meat fermentation.

For this, 27 *L. sakei* and 47 *L. curvatus* strains were screened for prophage-mediated lysis, indicating the presence of intact prophages. After treatment with ultraviolet (UV) light or the genotoxic antibiotic mitomycin C (MitC), two common phage inducers, lysis was observed in nine *L. sakei* and 24 *L. curvatus* strains, albeit with varying intensities. Phages from five *L. sakei* and six *L. curvatus* post-induction lysates were precipitated and sequenced. This proved that simultaneous induction of multiple prophages of a multi-lysogenic strain is possible. Distinctive sequencing depths of phage-related sequences hinted at varying induction intensities of each prophage within multi-lysogenic strains. This could explain the presence of only one phage morphotype (originating from the most induced prophage) per lysate. All detected virions featured the siphovirus morphotype with icosahedral capsids and non-contractile tails. While their capsid sizes were primarily uniform, their tail lengths varied significantly.

Forty-three *L. sakei* and 45 *L. curvatus* genomes, including openly available ones, were screened for prophages via “Phage Search Tool Enhanced Release” (PHASTER), a web-based prophage search tool. A total of 302 prophage-related (intact, questionable, and incomplete) sequences were detected by PHASTER. After manual completeness evaluation, 29 putatively intact *L. sakei* prophages and 50 *L. curvatus* prophages were identified. The prophages shared a conserved genome synteny but were, with some exceptions, highly diverse. All prophages started with lysogeny-related genes, followed by replication, packaging, morphogenesis, and lysis genes. Some prophages encoded transposases, transfer ribonucleic acids (tRNAs), or

methyltransferases (MTases). While tRNAs and MTases could benefit the phage, transposons could have caused the incomplete virion assemblies of some prophages and, therefore, be a sign of their ongoing degradation and domestication. Seventy-eight *Latilactobacillus* phage integrases were analysed and assigned to 13 distinctive groups. Each group allowed integration into mostly one specific chromosomal locus. For integration, tRNA genes or genes known for their highly conserved nature were chosen almost exclusively.

To evaluate if an intact prophage does affect meat fermentation, a model system consisting of a prophage-harbouring wild-type (WT) strain and prophage-negative isogeneic (cured) control was created. This was done by screening for cells that lost their prophage after UV light induction. A prophage-free derivative (*L. curvatus* TMW 1.2406) that virions (TMW 1.591 P1) released by its WT strain (*L. curvatus* TMW 1.591) could infect was obtained for one of three selected strains. By determining released WT phage counts using the cured strain as an indicator, a more precise determination of phage induction compared to lysis observations during growth monitoring, which were more qualitative, was possible. This strain model identified Ca^{2+} ion concentration and the number of infecting phages per bacterial cell as critical factors for effective host lysis. Apart from the cured strain, 65 tested *Latilactobacillus* strains were generally resistant to the phages released by 12 previously identified lysogens. This demonstrates the narrow host spectrum of tested temperate phages.

Salami and meat model fermentations were conducted to evaluate the impact of the temperate phage TMW 1.591 P1 on the fitness and competitiveness of its host. The salami fermentation allowed examination of the final product after production in a close-to-industry setting. The simplified meat model fermentation allowed conclusions about the impact of the phage-contaminated substrate. It offered a higher temporal resolution concerning phage induction during the first five days of fermentation. Both experiments revealed that TMW 1.591 P1 is induced during meat fermentation, leading to the production of new phage progeny. Yet, the prophage seemingly did not impact host fitness or competitiveness. Analogically, phage addition into the meat before adding starter strains simulating phage-contaminated meat yielded no observable effect.

Induction experiments were performed to identify what caused the extensive phage production during fermentation. The analysed stressors were applied as a short-time shock to *L. curvatus* TMW 1.591 and its prophage-negative isogeneic control TMW 1.2406. This revealed high temperatures (45-60°C) and an acidic environment (pH 3.0) as phage inducers. Higher NaCl or

$NaNO_2$ concentrations or lack of nutrients (carbon source or total nutrients) had no observable inducing effect.

Moreover, other meat-associated bacteria interfered with TMW 1.591 P1 induction. Co-cultivation with *L. sakei* TMW 1.2 led to more phages being released than in the control sample. On the contrary, the presence of *Lacticaseibacillus* (*Lc.*) *paracasei* isolate 1, *Lactiplantibacillus* (*Lp.*) *plantarum* TMW 1.25, or *Pediococcus* (*P.*) *pentosaceus* TMW 1.1974 led to reduced phage release, despite all *L. curvatus* TMW 1.591 samples experiencing the same induction treatment previously. Similar phage counts as the control sample were obtained in samples containing *Staphylococcus* (*S.*) *carnosus* ssp. *carnosus* TMW 2.212, which was also added in conducted fermentations, *S. carnosus* ssp. *utilis* ME, and *S. xylosus* TMW 2.1521. Thus, TMW 2.212 was most likely not the cause for the observed phage induction during fermentation.

Once initiated, phage induction was maintained during cryopreservation of a lysogenic strain. This implies that avoiding inducing conditions could be crucial for the fitness of a lysogenic bacterial starter.

ZUSAMMENFASSUNG

Bakteriophagen (kurz: Phagen) sind Viren, die spezifisch Bakterien infizieren. Im Gegensatz zu virulenten Phagen, die ihren Wirt nach Infektion stets lysieren, können temperente Phagen entweder ihren Wirt lysieren oder ihr Genom als Prophagen in das Wirtsgenom integrieren. In diesem Zustand befinden sich Prophagen bis zur Reaktivierung (Induktion) in einem Ruhezustand und replizieren sich passiv während der Zellteilung. Während Prophagen als vorteilhaft für ihre Wirte diskutiert wurden, könnte exzessive Wirtslyse während des lytischen Zyklus die Fitness eines bakteriellen Starterorganismus negativ beeinflussen. Obwohl Phagen seit über 100 Jahren erforscht werden und immer mehr Arten auf ihre Prophagen hin untersucht wurden, verblieben *Latilactobacillus* (*L.*) *sakei* und *L. curvatus* auf der Streichliste. Unter Berücksichtigung ihres Werts für Fleischfermentationen ist dies überraschend. Auch der Einfluss temperenter Phagen auf Fleischfermentationen im Allgemeinen ist weitestgehend unerforscht. Daher befasst sich die vorliegende Arbeit mit beiden Themen, indem sie die Prophagenverteilung beider Stämme beschreibt und den Einfluss eines intakten Prophagen auf seinen Wirt während einer Fleischfermentation analysiert.

Siebenundzwanzig *L. sakei* und 47 *L. curvatus* Stämme wurden auf prophagenvermittelte Lyse untersucht, ein Hinweis auf das Vorhandensein von intakten Prophagen. Nach Behandlung mit ultraviolettem (UV) Licht oder dem genotoxischen Antibiotikum Mitomycin C (MitC), zwei gängigen Phageninduktoren, wurde bei neun *L. sakei* und 24 *L. curvatus* Stämmen Lyse unterschiedlicher Intensität beobachtet. Aus fünf *L. sakei* und sechs *L. curvatus* Lysaten wurden nach der Induktion Phagen gefällt und sequenziert, was eine gleichzeitige Induktion mehrerer Prophagen in einem multilysogenen Stamm bewies. Die unterschiedlichen Sequenzierungstiefen der phagenzugehörigen Sequenzen deuteten auf unterschiedlich starke Induktionen der einzelnen Prophagen innerhalb eines multilysogenen Stammes hin. Dies könnte das Vorhandensein von nur einem Phagenmorphotyp (vom am stärksten induzierten Prophagen) pro Lysat erklären. Alle nachgewiesenen Virionen wiesen mit ikosaedrischen Kapsiden und nicht-kontraktilen Schwänzen den Siphovirus-Morphotyp auf. Während deren Kapside sich in Größe ähnelten, variierten deren Schwanzlängen deutlich.

Es wurden 43 *L. sakei* und 45 *L. curvatus* Genome, darunter auch offen zugängliche, mit dem webbasierten Prophagen-Suchwerkzeug “Phage Search Tool Enhanced Release” (PHASTER) durchsucht. Mittels PHASTER wurden insgesamt 302 Prophagen-bezogene Sequenzen (intakte, fragliche und unvollständige) detektiert. Nach manueller Vollständigkeitsprüfung wurden 29 mutmaßlich intakte *L. sakei* und 50 *L. curvatus* Prophagen identifiziert. Die

Prophagen wiesen eine konservierte Genomsyntenie und, mit wenigen Ausnahmen, hohe Diversität auf. Alle Prophagen begannen mit Lysogenie-bezogenen Genen, gefolgt von Genen für Replikation, Verpackung, Morphogenese und Lyse. Einige Prophagen kodierten außerdem Transposasen, Transfer-Ribonukleinsäuren (tRNAs) oder Methyltransferasen (MTasen). Während tRNAs und MTasen von Vorteil für den Phagen sein könnten, könnte das Vorhandensein von Transposons die unvollständigen Virionenzusammensetzungen mancher Prophagen verursacht haben und somit ein Zeichen für deren fortschreitenden Abbau und Domestizierung sein. Es wurden 78 *Latilactobacillus* Phagenintegrasen untersucht und in 13 verschiedene Gruppen eingeteilt, die die Integration in meist eine spezifische Stelle im Wirtschromosom ermöglichten. Für die Integration wurden fast ausschließlich tRNA-Gene oder Gene ausgewählt, die für ihre hohe Konservierung bekannt sind.

Um festzustellen, ob ein intakter Prophage Fleischfermentationen beeinflussen kann, wurde zunächst ein Modellsystem, bestehend aus einem Prophagen-tragenden Wildtyp (WT)-Stamm und einer Prophagen-negativen, isogenen (gecurten) Kontrolle, geschaffen. Dies geschah durch Screening auf Zellen, die ihren Prophagen nach UV-Licht Induktion verloren hatten. Für einen von drei ausgewählten Stämmen konnte ein prophagenfreies Derivat (*L. curvatus* TMW 1.2406) gewonnen werden, welches mit den von seinem WT-Stamm (*L. curvatus* TMW 1.591) freigesetzten Virionen (TMW 1.591 P1) erneut infiziert werden konnte. Durch Quantifizierung der freigesetzten WT-Phagen unter Verwendung des gecurten Stammes als Indikator, war, verglichen mit den zuvor eher qualitativen Lysebeobachtungen, ein genauerer Induktionsnachweis möglich. Durch das Stammmodell wurden die Ca^{2+}-Ionenkonzentration und die Anzahl der infizierenden Phagen pro Zelle als kritische Faktoren für effiziente Wirtslyse identifiziert. Abgesehen vom gecurten Stamm, waren die 65 getesteten *Latilactobacillus* Stämme gegen die freigesetzten Phagen der 12 zuvor identifizierten Lysogenen resistent. Dies demonstriert das enge Wirtsspektrum der getesteten temperenten Phagen.

Um die Auswirkungen des temperenten Phagen TMW 1.591 P1 auf die Fitness und Wettbewerbsfähigkeit seines Wirts zu bewerten, wurden Salami- und Fleischmodellfermentationen durchgeführt. Während die Salamifermentationen Untersuchungen im Endprodukt nach Produktion in einer industrienahen Umgebung ermöglichten, erlaubte letzteres Rückschlüsse auf die Auswirkungen von phagenkontaminiertem Substrat und bot eine höhere zeitliche Auflösung hinsichtlich Phageninduktion während der ersten fünf Fermentationstage. Beide Experimente zeigten, dass

TMW 1.591 P1 während der Fermentation induziert wurde, was zur Herstellung neuer Phagen führte. Der Prophage hatte jedoch offenbar keinen Einfluss auf die Fitness oder Wettbewerbsfähigkeit seines Wirts. Auch die Zugabe von Phagen in das Fleisch vor Zugabe der Starter, welche phagenkontaminiertes Fleisch simulierte, hatte keine erkennbaren Auswirkungen.

Um die Ursache für die ausgeprägte Phagenproduktion während der Fermentation zu ermitteln, wurden weitere Induktionsexperimente durchgeführt, bei denen Stressoren als Kurzzeitschock auf *L. curvatus* TMW 1.591 und seine prophagennegative, isogene Kontrolle TMW 1.2406 angewendet wurden. Es zeigte sich, dass hohe Temperaturen (45-60°C) und eine saure Umgebung (pH 3,0) phageninduzierend wirkten. Dahingegen hatten erhöhte Konzentrationen an NaCl oder $NaNO_2$, oder Nährstoffmangel (Kohlenstoffquelle und Gesamtnähstoffgehalt) keine erhöhte Phageninduktion zur Folge.

Die Anwesenheit anderer fleischassoziierter Bakterien beeinflusste die Induktion von TMW 1.591 P1 ebenfalls. So führte die Co-Kultivierung mit *L. sakei* TMW 1.2 zu einer erhöhten Freisetzung von Phagen im Vergleich zur Kontrollprobe. Im Gegensatz dazu führte die Anwesenheit von *Lacticaseibacillus* (*Lc.*) *paracasei* Isolat 1, *Lactiplantibacillus* (*Lp.*) *plantarum* TMW 1.25 oder *Pediococcus* (*P.*) *pentosaceus* TMW 1.1974 zu einer verringerten Freisetzung, obwohl alle *L. curvatus* TMW 1.591 Proben zuvor die gleiche Induktionsbehandlung erfuhren. Ähnliche Phagenzahlen wie in der Kontrollprobe wurden in Proben erzielt, die *Staphylococcus* (*S.*) *carnosus* ssp. *carnosus* TMW 2.212 enthielten, der auch in den durchgeführten Fermentationen eingesetzt wurde, sowie *S. carnosus* ssp. *utilis* ME und *S. xylosus* TMW 2.1521. TMW 2.212 war demnach höchstwahrscheinlich nicht die Ursache für die beobachtete Phageninduktion während der Fermentationen.

Einmal initiiert, blieb Phageninduktion während der Kryokonservierung eines lysogenen Stamms erhalten. Dies deutet darauf hin, dass die Vermeidung induzierender Bedingungen entscheidend für die Fitness eines lysogenen bakteriellen Starters sein könnte.

1 INTRODUCTION

This thesis describes the prophages of *L. sakei* and *L. curvatus* and assesses their fate during meat fermentation. This chapter provides information about the genus *Latilactobacillus*, bacteriophages, and raw meat fermentation.

1.1 *L. sakei* and *L. curvatus* – "Meat" and Greet

In 2020, the genus *Lactobacillus* was reclassified into 25 genera [1]. The genus *Latilactobacillus*, which means "a widespread *Lactobacillus*", comprises five species: *L. curvatus*, *L. fuchuensis*, *L. graminis*, *L. sakei,* and *L. fragifolii*, which was recently [2] isolated from strawberry plant leaves. Members of this genus are homofermentative [1], although *L. curvatus* [3], *L. graminis* [4], *L. sakei* [5], and *L. fragifolii* [2] are also described as facultative heterofermentative. The GC content of their 1.82 to 2.12 Mbp long genomes ranges between 40 and 42 mol% [1]. *L. sakei* and *L. curvatus* produce lactic acid in D-(-)- and L-(+)-form and are commercially relevant meat starters [1]. They generally dominate the meat microbiota during spontaneously fermented European sausages [6].

L. sakei was first isolated from moto [7], a yeast mash used in the production of sake, and can be isolated from vacuum-packaged meat, sauerkraut, silage and meat products [8]. *L. sakei* cells are irregular and slightly curved [1], feature rounded ends, are rod-shaped, 0.6-0.8 µm in diameter and 2-3 µm long [8]. *L. sakei* has high intraspecies diversity, reflected phenotypically in strain-specific differences like variable growth speeds and tolerances to temperature and salt concentration, variable acidification dispositions [9], and the ability to perform agmatine and citrate metabolism [10]. The genotypic diversity of *L. sakei* is reflected in a large accessory genome of approximately 50% of its pangenome [10]. Like *L. curvatus*, *L. sakei* was shown to harbour remnant or complete bacteriocin genes (coding for antibacterial toxins), which was speculated to give this species a competitive advantage in their natural habitat [10, 11]. In contrast to *L. curvatus* [10], *L. sakei* can produce energy in the form of adenosine triphosphate (ATP) via the arginine deiminase (ADI) pathway by degrading arginine with ammonia [12] or using the agmatine pathway (the latter being a strain-specific trait) [10]. *L. sakei* is recognised as more competitive during raw meat fermentation compared to *L. curvatus* [6].

While *L. curvatus* shares the ecological niches of *L. sakei* [1, 13], it seems less restricted in its habitat and can be found in honey [14], Korean sourdough [15], Spanish goat cheeses [16] and kimchi [17]. "*Curvatus*" derives from the bean-shaped, curved cells with rounded ends, which

are 0.7 to 0.9 µm in diameter and 1 to 2 µm long [8]. This species was recently discussed to offer probiotic properties to feed and food [17–19]. Furthermore, *L. curvatus* protects food fermentations effectively against spoilage and pathogenic bacteria by producing bacteriocins like sakacin P and curvacin A [20]. *L. curvatus* NRIC 0822, isolated from kabura-zushi, displayed flagellum-mediated motility [21]. Concerning lactobacilli, this trait is primarily found in the genera *Ligilactobacillus* and *Liquorilactobacillus* [1, 21].

1.2 Bacteriophages - the Good, the Bad, and the Ugly

Bacteriophages (short: phages) are viruses that infect bacteria. They are known bacterial fitness modulators that shape and stabilise the microbial equilibrium, leading to a higher biological diversity [22]. Frederick William Twort in 1915 [23] and Felix D'Herelle in 1917 [24] were the first scientists who discovered phages. With an estimated number of 10^{31} particles [25], which was suggested to be referred to as "the Hendrix product" [26], phages are the most abundant biological entity on Earth. Despite the sheer number, with 0.2 gigatons of carbon (Gt C), they only account for a minor part of the approximately 550 Gt C of biomass across all taxa on Earth [27].

The following segments contain information about bacteriophages, their applications and effects on food fermentations and human health, and their degradation, domestication, and usefulness to their host. After an overview of phages infecting lactic acid bacteria (LAB), phage induction mechanisms are discussed.

1.2.1 The Good – Bacteriophage Applications

The concept of using bacteriophages to combat bacterial infections, called phage therapy, is nearly as old as the discovery of phages itself [28]. Felix D'Herelle concluded his article titled "Bacteriophage as a Treatment in Acute Medical and Surgical Infections" in 1931 with the following words:

> "Bacteriophage therapy is still in its infancy and many studies are still necessary before we will learn all the results that we may anticipate, but that which has already been done in many diseases justifies the belief that this is the specific treatment *par excellence* and that it will attain a wider and wider application." [28]

This statement was held two years after the discovery of the antibiotic substance penicillin [29]. Phages offer many advantages compared to antibiotics, like biofilm clearance, single-dosing,

and auto-dosing (due to their self-replicative nature upon bacterial cell infection) and fewer adverse side effects after treatment [30]. Yet, even a combined phage administration as a phage cocktail is usually more selective in its activity spectrum than most antibiotics [30], which can, thus, cure a broader spectrum of bacterial infections. Additionally, controversies surrounding phage therapy supported its decline in Western medicine [31]. According to a recent assessment by Brives and Pourraz [32], the progress of utilising phage therapy on a broader spectrum is nowadays hampered by multiple reasons. Amongst others, phages would not adhere to current regulations of industrial, medicinal products (i.e., forced scalability and commodification of living organisms), the effect of mass utilisation of phage cocktails would be unpredictable, and a high expected price of phage treatment [32].

Today, bacterial antimicrobial resistance (AMR) is a considerable burden to overcome. The higher frequency of AMR is caused by the extensive use of antibiotics and the selection of pathogenic bacteria resistant to those drugs [33]. In 2019, 4.95 million deaths were estimated to be associated with AMR, among which 1.27 million could be attributed to AMR [34]. Next to good flock and herd management and vaccination of livestock, it is hoped that bacteriophage application reduces the use of antibiotics in animal agriculture and thus decreases the chance of AMR formation in the future [35]. In phage therapy, virulent phages are primarily used due to their obligate lytic behaviour and to avoid the potential transfer of virulence factors upon lysogenic conversion, as may be caused by temperate phages [36]. Nonetheless, the nature of temperate phages to lysogenise instead of killing the host directly is considered useful for phage therapy [37], e.g., for sensitising bacteria to antibiotics [38].

Next to medical applications, phages are also utilised during food production. Phages that suppress spoilage bacteria like *Listeria* [39] and *Salmonella* [40] in meat products serve as an additional intervention strategy to preserve especially ready-to-eat [41] and other fresh foods [42]. Moreover, phages proved effective against biofilms, which deliver high resistance against industrial cleaning/disinfection processes and act as reservoirs of spoilage and pathogenic bacteria [43].

Besides the “whole” phage, phage components are utilised in molecular biology. Cosmids, special plasmids packed inside phage particles, use the cos sites of phage λ to integrate large pieces of Deoxyribonucleic acid (DNA) into bacterial genomes after transduction by the phage particles and offer a highly effective method for the generation of genetically modified organisms [44]. Specific binding partners can be found via phage display, which combines a peptide library outside the phage capsids with the genetic information for their expression

packed inside the phage. This can be used, for example, to develop new assays against pathogenic viruses like coronavirus 2 [45]. Moreover, digested or via polymerase chain reaction (PCR) amplified phage genomes are commercially available ladders for gel electrophoresis [46]. Also, the regulation systems of phages are utilised to produce recombinant strains, enabling high-level expression [47] or temperature-controlled gene expression [48]. For example, the temperature-sensitive system p_R/cI857 of phage λ offers temperature-controlled gene expression regulated by mutations of the promoter p_R [48]. The T7 late promoter controls the highly selective T7 RNA polymerase, which forms a high-level expression system that can be utilised for gene expression [49].

1.2.2 The Bad – Phages Impacting Food Fermentations and Human Health

The beneficial aspects of phages discussed in the previous chapter mostly derive from their ability to lyse their host effectively and with high specificity. Vice versa, this property can negatively influence applications, e.g., food fermentation, that utilise beneficial bacteria as starter cultures. According to Josiane E. Garneau and Sylvain Moineau [50], phages could enter manufacturing facilities over raw, processed, or recycled ingredients, through air and surfaces, or by the starter strains themselves when they carry prophages. Amongst others, they suggest good sanitation and treatment of raw materials to reduce the spread of phages within facilities and starter strain rotation to prevent repeating phage amplification throughout multiple consecutive fermentation steps [50]. While the authors focused their work on dairy fermentation, these points are undoubtedly valid for most food fermentations. Nonetheless, not all food fermentations are influenced equally strongly by phages. The number of different added starter organisms or strains on the one side and the consistency/viscosity of the fermented substrate on the other influence the chance of complete lysis of the added starter culture. Highly viscose food matrices can immobilise the phage particles and restrict access to new host cells [51]. In such a substrate, an initial phage-mediated cell-killing step would be followed by re-growing hosts without new phage particles infecting those cells [52]. While the fermentation does not proceed during the first few fermentation hours due to starter lysis, it was shown during raw meat fermentation that the surviving starter cells can recover and continue to grow [53].

Different starter composition types that vary in strain diversity and characterisation level are used in food fermentations. Regional fermented products often rely on starters comprised of an undefined mix of fungi, thermophilic or mesophilic bacteria originating from the indigenous microbiota of the production vessel or substrate [54]. Defined, industrially applied starter cultures rely on fewer redundant strains [54]. Using a diverse set of redundant starter organisms

and rotating the primary starter cultures can decrease the risk of phages impacting fermentation [54]. However, starter strain rotation can entail unintended aroma profile changes [55]. Despite optimised phage-targeted disinfection strategies being applied, i.e., combined administration of multiple biocidal agents [56], many fermented products, including salami produced on an industrial scale [53] or cheddar-style cheeses [54], are made by a defined set of starter strains and are, therefore, at risk of phage attacks.

Usually, phages do not interact directly with human health due to their host-specific nature. Yet, upon transduction of specific genes, prophages can alter their host's phenotype in a human health-concerning way. Commensal bacteria provided with virulence factors can lead to botulism, diphtheria, or cholera or increase antibiotic resistance. [57]

1.2.3 The Ugly – Prophage Degradation and Domestication

The bacterial cell uses many anti-phage-defence systems. This includes degrading intact prophages by gene deletion. These deletion events do not occur at a steady frequency but happen in two distinct phases. During the first, the cell rapidly inactivates a prophage. The second genetic degradation step then proceeds much slower. [58]

Notably, prophage inactivation cannot only be achieved by deleting prophage-related genes but also by the insertion of mobile elements into the prophage. Two transposases were found in phage φ-DJ1812 harboured by *L. sakei* TMW 1.1398, one of which was discussed to cause an incomplete phage particle assembly. This strain still lysed extensively after phage induction, suggesting that the transposase only impaired the phage's ability to infect new host cells. [59]

Another form of prophage inactivation can be caused by genetic events that cause irreversible lysogeny, the so-called “grounding” of prophages [60]. This can happen, for example, through resected *att* sites (attachment sites involved in the integration and excision of phage genomes into and from the bacterial chromosome), defective recombinase proteins (the enzyme responsible for integration and excision), or homologous recombination with related phages during superinfection [60]. Over time, the host cells can domesticate prophages by keeping and exchanging prophage genes for their advantage [58]. One example of this is the utilisation of prophage-encoded endolysins to offset the loss of the major autolysin AcmA in *Lactococcus lactis* [61]. Autolysis (self-digestion) is the intrinsic mechanism of a cell to lyse via autolysins [62]. These enzymes are vital during bacterial cell growth, development, and division as they allow the rigid peptidoglycan cell wall to be partially broken up and expanded [63]. Thus, endolysins encoded within prophages, usually utilised for complete host lysis to release new

phage progeny, are convenient alternatives for the cell to carry out these essential functions. Next to genes coding for phage-related functions, the host can also domesticate so-called "moron" genes, which are sometimes carried by prophages. The name of these genes stems from the fact that there is "more on" the phage genome with this type of mobile DNA present than without those genes [64]. These moron genes may provide the phage and the host beneficial traits, like the prevention of phage superinfection [64], increasing the antibiotic resistance of the host [57], or enabling bacteriocin production, which is used to suppress other microorganisms and therefore boost host fitness [65]. Consequently, domesticated or "grounded" prophages can still affect their hosts.

1.2.4 The Phages of Lactic Acid Bacteria

Earlier publications state that all phages infecting LAB would belong to the order *Caudovirales* [54, 66], which included phages with tails, icosahedral capsids, and double-stranded DNA (dsDNA) [67]. The *Caudovirales* contained three families, namely the *Siphoviridae,* described as the most frequent family amongst LAB phages, and of which members feature long non-contractile tails*, Myoviridae* with long contractile tails, and *Podoviridae*, the least frequent family amongst LAB phages, with short tails [67]. In 2022, the order *Caudovirales,* including the three morphology-based families *Siphoviridae*, *Myoviridae*, and *Podoviridae* [67] within the class *Caudoviricetes* was abolished by the "International Committee on Taxonomy of Viruses" (ICTV) due to their polyphyly, meaning an inaccurate reflection of shared evolutionary history [68]. Today, the *Caudoviricetes* contain all archaeal and bacterial viruses with dsDNA genomes, tails, and icosahedral capsids [68]. "Siphovirus", "myovirus", and "podovirus" are now non-taxonomic terms used to describe morphological phage features [68]. Examples of those morphotypes are depicted in Figure 2.

Phages infecting *Lactobacillus* are reported to have a high biological variability [69], hindering the implementation of a broad classification system [70]. A recent study [71] scanned 1,472 strains amongst 16 *Lactobacillus* species for prophages and identified prophage fragments in 99.8% of analysed genomes, with 64.1% harbouring intact predicted prophages. The authors confirmed that prophages were highly diverse and unevenly distributed amongst different species and suggested that species restricted in their habitat would retain fewer prophages in their genomes. Their antibiotic resistance gene (ARG) screening revealed that 11.1% of detected LAB prophages encode one to four ARGs, but *L. sakei* prophages encoded none.

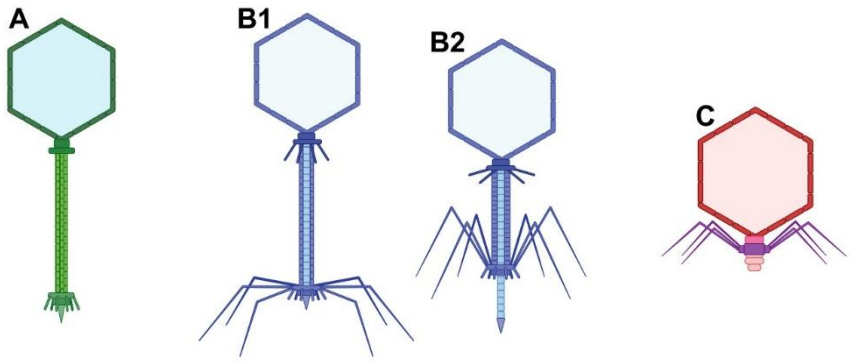

Figure 2. Overview of LAB phage morphotypes. (A) Siphovirus with a long, non-contractible tail. (B) Myovirus with an extended (B1) and a contracted (B2) tail sheath. (C) Podovirus with a short tail. Adapted from [72] with modifications.

1.2.5 Phage Life Cycles

Phages replicate via lytic or temperate cycles (Figure 3). Access to those life cycles is phage-dependent [70]. During lytic infection and after attachment of the phage particle to the bacterial cell, the phage injects its genetic material into the cell [73]. Environmental factors, like temperature and pH, affect phage infection [74]. Some LAB phages depend on divalent cations like Mg^{2+} and Ca^{2+} to properly adsorb to the host cell [70] or perform their lytic cycle [75].

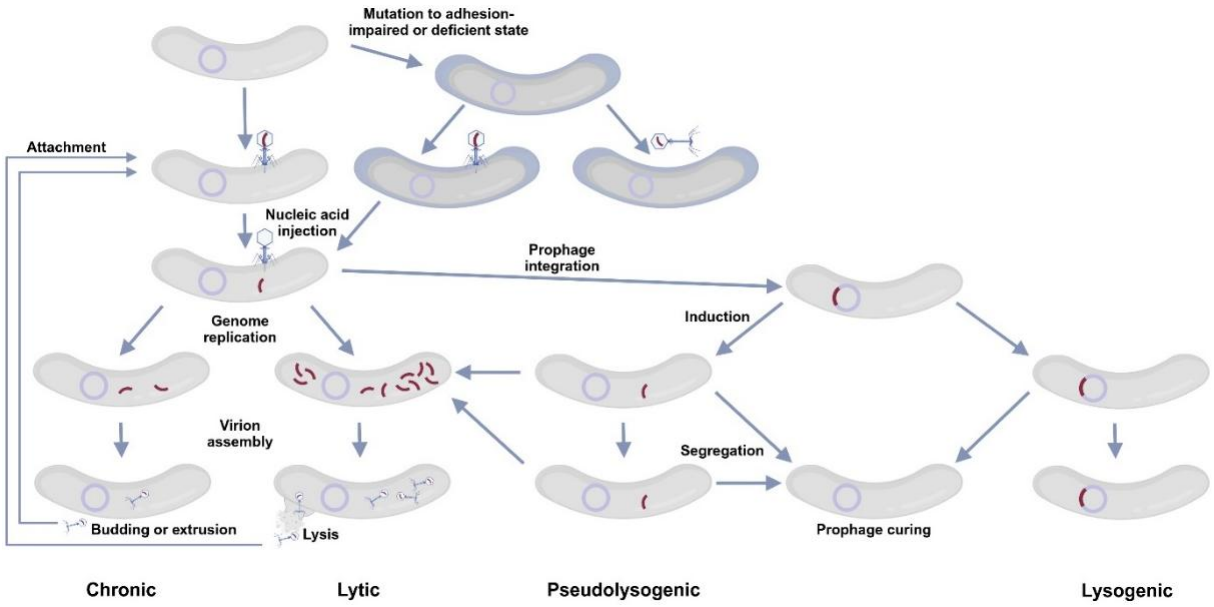

Figure 3. Overview of phage life cycles. After attaching and injecting their genetic material, phages replicate in chronic, lytic, pseudolysogenic, or lysogenic cycles, depending on their type. Mutations can cause an adhesion-impaired or deficient cell state, which grants protection against specific phages. Adapted from [73, 76] with some modifications.

Mutations of the host cell can cause an adhesion-impaired or a deficient cell state [73] and confer protection against specific phages. After the successful injection of their nucleic acids, virulent (strictly lytic) phages take over the replication and translation mechanisms of their host, replicate their genomes, and produce all necessary components for phage assembly. The release of phage particles is usually accompanied by cell lysis (disintegration of the cell), although chronic phage infections were also reported. These are characterised by a slow release of phage virions (phage budding or extrusion) without causing cell lysis. In addition to the lytic life cycle, temperate phages can integrate their genome into the bacterial chromosome, which are then called prophages. The prophages are replicated in concert during cell division and remain dormant until induction. Upon induction, prophages re-enter the lytic life cycle. If the prophage is excised from the bacterial chromosome and not digested within the cell but propagated similarly to plasmids, it is called pseudolysogeny. A prophage can be lost (prophage curing). This can happen by degradation of the excised prophage or during cell segregation after induction. [73, 76]

1.2.6 Phage Induction

Induction is the process of a phage re-entering its lytic life cycle. Induction can happen if the host cell is exposed to DNA-damaging agents that activate its SOS response, such as genotoxic chemicals or UV radiation [77, 78].

UV light, mostly UV-B with wavelengths between 280 to 315 nm, causes DNA strand breaks and multiple DNA lesions, like cyclobutane-pyrimidine dimers, 6-4 photoproducts, as well as their Dewar valence isomers [79]. After the accumulation of DNA lesions, the SOS response of the damaged cell is activated by the expression of the protein RecA, which supports the auto-proteolysis of LexA, the repressor of the DNA damage repair genes [79]. Some temperate phage repressors (e.g., cI of coliphage λ) are structural homologs to LexA and are also inactivated by the presence of RecA, leading to phage induction [80, 81].

First isolated from *Streptomyces caespitosus* in the 1950s, MitC is an antitumor antibiotic substance that causes the formation of covalent crosslinks between the complementary DNA strands and binds the DNA via its UV chromophore covalently, causing DNA alkylation [82]. Thus, it selectively inhibits DNA replication and strongly activates the SOS response of the cell [82]. Other antibiotics inducing the pro-mutagenic SOS response include ciprofloxacin and other fluoroquinolones like enrofloxacin and danofloxacin (DNA gyrase and topoisomerase IV inhibitors) [83], trimethoprim (causing overproduction of reactive oxygen species leading to

DNA damage) and nitrofurantoin (mechanism still poorly understood; discussed to inhibit protein synthesis or cause direct DNA damage) [84].

A prophage may also undergo induction during "normal" growth of the host, which is called "spontaneous phage induction" (SPI). SPI can be influenced by environmental factors, including temperature, pH, osmotic pressure, and nutrient availability [85]. The multiplicity of infection (MOI; the number of infecting phages per bacterial cell; higher MOI most often favours lysogeny), the physiological state of the cell upon infection, the host density, and the presence of heavy metals can also influence the lysis-vs-lysogeny decision [86–88]. Notably, the effect of those conditions is highly phage and host-dependent, represented by inhomogeneous literature [85, 89].

1.2.7 Genomic Composition of Lactic Acid Bacteria Phages

Temperate phages require a specific repertoire of genes to fulfil all essential functions. These genes are often arranged in syntenic blocks and summarised according to function. [90, 91]

Figure 4. Gene module composition of temperate LAB phages. The module sequence is displayed in the example of temperate *Lactococcus lactis* phages [90], modified.

These gene modules cover the functions for lysogeny, replication/transcription, DNA packaging into the capsid, morphogenesis (head- and tail-related genes, last including baseplate genes and genes for host recognition), and host lysis [90]. The lysogeny gene module comprises genes, ensuring the phage genome is stably integrated into the bacterial chromosome. The phage integrase performs this site-specific recombination by recombining the bacterial attachment site (*attB*) and the phage attachment site (*attP*) [92]. As a result of the integration, a left attachment site (*attL*) and a right attachment site (*attR*) are formed as hybrids from the previous *att* sites and represent the junctions between the integrated prophage and the bacterial chromosome [93]. The repressor genes in this module ensure the dormancy of the prophage until induction [94]. Notably, the number of chromosomal integration sites seems restricted and can be conserved for millions of years [95]. These sites were found located in tRNA, transfer-messenger RNA (tmRNA), and well-conserved genes, which are sometimes disrupted by the integrated prophage, as well as in intergenic regions, which are discussed to be under strong purifying selection [95].

The replication module is reported to contain highly conserved genes with a conserved synteny and harbours genes for replicating the phage genome upon induction [90, 96]. Amongst others, genes coding for topoisomerases and resolvases are located in the replication module, as well as primosome-related genes, which are responsible for the initiation of DNA replication, like helicases (separation of DNA strands) or primases (RNA-polymerase) [90, 96, 97].

The packaging module mainly consists of genes coding for the large (TerL) and small (TerS) subunits of the terminase complex, which are responsible for the packaging of the phage DNA into the phage capsid [98].

The head gene module harbours, amongst others, genes for the major and minor capsid proteins, which mainly form the head structure during lytic phage development, as well as scaffolding proteins (supporting the head structure during prohead formation), portal proteins (involved in DNA packaging), and neck proteins. [99]

The tail, baseplate, and receptor-binding gene modules are all involved in the construction of the tail. Tail construction of the siphovirus and myovirus morphotypes starts at the distal end of the phage tail, called the initiator complex. The tail gene module comprises genes that form the tail structure, which is, for phages with the siphovirus and myovirus morphotypes, pre-formed during lytic development and attached to the head after its assembly. In contrast, podovirus tail proteins are connected sequentially to the head. [99] Some genes involved in tail construction include the genes for distal tail proteins, the tail-associated lysin, receptor-binding proteins (RBPs), (major) tail protein(s) [54], and the tape measure protein (TMP), which determines the length of the tail (together with tail assembly chaperons) [100]. Notably, Myophages and Podophages feature two-layered tails [99] and harbour genes for forming the inner tube and the outer sheath. Some phages were reported to feature multi-protein complexes, called baseplates, which include the RBPs [54].

1.2.8 Phage Receptor-Binding Sites

Phages infecting Gram-positive bacteria are meant to infect their hosts in two steps [74]. After the first reversible binding step, in which the phage interacts with the saccharides on the cell surface, the phage irreversibly binds the same or a different surface component [74]. These secondary binding partners can be cell wall polysaccharides, wall teichoic acids, or lipoteichoic acids [74]. The host range of LAB phages has been described as very narrow [74]. For lactococcal siphovirus morphotype phages, this host-specific binding is enabled by the adhesion module consisting of the “initiator complex” as well as the peripheral baseplate and/or RBP

gene(s) [101, 102]. The initiator complex, in turn, includes the genes for the TMP, the distal tail protein, and the tail-associated lysin [101, 102]. An atomic model of the lactococcal phage TUC2009 baseplate suggests that even multiple carbohydrate-binding modules can be present within one phage baseplate [103].

1.3 Raw Sausage Fermentation

For the production of fermented sausages, cured and seasoned meat batter is stuffed into casings and maturated and/or dried [104]. Various antimicrobial hurdles are utilised in the production process to increase shelf life and secure product safety. These include (non-exhaustively) the reduction of water activity (a_w), the addition of nitrite/nitrate curing salts, smoking, and acidification by LAB [104]. Jensen and Paddock patented the idea of adding pure or mixed lactobacilli cultures to raw meat to improve and control its organoleptic properties in 1940 [105]. Next to homofermentative pediococci and/or lactobacilli, catalase-positive and Gram-positive cocci (e.g., coagulase-negative and non-pathogenic staphylococci or kocuriae), as well as moulds and yeasts are utilised in the production of fermented raw sausage products [6]. Notably, many different animals are processed as meat sources worldwide. Thus, the animal-associated, autochthonous microbiota in the meat batter, which originates mainly from the intestines and skin of the animal and is mixed into the meat during slaughtering (another critical source of contamination), varies also. In descending order based on consumption, the three most consumed meat types worldwide are poultry (mostly chicken), pork, and beef. [104]

As depicted in Figure 5, the genus *Latilactobacillus* was found to be part of the microbiota in all three meat types (mainly during storage or processing). Therefore, Latilactobacillus represents an unsurprisingly effective source of starter organisms for meat fermentation.

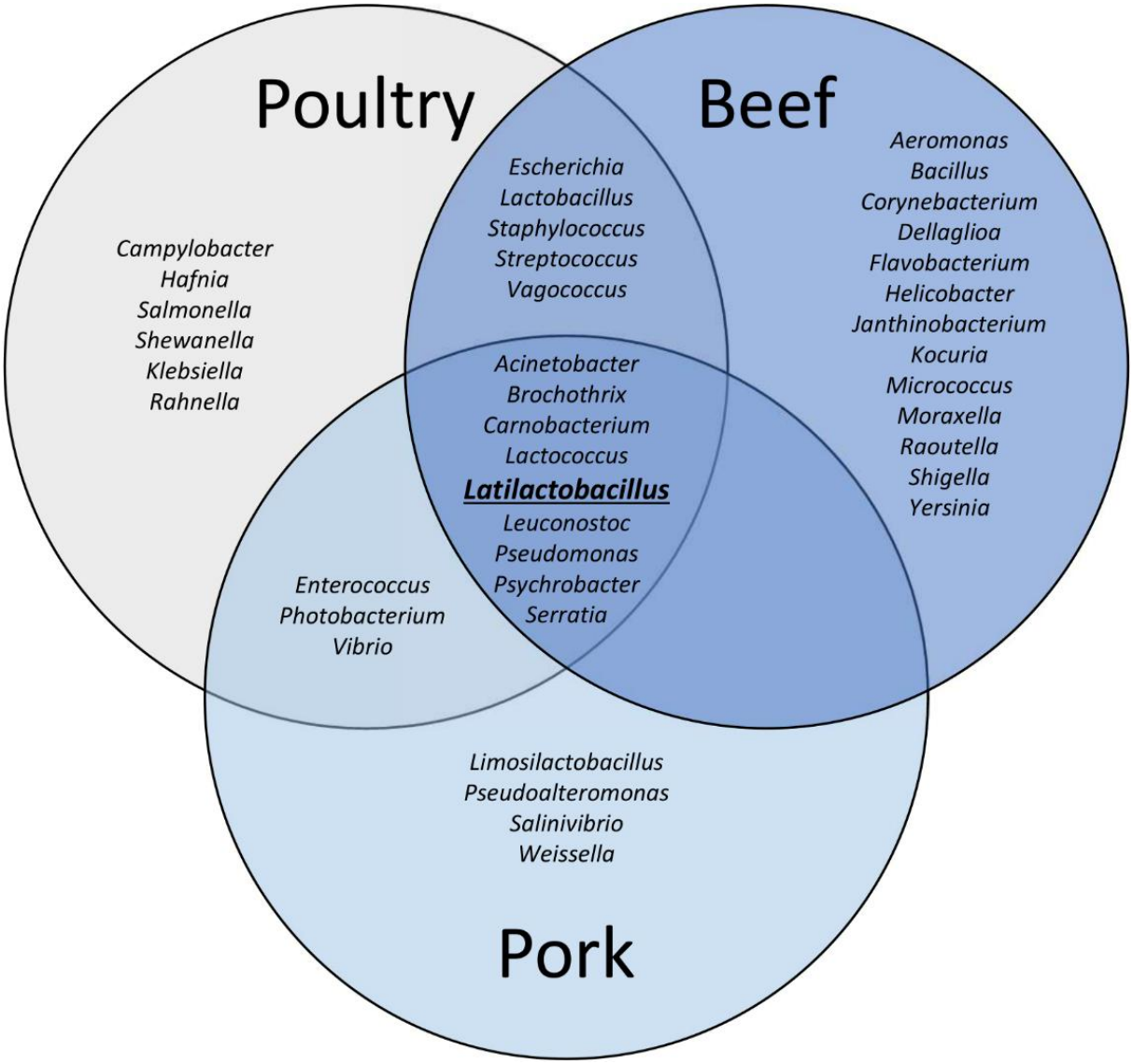

Figure 5. The Microbial composition found during the storage or processing of meat. The species identified in poultry, beef, and pork meat are shown, according to [104]. Notably, this does not strictly include genera identified in the final fermented meat products and may be non-exhaustive.

2 WORKING HYPOTHESES

This thesis started with the idea of partial bacterial lysis being a potential booster for the competitiveness of meat starter cultures. Partial lysis of the starter organism could lead to the release of growth factors and cytoplasmic enzymes, which break down substrate and provide the surviving cells with additional nutrients, increasing the long-term persistence within the fermentation. Furthermore, releasing bacteriocins or other suppressing agents impeding competing microorganisms and enhanced biofilm formation could potentially boost competitiveness after partial lysis.

Lysis may be caused by the intrinsic enzymes controlled by the cells, called autolysis or lytic phages. Two types of phages are discerned: virulent (strictly lytic) and temperate, which can integrate their genome into the host chromosomes in a dormant state (called prophages) until reactivated. The presence of virulent phages is mostly substrate and factory-specific and can thus vary wildly. Temperate phages, in contrast, can be carried stably by the starter organism for many generations and represent, until their degradation, vertically inherited lysis cassettes. Considering the ubiquity of temperate phages amongst LAB, the two species *L. sakei* and *L. curvatus*, commonly used for raw sausage fermentation, are compelling candidates to research.

In summary, this thesis accommodates two major research hypotheses:

1. Strains of the widely used meat starters *L. sakei* and *L. curvatus* contain intact prophages.
2. Prophages affect the competitiveness of their host during meat fermentation.

3 MATERIALS AND METHODS

3.1 Bacterial Strains

Table 1. *L. sakei* strains included in this thesis.

***L. sakei* strain**	**Isolation source**
TMW 1.2 = CTC 372	Fermented sausage (Spain)
TMW 1.3	Fermented sausage (Spain)
TMW 1.4	Fermented sausage (Spain)
TMW 1.13	Starter culture (Germany)
TMW 1.23	Fermented sausage (Germany)
TMW 1.46	Starter culture (Germany)
TMW 1.114	Starter culture (Germany)
TMW 1.411	Sauerkraut (Germany)
TMW 1.417	Starter culture (Germany)
TMW 1.578	Unknown
TMW 1.1189 = DSM 20017^T	Moto (rice wine starter)
TMW 1.1239	Wheat sourdough (France)
TMW 1.1290	Fermented sausage (Germany)
TMW 1.1322 = 23K	Meat
TMW 1.1383	Starter culture (Germany)
TMW 1.1385	Starter culture (Germany)
TMW 1.1386	Starter culture (Germany)
TMW 1.1388	Starter culture (Germany)
TMW 1.1392	Starter culture (Germany)
TMW 1.1393	Starter culture (Germany)
TMW 1.1395	Starter culture (Germany)
TMW 1.1396	Starter culture (Germany)
TMW 1.1397	Starter culture (Germany)
TMW 1.1398	Starter culture (Germany)
TMW 1.1399	Starter culture (Germany)
TMW 1.1500	Fermented sausage (Germany)
TMW 1.2292	Prophage-free derivative of TMW 1.1398 [59]

Table 2. *L. curvatus* strains included in this thesis.

***L. curvatus* strain**	**Isolation source**
TMW 1.7 = DSM 20019^T	Milk
TMW 1.17	Raw sausage
TMW 1.27	Unknown
TMW 1.47	Unknown
TMW 1.48	Unknown
TMW 1.49	Unknown
TMW 1.50	Unknown
TMW 1.51	Unknown
TMW 1.167	Unknown
TMW 1.266	Palm wine
TMW 1.401	Sauerkraut
TMW 1.407	Sauerkraut

***L. curvatus* strain**	**Isolation source**
TMW 1.408	Sauerkraut
TMW 1.421	Unknown
TMW 1.439	Unknown
TMW 1.440	Unknown
TMW 1.591	Unknown
TMW 1.593	Unknown
TMW 1.594	Unknown
TMW 1.595	Unknown
TMW 1.596	Unknown
TMW 1.624	Italian raw sausage
TMW 1.700	TMW 1.624 with deleted dextran sucrose (knockout mutant)
TMW 1.706	Sourdough
TMW 1.1291	Raw sausage
TMW 1.1365	Unknown
TMW 1.1381	Raw sausage starter culture
TMW 1.1382	Raw sausage starter culture
TMW 1.1384	Raw sausage starter culture
TMW 1.1389	Raw sausage starter culture
TMW 1.1390	Raw sausage starter culture
TMW 1.1391	Raw sausage starter culture
TMW 1.1403	Unknown
TMW 1.1408	Fermented freshwater fish (Norway)
TMW 1.1437 = LTH 1683	Lc2-c: pNZ12 (Cmr, Kmr, Neor, *E. coli-Streptococcus* shuttle vector, 4.3 kbp)
TMW 1.1438 = LTH 1831	Lc2-c: pLipPS1 (Cmr, lip gene from *S. hyicus* under control of an *S. carnosus* promoter, 5.4 kbp)
TMW 1.1439 = LTH 1432 = Lc2-c	Unknown
TMW 1.1447	Sardegna pecorino cheese
TMW 1.1449	Italian brenta cheese
TMW 1.1450	Italian brenta cheese
TMW 1.1813	Belladonna/honey ferment
TMW 1.1876	Raw sausage starter culture
TMW 1.1928	Italian raw sausage
TMW 1.1940	Italian raw sausage
TMW 1.1948	Hungarian salami
TMW 1.2270	Rye sourdough
TMW 1.2272	Mealworm
TMW 1.2406	Prophage-free derivative of TMW 1.591 (this thesis)

Table 3. Non-*Latilactobacillus* strains included in this thesis.

Strain	Isolation source
Lc. paracasei isolate 1	Raw sausage (this thesis)
Lp. plantarum TMW 1.25	Portuguese raw sausage
P. pentosaceus TMW 2.1974	Raw sausage
S. carnosus ssp. *carnosus* TMW 2.212	Fermented fish sauce (shrimp)
S. carnosus ssp. *carnosus* MC	Unknown (provided by Meat Cracks GmbH for salami fermentations)
S. carnosus ssp. *utilis* ME	Raw sausage
S. xylosus TMW 2.1521	Raw sausage

3.2 Media and Buffers

3.2.1 Media

Hydrochloric acid or sodium hydroxide was used to adjust the pH of the media.

Baird-Parker (BP) Agar

For 1 L BP agar, 63 g of Baird Parker Base (Carl Roth) was solubilised in 800 mL demineralised water (dH_2O). Water was added to 950 mL, and the medium was autoclaved at 121°C for 15 min. 50 mL egg yolk tellurite emulsion (VWR™) was added directly before pouring.

Modified De Man, Rogosa, and Sharpe Medium (mMRS)

MRS medium/agar was prepared according to [106], with a substitution (mMRS) of ammonium citrate for di-ammonium hydrogen citrate. For 1 L mMRS, 10 g tryptone/peptone from casein (Carl Roth), 10 g meat extract (Millipore), 5 g yeast extract (Carl Roth), 2.6 g di-potassium hydrogen phosphate trihydrate (Merck), 8.3 g sodium acetate trihydrate (Carl Roth), 2 g di-ammonium hydrogen citrate (Carl Roth), and 1 g Tween 80® (Fisher Scientific) was solubilised in 800 mL dH_2O. After addition of 2 mL magnesium sulfate heptahydrate (Sigma-Aldrich) and 0.5 mL manganese(II)sulfate monohydrate (Carl Roth) stock solutions (both 0.1 g/mL, solubilised in dH_2O), dH_2O was added to 900 mL and pH was adjusted to 6.3. dH_2O was added to 950 mL, and the medium was autoclaved at 121°C for 15 min. A 22 g D-glucose monohydrate (Gerbu) was solved in 50 mL demineralised water, autoclaved separately, and added after sterilisation. For mMRS agar [mMRS(A)], 15 g agar-agar (Carl Roth) was added before pH adjustments.

For phage quantification or reinfection assays, mMRS(A) or medium containing 6.8 mM $CaCl_2$ (final concentration) was used if not otherwise stated. For 1 L of medium or agar, 10 mL of

sterile-filtered 0.68 M $CaCl_2$ stock solution was added to the liquid medium or agar (directly before plate pouring)

Tryptone Soya Broth (TSB)

For 1 L TSB, according to [107], 17 g peptone from casein (Carl Roth), 3 g peptone from soymeal (Carl Roth), 5 g NaCl, and 3.25 g di-potassium hydrogen phosphate trihydrate (Merck) was solubilised in 800 mL dH_2O. pH was adjusted to 7.3, dH_2O was added to 950 mL and the medium was autoclaved at 121°C for 15 min. 2.75 g D-glucose monohydrate (Gerbu) was solved in 50 mL demineralised water, autoclaved separately and added after sterilisation. For agar TSB-agar (TSA), 15 g agar-agar (Carl Roth) was added before pH adjustments

3.2.2 Buffers

$CaCl_2$ Stock Solution (0.68 M)

For 100 mL $CaCl_2$ stock solution (0.68 M), 10 g $CaCl_2$ dihydrate (Sigma-Aldrich) was solubilised in 100 mL dH_2O.

Ethylenediaminetetraacetic Acid (EDTA) Stock Solution (0.5 M)

For 500 mL EDTA (0.5 M), 93.05 g EDTA-dihydrate (vwr™) was added to 200 mL dH_2O. The pH was adjusted to 8.0, and volume was adjusted to 500 mL.

Polyethylene Glycol (PEG) 8000/NaCl Stock Solutions

For 500 mL 5× PEG8000/NaCl stock solution used for phage precipitation before TEM, 100 g (≙20% w/v) Poly(ethylenglykol) with an average molecular weight of 8000 (Sigma Aldrich) and 73.05 g (≙2.5 M) NaCl (Carl Roth) were dissolved in 400 mL dH_2O and volume was adjusted to 500 mL.

For 500 mL 2× PEG8000/NaCl stock solution used for phage precipitation before viral DNA sequencing, 100 g (≙20% w/v) PEG8000 (Sigma Aldrich) and 29.25 g (≙1 M) NaCl (Carl Roth) were dissolved in 400 mL dH_2O and volume was adjusted to 500 mL.

Ringer's Solution (1×-Concentrated)

For 1 L 1×-concentrated Ringer's solution, eight Ringer tablets (Merck) were solubilised in 1 L dH_2O. Sterilisation by autoclaving was performed at 121°C for 15 min. Two tablets were used instead for 1:4-diluted Ringer's solution.

SM Buffer

For 1 L SM buffer according to [108], 2 g $MgSO_4$ heptahydrate (Sigma-Aldrich) and 5.8 g NaCl (Carl Roth) were dissolved in 800 mL dH_2O. A 50 mL 1 M Tris-Cl was added, and the volume was adjusted to 1 L with dH_2O. Sterilisation by autoclaving was performed at 121°C for 15 min. For 1 L SM buffer with gelatine according to [109], 5 mL aqueous gelatine solution (containing 2% w/v gelatine (Carl Roth)) was added before volume adjustment to 1 L.

50× TAE Buffer

For 1 L 50× TAE buffer, 242 g Tris base (MP Biomedicals) was dissolved in 600 mL dH_2O. A 57.1 mL acetic acid (Carl Roth) and 100 mL 0.5 M EDTA stock solution were added and the volume was adjusted to 1 L. To obtain 1× TAE buffer for gel electrophoresis, 100 mL 50× TAE buffer was dissolved in 5 L dH_2O.

TE Buffer, pH 8.0

For 1 L TE buffer, 0.37 g EDTA-dihydrate (vwr™) and 1.21 g Tris base (MP Biomedicals) was dissolved in 800 mL dH_2O and the pH was adjusted to 8.0 with HCl. The volume was adjusted to 1 L with dH_2O.

Tris-Cl (1 M)

For 1 L Tris-Cl, 121.1 g Tris base (MP Biomedicals) was dissolved in 800 mL dH_2O. The pH was adjusted to 7.5 with concentrated HCl (Carl Roth). The volume was adjusted to 1 L with dH_2O.

3.3 Bacterial Cultivation and Storage

Unless otherwise indicated, LAB were cultured on mMRS(A) or in mMRS medium static with a closed lid at 30°C. Staphylococci were cultured at 37°C aerobically shaken in TSB or static on TSA. LAB and staphylococci were inoculated 1:1000 with bacterial glycerol stocks. To prepare bacterial glycerol stocks, strains from the TMW strain collection were cultured on an appropriate agar for one to two days. Four colonies were isolated and incubated as before. Species identity of the isolates was verified via matrix-assisted laser desorption/ionisation time-of-flight mass spectrometry (MALDI-TOF MS; Chapter 3.6), and strains were grown overnight in 15 mL (LAB) or 30 mL (staphylococci) medium. Cells were harvested (6000 × g, 10 min) and solubilised in 900 µL or 1.8 mL (if two glycerol stocks were prepared) medium. A 900 µL of cells was added to cryovials with 900 µL 80% (w/v) sterile glycerol [prepared from 99.5%

glycerol (Carl Roth) diluted with demineralised water]. Bacterial glycerol stocks were stored at -80°C.

3.4 Growth Kinetics

Single optical density measurements at a wavelength of 600 nm (OD_{600}), e.g., of overnight cultures for optical density adjustments, were determined using a Novaspec Plus spectrophotometer (Amersham Biosciences) in combination with polystyrene cuvettes (Sarstedt).

For growth monitoring (e.g., after induction via UV light or supplementation of MitC), samples were transferred into a 48-well cell culture plate (Greiner) with a 1 mL sample volume per well, and OD_{600} was measured using a FLUOstar® Omega reader (BMG LABTECH GmbH) at 30°C. Samples were mixed by double orbital shaking at 200 rpm for 5 s before each cycle.

3.5 Bacterial DNA Extraction, Sequencing, Genome Assembly and Annotation

3.5.1 Cell Disruption and DNA Extraction

Bacterial genomic DNA was extracted using the "E.Z.N.A.® Bacterial DNA Kit" (Omega Bio-Tek) according to the manufacturer's instructions. 0.8 mL to 1.5 mL of overnight culture was used for extraction. Samples were treated twice in size during the cell disruption phase. DNA was eluted later with regular elution buffer volume. Cells were centrifuged. For cell disruption, the cell pellet was resuspended in 220 µL lysozyme solution (10 mg/mL lysozyme from Omega Bio-Tek solubilised in TE buffer (pH 8.0)) and incubated at 37 °C for 1.5 h. Cells were additionally disrupted using glass beads in combination with the FastPrep®-24 (20 s, 4 m/s, 24/2) from MP.

3.5.2 Genome Sequencing, Assembly and Annotation

The genomes were sequenced using the Illumina HiSeq technology by Eurofins Genomics. The raw reads were assembled with Unicycler version 0.4.8 [110] (usegalaxy.eu) using default parameters and a contig length cutoff of 1000. The genome annotation was performed via the NCBI Prokaryotic Genome Annotation Pipeline (PGAP) [111–113]. Sequencing of PCR amplicons was performed via Illumina HiSeq technology by Eurofins Genomics after purification using the E.Z.N.A.® Cycle Pure Kit (Omega Bio-Tek) according to the manufacturer's instructions. For sequencing information about viral DNA, see Chapter 3.9.

3.6 Microbial Identification

For microbial identification via MALDI-TOF MS, bacterial colonies were picked onto an MSP 96 polished steel BC target (Bruker Daltonics) and overlaid with 1 µL of 70% formic acid (Sigma-Aldrich). Samples were left for air drying. Samples were then overlaid with 1 µL of 10 mg/mL α-cyano-4-hydroxycinnamic acid (Tokyo Chemical Industry) solubilised in Bruker Standard Solvent (Sigma-Aldrich), consisting of 50% acetonitrile, 47.5% water, and 2.5% trifluoroacetic acid and again air dried. Proteome spectra were recorded with a microflex® LT spectrometer (Bruker Daltonics). The programs flexControl version 3.4 (Bruker Daltonics) and MBT Compass version 4.1 (Bruker Daltonics) were used for measurement and spectra analysis. Obtained mass spectra were matched against the reference spectra of the in-house database and the integrated database. Calibrations were performed regularly using Bruker Bacterial Test Standard (Bruker Daltonics).

3.7 Phage Induction

Prophages were induced using UV light or the genotoxic antibiotic MitC. The following protocols were applied.

3.7.1 Ultraviolet Light

Overnight cultures of LAB were diluted 1:50 in 50 mL, 30°C preheated mMRS. When an OD_{600} of 0.3-0.4 was reached, 10 mL of bacterial culture was transferred into sterile 100 mL Erlenmeyer flasks. UV light irradiation was performed using a UVT-28 M (Herolab) transilluminator featuring eight 8 W UV-B light tubes (Herolab; Cat. No. 2984400; spectrum optimum at 312 nm) on the “high” light intensity setting for 4 minutes. The bacterial cultures were shaken periodically during irradiation.

3.7.2 Mitomycin C

A 15 mL of 30°C preheated mMRS medium was set to an OD_{600} of 0.05 with LAB overnight cultures. After bacterial growth to OD_{600} of 0.1, MitC from *Streptomyces* (Sigma-Aldrich) was added in different concentrations (20, 10, 5, 0.5, 0.2, 0 µg/mL MitC).

3.8 Phage Isolation and Purification

Two purification protocols were applied depending on whether phages were used for TEM or viral DNA sequencing. Phage-containing lysates were harvested one day after UV induction. For this, lysates were optionally centrifuged [6000 × g, 5 min, room temperature (RT)].

Lysates/supernatants were sterile-filtered using Filtropur S 0.45 µm filters (Sarstedt) to remove residual cells and debris. Lysates were stored at 4°C until precipitation was performed.

3.8.1 Purification for TEM

A 1.2 mL sample was supplemented with 300 µl of 5× PEG8000/NaCl stock solution (final concentrations in sample: 4% w/v PEG8000, 0.5 M NaCl). The samples were incubated for 1 hour on ice and then centrifuged (13,000 × g, 10 min, 4°C). The supernatants were discarded, and the phage pellets were solubilised in 120 µL of SM buffer with gelatine corresponding to 1/10th of the former sample volume. Purified phage samples were stored at 4°C.

3.8.2 Purification for Viral DNA Sequencing

Phages in 10 mL lysate were precipitated overnight at 4°C after adding 10 mL 2× PEG8000/NaCl stock solution (final concentrations in sample: 10% w/v PEG8000, 0.5 M NaCl). The samples were centrifuged (16,000 × g, 30 min, 4°C), and the supernatants were discarded. The phage-containing pellets were resuspended in 500 µL SM buffer.

3.9 Phage DNA Extraction and Sequencing

A 1.25 µL DNase I (Quiagen) and 2.5 µL RNase (10 mg/mL; Carl Roth) were added to 500 µL of phage precipitate. Bacterial DNA and RNA were digested at 37°C for 1 h. 1.25 µL Proteinase K (20 mg/mL; Omega Bio-tek), 25 µL 10% (w/v) sodium dodecyl sulfate (SDS; Serva) stock solution and 20 µL 0.5 M EDTA (pH 8.0; vwr™) were added and phage capsids were digested at 60°C for 1 h. Samples were allowed to cool down to RT. The Phage DNA was extracted via phenol-chloroform extraction and precipitated using ethanol according to [49] with slight modifications.

An equal volume of a 1:1 mixture of Roti®-Aqua-Phenol (Carl Roth) and chloroform:isoamyl alcohol 24:1 (Sigma) was added to the app. A 500 µL phage DNA-containing digest. Samples were inverted multiple times and centrifuged (3000 × g, 5 min, RT). The supernatants were transferred into new 2 mL microcentrifuge tubes, and extraction via phenol, chloroform, and isoamyl alcohol was repeated. After transferring the supernatants into new tubes, an equal volume of chloroform was added, and samples were inverted and centrifuged as before. The supernatants were transferred into new microcentrifuge tubes, and 1/10th volume 3 M sodium acetate (Carl Roth) and 2.5 volumes ice-cold ethanol (96%, vwr™) were added. Samples were mixed, and the DNA was precipitated at -20°C overnight. Samples were centrifuged (16,000 × g, 20 min, RT), and the supernatants were removed. The phage DNA was washed by

adding 1 mL 70% ethanol (from 96% stock; vwr™), and samples were centrifuged (16,000 × g, 2 min, RT). The washing step was repeated. The ethanol was removed, and the tubes were left open until the residual ethanol evaporated. The DNA was dissolved in 30 µL Elution Buffer (E.Z.N.A.® Bacterial DNA Kit; Omega Bio-tek) and was quantified using a NanoDrop® ND-1000 (Peqlab) spectrophotometer. The phage genomes were sequenced using Eurofins INVIEW Virus Sequencing for dsDNA viruses and assembled as described before. A 100 bp contig cut-off was set during the assembly process. Fragmented genomes were completed by alignment with their corresponding prophage before uploading at NCBI (accession numbers: Appendix; Chapter 8.1).

3.10 Transmission Electron Microscopy

Negative staining TEM of purified phage solutions (Chapter 3.8) was performed according to [114] by the Chair of Plant Development (LMU). Therefore, 5 µL of the sample was transferred onto glow-discharged and carbon-coated copper grids. Samples were blotted on filter paper and were washed twice using double-distilled water. Negative staining was performed using 2% uranyl acetate for 20 s. After additional blotting, samples were air-dried. A Zeiss EM912 (operated at 80 kV in the zero-loss mode) featuring an integrated Omega filter (Zeiss) was used with a 2k×2k slow-scan CCD camera (TRS) to generate the electron micrographs. The procedures for purification and TEM are depicted in Figure 6.

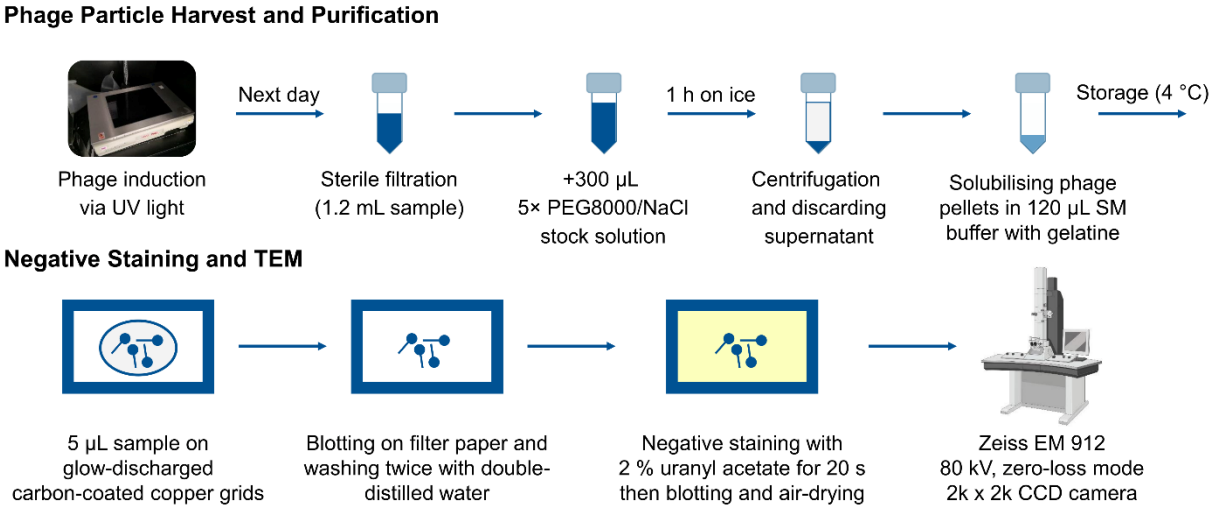

Figure 6. Procedures for phage harvest, purification, negative staining, and TEM. After phage induction via UV light, phages are precipitated, harvested, and stored until TEM. Negative staining of samples and TEM was performed externally, according to [114].

3.11 Prophage Mining and Collinearity Analysis

With JSpeciesWS Webtool (Ribocon GmbH; version 3.9.5) [115], similar genomes [99.00 average nucleotide identity based on BLAST+ (ANIb) over an alignment percentage (AP) cut-off of 95%] were excluded. Prophages were predicted in whole genome sequences of *L. sakei* and *L. curvatus* strains using the web tool PHASTER on phaster.ca [116, 117]. While writing this thesis, this tool was replaced by the "Phage Search Tool with Enhanced Sequence Translation" [116–118]. Found phages were classified as intact, questionable, or incomplete. Prophages were checked manually to see if the assignment was performed correctly. Prophage gene annotation was based on the annotation provided by PHASTER and checked manually by BLASTing the gene sequences or their translated amino acid products against the database on uniprot.org, restricted by the taxonomic filter "viruses." Intact prophages were named based on the host strain identifier followed by a capitalised "p" for "prophage" and a number to distinguish different prophages within the same host. Following the ICTV [119], prophage names are displayed in non-italic, even when the host is included (e.g., L. curvatus TMW 1.591 P1 or TMW 1.591 P1).

Prophage genes were colourised according to their predicted function using SnapGene Viewer (Insightful Science). The colour scheme was based on [98]. In the prophage collinearity analysis, phage sequences with higher similarity were depicted next to each other. Sorting was based on a whole genome alignment and pairwise comparison of those phage genomes using CLC Main Workbench version 8.1.4 (Qiagen). Higher similarities between phage sequences were depicted as bars derived from BLAST analysis using Easyfig 2.2.5 [120] with the following settings: min. length: 0; max. E-value: 0.001; min identity value: 0; outline BLAST hits in black: yes; filter small BLAST hits/annotations: yes.

3.12 Polymerase Chain Reaction and Gel Electrophoresis

The PCRs were performed using a Mastercycler® gradient (Eppendorf) and the Taq DNA Core Kit 10 (MP Biomedicals™). A 25 µL reaction contained 0.15 µL *Taq* polymerase, 0.5 µL dNTPs mix (10 mM each), 2.5 µL 10× reaction buffer, 1.00 µL primer mix (10 µM each; 0.4 µM final concentration; Eurofins Genomics), 19.85 µL water and 1.00 µL DNA or in TE buffer (pH 8.0) dissolved bacterial biomass (colony PCR). All primers were designed to allow annealing at 53°C. For amplification, the following protocol was used: (93°C / 240 s) 1×, (93°C / 45 s, 53°C / 60 s, 72°C / t_E) 35×, (72°C / 600 s) 1× with t_E as elongation time.

For gel electrophoresis, gels with 1% (w/v) agarose (Biozym Scientific) solubilised in 1×-concentrated TAE buffer were used. After the separation of DNA, gels were stained for 15 min in dimidium-bromide (ThermoFisher) and decolourised for 30 min in demineralised water.

3.13 Prophage Curing

After the cultivation of lysogenic strains, UV light induction was performed. Bacterial glycerol stocks were prepared with induced cells. The stocks were stored at -80°C. Then, cells were centrifuged (2 min, 16,000 × g, RT). The supernatant was discarded and the cell pellet was resuspended in 1 mL mMRS medium. Growth was monitored until the OD_{600} reached minimal values after the lysis event. The surviving cells were separated on mMRS(A) plates and were incubated for one to two days at 30°C. One hundred colonies were isolated on mMRS(A) and incubated as before. Ninety-three isolates were checked for prophage loss via colony PCR. Primer sequences are listed in Table 4, and binding sites are displayed in Figure 7.

Table 4. Primers for prophage curing. The sequences are listed in a 5'→3' direction.

Primer	Sequence (5'→3')
1.591_INT_FWD	CAATTCACCTTTACGCATTCC
1.591_INT_REV	TGATAAACAAGAGCTGCTAACC
1.591_PC_INT-site_FWD	GCGACTGCAATTGAGCGTG
1.591_PC_LYS-site_REV	CCGATTAATTGACCGTTACGTGC
1.1290_INT_FWD	CCAAAACTTTTGAAGCAGCC
1.1290_INT_REV	CAAAAAGTACCCCGATAGATCC
1.1290_PC_INT-site_FWD	CCAGTTCCGACACGATTCCG
1.1290_PC_LYS-site_REV	CCGTGCTGGTTCAAAGTGTTTC
1.2272_INT_FWD	GATTTCTTCCACACGCCAC
1.2272_INT_REV	CAAAGAAAGGCAAACGCTAC

For the curing of TMW 1.591 P1, the primers 1.591_ INT_FWD and 1.591_ INT_REV were used with t_E = 60 s, expecting a 112 bp long amplicon in the presence of the prophage. For TMW 1.1290 P1, the primers 1.1290_ INT_FWD and 1.1290_ INT_REV were used with t_E = 30 s, expecting a 431 bp long amplicon in the presence of the prophage. For the curing of TMW 1.2272 P1, the primers 1.2272_ INT_FWD and 1.2272_ INT_REV were used with t_E = 30 s, expecting a 238 bp long amplicon in the presence of the prophage. All primers bind within the integrase gene of the respective prophage.

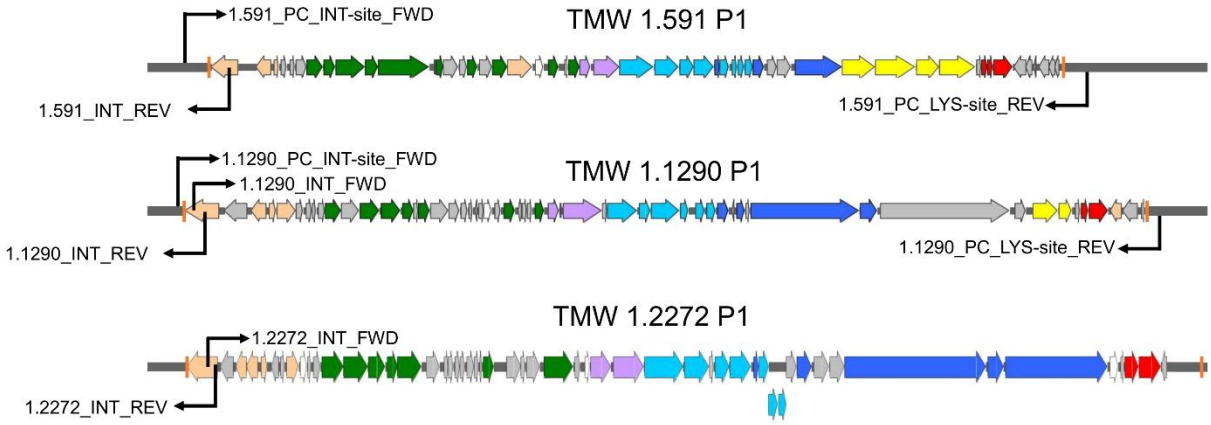

Figure 7. Primer-binding sites for phage curing. Forward (FWD) primers amplify in the sequences from left to right, and reverse (REV) primers from right to left. "INT" primers bind within the phage integrase gene. The PC_INT-site_FWD and PC_LYS-site_REV primers bind near the integrase and lysin genes outside of the prophages and amplify in the direction of the prophage. The attachment sites that indicate the joints between the prophage and bacterial genome are displayed as orange lines.

Subsequent UV-induction was performed of prophage-negative clones to check for the absence of lysis. The integration/excision site of the prophage was amplified, purified, sequenced (Eurofins Genomics), and BLASTed onto the WT genome as additional proof for complete prophage excision. For the amplification of the exclusion site of TMW 1.591 P1, the primers 1.591_PC_INT-site_FWD and 1.591_PC_LYS-site_REV were used with t_E = 240 s expecting a 2.2 kbp amplicon in the case of successful curing. For TMW 1.1290 P1, the primers 1.1290_PC_INT-site_FWD and 1.1290_PC_LYS-site_REV were used with t_E = 240 s expecting an amplicon of 738 bp in the case of successful curing. A 1 µL of the diluted bacterial glycerol stock of the respective cured candidate [1 µL bacterial glycerol stock solubilised in 10 µL TE buffer (pH 8.0)] was used in each reaction. The E.Z.N.A.® Cycle Pure Kit (Omega Bio-Tek) was used to purify amplified DNA.

3.14 Phage TMW 1.591 P1 Quantification

To quantify TMW 1.591 P1 phages via Spot Assay, an *L. curvatus* TMW 1.2406 overnight culture was plated on mMRS(A) containing 6.8 mM $CaCl_2$ (Sigma-Aldrich). The (diluted) phage-containing solution was applied as (multiple) 10 µL drops and was allowed to air dry for 5-10 min under the laminar flow workbench. This allowed the phage particles to come into direct contact with the permissive host cells in each "spot". After incubation (30°C) for two

days, plaques within each spot were counted. The lower reliable detection limit of this assay is estimated to be ~1 × 10^3 PFU/mL or ~1 × 10^4 PFU/g meat (the more solid matrix of the meat must be diluted at least 1:10 to be applicable as a sterile-filtered solution). This corresponds to ~ten plaques per spot. The phage quantification technique is displayed in Figure 8.

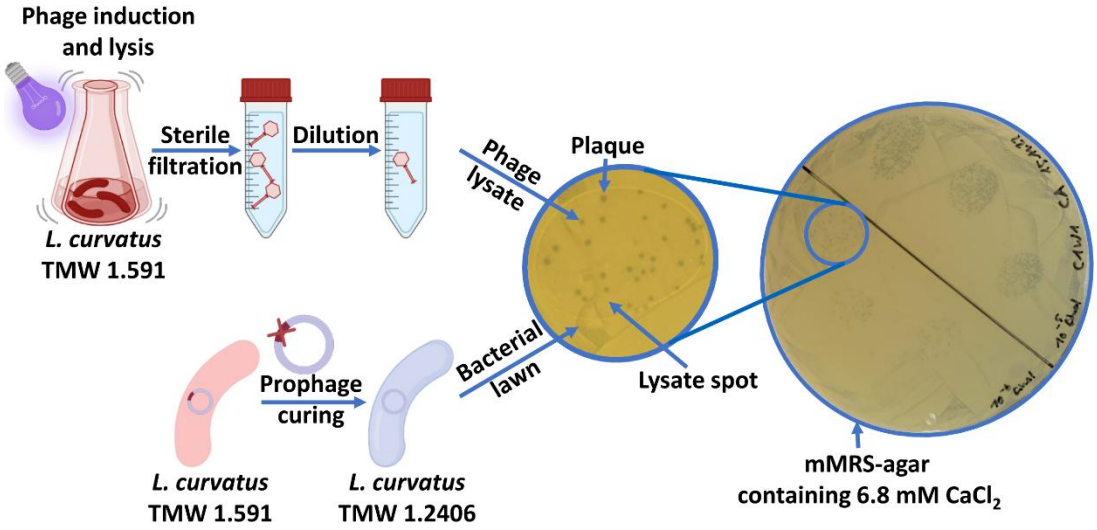

Figure 8. Quantification of TMW 1.591 P1 phages via spot assay. Phage induction of *L. curvatus* TMW 1.591 via UV light produces TMW 1.591 P1 phage particles that cause clear plaques within the turbid *L. curvatus* TMW 1.591 lawn.

3.15 Bioinformatic Tools and Analyses

CLC Main Workbench version 8 was used with default settings to create alignments for phylogenetic analyses. MEGA X (version 10.2.6) [121] was used to create phylogenetic trees. For this, the neighbor-joining method (distance measure method: Maximum composite likelihood) was applied, and bootstrapping was performed using 1000 replicates. Marker genes of *Latilactobacillus* prophages were extracted manually for phylogenetic analysis. Out-grouping marker genes from phages infecting lactobacilli outside the *Latilactobacillus* genus were extracted from phage genomes (Appendix; Chapter 8.1) using the "extract annotation" feature of CLC Main Workbench 8. Phage tRNA genes were analysed with tRNAscan-SE version 2.0 [122, 123] to determine isotype and anticodon. CLC Main Workbench 8 was used to assess codon usage propensities. The tRNA secondary structures were checked manually after prediction with CLC Main Workbench 8 and tRNAscan-SE 2.0. Predicted phage MTase genes were BLASTed (date: 23 February 2023) at rebase.neb.com [124] to verify the correct annotation and type of methylation. For ARG prediction, the curated lists with intact predicted prophages were analysed with the "Comprehensive Antibiotic Resistance Database" (CARD) web tool on card.mcmaster.ca [125].

3.16 Phage Reinfection

3.16.1 Ion Dependency of TMW 1.591 P1 for Reinfection

A 50 µL of TMW 1.591 P1 phages was added to 950 µL *L. curvatus* TMW 1.2406 culture (OD_{600} = 0.05; mMRS medium) supplemented with different amounts of $CaCl_2$, $MgCl_2$, or $ZnCl_2$ (0, 0.5, 1.0, 5.0, 10.0 mM final concentration). The phages were added as a sterile-filtered $1:10^2$ diluted ($1:2\times10^3$ final dilution) lysate of UV-induced *L. curvatus* TMW 1.591. Growth was monitored in triplicates. For a more precise resolution of the required $CaCl_2$ concentration for reinfection, additional concentrations were tested (0, 0.16, 0.32, 0.64, 1.28, 1.60, 1.92, 2.24, 2.59, 2.88, 3.20, 4.79, 6.39, and 12.78 mM final concentration).

3.16.2 Lysate Dilution Dependency of TMW 1.591 P1 for Reinfection

The experimental procedure was performed as described in Chapter 3.16.1. The medium contained 6.8 mM $CaCl_2$ and was also used for lysate dilution. The phages were added prediluted as sterile-filtered post-induction lysate of *L. curvatus* TMW 1.591 P1 in the dilutions "undiluted," 1:10, $1:10^2$, $1:10^3$, $1:10^4$, $1:10^5$, $1:10^6$, and $1:10^7$ resulting in the final dilutions (within the well) 1:20, 1:200, 1:2000, $1:(2\times10^4)$, $1:(2\times10^5)$, $1:(2\times10^6)$, $1:(2\times10^7)$, and $1:(2\times10^8)$. Samples with sterile demineralised water instead of lysate and 1:20 diluted lysate (final dilution) without $CaCl_2$ supplementation served as negative controls.

3.16.3 *Latilactobacillus* Phage Resistance

A combi-strain lysate was prepared by combining (1:12 dilution) equal parts of phage-containing lysates from the following lysogenic strains harvested after UV light induction: *L. sakei*: TMW 1.23, TMW 1.46, TMW 1.1290, TMW 1.1386, TMW 1.1393, TMW 1.1398; *L. curvatus*: TMW 1.591, TMW 1.706, TMW 1.1365, TMW 1.1381, TMW 1.1447, TMW 1.2272. A 950 µL of each tested *Latilactobacillus* strain was grown (OD_{600} = 0.05) mMRS medium containing 6.8 mM $CaCl_2$ and was supplemented with 50 µL combi-strain lysate (1:240 dilution per strain lysate) or demineralised water (negative control). *L. curvatus* TMW 1.2406 was used as the positive control (susceptible to TMW 1.591 P1 phages). Growth was monitored. The procedure is depicted in Figure 9.

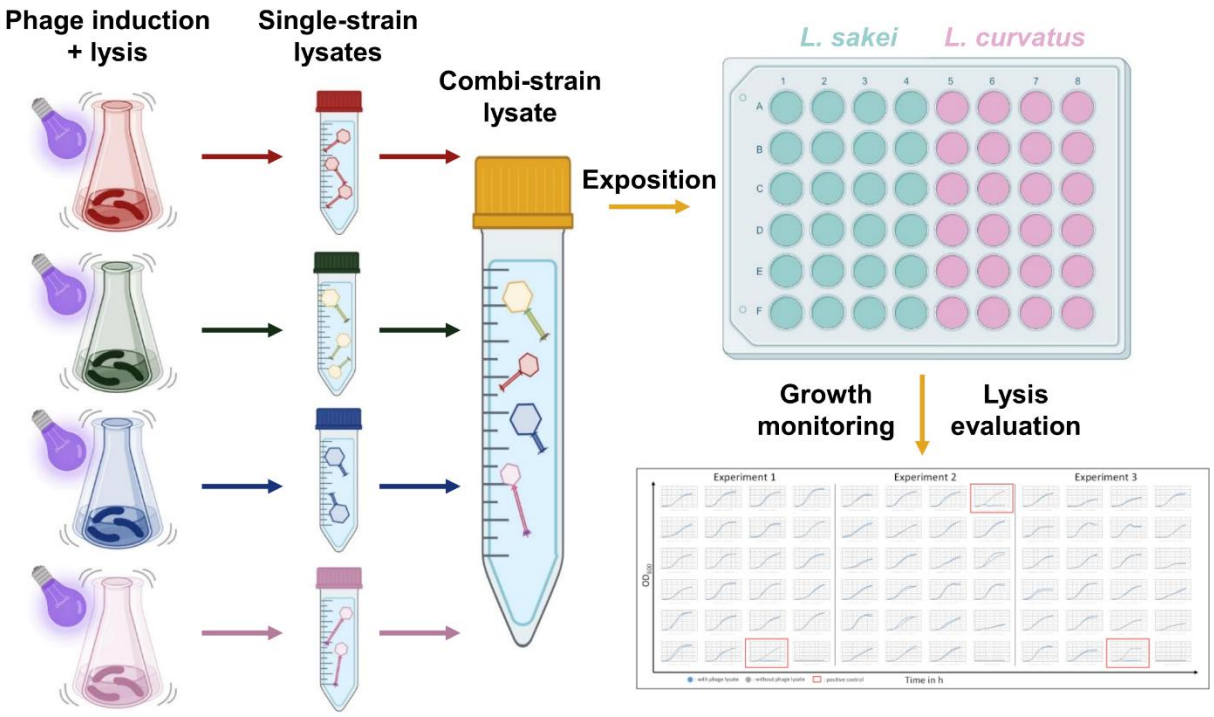

Figure 9. Experimental design of the *Latilactobacillus* phage resistance screening. Single-strain lysates were produced by UV light induction of lysogenic *L. sakei* and *L. curvatus* strains. The strain resistance to phages was checked by exposing the strains to a mixture of all single-strain lysates (combi-strain lysate). *L. curvatus* TMW 1.2406 was used in all experiments as the positive control (red rectangles) due to its susceptibility to TMW 1.591 P1 phage particles.

3.17 Salami Fermentation

LAB starter strains were sent to Meat Cracks GmbH for cultivation and raw sausage fermentation. To allow proper fermentation, the provided strain *S. carnosus* ssp. *carnosus* MC was added to each fermentation. The salamis comprised 22% w/w frozen back fat, 23% w/w frozen shoulder, and 55% w/w fresh shoulder from pork. The frozen raw materials were seasoned and mixed with the LAB and staphylococci starter cultures (5×10^6 CFU/g). The mix was ground to a grain size of 3 mm. 2.6% w/w nitrite curing salt was added. After mixing with the fresh meat, the mix was filled into 45 mm calibre fibrous artificial casings and fermented at 24°C and 96% relative humidity until pH 5.2 was reached. Salamis were ripened at gradually decreasing temperatures (24°C-16°C) for 16 days until a weight reduction of 30%. Cell counts of staphylococci (on BP agar) and LAB (on MRS agar), as well as the total cell counts (on plate count agar), were determined in duplicate for each experimental setting on the days zero, one, three, and seven. After 16 days of fermentation, salamis were cooled at 4°C until day 34. Then, two raw sausages for each experimental setting were sampled for cell count determination on BP and mMRS(A), LAB species distribution, and phage count determination. For this, 10 g of

each tested salami was pre-minced and added to 90 mL (≙1:10 dilution) sterile 1×-concentrated Ringer's solution. After homogenisation in 400 mL sterile lateral filter blender bags (VWR®) for 3 min using a BagMixer 400 W (INTERSCIENCE) laboratory blender, samples were diluted with 1×-concentrated Ringer's solution and cell counts were determined in duplicates on mMRS(A) and BP agar for each sausage. After centrifugation (6,000 × g, 10 min, 25°C), the supernatants of the 1:10 diluted samples were sterile-filtered using filters with 0.45 µm pore size (Sarstedt AG) and were stored at 4°C for later phage quantification. Phage counts for each sample were determined in triplicates. For the distribution of LAB species, the mass spectra of LAB starter strains were recorded and deposited in the in-house database before measurements. Two salamis per experimental setting were analysed 34 days after fermentation start (storage of sausages between day 16 and day 34 at 4°C). The distribution was based on 94 colonies per sausage grown on mMRS(A).

For TMW 1.591 P1 detection and verification of its excision in *L. curvatus* isolates, four primers (1.591_ INT_FWD/1.591_ INT_REV/1.591_PC_INT-site_FWD/1.591_PC_LYS-site_REV; Table 4) were used. The standard PCR protocol (Chapter 3.12) with t_E = 180 s was utilised. DNA is amplified when the prophage is present (112 bp) or excised (2.2 kbp). For verification of TMW 1.591 P1, the primers TMW_1.591_P1_INT_FWD_NEW (**5'-**ATTGCT CGCTTGGTTCTT-**3'**) and TMW_1.591_P1_INT_REV_NEW (**5'-**GGCACGGATCACC GATAA-**3'**) were used. In the presence of the prophage, a 983 bp large amplicon was generated. Both primers bind within the phage integrase gene. The standard PCR protocol (Chapter 3.12) with an elongation time of t_E = 90 s was used for amplification. DNA was applied as 1 µL of TE buffer (pH 8.0) solubilised cells grown on mMRS(A).

3.18 Meat Model Fermentation

The experimental design of the performed meat model fermentations is depicted in Figure 10. One kilogram of pork meat batter consisted of 534 g sow shoulder meat, 277 g shoulder meat from a young pig, and 158 g bacon from a young pig. Moreover, it contained 0.4 g/kg sodium ascorbate, 2.6 g/kg pepper, and 28.7 g/kg pickling salt (NaCl; 0.6% w/w nitrite). The recipe was similar to [126]. 3 mL of *L. curvatus* TMW 1.591 post-induction lysate containing $(1.1\pm0.1)\times10^9$ PFU/mL of TMW 1.591 P1 phages (MOI of 0.1 in relation to the added *L. curvatus* starter organism) and 2 g D(+)-glucose monohydrate (≙0.6% w/w final concentration; Gerbu) were mixed into 300 g of meat batter. A 3 mL of sterile-filtered overnight culture supernatant of *L. curvatus* TMW 1.2406 was used instead of the phage solution as a negative control to compensate for crude phage lysate.

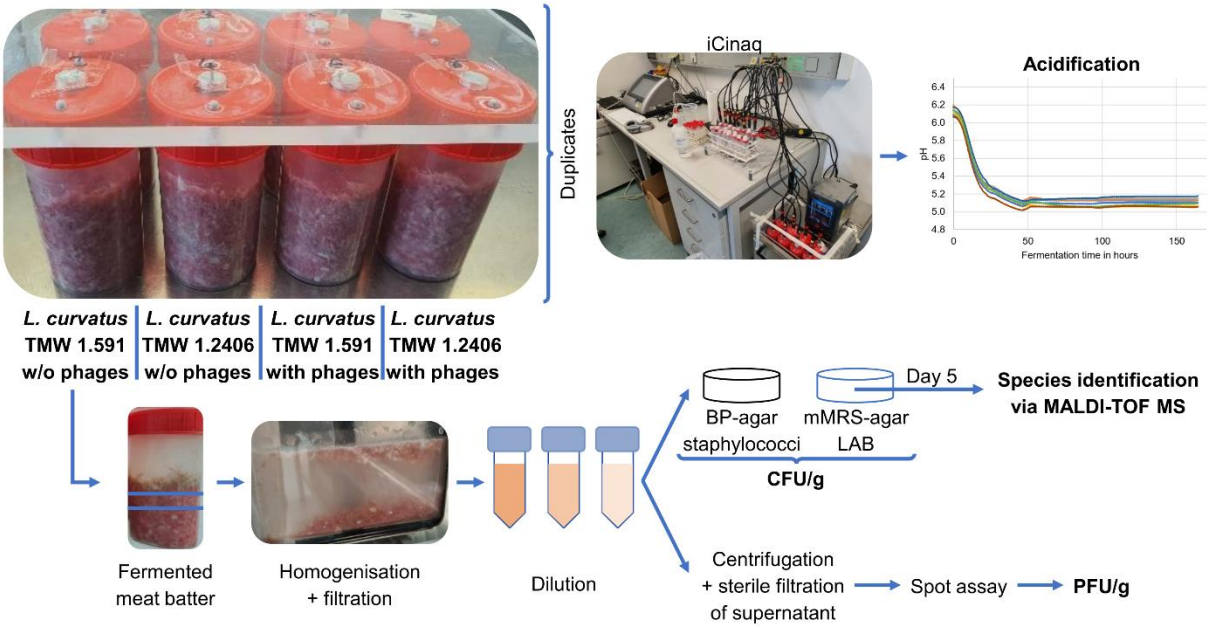

Figure 10. Experimental design of the performed meat model fermentation. The meat batter was fermented in sterile polypropylene cups with *L. curvatus* TMW 1.591 or *L. curvatus* TMW 1.2406 with and without phage TMW 1.591 P1 addition. For sampling of the meat batters on days zero, one, two, and five, the oxidised layers on top of the meat batters were discarded, and aliquots were homogenised and diluted. In the diluted samples, cell and phage counts were determined. The presence of added starters was verified using MALDI-TOF MS on day five of the fermentation.

L. curvatus TMW 1.591 and *L. curvatus* TMW 1.2406 starter strains were added at 1×10^8 CFU/g and *S. carnosus* ssp. *carnosus* TMW 2.212 was added at 1×10^7 CFU/g. Each overnight culture was centrifuged (6,000 × g, 10 min, RT), the supernatants were discarded, and each cell pellet was resuspended in 3 mL 1×-concentrated Ringer's solution (final volume). The starter strains were thoroughly mixed into the meat batter, and after bisecting, each meat batter was transferred into sterile 185 mL polypropylene cups (Kuhnle). Temperature and pH were monitored with an iCinac system (AMS Systea) every hour for five days. For fermentation, the following temperature program was applied: 0-24 h: 24°C; 24-48 h: 20°C; 48 h-end: 16°C.

Sampling was performed on days zero, one, two, and five as described for the salami fermentations and under sterile conditions. Before sampling, the oxidised meat layer on top was discarded. Before reapplication into the samples, the electrodes were cleaned, disinfected in 96% ethanol (VWR™) for one minute, and rinsed with autoclaved demineralised water.

3.19 Evaluation of Phage-Inducing Parameters

L. curvatus TMW 1.591 or *L. curvatus* TMW 1.2406 were grown in mMRS medium from OD_{600} 0.05 to 0.1. Then, 1.5 mL (once per strain, stressor, and exposure time) was centrifuged (16,000 × g, 2 min, RT), each supernatant was discarded, 1.5 mL stressor-containing medium was added, and samples were vortexed.

Following stressors were applied for 10 min, 45 min, and 90 min: NaCl (w/v: 0%, 1%, 2%, 3%, 4%, 8%), $NaNO_2$ (0 ppm, 20 ppm, 50 ppm, 100 ppm, 200 ppm, 1000 ppm), acidity/pH (6.3, 5.0, 4.5, 4.0, 3.5, 3.0), temperature (5, 20, 30, 37, 45, 50, 55, and 60°C), carbon source starvation (glucose supplementation in w/v: 0%, 0.25%, 0.5%, 1%, 1.5%, 2%) and total nutrient starvation (0% starvation ≙ 100% mMRS broth, 20%, 40%, 60%, 80%, 100% ≙ pure 1:4-diluted Ringer's solution. MitC (10 µg/mL; final concentration) induced samples of both strains served as controls. While samples were generally incubated at 30°C, temperature-stressed samples were incubated at the desired temperature during the stressing procedure instead. After stressing, cells were transferred into standard mMRS and growth was monitored for 12-18 hours. The next day, each *L. curvatus* TMW 1.591 sample was sterile-filtered. Filtrates were stored at 4°C until phage detection. The release of phage progeny was verified qualitatively via spotting in duplicates. The experimental procedure is summarised in Figure 11.

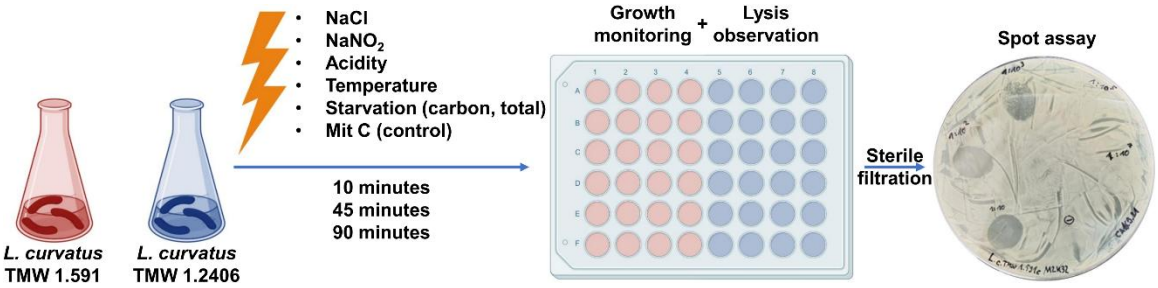

Figure 11. Evaluation of phage-inducing parameters. Tested conditions were higher salt concentrations (NaCl and $NaNO_2$), acidity, temperature, and starvation (carbon source and total nutrients). MitC was used as the control for successful phage induction. Stressors were applied for 10 min, 45 min, and 90 min on growing cultures of *L. curvatus* TMW 1.591 and *L. curvatus* TMW 1.2406 (negative control). Spot assays were performed with *L. curvatus* TMW 1.591 samples 24 hours after stressor application.

3.20 Maintenance of Phage Induction During Strain Cryopreservation

3.20.1 Cryopreservation of Phage-Induced Cells

An overnight culture of *L. curvatus* TMW 1.591 was set to an OD_{600} of 0.1 with 50 mL fresh medium and incubated at 30°C, static, with a closed lid until an OD_{600} of 0.3 was reached. 4× 10 mL of this bacterial culture was then transferred into sterile Erlenmeyer flasks and UV light irradiated as described before. The induced cells were pooled and vortexed after UV light treatment. As described, 3× 1 mL (triplicate) was used for growth monitoring at 30°C. Measurements were taken every 20 minutes for 12 hours. Samples were shaken before measurement. The remaining induced bacterial culture was set on ice for 10 min. After centrifugation (6,000 × g, 10 min, 4°C) and removing the supernatant, the cell pellet was resuspended in fresh, ice-cold mMRS broth in a 10^{th} of the former culture volume. Then, 300 µL of 10×-concentrated cells were added to 300 µL 80% (w/v) sterile-filtered glycerol. The preparation of bacterial glycerol stocks was performed on ice. Bacterial glycerol stocks were stored at -80°C until growth monitoring/cell lysis.

On each sampling day, one cryopreserved bacterial glycerol stock was melted on ice for 10 min. 2× 220 µL cells (duplicates) were transferred into sterile 1.5 mL microcentrifuge tubes for a washing step. The samples were centrifuged (16,000 × g, 2 min, RT = 25°C), the supernatants were discarded, and the cell pellets were resuspended in 1.1 mL fresh, preheated (at RT) mMRS broth. The samples were vortexed briefly. The washing procedure was repeated once. 1 mL of each sample was used for growth monitoring (duplicates) at 30°C. Phage-containing bacterial lysates were harvested 24 hours after reconstitution of ideal growth conditions by sterile filtration, and phages were quantified in both samples. Quantification [mean ± standard deviation (SD)] was performed in triplicate for each sample (six spots were counted for each duplicate).

3.20.2 Determination of Cell Viability After Cryopreservation

Bacterial cultures of *L. curvatus* TMW 1.591 (1× 50 mL) and *L. curvatus* TMW 1.2406 (2× 50 mL) were prepared and grown to an OD_{600} of 0.3. One *L. curvatus* TMW 1.2406 culture was UV-light-induced, as described before. The other two bacterial cultures were incubated at RT during UV induction. After induction, the induced *L. curvatus* TMW 1.2406 samples were pooled. All samples were cooled on ice for 10 min. Cells were harvested, and bacterial glycerol stocks were prepared and stored at -80 °C, as described above. Bacterial glycerol stocks were used once per cell count determination and were discarded afterwards. After storage, bacterial

glycerol stocks were melted for ten minutes on ice. Dilution series were prepared using 1×-concentrated Ringer's solution. Cell counts were determined on mMRS(A) once before -80°C storage (day zero), after one day at -80°C, then once every seven days for five weeks, at seven weeks and ten weeks. Plates were incubated at 30°C for one to two days before cell counting.

3.21 Effect of Species Interference on Phage Induction

An overnight culture of *L. curvatus* TMW 1.591 was set to an OD_{600} of 0.05 with fresh mMRS medium and incubated at 30 °C with a closed lid until OD_{600} of 0.3 was reached. 3× 10 mL was transferred into sterile 100 mL Erlenmeyer flasks and UV-light-induced as described previously. Induced cultures were pooled afterwards. The following meat-associated species/strains were tested for their ability to modulate phage induction: *L. sakei* TMW 1.2, *Lp. plantarum* TMW 1.25, *Lc. paracasei* isolate 1 (isolated from raw sausage from model salami fermentationin; Chapter 4.2.5), *P. pentosaceus* TMW 2.1974, *S. carnosus* ssp. *carnosus* TMW 2.212, *S. carnosus* ssp. *utilis* ME, and *S. xylosus* TMW 2.1521. From overnight cultures of each tested species/strain, a certain amount was transferred into sterile 1.5 mL microcentrifuge tubes and centrifuged (16,000 × g, 2 min, RT). The amount of overnight culture was determined in a way that, after discarding the supernatant, the overnight culture equalled OD_{600} of 0.3 after resuspension of its cell pellet with 1 mL of (non-)induced *L. curvatus* TMW 1.591 culture (resulting in a total OD_{600} of 0.6, thus corresponding to a ~1:1 strain mixture). As described, 1 mL of each sample was used for growth monitoring (duplicates). Measurements were taken every 5 min for 12 hours. The next day, duplicate samples were pooled, sterile-filtered as described before and stored at 4 °C until phage quantification (means ± SD of triplicates).

3.22 Software

BioRender.com was used to create Figure 1, Figure 2, Figure 3, Figure 6, Figure 8, Figure 9, Figure 11, and Figure 17, or parts thereof. The AI-based services Grammarly and DeepL were used as writing assistants during text correction (grammar, spelling, and punctuation) of this thesis. CLC Main Workbench version 8.1.4 (Qiagen) was used for (whole genome) alignments, BLAST analyses, creation of some phylogenetic trees and bootstrap analyses. Easyfig version 2.2.5 [120] was used to perform prophage collinearity analyses. SnapGene Viewer version 5.2.3: SnapGene software (Insightful Science) was used for prophage gene colourisation according to the predicted function. Unicycler version 0.4.8 [110] on usegalaxy.eu was used for genome assembly of raw reads.

4 RESULTS

The following chapter displays the results of the experiments and analyses performed. It is structured in two major sections. The first section (Chapter 4.1) includes the evaluation of phage-dependent post-induction lysis during the lysogen screening, the genome mining for *Latilactobacillus* prophages, and the morphological analysis of released phage particles. This data is extensively discussed in the publications [127] for *L. sakei* prophages and [128] for *L. curvatus* prophages. Furthermore, the impact of L. curvatus phage TMW 1.591 P1 on raw meat fermentation, containing information published in [129], was examined in the second section (Chapter 4.2). The generation and characterisation of a model system (a prophage-free strain that serves as the negative control during fermentation), the fermentation of raw meat with a prophage-harbouring WT strain and its cured counterpart, and induction experiments to investigate the cause for phage induction during the fermentation are described.

4.1 Distribution, Inducibility, and Characterisation of *Latilactobacillus* Prophages

4.1.1 Identification of Lysogenic *Latilactobacillus* Strains

Twenty-seven *L. sakei* (Table 1) and 47 *L. curvatus* strains (Table 2) were screened for phage-mediated lysis after UV light or MitC treatment to identify prophage-harbouring candidates. Lysis was strain and inducer-dependent and was observed either as a fast decline (≙strong lysis; e.g., TMW 1.591) or a short plateau (≙weak lysis; e.g. TMW 1.23) in OD_{600} during growth two to six hours after induction (Figure 12). Nine *L. sakei* (Table 9; Appendix; Chapter 8.4) and 24 *L. curvatus* strains (Table 10; Appendix; Chapter 8.4) lysed after induction.

L. sakei strains that lysed after UV light treatment also lysed after MitC administration. This differed from lytic *L. curvatus* strains, some exclusively lytic after UV light or MitC treatment (but not both). Preliminary experiments have shown that MitC must be administered early and at lower optical density than UV light (growth from OD_{600} 0.05 to 0.1 instead of OD_{600} ~0.1 to 0.3) to achieve the strongest phage-mediated lysis. MitC must also be administered in high concentration (5-20 µg/mL MitC). Lysis was observable at MitC concentrations as low as 0.5 µg/ml in MitC-sensitive strains (e.g., *L. sakei* TMW 1.23). During screening, fast or slow bacterial growth leading to weaker lysis and undetected lysogens was found disadvantageous.

Seven inducible *L. sakei* (Figure 12) and six *L. curvatus* (Figure 13) strains were selected for closer investigation of their prophages (Chapter 4.1.4) after missing genomes were sequenced

(Appendix; Chapter 8.1). The growth of other tested strains after UV light (*L. sakei*: Figure 35; *L. curvatus*: Figure 36) or MitC treatment (*L. sakei*: Figure 37; *L. curvatus*: Figure 38) are provided in the Appendix (Chapter 8.2). This contains non-lytic strains, excluded strains due to a close genetic relationship with strains in Figure 12 or Figure 13, or strains that were not sequenced at the time of the analysis. Of note, *L. sakei* TMW 1.1386 and *L. sakei* TMW 1.1398 were included despite similar genomes (TMW 1.1398 shares 99.7% ANIb over 95.11% of aligned nucleotides with TMW 1.1386). This was done because both strains varied in their lysis responses after induction, with TMW 1.1398 lysing stronger than TMW 1.1386 after UV light or MitC treatment.

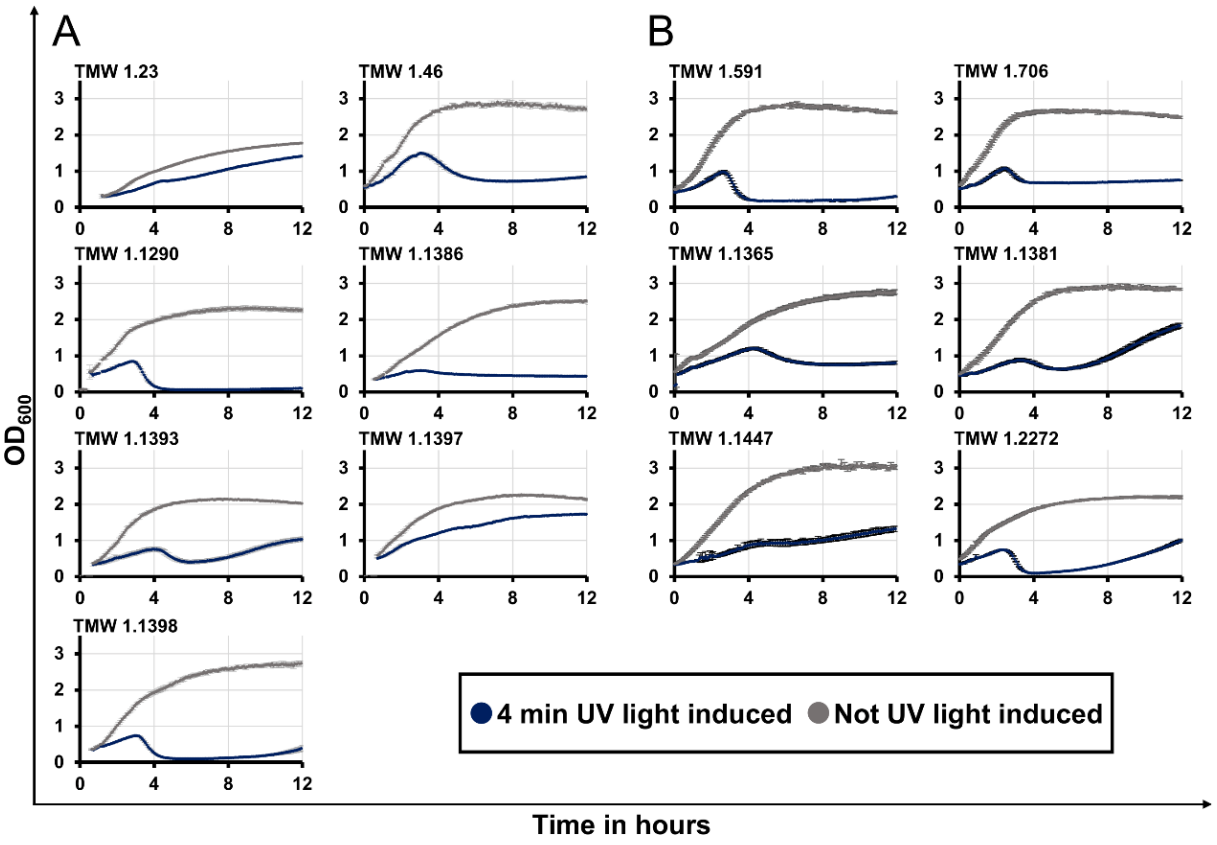

Figure 12. Growth (OD_{600}) of lytic *Latilactobacillus* strains after UV light induction. Samples were induced for four minutes (blue data points). Samples without prior UV treatment (grey data points) served as negative controls. (A) *L. sakei* strains. (B) *L. curvatus* strains.

Next to strain lysis observation, viral DNA from a selection of post-induction lysates was isolated and sequenced as additional proof for phage induction. Before sequencing, phages of strains depicted in Figure 12 and Figure 13 (exceptions: TMW 1.1397 and TMW 1.1398) were precipitated, and bacterial genomic DNA and phage capsids were digested. While DNA from all eight intact *L. sakei* phages and nine intact *L. curvatus* phages (Figure 39 and Figure 40;

Appendix; Chapter 8.3) was detected, the completeness of obtained genomes after assembly varied phage-dependently.

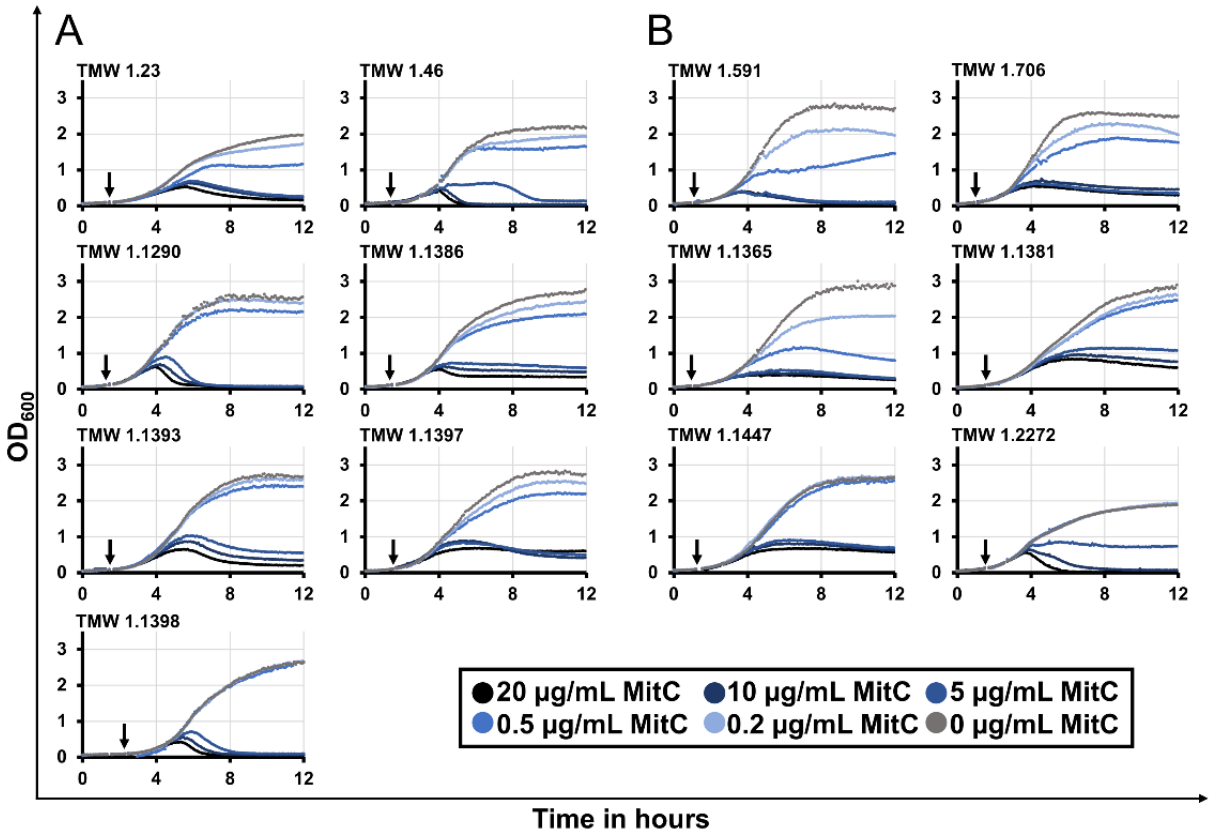

Figure 13. Growth (OD_{600}) of lytic *Latilactobacillus* strains after MitC induction. MitC was applied in concentrations ranging from 0.2-20 µg/mL (blue data points). Untreated samples (grey data points) served as negative controls. (A) *L. sakei* strains. (B) *L. curvatus* strains. The black arrows indicate the time of the MitC administration.

Five *L. sakei* (TMW 1.46 P1, TMW 1.46 P2, TMW 1.1386 P1, TMW 1.1393 P1, TMW 1.1397 P1) and five *L. curvatus* (TMW 1.591 P1, TMW 1.706 P1, TMW 1.1365 P2, TMW 1.1365 P3, TMW 1.1381 P1) phage genomes were fully sequenced. Of the fully sequenced phage genomes, three *L. sakei* (TMW 1.1386 P1, TMW 1.1393 P1, TMW 1.1397 P1) and three *L. curvatus* (TMW 1.1365 P2, TMW 1.1365 P3, TMW 1.1381 P1) were annotated as circular while the rest was annotated as linear after assembly. The two phages of strain TMW 1.46 were fully sequenced in three contigs. TMW 1.46 P1 was primarily located on contig 1 (sequencing depth = 1.00×), and TMW 1.46 P2 on contig 2 (sequencing depth = 4.46×). The missing tail gene part, identical for both phages and necessary for full coverage, was located on the 227 bp long contig 3 (sequencing depth = 5.65×).

Phage TMW 1.46 P2 might have experienced stronger induction or phage assembly according to the four- to fivefold higher sequencing depth (a measure for the number of times the sequence was read during sequencing). TMW 1.1365 P1 (sequencing depth of fragments = ~200-300×) might have been induced/assembled more than TMW 1.1365 P2 (sequencing depth = 1.00×) and TMW 1.1365 P3 (sequencing depth = 0.16x), despite its fragmented genome after assembly. Similarly, TMW 1.706 P1 (sequencing depth = 1.00×) had a lower sequencing depth and might be induced less than the fragmented TMW 1.706 P2 (sequencing depth of fragments = ~5-8×). Interestingly, a transposase was detected in the sequenced viral DNA of TMW 1.1365 P2, which was previously not harboured by the respective prophage.

L. sakei TMW 1.23 P1 and L. curvatus TMW 1.1447 P1 were sequenced as prophages (phage sequences embedded in chromosomal host DNA), confirming the poor inducibility of both phages. While contig 15 (length = 38874), which harboured TMW 1.1447 P1, had a higher depth (131.29×), TMW 1.23 P1 was located on contig 1 (length = 229008) with depth = 1.00×. The sequencing of TMW 1.23 P1 as prophage enabled the identification of both adjacent bacterial border regions, and its integration into a tmRNA gene was confirmed (Chapter 4.1.5).

The genomes of the remaining two *L. sakei* (TMW 1.1290 P1 and TMW 1.1398 P1) and three *L. curvatus* (TMW 1.706 P2, TMW 1.1.1365 P1, and TMW 1.2272 P1) phages were only partially sequenced and, thus, fragmented. Except for TMW 1.1290 P1 contigs (depth: ~1.03-1.25×), all other phage-related contigs featured higher sequencing depths suggesting their induction (φ-DJ1812: ~250-300×; TMW 1.706 P2: 5.26-8.02×; TMW 1.1.1365 P1: 235.19-330.19×; TMW 1.2272 P1: 1238.18-2981.81×).

In conclusion, the lysis responses were strain- and inducer-dependent after UV light or MitC treatment. Administration of a high concentration of MitC (5-20 µg/mL) led to the strongest host lysis. A 4-minute UV light treatment was also effective for phage induction. The successful extraction and sequencing of phage DNA originating from different prophages within post-induction lysates of one multi-lysogenic strain prove their synchronous inducibility despite only one phage morphotype being detected via TEM (Chapter 4.1.2).

4.1.2 *Latilactobacillus* Phage Morphotypes

The PEG8000/NaCl precipitated phages from lysates of five post-UV-light-induced lysogenic *L. sakei* strains (Figure 14A-E) and six *L. curvatus* strains (Figure 14F-K) were examined via TEM as additional proof for phage induction next to lysis monitoring and DNA sequencing and to verify successful phage assembly. The micrographs showed assembled phage virions in four

L. sakei lysates (Figure 14; A: TMW 1.23; B: TMW 1.46; C: TMW 1.1290; E: TMW 1.1393) and four *L. curvatus* lysates (Figure 14; F: TMW 1.591; G: TMW 1.706; H: TMW 1.1365; K: TMW 1.2272). No fully assembled phages were detected in three lysates (Figure 14; *L. sakei*: D: TMW 1.1386; *L. curvatus*: I: TMW 1.1381; J: TMW 1.1447).

All detected phages feature similar-sized icosahedral heads ~43-77 nm in diameter and long, flexible tails with tail widths of ~10-19 nm. Therefore, all detected phages belong to the *Caudoviricetes* class. As no sheath tubes were detected (indicating a myovirus morphotype), they most likely belong to the siphovirus morphotype with long, non-contractile tails. The tail lengths varied between ~126-365 nm. TMW 1.591 P1 virions featured the shortest tails, while the longest tails were detected for TMW 1.2272 P1. The phage capsid diameters, tail diameters and tail lengths are listed in Table 5.

Table 5. Dimensions of *L. sakei* and *L. curvatus* phages. Measurements were determined using TEM micrographs (Figure 14). "nd": No phage virions were detected within the lysate.

Species	Strain	Tail length [nm]	Tail diameter [nm]	Capsid diameter [nm]
L. sakei	TMW 1.23	187	10	43
	TMW 1.46	231	19	77
	TMW 1.1290	262	14	76
	TMW 1.1386	nd	nd	nd
	TMW 1.1393	170	13	53
L. curvatus	TMW 1.591	126	15	47
	TMW 1.706	129	14	54
	TMW 1.1365	186	14	61
	TMW 1.1381	nd	nd	nd
	TMW 1.1447	nd	nd	nd
	TMW 1.2272	365	12	65

Of note, the dark coronas surrounding some phage particles (e.g., Figure 14: B1, C1, G1, K1) hindered exact measurements, and the sizes of those phage particles could be smaller. Protruding baseplates were detected in *L. sakei* TMW 1.46 (Figure 14B1), *L. sakei* TMW 1.1393 (Figure 14E3-4), *L. curvatus* TMW 1.591 (Figure 14F2), and *L. curvatus* TMW 1.1365 (Figure 14H1) phage precipitates. Only one phage morphotype was detected per multi-lysogenic strain (*L. sakei* TMW 1.46, *L. curvatus* TMW 1.706, *L. curvatus* TMW 1.1365).

Cell and phage debris was detected in all samples. Amongst others, separated capsids (Figure 14A3-4) or tails (Figure 14E4) and empty phage capsids (Figure 14E3) were present in samples

with fully assembled virions. Misshapen, tail-less, head-like structures ~50-200 nm in size were detected in *L. sakei* TMW 1.1386 (Figure 14D1-4) and *L. curvatus* TMW 1.1381 (Figure 14 I2-3) samples.

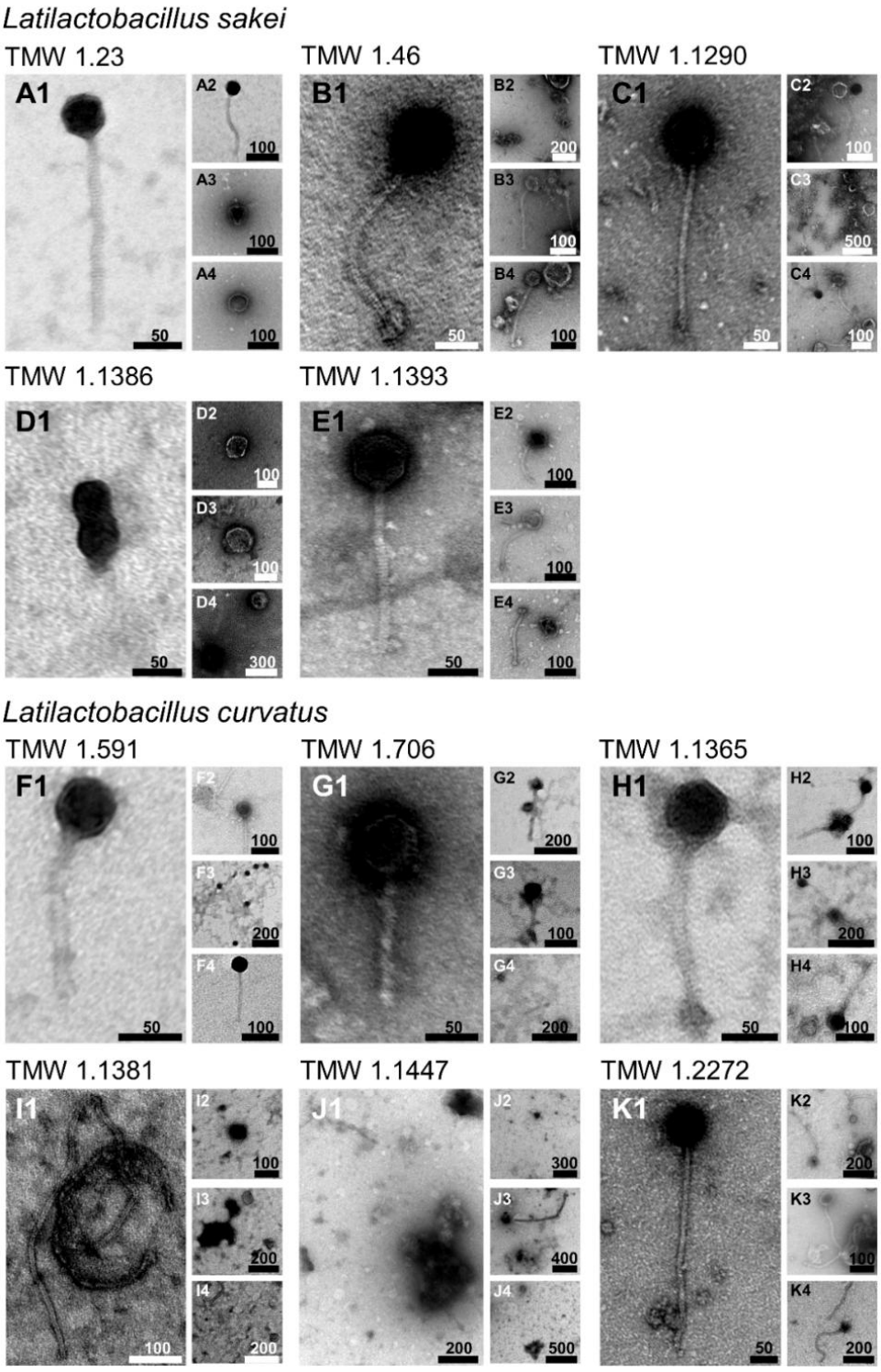

Figure 14. *Latilactobacillus* phage morphotypes. Displayed are TEM micrographs of negatively stained phage precipitates from lysates of UV-light-induced, lysogenic *L. sakei* (A-F) and *L. curvatus* (F-K) strains. Following *L. sakei* strains were analysed: A1-A4: TMW 1.23.

B1-B4: TMW 1.46. C1-C4: TMW 1.1290. D1-D4: TMW 1.1386. E1-E4: TMW 1.1393. Following *L. curvatus* strains were analysed: F1-F4: TMW 1.591. G1-G4: TMW 1.706. H1-H4: TMW 1.1365. I1-I4: TMW 1.1381. J1-J4: TMW 1.1447. K1-K4: TMW 1.2272. The bar size is depicted in nanometres. Adapted from [127, 128], modified.

4.1.3 Prophage Distribution in *L. sakei* and *L. curvatus*

To date, only limited information about the prophage distribution of *L. sakei* and *L. curvatus* is accessible. Therefore, all strains with available genomes analysed within Chapter 4.1.1 were mined for prophages. Additionally, seven *L. sakei* and five *L. curvatus* strains were sequenced (Appendix; Chapter 8.1) and analysed. Forty openly available *L. sakei* and fifty-six *L. curvatus* genomes (Appendix; Chapter 8.1) were downloaded from the NCBI genome database to further extend the mined genome set. Similar genomes (99.00 ANIb over an alignment percentage cut-off of 95%) were identified using JSpeciesWS (Ribocon GmbH; version 3.9.5) [115] and were excluded with some exceptions (Appendix; Chapter 8.4) to ascertain strain diversity in further analyses. In total, 43 *L. sakei* and 45 *L. curvatus* genomes remained in the analysis and were analysed with PHASTER (*L. sakei*: Table 9, *L. curvatus*: Table 10; Appendix; Chapter 8.4).

PHASTER detected 302 prophage sequences of any completeness in the 88 analysed *Latilactobacillus* genomes. Of those, 73 sequences were predicted as intact, 49 as questionable and 180 as incomplete. In the 43 analysed *L. sakei* genomes, 26 of the 89 detected sequences were predicted as intact, 11 as questionable, and 52 as incomplete. *L. sakei* harboured 2.07±1.12 (mean ± SD) prophage sequences of any completeness and 0.60±0.73 intact prophages per strain. Twenty-one *L. sakei* strains contained intact prophages (48.8% of analysed strains). Encoding three prophages, strain J64 harboured the highest number of intact prophages. Of the *L. sakei* strains, the highest number of prophage sequences (any completeness) was predicted for TMW 1.1398 with five sequences. In the 45 analysed *L. curvatus* genomes, 47 of the 213 detected sequences were predicted as intact, 38 as questionable, and 128 as incomplete. *L. curvatus* harboured 4.73±3.60 prophage sequences (any completeness) and 1.04±1.00 intact prophages per strain. Twenty-eight *L. curvatus* strains contained intact prophages (62.2% of analysed strains). With three sequences each, *L. curvatus* strains DRD-164, TMW 1.7, TMW 1.624, and VRA_2sq_f carried the highest number of intact prophages. Of the *L. curvatus* strains, the highest number of prophages of any completeness was predicted for TMW 1.1928 with 14 sequences. In summary, *L. curvatus* harboured more prophages (intact and of any completeness) than *L. sakei*.

The further analysis focused on intact-predicted prophages, as distinguishing between incomplete prophages and parts of plasmids or transposon-rich sequences was often difficult. While PHASTER effectively identified prophage-related sequences, the tool often misevaluated their completeness (e.g., a bacterial genome region rich in transposases of *L. curvatus* TMW 1.411 was predicted as an intact prophage) and their exact chromosomal integration sites. This led to wrong prophage lengths and coding sequence (CDS) counts. Therefore, prophage completeness was revised manually. This way, 29 *L. sakei* prophages and 50 *L. curvatus* prophages were identified with the potential to be intact. The intact predicted prophages after manual revision are listed with their general features in Table 11 (*L. sakei* prophages) and Table 12 (*L. curvatus* prophages).

4.1.4 Genomic Features of *Latilactobacillus* Prophages

The intact predicted prophages harboured by a selection of strains (Figure 12 and Figure 13) were further analysed to obtain insights into the genomic architecture of *Latilactobacillus* prophages. Each phage-related gene was manually BLASTed against a virus gene database (uniprot.org) and gene colourisation was adjusted to predicted functions. The genomes of *L. sakei* prophages are displayed in Figure 15A and of *L. curvatus* prophages in Figure 15B. Prophage φ-DJ1812 (harboured by *L. sakei* TMW 1.1398) [59] was included in this analysis as a reference. While the intact *Latilactobacillus* prophages were highly diverse from one another, four prophage pairs were found to be closely related. L. sakei phage φ-DJ1812 shared 99.99% ANI over 96.26% AP with L. sakei phage TMW 1.1386 P1, L. sakei phage E28G P1 shared 99.98% ANI over 98.60% AP with MFPB19 P1, L. curvatus phage TMW 1.706 P1 shared 97.75% ANI over 100.00% AP with DSM 20019 P2, and L. curvatus phage TMW 1.706 P2 shared 97.60% ANI over 100.00% AP with DSM 20019 P1.

Although the prophage structure is demonstrated by the seven *L. sakei* and six *L. curvatus* strains in Figure 15, the other prophages listed in Table 11 and Table 12 (Appendix; Chapter 8.5) featured the same highly conserved gene module arrangement. All intact prophages start (Figure 15; left to right) with lysogeny-related genes (ochre), followed by genes coding for replication (green) and packaging (lilac) functions. The morphogenesis gene module follows, consisting of genes for capsid (dark blue), tail (light blue), and fibre/receptor (yellow) formation. If BLAST hits were ambiguous, the baseplate, fibre, and receptor genes were classified as tail-related.

The lysis gene cassette (red) was located at the end of each prophage and occasionally followed by genes with hypothetical genes with unknown functions. The replication, head, and tail gene

modules showed the highest conservation. The lysis cassettes consisted of one to two holin genes and one lysin. The lysin genes, used by phages for leaving the bacterial host cell, coded primarily for N-acetylmuramoyl-L-alanine amidases. A gene coding for lysozyme was found in the genome of TMW 1.46 P2 instead. Lysozyme-like genes were mainly found for the tail-associated lysin, which the phages use to enter the bacterial host cell.

Most intact predicted phage genomes encoded all gene modules necessary for completeness. Nonetheless, partial sequence information was missing for some prophages due to incomplete sequencings. For example, the lysogeny module of TMW 1.1447 P1 was partly unsequenced. Analogically, the tail gene module regions of DRD-164 P1 and DRD-164 P2 contained assembly gaps, with the latter also lacking its lysis genes because of this. Although conclusive evidence is missing, the absent prophage-completing genes may, thus, still be present. Besides the lack of complete sequencing information, transposases impeded the correct prediction of prophage intactness. Yet, prophages with a complete set of gene modules encoding transposases were tentatively classified as intact. Transposases (light yellow) were identified in three *L. sakei* prophages (LK-145 P1, φ-DJ1812 and TMW 1.1386 P1), as well as in five *L. curvatus* prophages (ELA214388 P1, ELA214388 P2, KG6 P1, TMW 1.624 P1, TMW 1.1928 P1). While phages TMW 1.1386 P1 and φ-DJ1812 were almost identical, φ-DJ181 encoded an additional set of transposases in its tail gene module and a presumably disrupted gene caused by an SNP. The intact predicted *Latilactobacillus* prophages were searched for ARGs using CARD, but no ARGs were identified.

After excluding Probio65 P2 and DRD-164 P2 for the reasons explained in Table 11 and Table 12 (Appendix; Chapter 8.5), the 77 remaining intact *Latilactobacillus* prophages were compared in length, GC content and number of CDS. The shortest and longest intact *L. curvatus* prophages (and *Latilactobacillus* prophages overall) were WiKim38 P2 (29.3 kbp) and MRS6 P1 (51.2 kbp). The shortest and longest intact *L. sakei* prophages were J54 P1 (33.2 kbp) and CBA3635 P1 (45.6 kbp). With 38.5±3.0 kbp [median ± interquartile range (IQR)], *L. sakei* prophages were similar in size compared to *L. curvatus* prophages with 37.7±4.9 kbp. Overall, *Latilactobacillus* prophages were 38.0±4.2 kbp long.

The GC content of *L. curvatus* prophages ranged from 37.9% (VRA_2sq_f P2) to 43.5% (TMW 1.1365 P1). The GC content of *L. sakei* prophages ranged from 39.0% (TMW 1.1397 P1) to 42.0% (J54 P1). With 39.8±0.8% (median ± IQR), *L. sakei* prophages featured the same GC content as *L. curvatus* prophages with 39.8±1.2%. Overall, *Latilactobacillus* prophages featured a GC content of 39.8±1.1%.

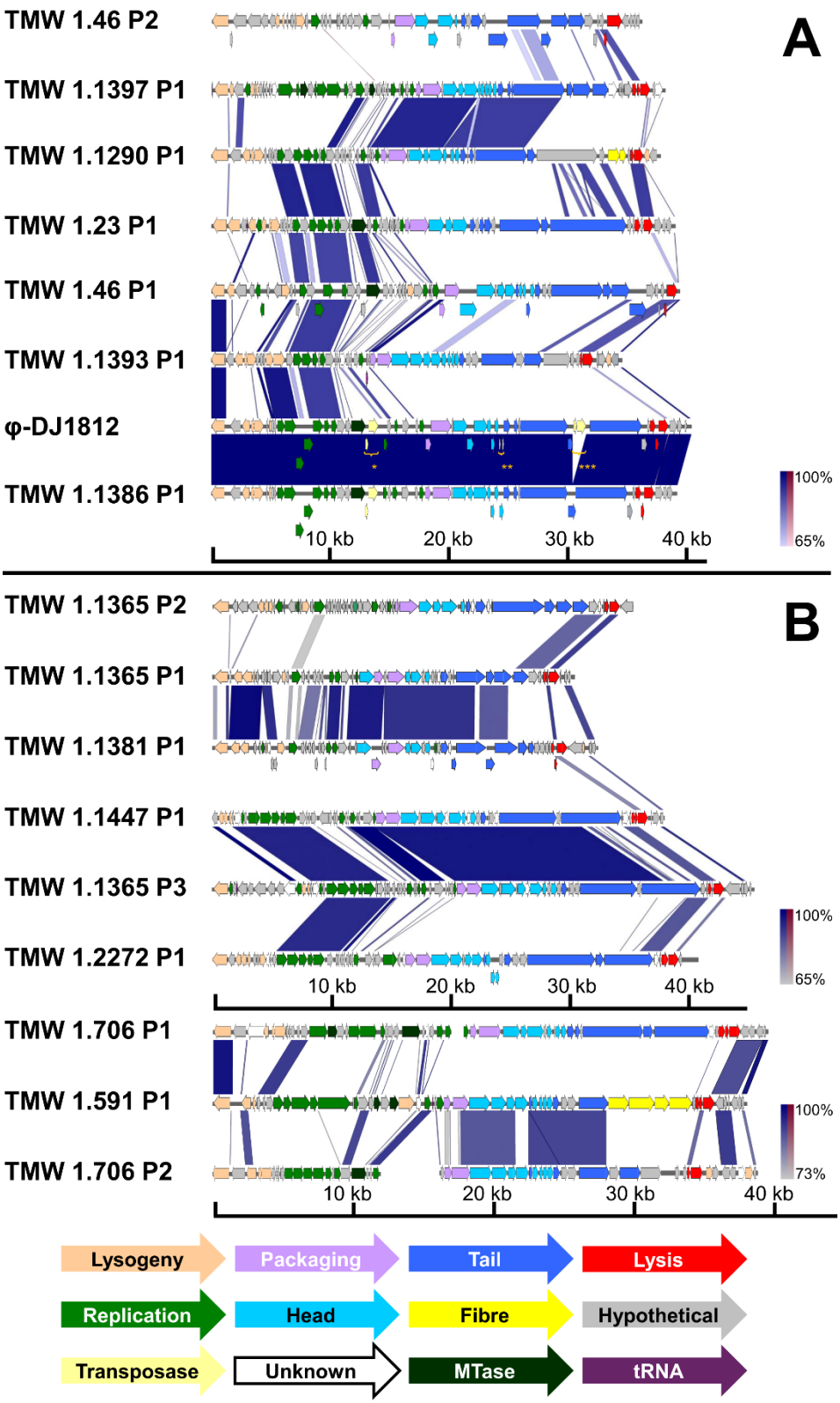

Figure 15. Genomic organisation of *Latilactobacillus* prophages. Displayed are intact predicted prophages of (A) *L. sakei* and (B) *L. curvatus* strains with lytic behaviour after UV light and/or MitC induction. Phage φ-DJ1812 is harboured by *L. sakei* TMW 1.1398. The predicted gene (arrows) functions are indicated by colourisation. Prophages were pre-sorted according to their genetic relationship. Collinearity between phages is depicted as blue bars (red bars if a reverse

correlation is given). Darker bar colours indicate closer relationships. The legends on the right side of each alignment show the nucleotide similarity range of the depicted collinearity bars. The scale below each alignment refers to the length of the sequences in kilobases. "*", transposase in the replication module of φ-DJ1812, which is also located in TMW 1.1386 P1 and caused a contig separation during whole genome sequencing of *L. sakei* TMW 1.1386 (the sequence within this figure was completed using the viral DNA sequencing data of TMW 1.1386 P1). "**", single nucleotide polymorphism (SNP) disrupting an ORF compared to TMW 1.1386 P1. "***", the transposase in the tail gene module potentially hinders correct tail assembly and attachment [59]. Adapted from [127], modified and extended by *L. curvatus* prophages.

Latilactobacillus prophages carried between 40 (L. curvatus KG6 P1, L. curvatus TMW 1.595 P1) and 72 (L. sakei CBA3635 P1) CDS. The *L. sakei* prophage with the least CDS was E28G P1, with a CDS count of 48. The *L. curvatus* prophages with the most CDS were MRS6 P1 and TMW 1.1365 P3, with a CDS count of 71. With CDS counts of 54.0±6.3 (median ± IQR), *L. sakei* prophages featured a similar count in coding regions compared to *L. curvatus* prophages with 55.0±7.0 kbp. Overall, *Latilactobacillus* prophages featured CDS counts of 55.0±7.0.

In summary, when comparing *Latilactobacillus* prophages, *L. sakei* prophages were slightly more homogeneous after exclusion of outliers than *L. curvatus* prophages. This is indicated by the overall smaller IQRs of listed *L. sakei* prophage features. There were no significant differences in size, GC content, and number of CDS between prophages infecting *L. sakei* and *L. curvatus*. Like transposases, some *Latilactobacillus* prophages carried features absent in other intact predicted prophages. In the following, encoded methyltransferases and tRNAs are described.

4.1.4.1 Methyltransferases

Thirty-two MTase genes were predicted (Table 13) in 28 intact *Latilactobacillus* prophages. Each prophage encoded one to two MTases within their replication module. Of the 14 MTase genes carried by the 12 *L. sakei* prophages, four were predicted as adenine-specific and nine as cytosine-specific (either through NCBI annotation or BLAST at rebase.neb.org). For one, no specificity could be identified. Of the 18 MTase genes carried by the 16 *L. curvatus* prophages, seven were marked as adenine-specific and eight as cytosine-specific. For three MTases, no specificity could be determined.

Only two *L. sakei* prophages and three *L. curvatus* prophages feature genes in direct proximity downstream of their MTase genes that encode a product with an endonuclease function (DNA-binding protein, tyrosine recombinase, HNH homing endonuclease; transposases omitted) with which restriction-modification (RM) systems could eventually be formed.

4.1.4.2 tRNAs

Omitting genes used for integration, the intact *L. sakei* and *L. curvatus* prophages encoded between 0 and 2 tRNAs (Table 11 and Table 12; Appendix; Chapter 8.5). Most (17) of the 28 analysed *L. sakei* prophages encoded no tRNAs, 10 prophages encoded one, and one prophage encoded two. Five isoleucine and five phenylalanine tRNA genes were identified, one for valine and one with an undeterminable isotype. Of the 50 analysed *L. curvatus* prophages, 29 lacked tRNA genes, 17 featured one tRNA gene, and four featured two tRNA genes. *L. curvatus* prophages encoded mostly tRNAs for isoleucine (11) or phenylalanine (10), but tRNAs for histidine (1×) and with non-assignable isotype (3×) were also predicted. Eight of the isoleucine tRNAs used CAU, one used AAU, one UAU, and one GAU as anticodon (Nucleotides: A: adenosine; T: thymidine; C: cytidine; G: guanosine; U: uridine). The phenylalanine tRNAs used exclusively GAA as the anticodon.

The use of isoleucine- or phenylalanine-specific codons of the respective prophages encoding these tRNAs was then compared with their hosts. For this analysis, only coding regions were considered. Notably, the prophage sequences were included for the codon usages of their host as they are part of the host genome. Nonetheless, interference is most likely negligible because each prophage only contributes to ~2% of the host genome size. Of the three isoleucine codons (ATA, ATC, ATT), the four isoleucine-tRNA-encoding *L. sakei* phages used ATT most frequently [59.57±3.07% (mean ± SD)], ATC less (26.56±2.63%), and ATA the least (13.87±2.11%). Similarly, their hosts used ATT (63.98±0.18%) most frequently, ATC less (31.79±0.19%), and ATA the least (4.23±0.17%). The nine isoleucine-tRNA-encoding *L. curvatus* phages used ATT most frequently [59.75±2.99% (mean ± SD)], ATC less (24.61±2.20%), and ATA the least (15.63±2.35%). Their hosts used ATT (64.55±0.87%) most frequently, ATC less (31.15±1.39%), and ATA the least (4.30±0.58%). The minor ATA codon was used more frequently by the analysed *Latilactobacillus* phages than their hosts.

Regarding phenylalanine tRNA codon usages, the five encoding *L. sakei* prophages preferred TTT (66.47±2.82%) over TTC (33.53±2.82%) at a similar frequency as their hosts (TTT: 61.40±0.10%; TTC: 38.60±0.10%). Analogically, the ten encoding *L. curvatus* prophages

preferred TTT (63.69±3.22%) over TTC (36.31±3.22%) and at a similar frequency as their hosts (TTT: 58.65±0.66%; TTC: 41.35±0.66%).

Priorly stated phage and host codon usages for isoleucine and phenylalanine tRNAs were similar compared to L. sakei phage TMW 1.1290 P1 (ATA: 12.22%; ATC: 27.73%; ATT: 60.05%; TTC: 34.94%; TTT: 65.06%), a phage harbouring no tRNA genes, and its host (ATA: 3.97%; ATC: 31.96%; ATT: 64.07%; TTC: 38.95%; TTT: 61.05%).

4.1.5 Genomic Integration Loci of *Latilactobacillus* Prophages

The analysis of chromosomal prophage integration sites can provide helpful data for identifying new prophages and estimating the vulnerability of strains to become lysogenic. To identify conserved integration loci shared by intact *Latilactobacillus* phages, the attachment sites *attL* and *attR* were determined for each phage using BLAST alignments. *attL* and *attR* are listed in Table 11 (*L. sakei* prophages) and Table 12 (*L. curvatus* prophages) in the Appendix (Chapter 8.5).

The phage integrase carries out the recombination of the phage genome with the bacterial chromosome. To examine correlations between the phylogenetic relationship of phage integrase genes and the prophage integration sites, groups were assigned to each cluster of closely related integrase genes that reflect their integration sites (Figure 16). Thirteen distinctive *Latilactobacillus*-phage-integrase-specific groups containing the 78 analysed integrases (29 *L. sakei* prophages and 49 *L. curvatus* prophages) were established. Of note, L. curvatus phage TMW 1.1447 P1 was excluded in this analysis as no integrase gene could be detected.

L. sakei phages utilised integrases of groups I-VI [127] for integration. *L. curvatus* phages carried integrase genes belonging to all groups but Group III [128]. Eleven *L. sakei* and 11 *L. curvatus* phages utilised Group I integrases that facilitated integration into arginine or leucine tRNA genes. Two *L. sakei* and two *L. curvatus* phages integrated into transfer-messenger RNA (tmRNA) or serine tRNA (TMW 1.2270 P1; typically Group VIII) genes and featured Group II integrases. Group III integrases were encoded by 11 *L. sakei* prophages (including Probio65 P2, which might be an assembly artefact; Table 11; Appendix; Chapter 8.5). These allowed integration into a gene with an unknown function. Two *L. sakei* and two *L. curvatus* phages used Group IV integrases, which enabled integration into a *sufB*-like gene. Two *L. sakei* and three *L. curvatus* phages used Group V integrases to integrate into a gene coding for a glutamine-hydrolysing guanosine monophosphate (GMP) synthase. One *L. sakei* phage and

three *L. curvatus* phages used Group VI integrases for integration into a gene with a glucose-6-phosphate isomerase as the product.

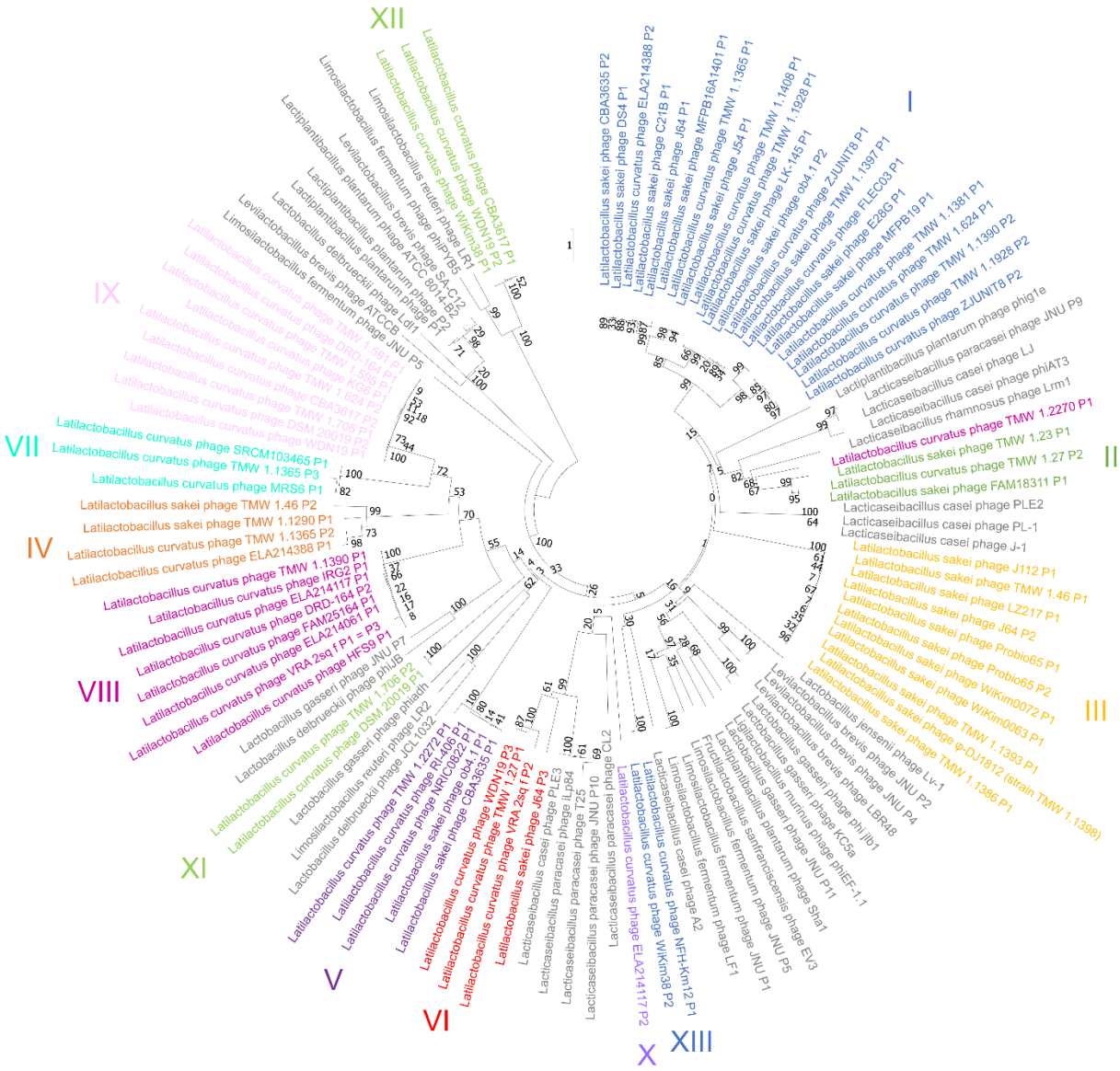

Figure 16. Phylogenetic relationship of *Latilactobacillus* phage integrases. The tree was constructed using the neighbor-joining method with "maximum composite likelihood" as the distance measure method. Bootstrapping was performed using the Jukes-Cantor model with 1000 replicates. The integrases of other lactobacilli-genera-infecting phages served as outgroups (grey). Closely related *Latilactobacillus* phage integrases were assigned to groups (Roman numerals) indicated by the same colour. Adapted from [128], modified.

The remaining groups VII-XIII exclusively contained integrases encoded on *L. curvatus* prophages. The three phages with Group VII integrases integrated into a *lepA* gene with translation elongation factor 4 as the product. Eight phages utilising Group VIII integrases integrated into tRNA genes for serine. Nine phages integrated into glutamine tRNA genes

(Group IX), and one phage utilising a Group X integrase integrated into a glutamic acid tRNA gene. While L. curvatus phage DRD-164 P1 utilised a Group IX integrase, its predicted *attR*-site was located before its lysis genes. Due to this, the phage might not be intact. Notably, an alternative pair of attachment sites was found (Table 12: *attL:* TATTCGTTGATGATATT, *attR:* TATTCGTTGATCATTTT), which would allow correct excision upon phage induction and would correspond to a gene coding for a FtsX-like permease family protein as integration site. Two phages with Group XI integrases and three with Group XII integrases integrated into non-coding regions. The two phages featuring Group XIII integrases integrated into a different leucine tRNA gene as Group I integrases and were assigned to a new group. For example, the utilised tRNA for integration of NFH-Km12 P1 shared a nucleotide similarity of 66-67% with Group I leucine tRNAs, which shared ~100% nucleotide similarity.

In summary, closely related phage integrases enable integration into the same gene. Only one outlier (TMW 1.2270 P1 integrase) used an unexpected integration locus compared to other integrase group members. The lactobacilli phages infecting other host genera served as effective outgroups for this analysis.

4.2 The Fate of Phage TMW 1.591 P1 During Raw Meat Fermentation

Prophages can alter the fitness and competitiveness of their host. It was previously unknown whether its prophages positively or negatively impact a *Latilactobacillus* starter during meat fermentation. A prerequisite for determining the influence of a prophage, whilst excluding any host-specific impact, is the generation of a prophage-free (cured) isogenic strain derivative. This way, a cured strain serves as the negative control during fermentation. If susceptible to the WT phage(s), a cured strain can additionally act as an indicator strain to quantify WT phages (e.g., via a plaque assay) or as the positive control when determining the phage resistance of a species. The following chapters describe the generation of a model system to study phage-host interactions, and the resistance of *L. sakei* and *L. curvatus* to *Latilactobacillus* phages is analysed. The salami and meat model fermentations with *L. curvatus* TMW 1.591 and its cured derivative (TMW 1.2406) are also described, and influences of temperate phage TMW 1.591 P1 on meat fermentation are determined. Induction experiments analyse the causes of enhanced prophage induction during fermentation. Last, it is examined if phage induction is maintained during cryopreservation. The working packages are summarised in Figure 17.

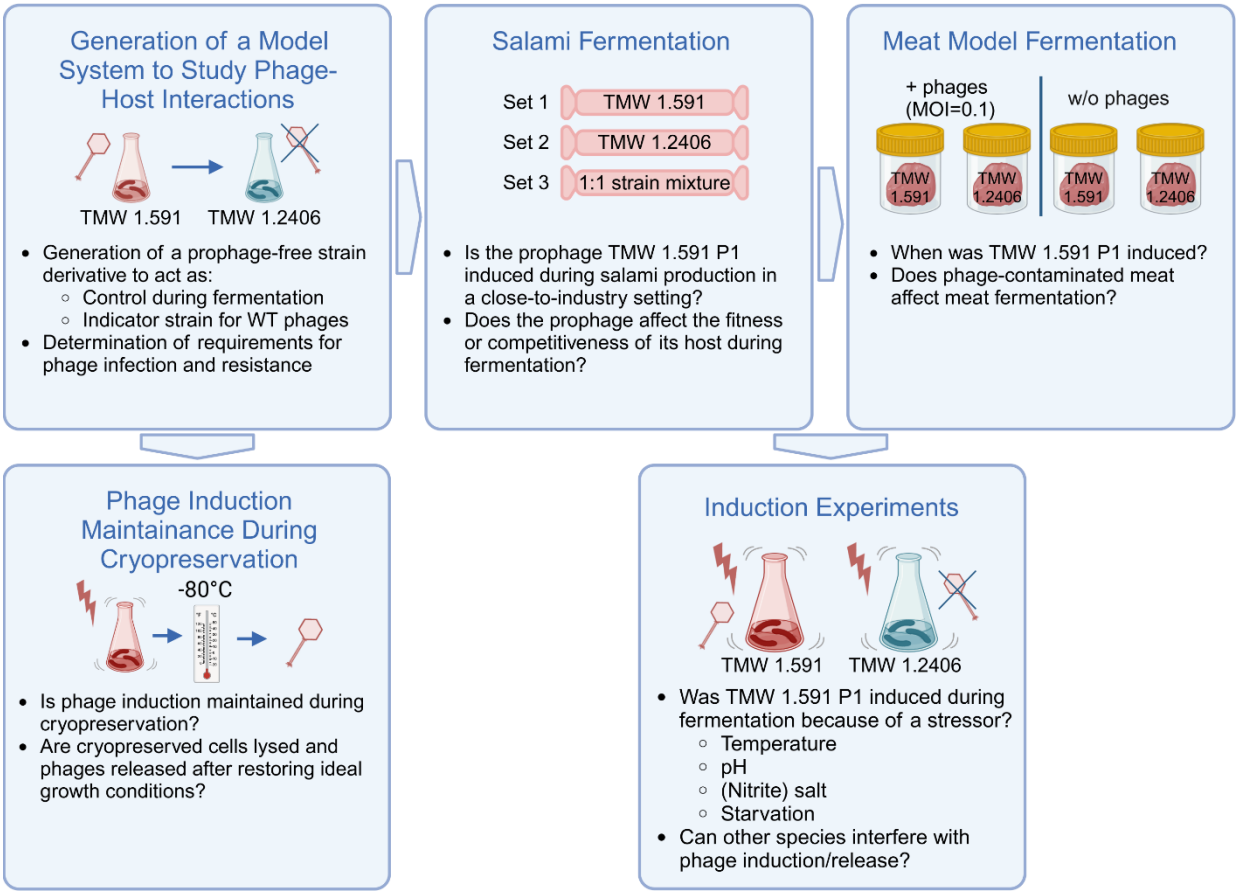

Figure 17. Working packages and research questions to evaluate the fate of TMW 1.591 P1 during raw meat fermentation.

4.2.1 Generation of a Model System to Study Phage-Host-Interactions

Prophage-negative strain derivatives are required to analyse the influence of an intact prophage on host fitness and competitiveness during meat fermentation and to compensate for strain-caused influences. Strains harbouring only one intact predicted prophage that showed strong lytic behaviour after phage induction were selected for curing. The presence of only one prophage in the WT strain ensured that a prophage-free strain was more likely to appear after induction. Curing multiple prophages within a multi-lysogenic strain requires the inducibility of all prophages and possibly multiple induction rounds, which could enhance spontaneous mutations altering the host phenotype. Moreover, an observed phage-related influence must be retraced to a specific prophage. Selecting a strain with only one prophage makes discussions about which prophage (or a combination of prophages) causes an observed effect unnecessary. *L. sakei* TMW 1.1290 and the *L. curvatus* strains TMW 1.591 and TMW 1.2272 fulfilled these criteria and were, thus, chosen for phage curing. Bacterial glycerol stocks were prepared with induced cells after a 4-minute UV light treatment. This streamlined the experimental procedure and allowed the same induced sample to be used in multiple screening rounds until prophage-

free isolates were obtained. Growth and phage-mediated lysis of revitalised cells were monitored after storage at -80°C (Figure 18). Cells were plated on mMRS(A) when minimal OD_{600} values were reached two to three hours after phage-mediated lysis to isolate prophage-free clones.

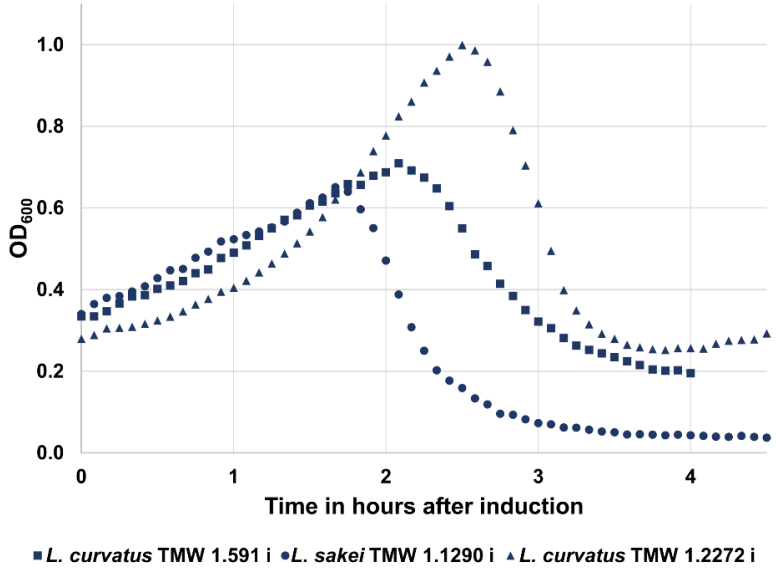

Figure 18. Induction verification of lysogenic strains before isolation of cured candidates. The growth of revitalised, 4-minute UV-light-induced *Latilactobacillus* strains is displayed. *L. sakei* and *L. curvatus* cells were plated after reaching minimal OD_{600} values to isolate prophage-free clones. *L. curvatus* TMW 1.591 growth was adapted from [129], modified.

Four of 186 *L. sakei* TMW 1.1290 and seven of 93 *L. curvatus* TMW 1.591 screened isolates were presumably prophage-free, indicated by a negative PCR result (Figure 41 and Figure 42; Appendix; Chapter 8.7). Data of unsuccessful screening attempts of *L. sakei* TMW 1.1290 and *L. curvatus* TMW 1.2272 are included in the Appendix (Figure 42; Chapter 8.7). To verify successful curing, the four potentially cured *L. sakei* TMW 1.1290 isolates and seven *L. curvatus* TMW 1.591 isolates were treated with UV light (Figure 19). All tested isolates showed no prophage-mediated lysis after the treatment, corroborating the curing success.

It was analysed whether released phages of respective WT strains could reinfect the potentially cured isolates. Therefore, *L. sakei* TMW 1.1290 isolate 6 and *L. curvatus* TMW 1.591 isolate 4 were exposed under the presence of 6.8 mM $CaCl_2$ to their post-induction WT strain lysate or a mixture of post-induction lysates from multiple lysogenic *Latilactobacillus* strains (combi-strain lysate; included lysates are listed in Chapter 3.16.3). *L. sakei* TMW 1.1290 isolate 6 (Figure 20A), its WT (Figure 20A), and *L. curvatus* TMW 1.591 [Figure 20B and Figure 43A (Appendix; Chapter 8.7)] were resistant to all tested phages, indicated by absent lysis. In

contrast, *L. curvatus* TMW 1.591 isolate 6 was susceptible to phage TMW 1.591 P1 (Figure 20B) but resistant to other tested phages (Figure 43B; Appendix; Chapter 8.7).

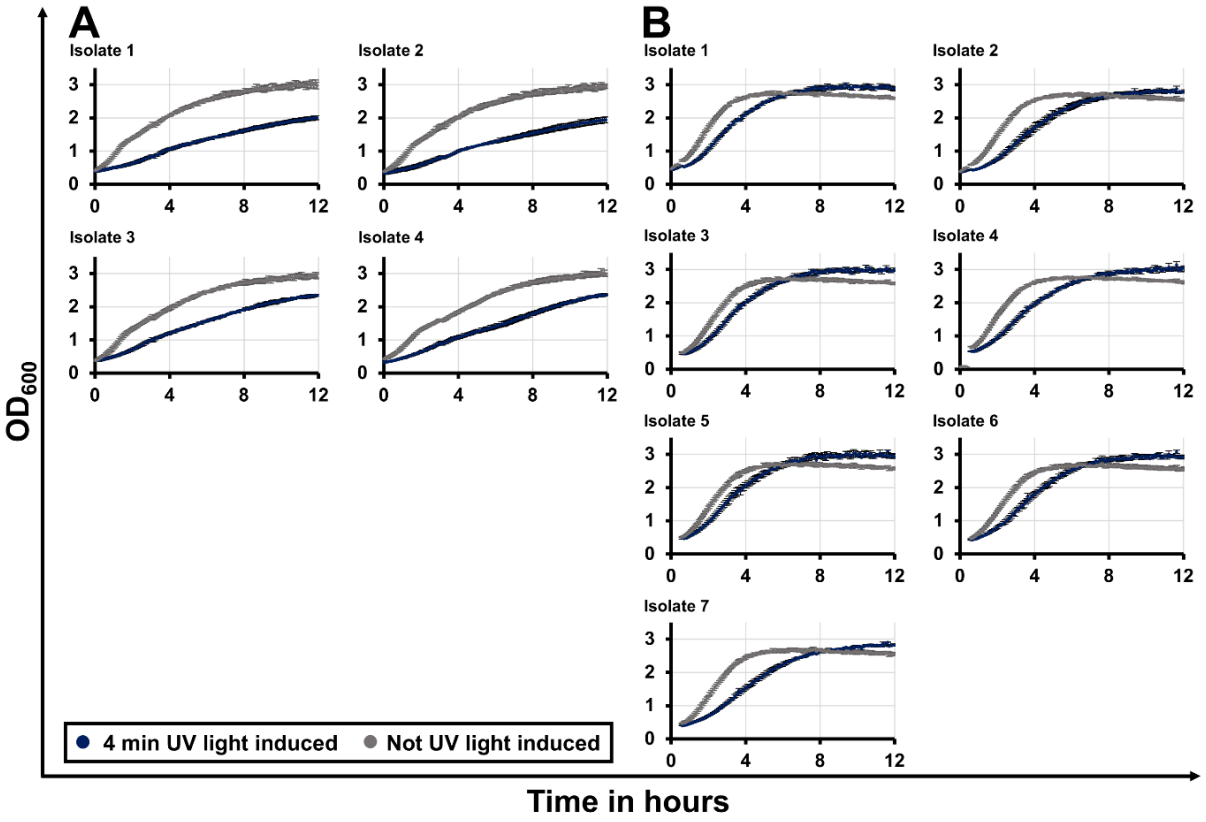

Figure 19. Curing verification of prophage-free *Latilactobacillus* candidates via UV light induction. (A) *L. sakei* TMW 1.1290 isolates. (B) *L. curvatus* TMW 1.591 isolates. The 4-minute UV light treatment (blue data points) did not lead to visible lysis. Untreated samples (grey data points) served as negative controls. B was adapted from [129], modified.

The ability of TMW 1.591 P1 to relysogenise a cured isolate was tested. For this, *L. curvatus* TMW 1.591 isolate 6 phage survivors (Figure 20, "TMW 1.591 isolate 6 + TMW 1.591 lysate") were plated one day after phage administration. All 20 tested survivors were found lysogenised by TMW 1.591 P1 (Figure 44; Appendix; Chapter 8.7).

The excision sites of prophages TMW 1.1290 P1 and TMW 1.591 P1 were amplified (Figure 21) and sequenced (one isolate per strain) to ensure complete excision of the respective prophages. All TMW 1.1290 isolates yielded an amplicon of >3 kbp despite the expected 738 bp amplicon if the prophage was successfully removed (Figure 21A). All seven TMW 1.591 isolates yielded an amplicon with the expected size of 2.2 kbp (Figure 21B). TMW 1.1290 isolate 4 and TMW 1.591 isolate 6 amplicons were sequenced, and retrieved sequences were aligned onto the WT genome (Figure 21C-D).

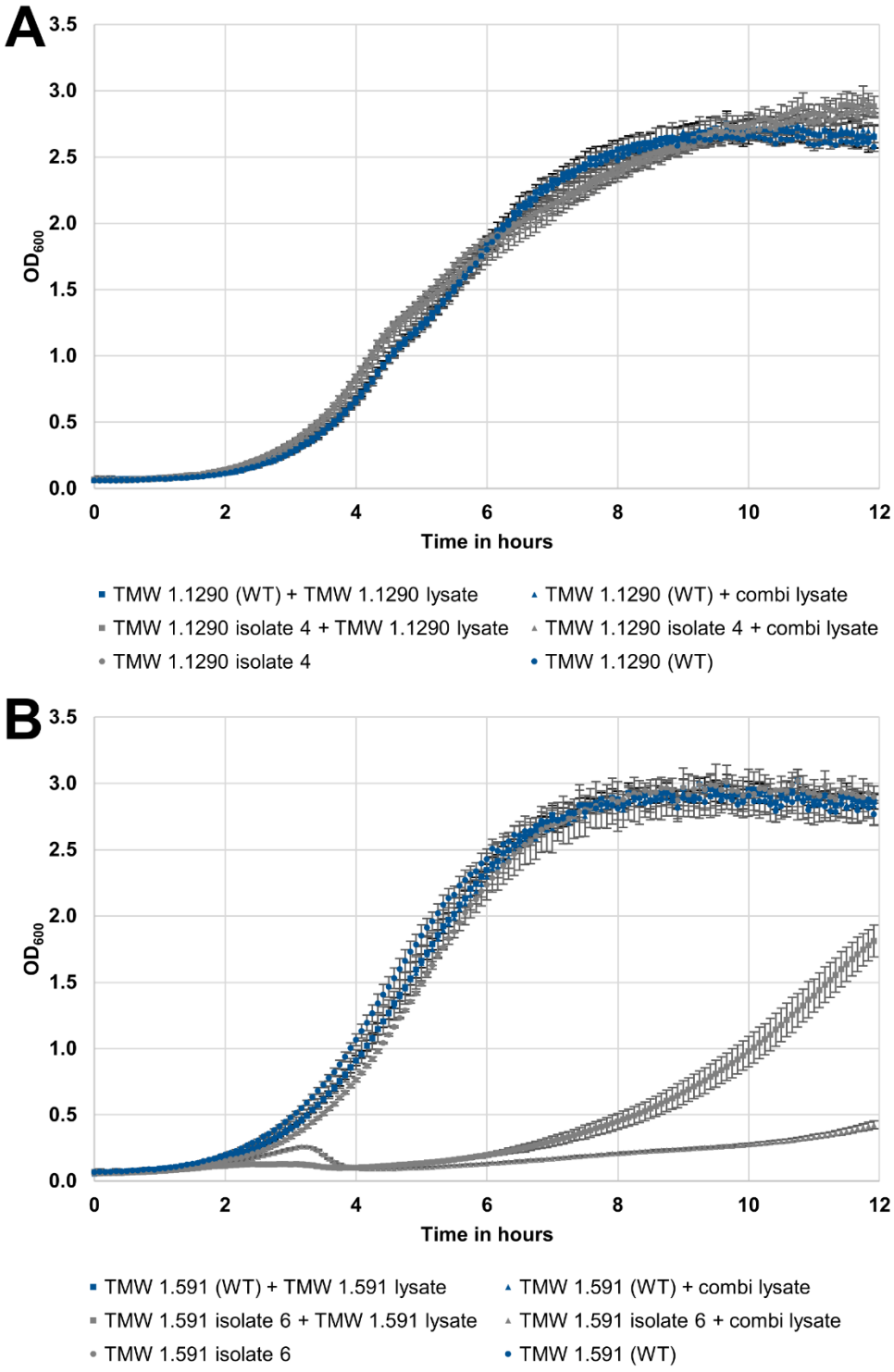

Figure 20. Phage resistance of cured *Latilactobacillus* isolates to *Latilactobacillus* phages. The growth of (A) *L. sakei* TMW 1.1290 isolate 6 (blue data points), (B) *L. curvatus* TMW 1.591 isolate 4 (blue data points), and their WT strains (grey data points) is displayed. The strains were treated with the respective WT post-induction lysate (rectangular data points) or a combi-strain lysate (triangular data points). Samples without lysate administration (circular data points) served as controls. All samples contained 6.8 mM $CaCl_2$ to enable phage reinfection. Lysis indicates successful phage infection. B was adapted from [129], modified.

BLAST analysis verified the correct excision of TMW 1.591 P1 within *L. curvatus* TMW 1.591 isolate 6 (Figure 21C). However, BLAST analysis of the TMW 1.1290 P1 revealed DNA of unknown origin (Figure 21D) in place of the prophage.

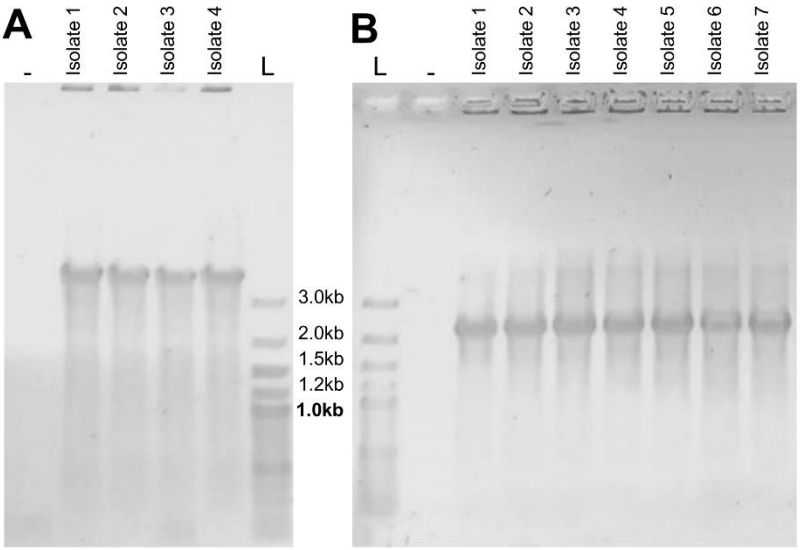

L: GeneRuler™ 100 bp Plus DNA Ladder (Thermo Fisher Scientific)
- : Negative control (water instead of cells)

C

TMW 1.591 isolate 6 5′-TTCTATCTTA----------ATTGGGTATATAGGGCTCGAA-3′
TMW 1.591 wild-type 3′-TTCTATCTTAATTGGGTATATAGG-TMW1.591P1-ATTGGGTATATAGGGCTCGAA-5′

D

TMW 1.1290 isolate 4 5′-TGGAAGGGTCCGTGGGGTAG-NNNNNNNNNNN-TAGGCTTTTTCTTATTTATTTTACCTAAGGCTAGTGACCTAAAACTTTT-3′
TMW 1.1290 wild-type 3′-TGGAAGGGTCCGTAGGGTAG-TMW1.1290P1-TGGAAGGGTCTGTAGGATAATAAAAAAGGCTAGTGACCTAAAACTTTT-5′

Figure 21. Verification of complete prophage excision via sequencing. (A) *L. sakei* TMW 1.1290 isolates 1-4 amplified using TMW-1.1290-P1-specific primers (1.1290_PC_INT-site_FWD/1.1290_PC_LYS-site_REV; Table 4) that produce a 738 bp long amplicon if the curing was successful. (B) *L. curvatus* TMW 1.591 isolates 1-7 amplified using TMW-1.591-P1-specific primers (1.591_PC_INT-site_FWD/1.591_PC_LYS-site_REV; Table 4) that produce a 2.2 kbp amplicon if the curing was successful. (C) BLAST alignment of the TMW 1.591 P1 integration/excision site between *L. curvatus* TMW 1.591 isolate 6 and its WT verified a correct prophage excision. (D) BLAST alignment of the TMW 1.1290 P1 integration/excision site between *L. sakei* TMW 1.1290 isolate 4 and its WT was unsuccessful. The "N"s represent the unsuccessfully aligned sequence without reference to its actual length. Successful alignments are shown in green. Failed alignments are shown in red. Prophage-related sequences are shown in blue. The *att* sites of each prophage are underscored. B and C were adapted from [129], modified.

Due to this sequence within the excision site of TMW 1.1290 P1 and the absence of host lysis after reinfection with WT phages, the curing of *L. sakei* TMW 1.1290 was deemed

unsuccessful. The successfully cured *L. curvatus* TMW 1.591 isolate 6 was renamed to *L. curvatus* TMW 1.2406 and was further analysed.

4.2.2 Calcium Dependency of TMW 1.591 P1 Infection

Some phages require the presence of multivalent ions like Ca^{2+}, Mg^{2+}, or Zn^{2+} for effective infection of their host. Thus, 6.8 mM $CaCl_2$ was supplemented in previous reinfection experiments (Figure 20). The minimal amount or type of ions that enable reinfection of *L. curvatus* TMW 1.2406 with TMW 1.591 P1 phages were still unknown and, thus, had to be tested. For this, three types of divalent cations (provided by $CaCl_2$, $MgCl_2$, or $ZnCl_2$) were added in concentrations ranging from 0.5-10 mM, and growth after phage supplementation was monitored (Figure 22A-C). While 5-10 mM $CaCl_2$ enabled effective lysis of *L. curvatus* TMW 1.2406 upon contact with TMW 1.591 P1 phages (Figure 22A), no cell lysis was observed when $MgCl_2$ (Figure 22B) or $ZnCl_2$ (Figure 22C) were added. Adding all three salts at 5 mM each (Figure 22C) suppressed lytic phage propagation. The experiment was repeated with several different $CaCl_2$ concentrations to receive a better resolution of the required minimal amount of this salt (Figure 23). A decrease in OD_{600} 8-10 hours after phage addition was observed from a minimum concentration of 1.92 mM Ca^{2+}. Higher Ca^{2+} concentrations led to an earlier observable host lysis.

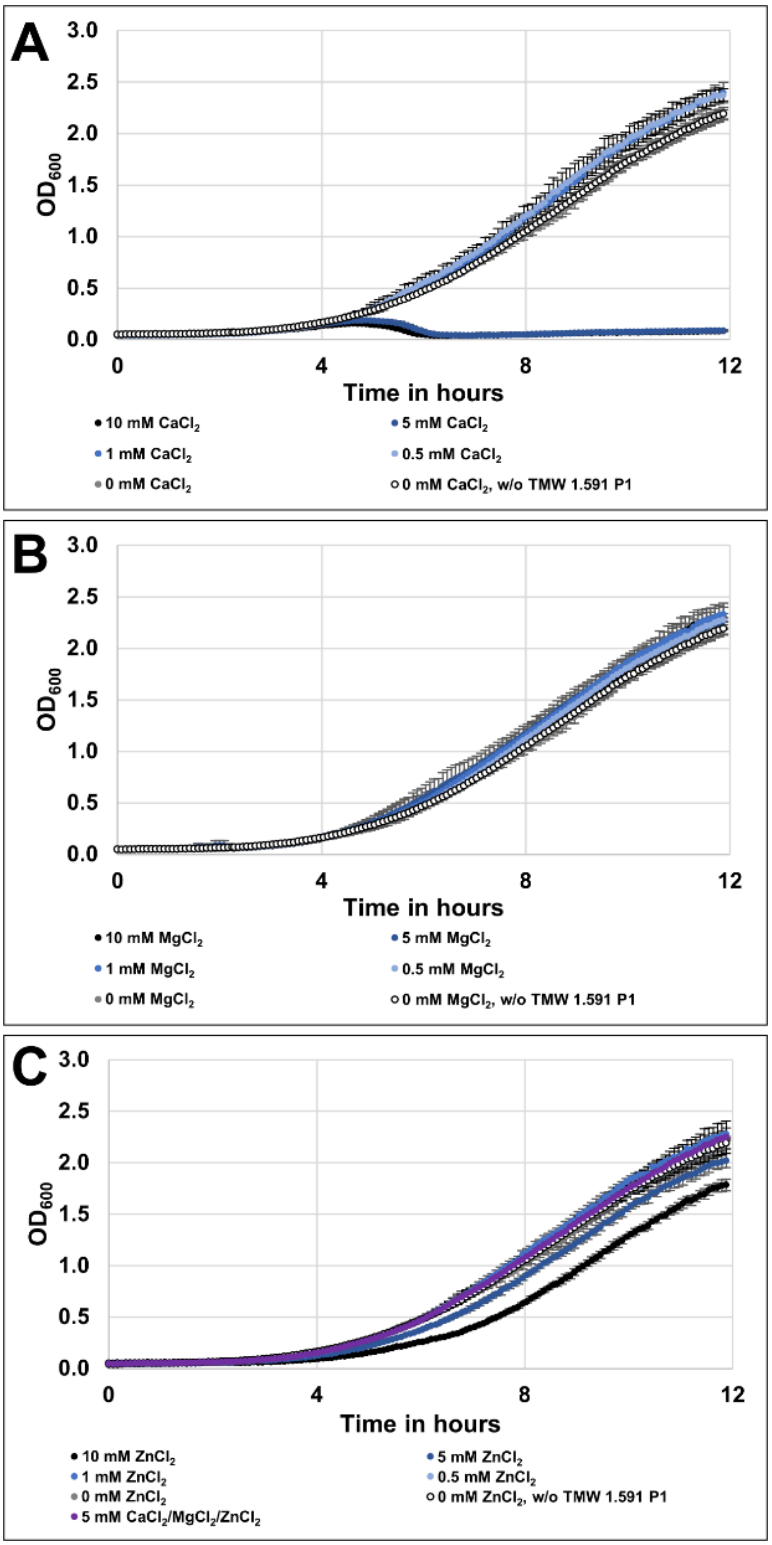

Figure 22. Effect of divalent cations on phage TMW 1.591 P1 infection. The growth of *L. curvatus* TMW 1.2406 in mMRS medium supplemented with 0.5-10 mM (A) $CaCl_2$, (B) $MgCl_2$, or (C) $ZnCl_2$ after the addition of phages (1:2000 dilution of sterile-filtered TMW 1.591 post-induction lysate) is displayed. Samples without the addition of divalent ions or phages served as negative controls. Lysis indicates a successful phage infection. Adapted from [129], modified.

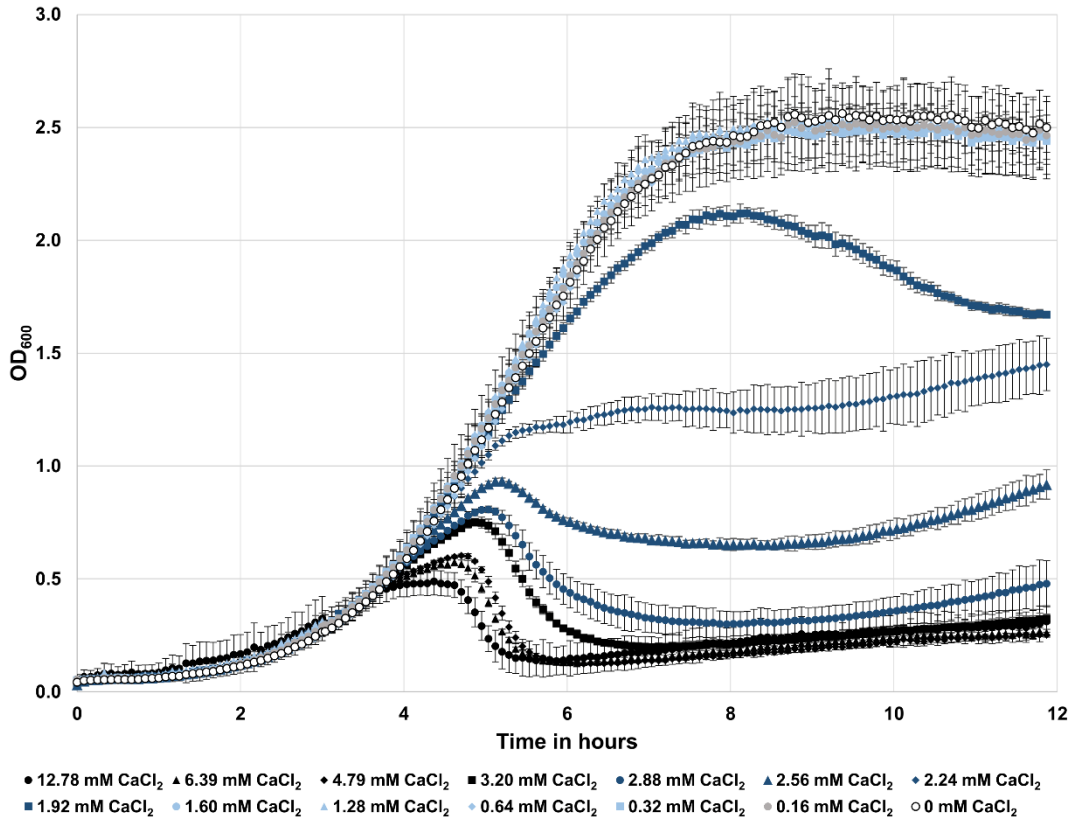

Figure 23. Effect of $CaCl_2$ on phage TMW 1.591 P1 infection. The growth of *L. curvatus* TMW 1.2406 in mMRS medium containing 0.16-12.78 mM $CaCl_2$ after phage supplementation (1:2000 dilution of sterile-filtered TMW 1.591 post-induction lysate) is displayed. A rapid lysis indicates an effective infection.

4.2.3 MOI Dependency of TMW 1.591 P1 Infection

Effective lysis of a bacterial culture can rely on the number of present phages. Therefore, *L. curvatus* TMW 1.2406 was exposed to different dilutions of TMW 1.591 P1 phage-containing post-induction lysate of *L. curvatus* TMW 1.591, and its growth was monitored. Notably, no assay for phage quantification was available at this experimental stage. Therefore, the MOI is represented by the amount of added lysate.

While exposure to 1:20-diluted lysate (final dilution in sample) led to the earliest observable lysis (app. 3 hours after lysate addition), the most significant, though later (4-5 hours after lysate addition) decrease in OD_{600} was observed for samples with 1:2000-diluted lysate (Figure 24). Lysates diluted more than $1:(2 \times 10^4)$ caused no observable lysis. Cells in samples with 1:20-diluted and 1:2000-diluted lysate restarted growing after the minimal OD_{600} was reached. Cells in samples with 1:200-diluted lysate recovered growth slower than in samples with 1:2000-diluted lysate.

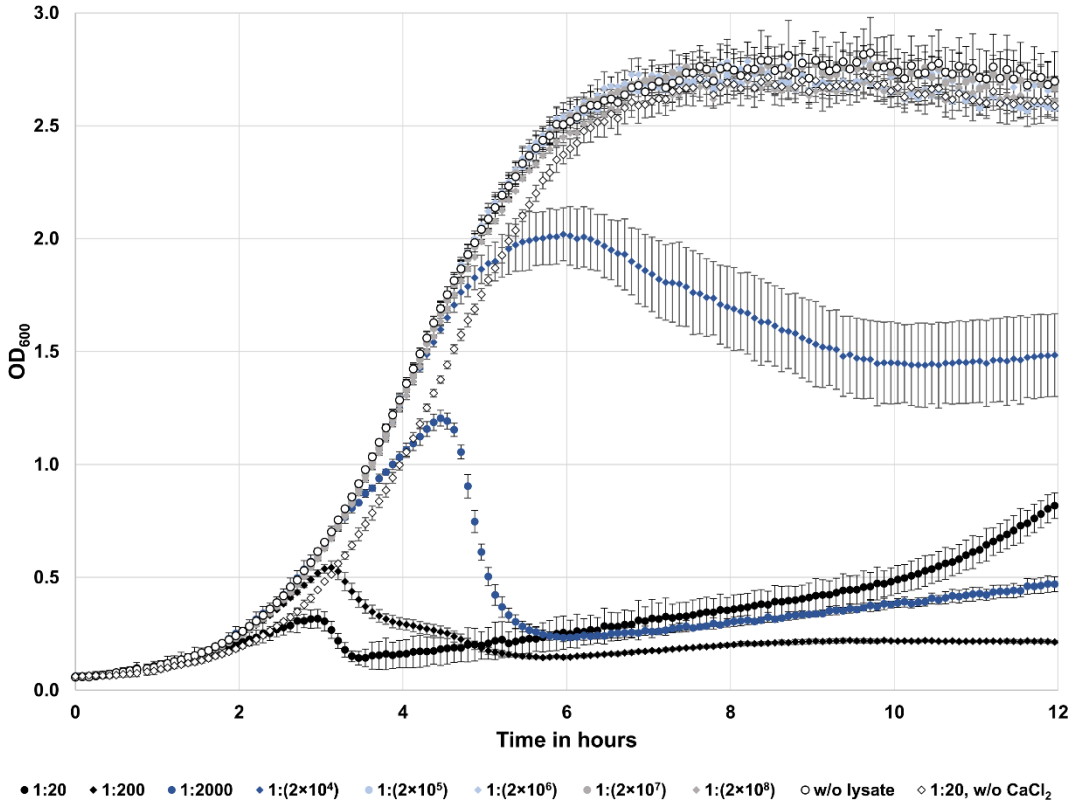

Figure 24. Effect of lysate dilution on phage TMW 1.591 P1 infection. The growth of *L. curvatus* TMW 1.2406 after administration of different (final) dilutions of phage-containing sterile-filtered *L. curvatus* TMW 1.591 post-induction lysate is displayed. Samples with demineralised water instead of phage lysate and samples with 1:20 diluted lysate without $CaCl_2$ supplementation served as negative controls (empty data points). A rapid lysis indicates an effective infection.

4.2.4 Phage Resistance of *L. sakei* and *L. curvatus*

L. sakei and *L. curvatus* are prophage-rich species (Chapter 4.1.3), suggesting susceptibility to phage attacks. Moreover, the cured strain *L. curvatus* TMW 1.2406 was growth-impaired by TMW 1.591 P1 WT phages if Ca^{2+} was sufficiently present but not by other *Latilactobacillus* phages (Chapter 4.2.2). Latter speaks for a narrow host range of the tested phages. Further experiments were necessary to test if temperate *Latilactobacillus* phages will likely impact the growth of multiple *L. sakei* and *L. curvatus* strains.

Thus, 24 *L. sakei* strains (Figure 25) and 41 *L. curvatus* strains (Figure 26) were exposed to a sterile-filtered mixture of phage-containing lysates harvested from 12 lysogenic strains (Chapter 3.16.3), and their growth was monitored. Resistance of a strain was evidenced by unimpeded growth. Of the 55 tested strains, only *L. curvatus* TMW 1.2406, the cured strain derivative of *L. curvatus* TMW 1.591 and positive control, lysed after phage administration

(Figure 26). Phage addition did not significantly impede the growth of most other strains. Yet, *L. sakei* TMW 1.1189 = DSM 20019^T grew slightly slower when the lysate was added. Many strains grew marginally faster upon lysate addition, most evident in *L. curvatus* TMW 1.591.

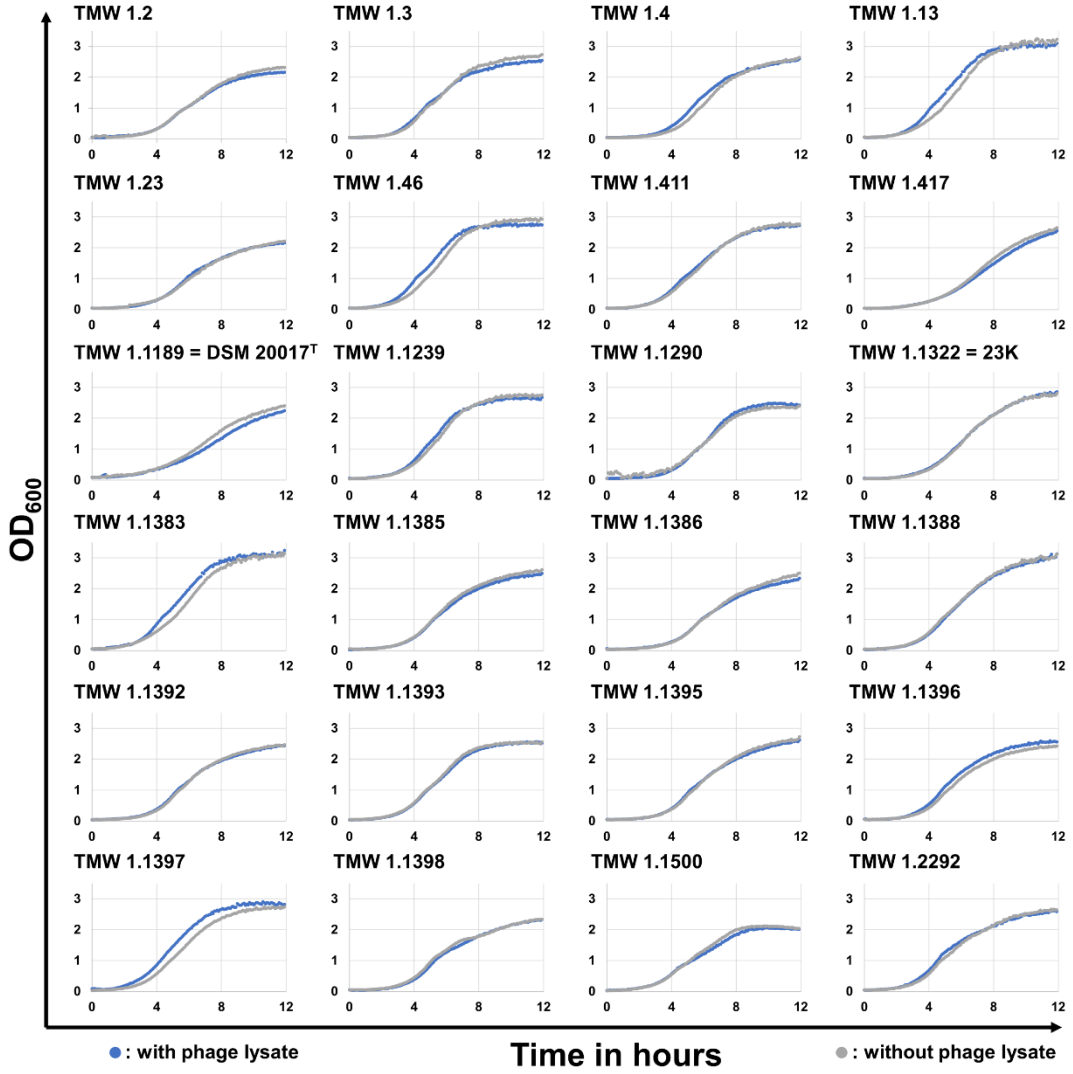

Figure 25. Phage resistance of *L. sakei* strains. The growth of *L. sakei* strains after *Latilactobacillus* phage administration is displayed. The administered combi-strain lysate (blue data points) contained lysates from six lysogenic *L. sakei* strains (TMW 1.23, TMW 1.46, TMW 1.1290, TMW 1.1386, TMW 1.1393, TMW 1.1398) and six lysogenic *L. curvatus* strains (TMW 1.591, TMW 1.706, TMW 1.1365, TMW 1.1381, TMW 1.1447, TMW 1.2272). Demineralised water (grey data points) instead of phage-containing lysates served as negative controls. Lysis or impeded strain growth after phage administration indicates susceptibility to at least one phage.

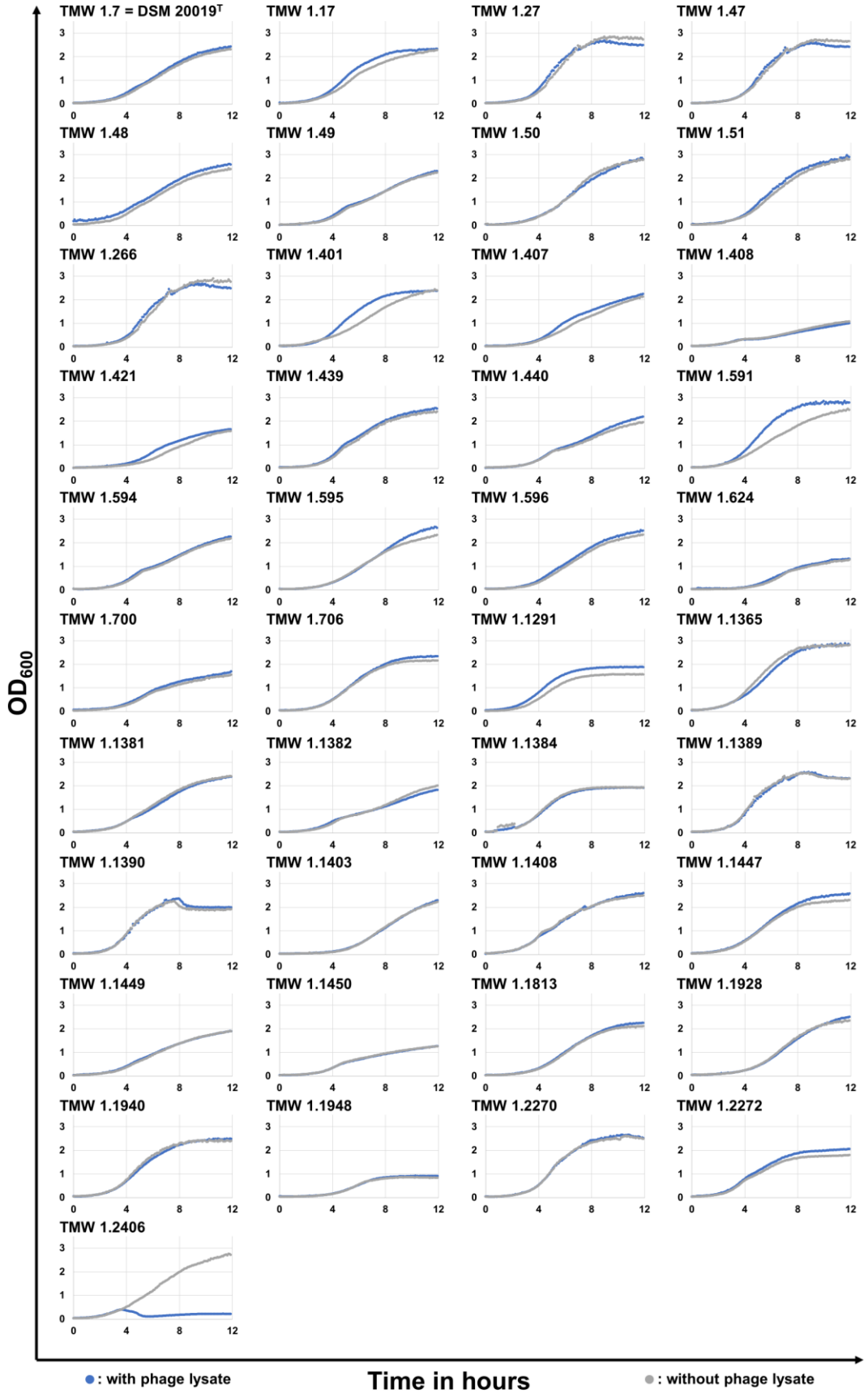

Figure 26. Phage resistance of *L. curvatus* strains. The growth of *L. curvatus* strains after *Latilactobacillus* phage administration is displayed. The administered combi-strain lysate (blue data points) contained lysates from six lysogenic *L. sakei* strains (TMW 1.23, TMW 1.46,

TMW 1.1290, TMW 1.1386, TMW 1.1393, TMW 1.1398) and six lysogenic *L. curvatus* strains (TMW 1.591, TMW 1.706, TMW 1.1365, TMW 1.1381, TMW 1.1447, TMW 1.2272). Demineralised water (grey data points) instead of phage-containing lysates served as negative controls. Lysis or impeded strain growth after phage administration indicates susceptibility to at least one phage.

4.2.5 The Release of Phages in Salami

The intact prophage of *L. curvatus* TMW 1.591 granted its host superinfection immunity against WT phages, preventing cell lysis upon infection. Nonetheless, most intact *Latilactobacillus* (pro)phages lysed their host effectively upon induction or during infection (TMW 1.591 P1 infecting *L. curvatus* TMW 1.2406). In summary, whether an intact prophage is a net positive or negative for its host during raw sausage fermentation is still unknown.

To answer this, salamis were fermented in a close-to-industry setting with the previously characterised strain model consisting of the lysogenic strain *L. curvatus* TMW 1.591 and its prophage-cured derivative *L. curvatus* TMW 1.2406. The cured strain served as the negative control during fermentation to compensate for strain-attributable influences and as the indicator for WT-released TMW 1.591 P1 phages, thus prophage induction. It was analysed if either strain led to faster meat acidification or was more competitive against the autochthonous meat microbiota. The fermentation and microbial analysis within the first week were carried out by a company well-versed in raw sausage production (Meat Cracks GmbH). Of the three produced sausage types, one was fermented with *L. curvatus* TMW 1.591, one with *L. curvatus* TMW 1.2406, and one with a 1:1 strain mixture (exact total inoculated cell count as in the first two types). All sausages contained *S. carnosus* ssp. *carnosus* provided by the production company (Meat Cracks GmbH). The fermentation was stopped after 16 days once the salamis were reduced by 30% in weight (Figure 27A), and salamis were stored at 4°C until later analysis. Notably, slow acidification of 0.1-0.2 (pH decrease) was characteristic for all salamis within the first two fermentation days (Figure 27B). Thirty-four days after the start of the fermentation, the LAB species occurrence (Figure 27C) was analysed for two raw sausages per batch, and TMW 1.591 P1 phages were quantified (Table 6). The added starter species, *L. curvatus* and *S. carnosus,* were isolated from all sausages, yet *L. sakei* and *Lc. paracasei* were also ubiquitous. The occurrence of *L. curvatus* differed slightly between the settings. While the lowest occurrence was found in TMW-1.591-fermented sausages, *L. curvatus* was most frequently isolated in TMW-1.2406-fermented sausages. The total cell counts (Figure 28A) and staphylococcal cell counts (Figure 28B) did not differ significantly between settings. Generally,

cell counts increased during the first seven fermentation days. The LAB cell counts after seven days (Figure 28C) were lowest in salamis fermented with the 1:1 strain mixture and highest in salamis fermented only with TMW 1.591. Overall, LAB cell counts varied only marginally. LAB cell counts of single-strain-fermented salamis remained stable between seven and 34 days but increased slightly in salamis fermented with the 1:1 strain mixture.

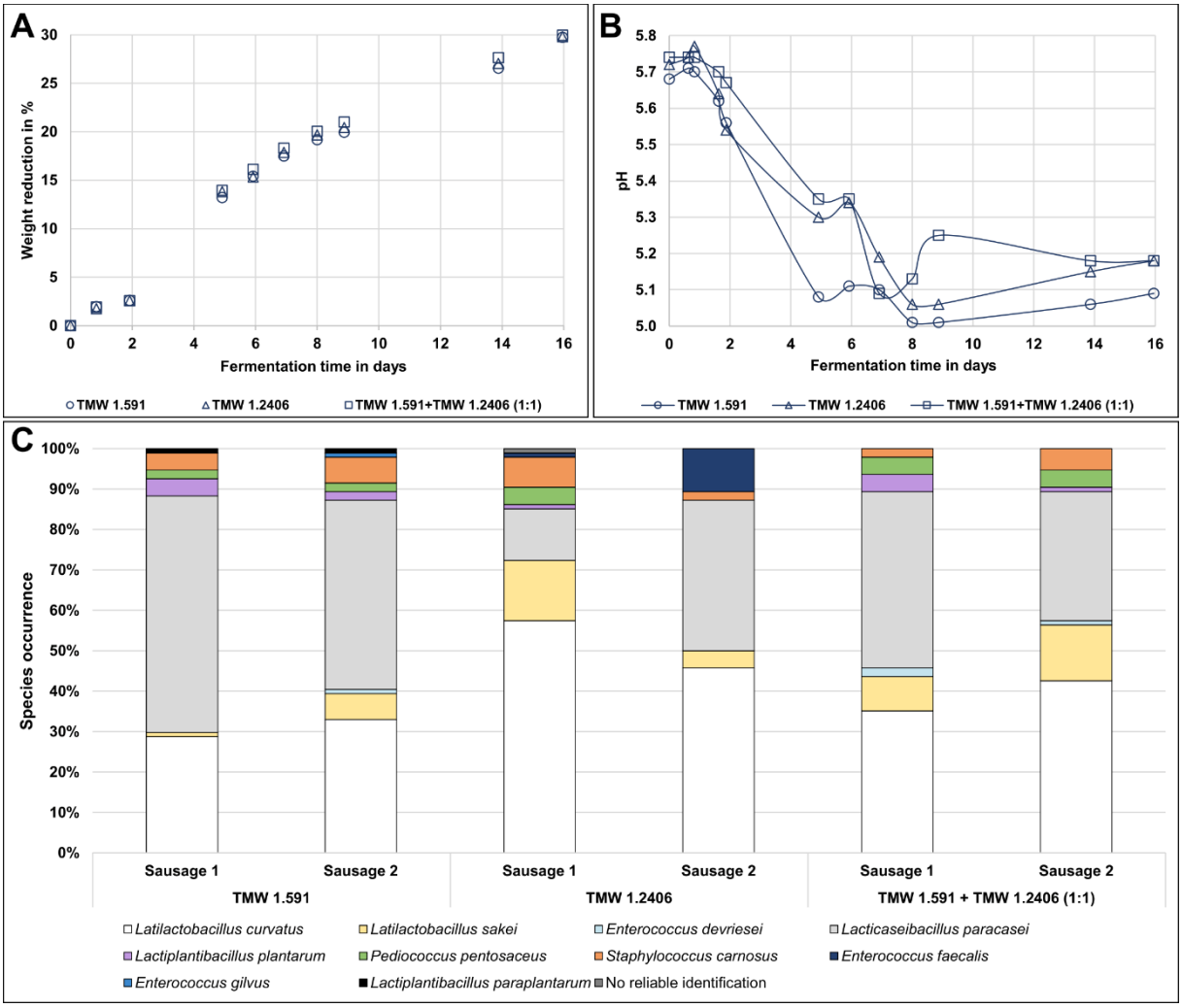

Figure 27. Salami fermentation data. The (A) weight reduction and (B) acidification of salamis during the fermentation are displayed. Moreover, the (C) species occurrence after fermentation in salamis fermented with TMW 1.591 (circular data points), TMW 1.2406 (triangular data points), and a 1:1 strain mixture of both strains (rectangular data points) is shown. The species occurrence was analysed 34 days after fermentation start via MALDI-TOF MS and is displayed as 100%-normalised columns. The species occurrence is based on mMRS(A)-cultured isolates and is, therefore, biased in favour of LAB. Adapted from [129], modified.

The phages in salamis that can reinfect *L. curvatus* TMW 1.2406 were quantified (Table 6). In salamis fermented exclusively with TMW 1.2406, no phages were detected above the

1×10^4 PFU/g detection limit. WT-fermented salamis contained $1.1 \pm 0.1 \times 10^7$ PFU/g (1:1 strain mixture; mean ± SD of both tested salamis) and $4.2 \pm 0.7 \times 10^7$ PFU/g (single-strain-fermented) TMW 1.591 P1 phages. Notably, the phage counts between both tested sausages within an experimental setting were consistent.

Table 6. TMW 1.591 P1 phage counts in TMW-1.591-fermented salamis. Plaques within three spots were counted for determination. Two salamis of each setting were analysed.

***L. curvatus* strains used for fermentation**	**Tested salami**	**Phage counts per g salami**
TMW 1.591	Salami 1	$4.2 \pm 0.7 \times 10^7$
	Salami 2	$4.3 \pm 0.7 \times 10^7$
TMW 1.591 + TMW 1.2406 (1:1 strain mixture)	Salami 1	$1.1 \pm 0.1 \times 10^7$
	Salami 2	$1.2 \pm 0.1 \times 10^7$

The prophage distribution of MALDI-TOF-MS-identified *L. curvatus* isolates in strain-mixture-fermented salamis was analysed (Figure 45A-C; Appendix; Chapter 8.8). This was done to determine whether the prophage was influencing the fitness of its host during fermentation. Each isolate was tested using two primer pairs that verify whether TMW 1.591 P1 was present (1.591_ INT_FWD/1.591_ INT_REV; 112 bp amplicon if present; Table 4) or excised (1.591_PC_INT-site_FWD/1.591_PC_LYS-site_REV; 2.2 kbp amplicon if excised; Table 4). In salamis fermented exclusively with TMW 1.591, 57 of 58 tested *L. curvatus* isolates were prophage-positive and excision-negative, representing the WT starter strain. All 97 tested isolates of salamis fermented with TMW 1.2406 were excision-positive. Nonetheless, 11 isolates featured an amplicon that indicated the presence of TMW 1.591 P1. Thirty-nine of 73 tested isolates from salamis fermented with the 1:1 strain mixture featured the WT amplicon pattern (prophage-positive and excision-negative). Twenty-six were prophage-negative and excision-positive, indicating TMW 1.2406. Fourteen excision-positive isolates were also potentially prophage-positive. If special-case isolates (excision-positive and prophage-positive) were neglected, 53% (39 of 73) of tested isolates in 1:1-strain-mixture-fermented salamis would possess the WT.

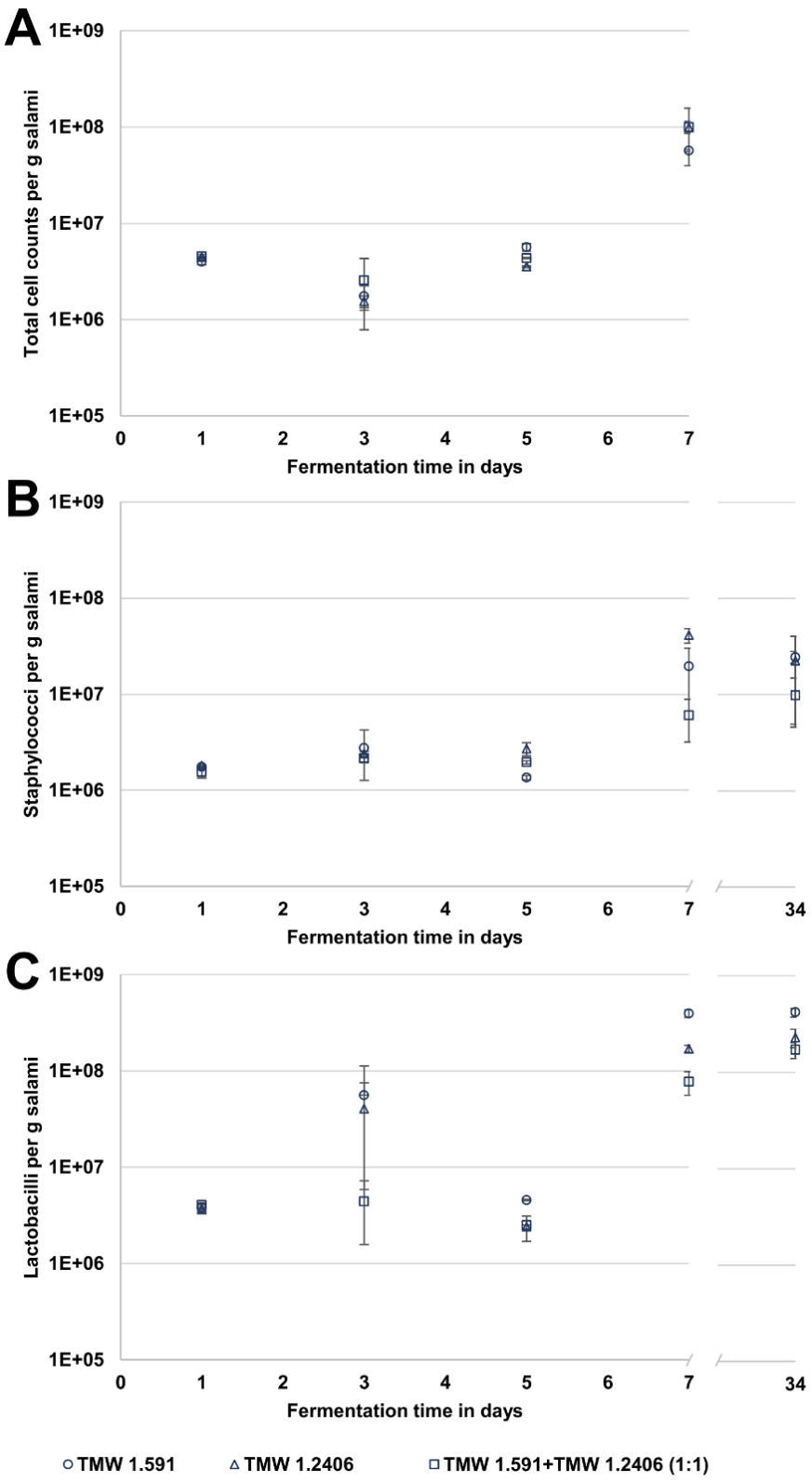

Figure 28. Cell counts during salami fermentation. The (A) total cell counts (PC-agar), (B) staphylococcal cell counts, and (C) lactobacilli cell counts per g salami fermented with TMW 1.591 (circular data points), TMW 1.2406 (triangular data points), or a 1:1 strain mixture of both strains (rectangular data points) are displayed. Cell counts (means ± SD) were analysed in duplicate (days one to seven) or quadruplicate (day 34). Adapted from [129], modified.

A new primer set was designed (TMW_1.591_P1_INT_FWD_NEW/ TMW_1.591_P1_INT_REV_NEW) that binds within the phage integrase gene but features a longer amplicon (983 bp instead of 112bp). This was done to separate the amplicon from the primer cloud during gel electrophoresis. The excision-positive prophage-positive isolates and the prophage-negative isolate E1 S2I30 of the TMW-1.591-single-strain-fermented salami were analysed with this primer set (Figure 45D; Appendix; Chapter 8.8). This verified the absence of TMW 1.591 P1 in isolate E1 S2I30 and its presence in six of 11 isolates originating from TMW-1.2406-single-strain-fermented salamis and eight of 14 isolates from 1:1-strain-mixture-fermented salamis. The data is summarised in Table 7.

Table 7. Summary of TMW-1.591-P1-specific colony PCR results. Listed are *L. curvatus* isolate counts from salamis fermented with TMW 1.591 and TMW 1.2406 (single-strain-fermented) and a 1:1 strain mixture of both strains that were tested prophage-positive/excision-negative indicating TMW 1.591, prophage-negative/excision-positive indicating TMW 1.2406, and prophage-positive/excision-positive.

***L. curvatus* strains used for fermentation**	**Tested isolates**	**prophage-positive/excision-negative (TMW 1.591)**	**prophage-negative/excision-positive (TMW 1.2406)**	**prophage-positive/excision-positive**
TMW 1.591	58	57	1	0
TMW 1.2406	97	0	91	6
TMW 1.591 + TMW 1.2406 (1:1 strain mixture)	73	39	26	8

The excision-positive prophage-positive isolate E2 S1I6 of TMW 1.2406-fermented salamis was sequenced to assess its identity. The assembled genome of the isolate was then compared with the genome of *L. curvatus* TMW 1.591 via JSpeciesWS. The genome of the isolate shared 99.96% ANIb over 99.10% of aligned nucleotides with *L. curvatus* TMW 1.591. In return, *L. curvatus* TMW 1.591 shared 99.99% ANIb over 97.66% aligned nucleotides compared to the new isolate. BLAST-analysis of the TMW 1.591 P1 phage integrase gene onto the genome of the isolate returned no hits. The chromosomal integration site of TMW 1.591 P1 was manually checked for the presence of a prophage in the genome of the isolate, but no prophage was found. While conclusive evidence as to why the isolate was tested prophage-positive is still missing, the identity of the isolate as TMW 1.2406 can be assumed.

In summary, the added starter strains could not suppress the autochthonous microbiota, and meat acidification was slow in all sausages, independently of TMW 1.591 P1 presence. Although TMW 1.591 P1 did not significantly influence host fitness or competitiveness during fermentation, its induction was proven by large quantities of virions detectable in WT-fermented salamis. Despite the availability of phage-susceptible TMW 1.2406 cells for lytic propagation, LAB cell counts, meat acidification, and *L. curvatus* species occurrence were not significantly different in strain-mixture-fermented salamis.

4.2.6 Phage Release During the First Days of Meat Fermentation

The salami fermentations proved the induction of TMW 1.591 P1 during fermentation. Thus, more simplified meat model fermentations were conducted to verify this data and elucidate when phage progeny can first be detected. Fast acidification is a prerequisite for effective spoilage bacteria suppression. Because meat acidification was slow during the previous fermentation, the LAB starter inoculum was increased to obtain an acidification profile that reflects the industry standard (pH < 5.2 within the first two days) more closely. Additionally, TMW 1.2406 growth was seemingly unaffected by the WT-released phages in salamis fermented with a 1:1 strain mixture of TMW 1.591 and TMW 1.2406. To verify this, a phage-contaminated substrate was simulated by spiking meat batters with TMW 1.591 P1 phages at an MOI of 0.1 before strain addition. Meat batters without spiked phages served as negative controls.

A higher starter inoculation (LAB: 1×10^8 CFU/g instead of 5×10^6 CFU/g; *Staphylococcus*: 1×10^7 CFU/g instead of 5×10^6 CFU/g) led to higher retrieved cell counts (Figure 29A-B). Through the faster acidification of the meat batter (Figure 29C), the desired pH of 5.2 was reached within the first two days of fermentation. LAB cell counts in all samples increased during day one and decreased after day two when the acidification process was completed and nutrients were mostly depleted (Figure 29B). After an initial increase in staphylococcal cell counts (Figure 29A) during day one, the fast acidification of the added LAB starters subsequently suppressed the added *Staphylococcus* starter. On day five, *L. curvatus* was identified in all meat batters as the most abundant species (Figure 29D).

Prophage-mediated differences in cell counts or meat acidification speed could not be observed, consistent with previous experimental data (Chapter 4.2.5). Spiking the substrate with phage TMW 1.591 P1 also did not significantly affect the acidification speed or growth of the cured strain during fermentation (Figure 29B). Yet, shortly after starter strain addition, phages were detected in WT-fermented meat batter without previous phage spiking (Figure 30;

1.0±0.2 × 10^4 PFU/g). No autochthonous TMW-1.2406-specific phages were detected in TMW-1.2406-fermented meat batters without prior phage spiking. Phage counts decreased in settings with spiked phages within the first day of fermentation. They remained constant in TMW 1.2406-fermented meat batters after day one and increased in WT-fermented meat batters between day one and two.

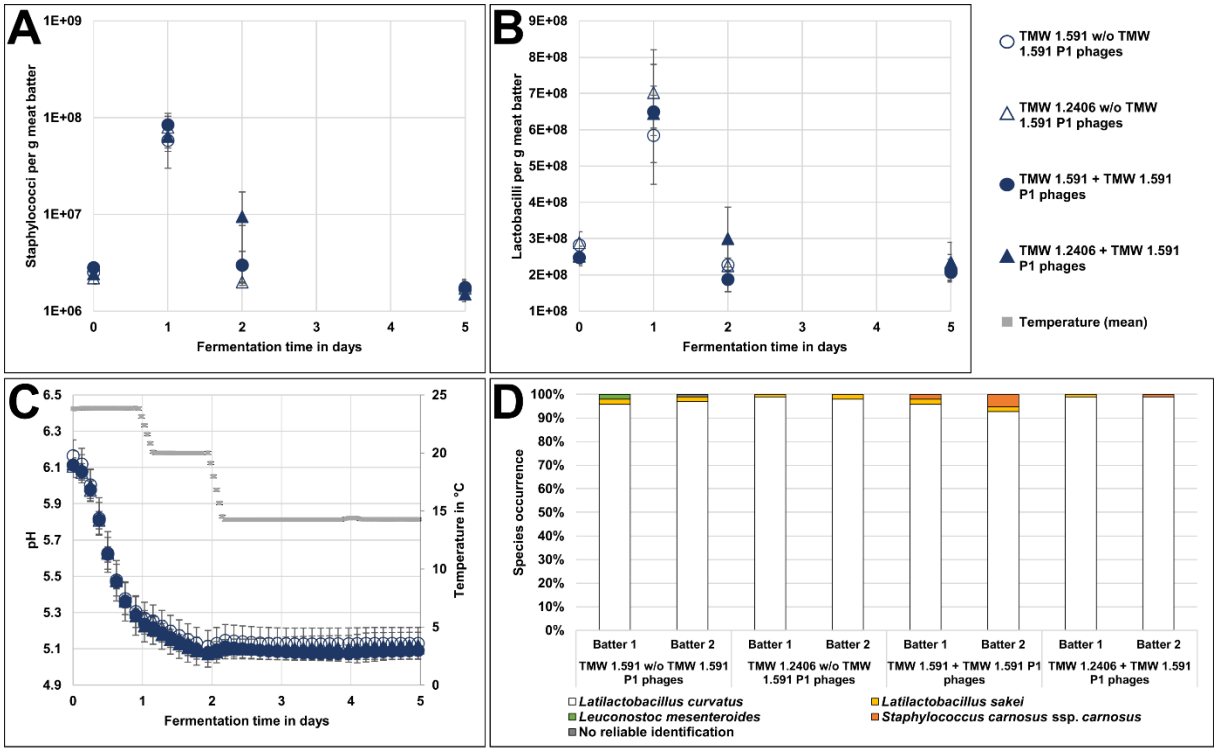

Figure 29. Meat model fermentation data. Displayed are the (A) staphylococcal and (B) lactobacilli cell counts, the (C) acidification and temperature profile, and the (D) species occurrence of meat batters fermented with TMW 1.591 (circular data points) and TMW 1.2406 (triangular data points). Filled data points indicate phage TMW 1.591 P1 spiking at an MOI of 0.1. Meat batters without spiked phages (empty data points) served as negative controls. The staphylococcal and lactobacilli cell counts (means ± SD of quadruplicates) were recorded on days zero, one, two and five. The acidification (means ± SD of duplicates) and temperature (means ± SD of all eight samples) were recorded continuously during the five days of fermentation (pH was recorded once per hour; every third measurement is displayed to improve visibility). The species occurrence on day five is displayed as 100%-normalised columns and was analysed via MALDI-TOF MS. The species occurrence is based on mMRS(A)-cultured isolates and is, therefore, biased in favour of LAB. Adapted from [129], modified.

The highest phage counts were detected on day two in WT-fermented meat batters with (8.0±1.6 × 10^7 PFU/g) and without prior phage addition (5.2±1.8 × 10^7 PFU/g). Thus, phage

counts were similar between the two settings on day two, independently of phage spiking. After day two, phage counts decreased in WT-fermented meat batters and remained at a lower but constant level in TMW 1.2406-fermented meat batters with prior phage spiking.

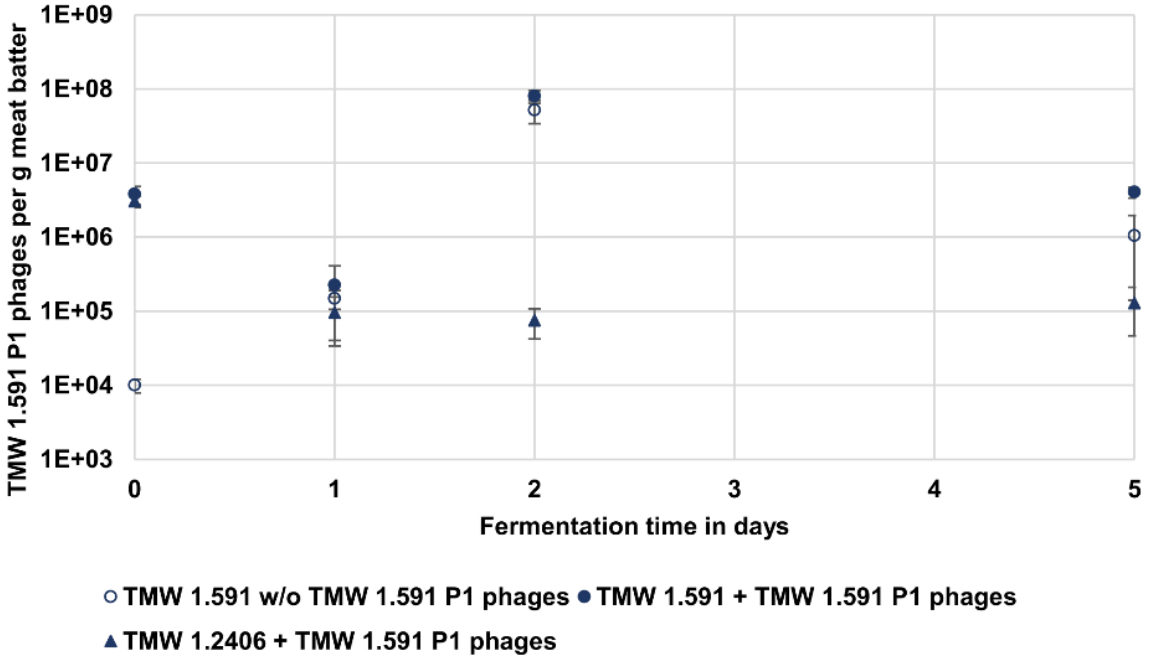

Figure 30. TMW 1.591 P1 phage counts during meat model fermentation. Displayed are the phage counts in meat batters with prior TMW 1.591 P1 phage addition at MOI = 0.1 (filled data points) and without phage addition (empty data points) during the five days of fermentation. Phage counts (means ± SD of sextets) in fermented meat batters with TMW 1.591 are indicated by round data points. Triangular data points indicate phage counts in fermented meat batters with TMW 1.2406. No phages above the reliable ~1×10^4 PFU/g detection limit could be detected in TMW 1.2406 fermented salami without prior phage supplementation. Adapted from [129], modified.

In summary, the experimental data retrieved from salami fermentation was verified. TMW 1.591 P1 was active during the meat model fermentation, releasing new phage progeny. Yet, phage-mediated lysis caused no observable effect on fermentation (e.g., reduced cell counts or acidification speed). Analogically, spiking with TMW 1.591 P1 phages to simulate phage-contaminated meat also had no significant influence on cell counts or acidification speed of the cured strain derivative.

4.2.7 Effect of Cultivation Conditions on TMW 1.591 P1 Induction

L. curvatus phage TMW 1.591 P1 phage progeny is continuously released during the first few days of meat fermentation when the metabolic activity of its host is the highest. It is unknown what caused these high levels of induction. Thus, a set of cultivation conditions that could appear during starter culture preparation or meat fermentation was applied to the *L. curvatus* TMW 1.591/TMW 1.2406 strain model as shock treatment and phage induction was analysed. The effects of temperature, an acidic environment, certain salts (NaCl and $NaNO_2$), and nutrient deficiency (total nutrient and carbon source) were examined. Phage-mediated lysis or high phage counts in the culture supernatant identified an inducing factor. Induction after treatment resulting in phage counts below the detection limit (1×10^3 PFU/mL), such as SPI, was treated as non-induced. While phage-mediated strain lysis after stress application was only observed for MitC-treated controls, a strongly acidic environment (pH 3.0; Figure 31A) and elevated temperatures (45-60°C; Figure 31B) led to increased phage counts (Table 8).

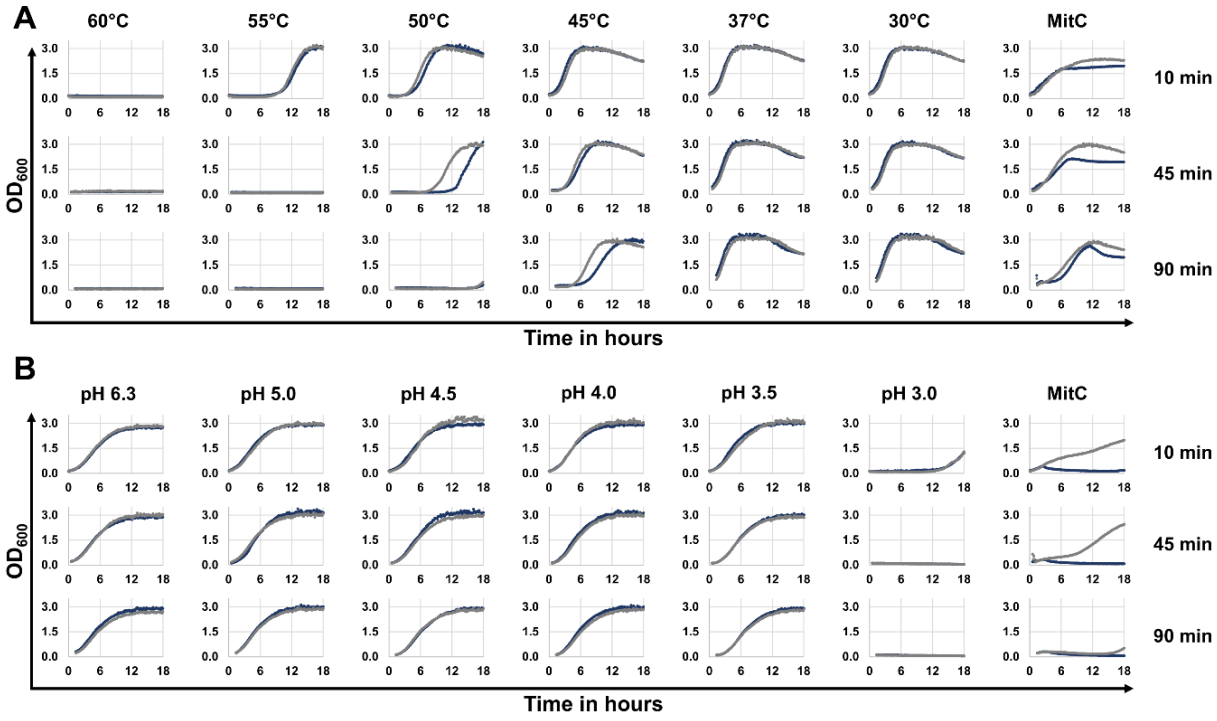

Figure 31. Influence of temperature and pH on TMW 1.591 P1 induction. The growth of *L. curvatus* TMW 1.591 (blue data points) and *L. curvatus* TMW 1.2406 (grey data points) after a 10-90 min (A) temperature and (B) acid shock is displayed. The temperature or pH is shown above the graphs, and the time of the shock treatment is shown on the right side. Lysis or impeded growth of the WT strain in relation to the cured strain indicates successful induction.

TMW 1.591 growth was more impeded than TMW 1.2406 when stressed at 45°C for 45-90 min and 50°C for 10-45 min. Excessively applied stress led to cell inactivation and no released phages. Starvation, colder temperatures (5°C and 20°C) and concentrations of NaCl ≤8% (w/v) or $NaNO_2$ ≤1000 ppm led to no phage release, thus, prophage induction (data not shown).

Table 8. TMW 1.591 P1 phage counts in temperature and pH induced samples. Phage counts of MitC-induced samples (positive control) are listed as a reference for successful prophage induction.

Experiment	Tested condition	Stress duration in minutes	PFU/mL
Temperature	10 µg/mL MitC	10	$2.04\pm0.60 \times 10^7$
		45	$9.03\pm5.36 \times 10^4$
		90	$1.38\pm0.97 \times 10^4$
	55 °C	10	$4.25\pm2.62 \times 10^3$
		45	$3.45\pm0.21 \times 10^4$
	50 °C	45	$2.39\pm0.82 \times 10^4$
		90	$1.54\pm0.77 \times 10^6$
	45 °C	90	$1.50\pm0.57 \times 10^3$
Acidic environment	10 µg/mL MitC	10	$3.37\pm0.43 \times 10^6$
		45	$2.41\pm0.43 \times 10^6$
		90	$1.89\pm0.55 \times 10^6$
	pH 3.0	10	$9.75\pm3.32 \times 10^4$
		45	$3.30\pm2.26 \times 10^3$

Notably, an inducing effect of carbon source deficiency (0% glucose in mMRS medium) was observed when *L. curvatus* TMW 1.591 (grown from OD_{600} = 0.1) was starved overnight. This led to $6.8\pm0.50 \times 10^4$ PFU/ml released phages without observable host lysis (Figure 46; Appendix; Chapter 8.9).

4.2.8 Effect of Species Interference on TMW 1.591 P1 Induction

To test whether the meat microbiota interferes with TMW 1.591 P1 induction, a set of meat-associated organisms was added to an induced and non-induced culture of *L. curvatus* TMW 1.591. Phage counts were recorded 24 hours after UV light treatment to determine induction differences. Additionally, cell growth was monitored after induction and the addition of cells (Figure 32). The set of tested microorganisms included *L. sakei* TMW 1.2, *Lp. plantarum* TMW 1.25, *Lc. paracasei* isolate 1, *P. pentosaceus* TMW 2.1974, *S. carnosus* ssp. *carnosus* TMW 2.212, *S. carnosus* ssp. *utilis* ME, and *S. xylosus* TMW 2.1521. Notably, differences in growth depending on the added species were expected due to mMRS, which favours LAB growth and impedes staphylococcal growth (Figure 32).

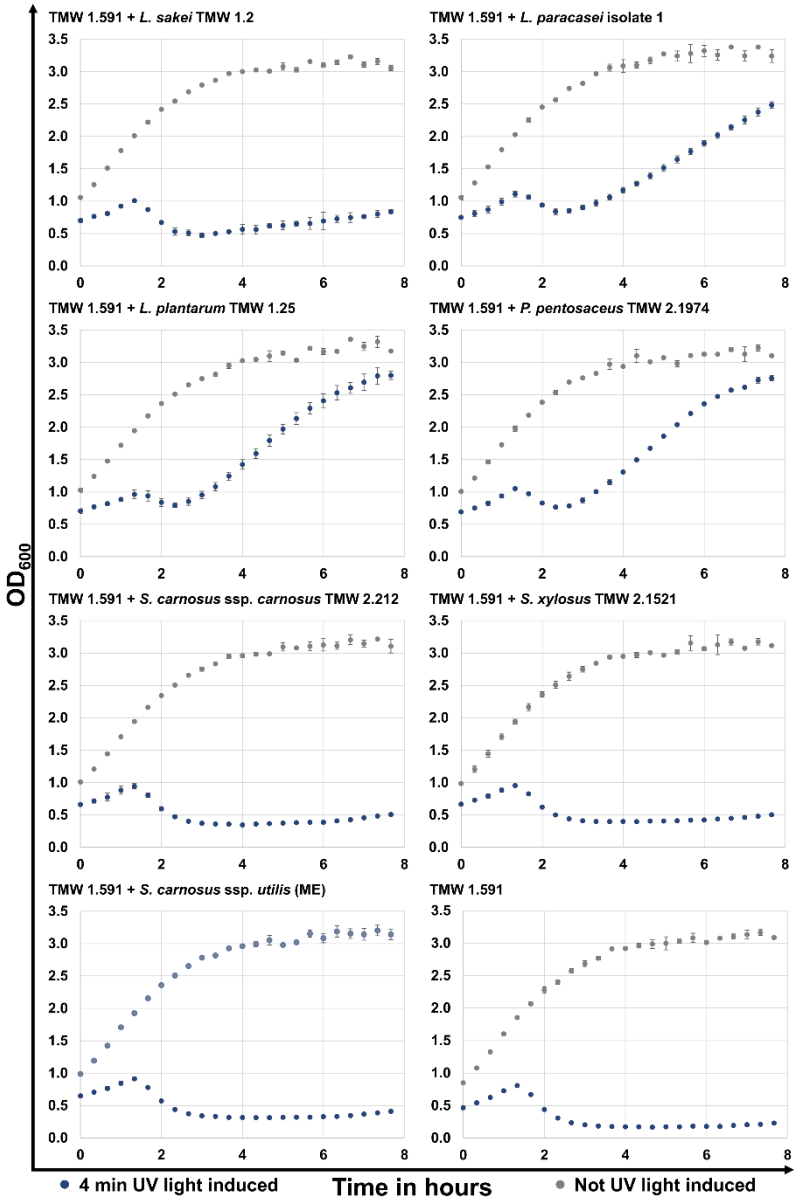

Figure 32. Species interference on TMW-1.591-P1-mediated lysis. The growth of *L. curvatus* TMW 1.591 after induction and supplementation with viable cells from different species is displayed. *L. curvatus* TMW 1.591 was 4-minute-UV-light-induced (blue data points) before adding four different genera of lactobacilli and three staphylococci associated with meat. Non-induced TMW 1.591 samples (grey data points) with respective supplemented foreign cells served as negative controls. Samples of induced and non-induced TMW 1.591 cells without foreign cell supplementation served as induction controls. Lysis indicates successful induction of TMW 1.591 P1.

The phage counts in induced (Figure 33A) and non-induced (Figure 33B) TMW 1.591 samples including beforementioned species were then compared to the phage counts in the induced control sample without added organisms. A 1.9±0.3 × 10^7 PFU/mL of TMW 1.591 P1 phages

were detected in the induced TMW 1.591 control sample without adding other species. *L. curvatus* TMW 1.591 presented a ~100-fold higher phage production (2.3±0.7 × 10^9 PFU/mL) when co-cultured with *L. sakei* TMW 1.2 and lower phage production when incubated with *Lc. paracasei* isolate 1, *Lp. plantarum* TMW 1.25 (phage counts for both samples were below the reliable ~1 × 10^3 PFU/mL detection limit), or *P. pentosaceus* TMW 1.1974 (2.4±0.2 × 10^5 PFU/mL). Similar phage counts compared to the induced control sample (without added species) were released in induced TMW 1.591 samples containing *Staphylococcus* cells (*S. carnosus* ssp. *carnosus* TMW 2.212: 5.0±0.4 × 10^6 PFU/mL; *S. carnosus* ssp. *utilis* ME: 6.5±0.6 × 10^6 PFU/mL; *S. xylosus* TMW 2.1521: 2.4±0.2 × 10^7 PFU/mL). The SPI was below the reliable detection limit in all non-induced *L. curvatus* TMW 1.591 samples.

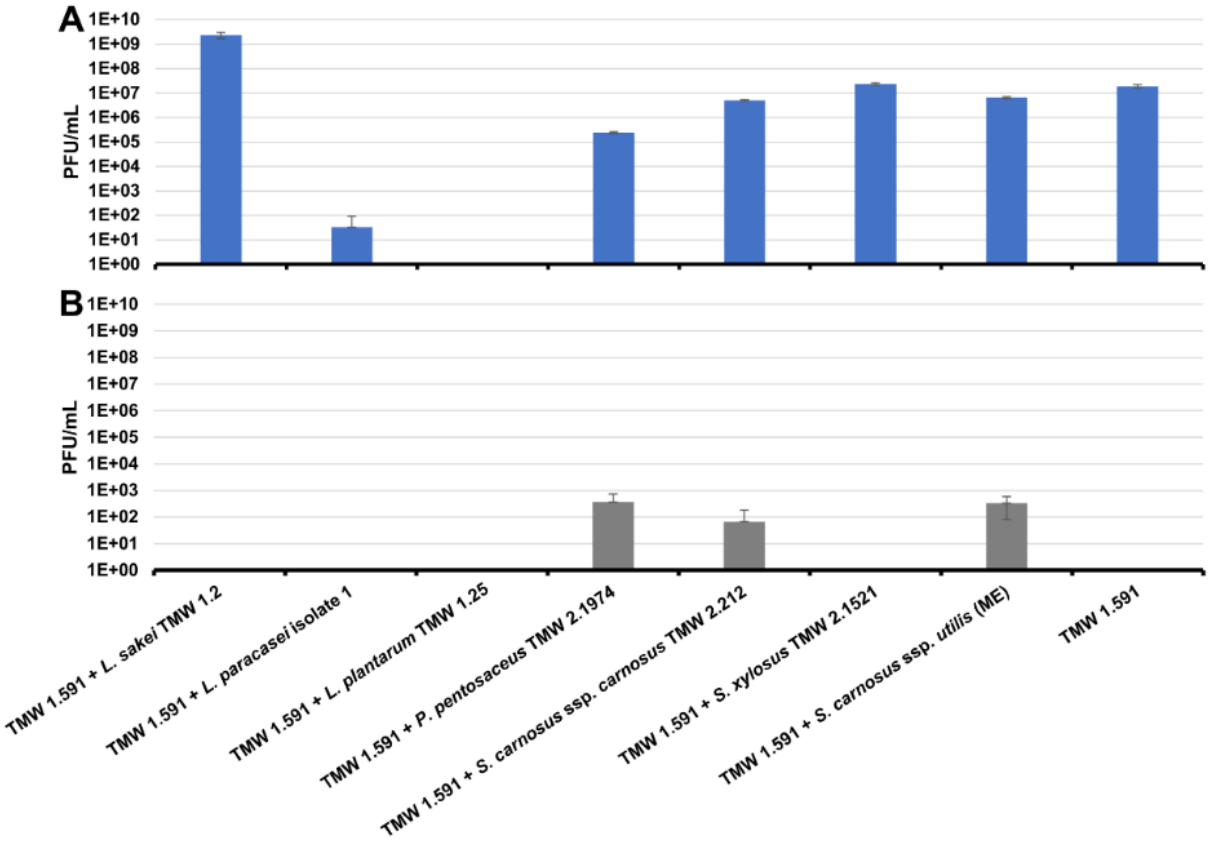

Figure 33. Species interference on TMW 1.591 P1 release. Displayed are the phage counts (means ± SD of triplicates) in (A) 4-minute-UV-light-induced *L. curvatus* TMW 1.591 and (B) non-induced *L. curvatus* TMW 1.591 samples after the addition of various species. Phage counts <1 × 10^3 PFU/mL were below the reliable detection limit. Higher/lower phage counts in samples in relation to the control (TMW 1.591 without other added species) indicate a positive/negative influence on TMW 1.591 P1 release.

The experiment was repeated once for *L. sakei* TMW 1.2 supplementation (growth not shown), and the phage-induction-boosting effect was reproduced. *L. curvatus* TMW 1.591 released 5.9±1.2 × 10^9 PFU/mL phages after induction and supplementation with *L. sakei* cells. In contrast, the induced sample without addition contained tenfold fewer phages (5.6±1.5 × 10^8 PFU/mL). Phage counts in non-induced samples were below the reliable detection limit.

In summary, this experiment demonstrates that the meat microbiota can alter the number of released phages upon induction depending on the present organisms. However, adding other species alone did not cause a strong induction of TMW 1.591 P1.

4.2.9 Phage Induction Maintenance During Cryopreservation

It was previously demonstrated [59] that *L. sakei* TMW 1.1398 maintains phage induction during cryopreservation and lyses after re-establishing optimal growth conditions. It was tested if *L. curvatus* TMW 1.591 behaves similarly and, thus, if phage induction maintenance during strain preservation represents a common phenomenon.

To analyse how long an induced cell status is preserved, *L. curvatus* TMW 1.591 was induced via UV light and bacterial glycerol stocks prepared directly after the treatment were stored for up to ten weeks at -80°C. After one day and once per week until five weeks, at seven weeks and ten weeks, the growth of preserved cells was monitored after restoring ideal growth conditions. Non-induced samples served as negative controls. After one day of growth, phages were harvested from induced samples and quantified. Notably, the growth of day zero samples was monitored directly after the UV light treatment without prior freezing. Prophage-mediated lysis (Figure 34A) leading to the release of phages (Figure 34B) was observed for all samples after two hours of growth. Day one cryopreserved cells released 450-fold fewer phages than cells of the non-frozen control on day zero. Phage counts of cryopreserved samples remained essentially constant across tested storage times. To analyse if the reduction in released phages was caused by lowered cell viability due to the preservation treatment, the viable cells in unfrozen (day zero) and frozen stocks (day one and weeks one to ten) of TMW 1.591, TMW 1.2406, and induced TMW 1.2406 were quantified (Figure 34C). This revealed that cryopreservation led to 40-60% fewer viable cells in all tested stocks compared to the respective unfrozen controls. While the induction treatment also decreased the number of viable cells (67% fewer viable cells in UV-light-treated TMW 1.2406 samples), the decline in viability due to the subsequent cryopreservation was similar to that of non-induced samples.

In summary, TMW 1.591 P1 induction was maintained during cryopreservation. After preservation, a 450-fold decrease in phage counts was observed, which might be explained by the cell-damaging effect of the preservation procedure itself, leading to ~50% fewer viable cells.

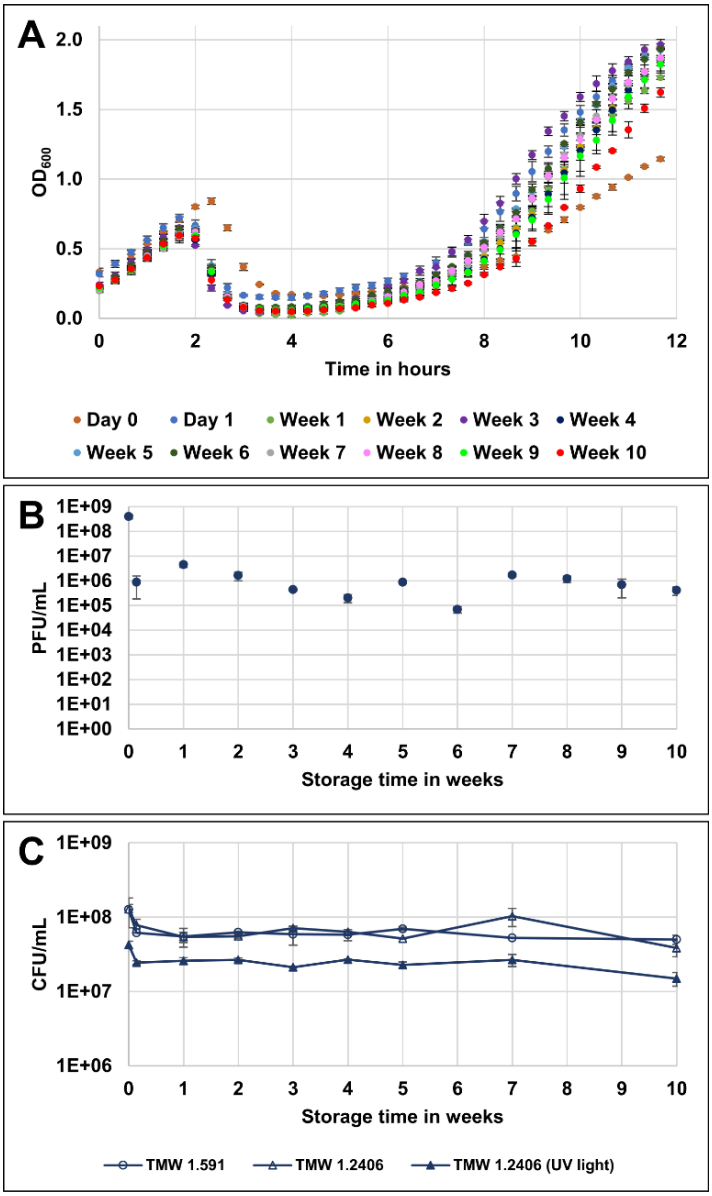

Figure 34. Maintenance of phage induction during cryopreservation. (A) Growth of UV-light-induced and cryopreserved *L. curvatus* TMW 1.591 after restoration of ideal growth conditions. Samples were stored at -80°C for up to ten weeks. The day zero sample was not cryopreserved but monitored directly after induction and served as the control. (B) Phage counts (means ± SD of sextets) in samples harvested 24 hours after restoration of ideal growth conditions. (C) Viable cells (means ± SD of duplicates) in cryopreserved bacterial glycerol stocks of TMW 1.591 (round empty data points), TMW 1.2406 (triangular empty data points), and UV-light-induced TMW 1.2406 (triangular filled data points) after storage at −80°C. Unfrozen day zero samples were plated directly after induction as controls. Adapted from [129], modified.

5 DISCUSSION

This chapter discusses the obtained results in the context of existing literature. This comprises prophage inducibility, phage morphology and prophage distribution in *L. sakei* and *L. curvatus*. Moreover, the chromosomal integration sites, genomic organisation and features of intact prophages are discussed, and phage induction- and infection-influencing factors are further analysed and explained. Lastly, the fate of TMW 1.591 P1 during raw meat fermentation and the phage induction maintenance during cryopreservation are debated.

5.1 Strain Dependency of *Latilactobacillus* Phage Induction

Screening for lytic strains with inducible lysis was an effective way of obtaining candidates that harbour intact prophages. Moreover, the induction experiments successfully elucidated if intact-predicted prophages lead to host lysis. The latter indicates the successful conversion of the lysogenic to the lytic life cycle of temperate phages. Genotoxic antibiotics like MitC and ciprofloxacin, or UV light, are commonly used to inflict DNA damage and achieve this conversion [77, 98, 100, 130]. In both approaches, transcription of *recA*, which is part of the SOS response, is enhanced. RecA binds the phage repressor, leading to its cleavage [80] and initiating phage induction [77, 78]. Although both treatments can lead to induction, they have different advantages. Induction via MitC might be easier for other laboratories to reproduce. However, the chemical is expensive and degrades rapidly under acidic conditions (pH<6), upon which it forms precipitates toxic to cells [131]. In contrast, induction reproduction using UV light may be more challenging, as different UV light sources can have different wavelength optima/spectra or intensities. Still, after an initial investment, it is cheaper, creates no toxic residues for cells and might be safer for the experimenter during handling.

Induction of φ-DJ1812 (harboured by *L. sakei* TMW 1.1398) using MitC ranging between 0.5-5.0 µg/mL at OD_{600} 0.3-0.4 was previously deemed unsuccessful, and UV light induction was most effective when applied for two and four minutes [59]. MitC is usually added in similar experimental settings, due to its acute toxicity, in amounts ranging between 0.1-2 µg/ml (e.g., for phage induction in *Lactococcus lactis* [89], *Streptococcus pyogenes* [132] and other lactobacilli [98, 133]). However, the strongest phage-mediated lysis responses in *Latilactobacillus* were observed at 5-20 µg/ml MitC, which is considerably higher. MitC must also be administered at a lower OD_{600} of 0.1 than UV light. A previous work inducing prophages in *Lactococcus lactis* [89] demonstrated the importance of the growth phase and inducer concentration on phage induction, which was also true for the screened *Latilactobacillus* strains.

A strong phage-mediated lysis after induction was not observed by all strains harbouring intact prophages. Yet, all strains with strong lytic behaviour contained intact predicted prophages. Some strains were closely related but differed in prophage content and, thus, inducibility. In other cases, prophages were nearly identical and only differed in their transposase content, yet caused distinctive host lysis responses. This suggests that host lysis is influenced equally by phage and host. In contrast, the number of intact prophages per strain seems to have a subordinate influence on lysis, indicated in different lysis intensities of strains within one species that harbour only one intact prophage. Also, strains with multiple intact prophages did not lyse faster or stronger/weaker than strains with only one intact prophage. However, successful sequencing of viral DNA from post-induction lysates verified induction of all intact prophages harboured by multi-lysogenic (and single-lysogenic) strains. Varying sequencing depths of prophage-related sequences indicate preferably induced prophages in a multi-lysogen.

Some phage genomes were marked as circular after assembly. Phage genome circularisation by attachment-site-specific recombination without prior induction commonly occurs after host infection [134] and during lytic development [135] but is highly amplified upon induction, e.g. via MitC [136]. However, the "circular" status of isolated viral DNA might be an artefact caused by the genome assembly process, as virions of all known tailed phages feature linear dsDNA chromosomes [137]. During phage packaging, the linear dsDNA chromosomes of tailed bacteriophages are bound and cut by the phage terminase subunits, then threaded through the narrow capsid portal [137]. Depending on the type of terminase involved and the DNA replication strategy, the DNA packaged into the phage capsid features one of multiple DNA terminus types [137]. Genomes with cohesive ends, genomes with terminal exact direct repeats, and circularly permuted genomes belong to the most common genome configurations after packaging [138] and are known to cause this artificial "circular" status [137].

5.2 *Latilactobacillus* Phage Morphology

Since 1967, so half a century after the first public mention of phages as "ultra-microscopic viruses" [23], the description of phage morphology was a significant step in early phage classification [139] due to the absence of modern bioinformatical and molecular methods. All LAB phages described to date belong to the *Caudoviricetes* class, and most of them feature the siphovirus morphotype, which is characterised by isomeric, icosahedral heads and long non-contractile tails [75, 140]. The isolated *Latilactobacillus* virions all featured these morphological traits. The high resolution of TEM, combined with the sample penetrating negative staining, allows the discrimination of empty/filled phage capsids and the detection of

phage fibre structures [141]. Besides fully assembled virions, the samples contained separated tails and (partially empty) capsids, which are precursors during siphovirus phage assembly [99] and were, thus, expected. While fibre genes were predicted in prophages L. sakei TMW 1.1290 P1 and L. curvatus TMW 1.591 P1, no fibre structures were observed in the TEM micrographs. One reason for this might lie in the sample preparation. The lysates were sterile-filtered to remove cells and larger debris. Then, phages were concentrated via precipitation, and samples were stored until microscopy. It is possible that the fibre structures were sheared off in one of these steps before the fixation of the samples was achieved.

The absence of fully assembled virions in *L. sakei* TMW 1.1386, *L. curvatus* TMW 1.1381, and *L. curvatus* TMW 1.1447 lysates could have multiple reasons. As previously discussed for φ-DJ1812 (harboured by *L. sakei* TMW 1.1398) [59], a pair of transposases in TMW 1.1386 P1 might have affected a correct phage assembly. Both phages share nearly identical sequence information except for a gene-disrupting SNP and a second pair of transposases in the morphogenesis gene module of φ-DJ1812. The latter was discussed previously to cause its defective head-tail joining [59]. Hence, the absence of virions might be caused by the transposase in the replication gene cluster of both prophages instead. It could also result from weak strain lysis after UV light induction, which was also observed for *L. curvatus* TMW 1.1447. Lastly, an unoptimised phage precipitation protocol could have further decreased the chance of finding intact phages. According to the micrographs, phage counts were low in all samples (Prof. Klingl; personal communication). Therefore, the phage purification protocol was optimised before viral DNA sequencing by increasing the PEG8000 concentration from 4% to 10%. Later experiments (plaque assay of "precipitated" TMW 1.591 P1 phage samples; data not shown) indicated that the number of phages was increased in purified samples when higher concentrations of PEG8000 (8-12% w/v) and NaCl (1.0-1.5 M) were used for precipitation.

The TMP gene dictates the length of the phage tail [100]. As a result, the simultaneous induction of multiple prophages encoding different-sized TMP genes should lead to phage particles with different-sized tails. Indeed, this hypothesis is corroborated by different phage morphotypes found within the lysate of a multi-lysogenic *Silicibacter* strain after MitC induction [142]. However, only virion type was found per multi-lysogenic *Latilactobacillus* lysate. This includes *L. sakei* TMW 1.46, *L. curvatus* TMW 1.706, and *L. curvatus* TMW 1.1365, harbouring two to three intact predicted prophages each. As previously mentioned, the DNA of each intact phage was successfully isolated from post-induction lysates and sequenced (although some genomes were fragmented after assembly), concluding that all intact phages were indeed induced and

assembled, although at different rates according to their sequencing depths. As a result, it is possible that only the most prevalent phage particle was found in the TEM micrographs.

5.3 The Prophage-Rich Species *L. sakei* and *L. curvatus*

To understand whether *L. sakei* and *L. curvatus* are prone to prophage accumulation, it is necessary to contextualise their prophage distribution with other LAB. Pei et al. [71] analysed 1,472 genomes across 16 lactobacilli species for their prophage content via PHASTER and demonstrated that prophage distribution between the species is uneven. According to the authors, multi-habitat species like *Levilactobacillus* (*Le.*) *brevis*, *Lp. plantarum*, or *Lc. paracasei* harbour more intact prophages than species occupying fewer habitats. With 98% of 134 analysed strains containing intact prophages (mean: 2.03 per strain) and zero to five intact prophages detected in strains, *Lp. plantarum* was identified as the species with the highest occurrence of intact prophages. *Lp. plantarum* contained 3.54 (mean) prophages of any completeness per strain, with a maximum of nine prophage-related (any completeness) sequences in a strain detected. *Lc. paracasei*, on the other hand, harboured more prophages of any completeness but had a lower occurrence of intact prophages. *Lc. paracasei* contained 4.39 prophages per strain and had the highest number of prophage-related sequences detected in a single strain (15 sequences). A 72.1% of 147 *Lc. paracasei* genomes contained intact prophages, with 1.39 (mean) intact prophages per strain ranging from zero to five intact predicted sequences. In contrast, *Lactobacillus acidophilus* was identified as the least likely species to harbour intact prophages (2.9% of 35 genomes contained intact prophages). It contained 1.06 (mean) prophage-related sequences with a maximum of two sequences detected in a strain and 0.03 (mean) intact prophages per strain (ranging from zero to one intact sequence detected in a strain). While *L. curvatus* was not included in this study, 44 *L. sakei* genomes were analysed, containing one to five prophage-related sequences (mean: 2.43) and zero to three intact prophages (mean: 0.77). 65.9% of analysed *L. sakei* strains by Pei et al. harboured intact prophages. [71]

Regarding *L. sakei*, a similar distribution was obtained in this thesis [2.07±1.12 (mean ± SD) prophage-related sequences per strain; 0.60±0.73 (mean ± SD) intact prophages per strain; 48.8% of strains contained intact prophages; most intact prophages in a strain: three; most phage-related sequences in a strain: five], although slight differences were caused by the partly different set of analysed genomes (excluded and newly sequenced strains). *L. curvatus* strains included in this thesis reached high numbers (up to 14) of phage-related sequences [4.73±3.60 (mean ± SD)] and intact prophages [1.04±1.00 (mean ± SD)] per strain. 62.2% of analysed

strains carried intact prophages. Compared to *Lp. plantarum* or *Lc. paracasei*, *L. curvatus* also seems to acquire many prophages but retains fewer intact prophages. Notably, the strains identified as lytic (and therefore likely to contain intact prophages) during the screening were included within the prophage distribution. As a result, the occurrence of intact prophages might be artificially increased to some extent.

Despite sharing phenotypically and phylogenetically close relationships, the two analysed *Latilactobacillus* species differ considerably in their prophage content. The higher prophage accumulation in *L. curvatus* could be explained, according to Pei et al. [71], by the less restricted habitat the species occupies. While both species share ecological niches like meat and meat-associated products [14–17, 143], *L. curvatus* indeed has a more diverse set of niches it was isolated from, like honey [14], Korean sourdough [15], Spanish goat cheese [16] or kimchi [17]. However, both species contained at least one prophage-related sequence per strain and, as a result, should be considered likely targets for phage attacks.

PHASTER, as a prediction tool, had its expected limitations, which were also acknowledged by Pei et al. [71] and emphasised by the creators of this tool [117]. Its database-driven prediction relies heavily on sequence similarity alignments with known phages. Therefore, novel prophages are more challenging to predict and most likely are classified as incomplete or, due to BLAST hit paucity, split into multiple prophage sequences (prediction of overlapping prophage regions within one prophage). PHASTER predicted 26 intact prophages in the 43 analysed *L. sakei* genomes and 47 intact prophages in the 45 analysed *L. curvatus* genomes. In contrast, 29 putatively intact *L. sakei* prophages and 50 *L. curvatus* prophages were identified after manual completeness evaluation. Although the number of intact sequences was similar, the predicted sequences by PHASTER deviated in part strongly from manually as intact predicted prophages. Because even manual prediction might be flawed (e.g., due to incomplete genome sequencing or poor gene annotation), induction experiments, as performed in this thesis, are necessary to obtain proof of prophage inducibility and intactness.

5.4 Preference of Conserved DNA Loci for Prophage Integration

Determining common prophage integration loci can provide valuable data when assessing the susceptibility of a species to phage attacks, as these represent the chromosomal “weak spots”. Conserved loci can indicate potential phage movement and integration and, thus, represent signs of phage and host evolution, fitness, and adaptability [98].

The integration loci of *L. sakei* prophages were analysed in the past [71]. However, the information was confined to relative genomic positions instead of gene-level predictions. Most likely, this choice was made due to the high number of screened genomes in this study (1,472 genomes across 16 LAB species). Chromosomal phage integration is performed by the phage integrase through site-specific recombination of an attachment site on the phage genome (*attP*) with an attachment site on the bacterial chromosome (*attB*), resulting in the prophage attachment sites *attL* and *attR* [144]. Because of this, an integration analysis starts by correctly predicting *attL* and *attR*. During the prophage distribution analysis, PHASTER often failed to predict both *att* sites correctly. Consequently, predicted *attL* and *attR* sites of all intact *Latilactobacillus* phages were manually checked and fixed/determined if possible. In some cases, incomplete sequencing data or ambiguous BLAST results hindered the exact prediction of *att* sites.

Prophages that integrated into the same locus shared similar or identical *att* sites and closely related integrase genes. In total, 13 distinctive phage integrase groups were identified for the intact *Latilactobacillus* prophages. The sharing of integration sites between closely related phages has also been reported for temperate phages infecting *Le. brevis* [98]. Notably, groups I and II integrases allowed integration into different chromosomal loci (two per group) reflected in different *att* sites. However, all loci were RNA genes that could feature similar recognised sequences. Consequently, a further subdivision into different integrase groups could be possible once more group members are identified.

While *L. sakei* prophages only harboured integrases of groups I to VI, *L. curvatus* prophages had a more diverse set of integrases, which belonged to 12 of the 13 groups (excluding group III integrases, which allowed into a gene with an unknown function). As aforementioned, a reason for this could be the more diverse set of ecological niches that *L. curvatus* occupies. In many cases, phage integration took place directly in a gene. Phages are known for restoring gene integrity, carrying a copy of the interrupted gene portion on their genomes [145]. This could explain why amber gene mutants (featuring premature stop codons within the coding sequence) were not observed and no vital pathways that ensure host survival were disrupted.

Of the 13 groups, one group facilitated integration into a gene with an unknown function and two groups into non-coding regions, making it difficult to hypothesise why the prophages chose these regions. Six groups facilitated integration into tRNA or tmRNA genes, including tRNAs for arginine, glutamine, glutamic acid, leucine, and serine. tRNA genes are common phage integration targets for integrases belonging to the tyrosine recombinase family [146]. These

integrases can specifically target a small DNA segment encoding the tRNA anticodon stem/loop, which contains well-conserved positions recognised by orthologous integrases [147].

Conserved genes are also often targets for integration [95]. This comprises genes like *lepA*, a gene coding for the translation elongation factor 4 [148], and a gene coding for a glucose-6-phosphate isomerase (PGI). PGI catalyses the isomerisation of glucose 6-phosphate and fructose 6-phosphate during glycolysis. Interestingly, an *Escherichia* (*E.*) *coli* isolate was described [149] that harboured phage mu, which was integrated into a PGI-gene.

Furthermore, a glutamine-hydrolysing GMP synthase coding gene was identified as an integration locus. While it cannot be said with certainty why this gene was chosen for integration due to missing literature data, its product supports proper growth (glutamine-hydrolysing GMP synthase is part of the purine metabolism) and could be chosen by the phage due to the benefits the cell has by keeping this gene.

Another integration site was identified in a *sufB*-like gene. This gene is part of an iron-sulfur cluster synthesis operon and was proposed to play a vital role during oxidative cell stress in *E. coli* [150]. Therefore, it is upregulated by hydrogen peroxide [151], which also induces some prophages [152], suggesting a relationship between the iron-sulphur cluster biosynthesis pathway and phage induction. This pathway was also shown to grant protection against infection with coliphage λ [153], which corroborates the hypothesis that this locus was not chosen arbitrarily for integration but intentionally provoked by the phage or host.

5.5 Genomic Synteny of *Latilactobacillus* Prophages

LAB phages were reported as highly diverse [69], making classification difficult [70]. Although, some prophages (TMW 1.1386 P1 and φ-DJ1812) only differed in their transposase content or were essentially identical (*L. curvatus* TMW 1.706 and *L. curvatus* DSM 20019^T prophages) due to close-to-identical host genomes (100.00 % ANIb over 99.95 % of aligned nucleotides), this was also true for most intact *Latilactobacillus* phages analysed within this thesis. Different genomic architectures between *L. sakei* and *L. curvatus* prophages indicating various lineages could have been anticipated due to their high diversity. However, a genome synteny shared by all intact prophages was evident. All intact predicted prophages started with lysogeny-related genes, followed by replication, packaging, morphogenesis, and host lysis genes. A higher sequence conservation between closer-related prophages was mainly found in the replication and morphogenesis gene modules. Compared to published information on

phages infecting *Le. brevis* [98], the genomic architecture of *Latilactobacillus* prophages was, at first glance, dissimilar in the succession of gene modules. Displayed *Le. brevis* phage genomes began with the small subunit terminase gene and ended with replication-related genes. In contrast, *Latilactobacillus* prophages start with lysogeny-related integrase genes and end with lysis-related genes. However, searching for previously described [98] *Le. brevis* SA-C12 prophages (e.g., TPSAC12-2) via PHASTER (data not shown) revealed they shared the same gene module succession with *L. sakei* prophages. Notably, a circular permutation between the virion genome (obtained from post-induction lysates after viral DNA sequencing) and its respective prophage can explain the discrepancies in gene module order. This was observed for Klebsiella oxytoca phage pKO2 [154] and the *Latilactobacillus* phages in this thesis. A prophage is chromosomally integrated by site-specific recombination of its *attP* site. As shown for coliphage λ [155], *attP* is located near the integrase gene, leading to prophages starting with an integrase gene. Similarly, terminases utilise particular sequences (e.g., *pac* or *cos* sites) for packaging of the phage genomes into the capsids, which can be in close vicinity of the terminase genes (e.g., in phage λ [155]). Hence, the phage genomes within viral capsids will likely start with the phage terminase DNA binding sites. In conclusion, a circular permutation between virion DNA and prophage is the consequence of using different recognition sites for integration and packaging.

According to previous literature regarding *L. sakei* prophages [71], the intact *Latilactobacillus* prophages encoded no ARGs. Interestingly, prophages were discussed to benefit their host independently of phage-provided ARGs in the past, e.g., by releasing virions that lyse susceptible competitors [156]. Despite ARGs not being carried, some of the intact *Latilactobacillus* prophages encoded non-ubiquitous features. The following chapters discuss the presence and function of transposases, tRNAs, and MTases.

5.5.1 Transposases as a Sign of Early Prophage Degradation

Transposases were identified in three intact predicted *L. sakei* and five *L. curvatus* prophages. These enzymes move DNA segments (transposons) within the genome to new loci without needing RNA intermediates. They are usually encoded on the transposed mobile element (autonomous transposon) or, less frequently, somewhere else on the genome (non-autonomous transposons). [157]

In contrast to virulent phages, temperate phages are much more likely to acquire transposons while integrated into the host chromosome [158]. It was demonstrated for phages infecting *Neisseria meningitidis* that transposons can interrupt or replace vital genes within a prophage

[159]. Interestingly, the integration of multiple identical transposons followed by homologous recombination excising the internal region (here: multiple morphogenesis-related genes) was discussed for the DNA loss caused by the IS30 transposase homologue [159]. The loss or interruption of those genes may hinder proper phage propagation. In fact, the rapid deletion of prophage-related genes by the host was discussed as an early step in the domestication of phage components and a rapid protective mechanism against phages [58].

No fully assembled virions were detected in lysates of *L. sakei* TMW 1.1386 and *L. sakei* TMW 1.1398 [59], which harbour transposon-containing and closely related prophages. Moreover, a putative transposase was identified in the genome of phage TMW 1.1365 P2 after sequencing that was not present in the prophage. Because this strain harbours multiple intact predicted prophages, it cannot be said with certainty if the observed fully assembled phage particles belong to TMW 1.1365 P2. It is questionable whether transposase-containing "intact-predicted" *Latilactobacillus* prophages can complete the lytic cycle and should be classified as "intact." For example, phage φ-DJ1812, harboured by *L. sakei* TMW 1.1398, was discussed as [59] and should be considered cryptic (defective) because of its inability to correctly assemble virions. This must be elucidated for each phage individually and requires more tests. In summary, transposases indicate the ongoing degradation of a prophage and can render it cryptic.

5.5.2 Phage-Host Codon Usage Differences Offset Through Phage-Encoded tRNAs

tRNAs are vital for protein synthesis and act as adaptors between transcribed genes and their encoded proteins during translation [160]. Some intact predicted *Latilactobacillus* prophages contained one to two tRNA genes (partial tRNA genes used for integration omitted). In phage genomes, tRNA genes are discussed to support translation during host chromosome degradation upon lytic infection [161] and compensate for different codon usages of infected hosts [162]. For example, Xanthomonas citri jumbo phage XacN1 and its host have different codon usages [163]. To circumvent this, the phage encodes tRNAs targeting codons used by the phage more frequently [163]. Hosts can also accommodate shifting demands in codon usage upon rapid influxes of maladapted foreign genes (e.g., through lateral gene transfer via temperate phage infection and prophage integration) by selectively retaining specific tRNA genes [164]. The transduced tRNA genes by *Latilactobacillus* prophages could, therefore, also contribute to offsetting codon usage differences. The following discusses this for the two most prevalently encoded tRNA genes.

Most often identified were isoleucine tRNAs using CAU as anticodon (ten of 16 isoleucine tRNAs) or phenylalanine tRNAs with GAA as anticodon (15 of 15 phenylalanine tRNAs) in

intact predicted *Latilactobacillus* prophages. Interestingly, the isoleucine tRNA with the CAU-anticodon ($tRNA^{Ile2}$(CAU)) is post-transcriptionally modified into $tRNA^{Ile2}$(LAU) by the enzyme $tRNA^{Ile}$-lysidine synthetase (TilS), which decodes ATA in *Lp. plantarum* [165]. All *Latilactobacillus* strains that feature intact prophages encoding isoleucine tRNAs also carry *tilS*. Hence, they could perform this modification. The *Latilactobacillus* prophages use ATA more often than their hosts. Therefore, the higher frequency of the minor ATA isoleucine codon within coding regions of prophage-related genes could necessitate and explain the carried $tRNA^{Ile2}$(CAU) genes.

In contrast, the prophages featuring phenylalanine tRNA genes used both corresponding codons (TTT and TTC) at similar frequencies as their hosts. Although TTC was used less than TTT by the prophages, exclusively phenylalanine tRNAs were encoded by the prophages that use GAA as the anticodon. The exclusive presence of $tRNA^{Phe}$(GAA) in nature and, in turn, the absence of natural tRNAs decoding the redundant codons NNC or NNT (N ≙ A, T, G, C) with an A in the wobble position of the anticodon [here: $tRNA^{Phe}$(AAA)] is a known phenomenon [166]. It was postulated [166] that this tRNA type was eliminated during evolution because $tRNA^{Phe}$(AAA) is not a suitable substrate for the enzyme phenylalanyl-tRNA synthetase (which catalyses the binding of the tRNA to its corresponding amino acid). However, the reason why *Latilactobacillus* prophages favourably carried phenylalanine tRNA genes is still unknown.

Conspicuously, phage TMW 1.1290 P1, despite encoding no tRNAs, had similar isoleucine and phenylalanine coding usages to phages encoding respective tRNAs. This suggests that its host might sufficiently provide tRNAs to ensure well-functioning translation of phage-related genes.

5.5.3 Methylation in *Latilactobacillus* Phages

MTase genes can occur alone (orphan MTases) or combined with restriction endonuclease (REase) genes, forming an RM system [167]. RM systems are found in most bacterial and archaeal genomes and protect against foreign DNA like viral genomes or transposons [168]. However, methylation also plays an important role in the DNA repair process of *E. coli* [169, 170]. In parallel, phage-encoded MTases can protect the phage genomes against the RM systems of their host after infection [171] or positively affect the packaging efficiency of the phage DNA into the capsid [172]. Methylation of the phage episome (extrachromosomal phage genome) was discussed to play a crucial role in the life cycle of phages and is likely connected to their replication rate [173]. MTases were only predicted in some intact predicted *Latilactobacillus* prophages, suggesting that (i) DNA methylation is no general requirement for DNA packaging in analysed species, (ii) the phage DNA is methylated as required by host-

encoded MTases, or (iii) MTase genes were present in all phages, but prediction occasionally failed due to poor database matching. These prophages mainly contained orphan MTases, although four *L. sakei* prophages (φ -DJ1812, J64 P1, TMW 1.1386 P1, TMW 1.1397 P1) and three *L. curvatus* prophages (phage FAM25164 P1, phage MRS6 P1, and phage TMW 1.591 P1) encoded genes for products with REase functions directly downstream of those MTases, with which RM systems could be formed. It is also unknown whether the detected phage MTases interact with the genomes of their host (e.g., upon phage induction) or exclusively with the prophage or phage episome. Methylome profiling could verify some of these hypotheses but is still costly. Fortunately, high-throughput methods are on the rise, which could make methylome profiling more affordable than the established bisulfite sequencing [174]. Because RM systems are considered a fundamental barrier during the genetic engineering of recalcitrant bacteria [175], prophage curing, potentially removing multiple prophage-encoded RM systems at once, could present a compelling alternative to classic deletion approaches.

5.6 Generation of Prophage-Free Strain Derivatives via SOS-Based Curing

Prophages can be segregated (prophage curing) from lysogenic strains by triggering the SOS response of their hosts via UV light irradiation [176] or by treatment with genotoxic agents like MitC [89]. This is possible due to the upon DNA-damage upregulated SOS-response-associated protein RecA that forms active extended DNA-bound filaments catalysing the autoproteolysis of LexA, the repressor of the DNA repair genes, and structural homologs, like many phage repressors [80, 81].

After the release of the phage repressor (induction), phages enter their lytic life cycle, where they successively kill and lyse their host during the production of new phage progeny. Non-lysogenic cells (e.g., cells that encountered prophage segregation after the inducing treatment) survive the induction treatment by avoiding lysis and repairing their inflicted DNA damage. Consequently, strong host lysis of lysogenic cells is the selective criterion for finding cured isolates. While in this thesis the SOS-based curing approach is applied, other non-SOS-based curing methods are described, like counterselection-based prophage curing [132, 177]), or curing via transcriptional silencing using clustered regularly interspaced short palindromic repeats interference [178].

The intact prophage TMW 1.591 P1 was removed from its lysogenic host *L. curvatus* TMW 1.591 by SOS-based curing. However, this was unsuccessful for *L. sakei* TMW 1.1290 and *L. curvatus* TMW 1.2272 prophages. For TMW 1.2272, no prophage-negative isolates were

retrieved after host lysis. For TMW 1.1290, multiple prophage-negative candidates that lacked phage-mediated lysis were isolated after induction. Yet, after sequencing the prophage integration/excision site, DNA of unknown origin was detected, leading to the exclusion of this strain from further analyses. Next, to cross-contamination, one possible explanation could be that this DNA originated from TMW 1.1290 but was not sequenced during whole-genome shotgun sequencing. This hypothesis could be tested via PCR, using primers targeting this sequence in the WT strain.

Consequently, only the cured strain derivative *L. curvatus* TMW 1.2406 (cured TMW 1.591) was used as prophage-negative control during fermentation. While some temperate phages influence the phenotype of their host upon infection (lysogenic conversion) [179], phenotypic changes of the cured strain derivative compared to the WT were not observed (except for the absence of lysis after the induction treatment and TMW 1.591 P1 phage susceptibility).

5.7 Requirements for TMW 1.591 P1 Infection

The TMW 1.591 P1 phage particles were able to reinfect the cured strain *L. curvatus* TMW 1.2406. However, an effective lytic reinfection was only possible when Ca^{2+} ions and phages were sufficiently present. This suggests that Ca^{2+} plays a crucial role during host adsorption or DNA-injection of phage TMW 1.591 P1 as phage production and release after induction did not require $CaCl_2$ addition. Divalent metal cations, like Ca^{2+} or Zn^{2+}, boost the effectiveness of phage cocktails [180] and are required by many LAB phages for adsorption to the host cell [70]. That said, not every phage adhesion strategy benefits from these ions, as demonstrated in the example of the two lactococcal phages, p2 [181] and TP901-1 [182]. The baseplate of p2 changes conformation based on the presence of $CaCl_2$ [181]. If $CaCl_2$ is present, its RBPs are exposed (from a resting to an active position), allowing host interaction and opening a channel through which DNA can pass during DNA injection [181]. The RBPs of TP901-1, on the other hand, are fixed permanently, and $CaCl_2$-independently, in an infection-enabling conformation [182].

Besides host density [183], the MOI affects the host reduction time of lytic phages [51] and influences the lysis-vs-lysogenisation decision of some temperate phages (e.g., coliphage λ) [86]. While the exact decision-making between the lysogenic and lytic cycle of phages is intricately regulated and complex and, as a result, remains predominantly unsolved, high MOIs favour lysogeny most often [88, 184]. Specific phages infecting *Bacillus* coordinate their lysis-vs-lysogenisation decision with the help of small “communication” peptides that are released

during infection and "measured" by progeny phages, which lysogenise at a certain threshold of this peptide [185]. This so-called "arbitrium" system seems phage-specific, reflected in different peptide versions encoded by different phages [185]. Another effect that is caused by a high number of simultaneously infecting phages, which is more likely at high MOIs (e.g., MOI of 100), is the concept of "lysis from without" [51]. In this case, the attaching phages kill the cell before new phage progeny is assembled. This leads to an absent phage burst reflected in decreased stable phage counts after infection [51].

A minimum concentration of TMW-1.591-P1-containing lysate (thus, MOI) was needed for a visible decrease in OD_{600} during the 12 h of growth monitoring. When the lysate was applied in higher amounts (1:20 final dilution), surviving cells restored growth much faster than samples with less lysate. This could result from a higher MOI favouring lysogeny, a higher concentration of growth-stimulating substances introduced by the added lysate, or, although highly speculative, even a similar mechanism as the aforementioned "arbitrium system." In the future, purified phage solutions with defined phage counts that lack growth-simulating substances could be applied to exclude their influence and more accurately analyse the impact of MOI on *Latilactobacillus* phage life cycle decisions.

Host density can also affect lytic phage propagation, although different theories exist to explain its influence [88]. "Kill-the-Winner" describes a phage preferentially lyses a highly abundant host population [88]. In contrast, the often challenged "Piggyback-the-Winner" theory suggests that the dominating population persists through favoured lysogeny [88]. Liquid cultures of *L. curvatus* TMW 1.591 reach an OD_{600} of ~5-6 and, thus, high host densities within less than one day. However, effective phage release was not observed for this strain without prior induction. Consequently, it is proposed that "Piggyback-the-Winner" might be more applicable to TMW 1.591 P1.

5.8 The Narrow Host Range of *Latilactobacillus* Temperate Phages

Most tested strains were resistant to a phage lysate mix from twelve lysogenic strains, indicating a narrow host range of *Latilactobacillus* phages. This was expected, as temperate phages have a much narrower host spectrum (higher host specificity) than virulent phages [158]. Nonetheless, some factors must be considered: TMW 1.591 P1 phages infecting the cured strain *L. curvatus* TMW 1.2406 (positive control during resistance screening) required Ca^{2+} ions for host lysis. However, it is unknown if other phage-strain combinations require higher amounts of this salt or have different prerequisites for effective lytic propagation. If infection conditions

were suboptimal, lysogenisation instead of host lysis could have been favoured. Moreover, taking the narrow host range of temperate phages into account, finding suitable hosts for a limited set of phages may be considered finding the "needle in the haystack." Yet, the fact that both species are rich in prophages indicates their susceptibility to phages within their respective environments, in which phage diversity is much higher.

Prophages can confer immunity against other similar phages to their hosts (superinfection immunity) by hindering the adsorption of superinfecting phage particles or injection of phage DNA [88]. Notably, secondary infection by heterologous temperate phages is not prevented, leading to multi-lysogenic strains and even (in some cases) to the SOS-based induction of an already established prophage [88]. *L. curvatus* TMW 1.591 did not visibly lyse after combi-strain lysate supplementation, suggesting that superinfection to TMW 1.591 P1 phages was indeed conferred. However, the heterologous phages in the lysate mix could not induce its prophage.

As discussed in Chapter 5.7, the observed marginally faster growth of strains upon lysate addition compared to the negative control (demineralised water) is most likely due to the additional nutrients or growth hormones contained in the lysate mix and presumably could have been averted by using purified phage solution.

5.9 The Phage-Inducing but Phage-Resilient Nature of Raw Meat Fermentation

Thirty years ago, phages were proposed to threaten raw sausage fermentation [53]. Despite this claim, meat fermentation failures caused by phages have not been reported. The missing knowledge about phages targeting meat starter cultures could undoubtedly cause a disconnection of a failed fermentation to a phage infection. It is equally likely that phage infection affects raw sausage production to a lesser extent than anticipated. If a prophage negatively affects a potential starter strain during fermentation, the strain will most likely not be commercialised. For this decision, in-depth phage-related knowledge is not required. Many of the *Latilactobacillus* strains examined in this thesis are starters for food fermentation or were isolated from fermented foods. Interestingly, intact prophages were frequently encoded by those strains. This could indicate a lack of or positive influence of prophages on strain fitness.

In a previous thesis [59], the influence of the cryptic prophage φ-DJ1812 on host fitness and competitiveness was assessed as ambivalent. While the phage-harbouring WT strain grew faster during *in vitro* experiments, the cured strain was more competitive in a raw sausage

fermentation setup [59]. LAB are responsible for suppressing spoilage bacteria by acidifying the meat substrate during the first days of fermentation. Thus, changes in competitiveness would be indicated by an altered acidification kinetic or decreased cell counts early during fermentation. None of that was observable for the strain model analysed in this thesis. Moreover, the prophage-specific PCR of salamis inoculated with both LAB starter strains (*L. curvatus* TMW 1.591/TMW 1.2406; 1:1 strain mixture) showed that the starters were present in virtually the same ratio after fermentation as during inoculation. This confirms that TMW 1.591 P1 did not affect host fitness or competitiveness during fermentation. Of note, this is only true if special-case isolates (tested excision-positive and prophage-positive) were counted as the cured strain derivative TMW 1.2406, which was confirmed by sequencing such isolate. Conspicuously, salami samples fermented exclusively with TMW 1.2406 also featured some special-case isolates (6 of 97). This could be caused by autochthonous phages that feature similar integrase genes but cannot infect TMW 1.2406. These autochthonous phages could then be introduced into the PCR reactions and cause a phage-integrase-positive result despite the isolates per se carrying no prophage. The infection disability of autochthonous phages was confirmed by the absence of lytic phages in salamis exclusively fermented with TMW 1.2406. This suggests that any present autochthonous phages have most likely not affected the starter growth. An integrase-positive result is also plausible due to the seemingly limited set of existing *Latilactobacillus* phage integrases (Chapter 4.1.5) and the high LAB species diversity present during fermentation that could have released phages because of the inducing properties of the meat environment. The latter is indicated by the high number of released TMW 1.591 P1 directly after starter inoculation.

The phage counts in meat batters fermented with the lysogenic WT strain or with added phages before starter addition followed a similar trend as previously described for raw meat fermentation [53]. Phage counts were high in the beginning and lower but stable at later phases of the fermentation. This indicates that phage induction and inactivation become less frequent after most nutrients are depleted and LAB starter growth slows down. As demonstrated for lactococcal temperate phages, SPI depends on the growth phase of the host cell and is most frequent during exponential and early stationary phases [89, 186]. Both phases are predominant during early fermentation. Later in the fermentation process, phage counts may be determined more by phage-degrading conditions, such as present proteases [187, 188]. During late ripening involving drying, these enzymes most likely lose activity due to the decreased water activity. The high number of phages isolated from the final raw sausage product (34 days after fermentation start) corroborates this hypothesis.

The meat batter supplemented with TMW 1.591 P1 phages and fermented with the phage-susceptible cured strain derivative (TMW 1.2406) experienced no phage increase. The following sections discuss reasons why the lytic propagation of TMW 1.591 P1 was restricted.

5.9.1 Restricted Access to New Host Cells Through Limited Diffusion

During phage infection experiments *in vitro* (Chapters 4.2.2, 4.2.3, and 4.2.4), host cells and phages were cultured in a liquid medium or agar. Both substrates allowed diffusion of released virions and, thus, unrestricted access to new host cells. In contrast, the meat matrix is regarded as a solid-state-type substrate with only limited diffusion possible. As no additional mixing occurs during fermentation, phage dispersal and access to new host cells are heavily impeded. To simulate phage-contaminated meat, TMW 1.591 P1 phages were added to the meat batter before the addition of bacterial starters. Although the meat batter was mixed thoroughly afterwards, not all phages might have adsorbed to suitable host cells. In contrast, Nes and Sørheim [53] added B_2 phages in high titre directly to a liquid *Lp. plantarum* starter culture and incubated the mixture for 15 minutes before adding it to the meat. This way, the direct contact of phages with their host ensured effective adsorption and ultimately led to extensive host lysis, delaying the fermentation. As shown for *Salmonella* Enteritidis phages [51], phage attachment is, in fact, more effective when performed in low-viscosity substrates. Consequently, phages could influence starter culture preparation more than the meat fermentation itself.

5.9.2 Impeded Phage Infection Through Insufficient Ca^{2+}

Phage TMW 1.591 P1 required Ca^{2+} to effectively lyse its host *in vitro*. Currently, $CaCl_2$ is not an integral part of typical raw sausage recipes, despite studies proposing $CaCl_2$ as a healthier alternative to NaCl or demonstrating its effects to increase meat tenderness [189–191]. Thus, if the natural meat concentration of Ca^{2+} were too low, lytic propagation could have been affected during fermentation. According to the United States Department of Agriculture [192], Italian-style pork-based salami contains 10 mg of calcium per 100 g of sausage. If all calcium were accessible to the phage in an ionic state, this would correspond to ~2.5 mM Ca^{2+} (approximation using the material density of water), representing one of the lowest concentrations where lytic propagation of TMW 1.591 P1 was observable. In conclusion, the actual accessible Ca^{2+} content in salami is most likely much lower and represents a limiting factor for effective lytic propagation of TMW 1.591 P1 during meat fermentation.

5.9.3 Increased Lysogenisation Through Unsuited MOI or Host Density

As previously discussed, the MOI and host density could affect the lysis-vs-lysogeny decision of a phage (Chapter 5.7). In salami and model fermentations, the host cell density was dictated by the performance of the fermenting bacterial starter. A low metabolic activity of *L. curvatus* TMW 1.591 and *L. curvatus* TMW 1.2406, reflected in slow acidification, required a higher inoculation to reflect a characteristic ripening step. Lower-titre crude phage lysate was used for phage supplementation instead of an enriched and purified high-titre phage solution. Because the addition of liquid into the meat batter had to be kept as low as possible, an MOI of 0.1 was chosen, which corresponds to one phage added for every ten cells. Thus, a higher lysogenisation rate or lysis-from-without phenomenon (simultaneous infection of multiple phages lyse the host cell upon cell entry) was not expected during the first infection cycle. Yet, phages or host cells could have been added in unsuited ratios or quantity for effective lytic propagation, potentially leading to the lysogenisation of the starter in successive infection rounds. To prove this hypothesis in the future, TMW 1.2406 candidates isolated directly after fermentation start from a phage-supplemented meat batter could be analysed for the presence of a prophage.

5.10 Phage Induction Through Low pH and High Temperature

Starter strains control food fermentations by suppressing the autochthonous microbiota and shape the final product. To do so, they must exhibit high fitness and competitiveness. Induced prophages causing host lysis due to specific environmental conditions can influence these traits. These conditions must be identified for prophage-rich starter species to ascertain proper fermentations. This thesis demonstrated the inducibility of prophages within *L. sakei* and *L. curvatus* strains using UV light and MitC. Although not treated with those inducers, *L. curvatus* TMW 1.591 released phages in high quantities during meat fermentation. Multiple cultivation conditions were tested to analyse which factor caused the induction during fermentation. *L. curvatus* TMW 1.591 released phages after exposure to heat (45-60°C) and an acidic environment (pH 3.0). Of note, excessively applied stress led to cell death before new phage progeny was produced. Unfortunately, because phage induction is highly phage- and host-specific, an overarching rule for phage induction is difficult to establish from literature with diverging observations on SPI. Taking lactococcal phage studies as an example, one study [89] observed decreased phage induction when nutrients were limited, while another [85] reported an inducing effect of cell starvation. While short-term starvation did not affect TMW 1.591 P1 induction, overnight starvation increased phage release, although less than induction via UV light or MitC. Both studies found an elevated temperature phage-inducing, as was

demonstrated for TMW 1.591 P1 in this thesis. Some strains in the first-mentioned study showed higher phage induction after an osmolarity upshift [89], which led to no observable induction of TMW 1.591 P1. While low pH led to a lowered SPI in the second study [85], it led to an increased induction of TMW 1.591 P1.

Phages with similar repressor systems can provide clues for the behaviour of TMW 1.591 P1 and, hopefully, *Latilactobacillus* phages in general. The repressor gene product of TMW 1.591 P1 was annotated as a putative CI-like repressor, a repressor type used by coliphage λ. Coliphage λ is one of the best-understood phage models and serves as a model for phage-associated regulation patterns. Despite phage λ infecting a Gram-negative host, comparing its regulation patterns to TMW 1.591 P1 could assist in understanding the induction mechanism of the latter. The lysis-vs-lysogeny-decision of phage λ is tightly regulated [87]. At high temperatures and low multiplicity of infection, it performs mostly its lytic cycle when host cells are cultured in a rich medium [87]. Higher temperatures are believed to stimulate the lytic cycle by supporting the rapid metabolic reactions during phage production [87]. Unsurprisingly, phage λ mutants have been identified that feature temperature-sensitive repressors that allow induction at high temperatures [193]. As shown for multiple phages infecting *Listeria monocytogenes* [194], temperature does affect adsorption and plaquing efficiencies. The authors suggested elevated temperatures (37°C instead of 30°C) to confer transient phage infection resistance to the host. Amongst other reasons, temperature-dependent changes in the regulation of the phage receptor-binding sites (presence of N-acetylglucosamine in and rhamnosylation of wall teichoic acids) were discussed to trigger this phenomenon.

Because LAB decrease the pH of their substrate effectively, the pH-induced DNA-damage-independent SOS response-mediated induction mechanism of the LexA repressor should be discussed. LexA is mimicked by the λ repressor CI, a structural homolog [80]. CI undergoes structural changes and quaternary structure formations (e.g., dimerisation and higher multimeric assembled states) that affect its activity by enabling cooperative binding to adjacent operator sites [195, 196]. Analogically, the repressor LexA (part of the *E. coli* SOS regulon) is also influenced by structural changes. At low pH (3.5-4.5), LexA forms predominantly aggregates that cannot bind DNA and (minorly) tetramers that bind DNA with low specificity. Although LexA does not bind SOS boxes (regulatory sequences in the operator region of SOS-controlled genes) at low intracellular pH, protein synthesis is still repressed due to the low pH. The cell metabolism is re-established upon restoration to a mildly acidic pH (~5-6). Because

SOS boxes are still predominately unrepressed, an initial RecA-independent SOS activation can occur. [197]

Under the premise that the repressor of TMW 1.591 P1 behaves similarly to LexA and closely related phage repressors (like CI), this proposed *in vivo* model could explain the observed phage induction of TMW 1.591 P1 after a short-time pH shock. Conspicuously, neither high temperature nor low pH were observed during the first hours of meat model fermentation. Yet, a synergistic effect of multiple inducing (partly unknown) factors causing the observed phage production during meat fermentation is still possible. Notably, no data is available regarding the microenvironment surrounding each cell. Because of the limited diffusion of acidic metabolites due to the solid-state nature of meat, an acidic microenvironment could also explain the observed phage induction.

In summary, enhanced induction of TMW 1.591 P1 was observed in an acidic environment and at elevated temperatures. An inhomogeneous literature indicates that inducibility is highly phage- and strain-specific. Still, the repressor regulation pattern of TMW 1.591 P1 could be explained by comparison to similar-behaving repressors.

5.11 Species Interfering With Phage Induction or Release

In the previous chapter, phage-inducing factors were discussed. These were tested *in vitro* using a pure culture approach. However, meat as a natural non-sterile substrate is inhabited by bacteria of many different genera (and some yeasts) [104]. Because this microbiota is also present during raw sausage fermentation, it was tested whether an assortment of meat-related bacterial species could influence phage induction/release. The experiment was focused primarily on the "pure presence" of foreign cells during phage production. This was ensured by harvesting foreign cells from overnight cultures, guaranteeing they were in their stationary growth phase (in contrast to *L. curvatus* cells, which were already in the early exponential phase during induction and co-cultivation). As a result, *L. curvatus* TMW 1.591 was supposed to have enough "lead" during phage production without the danger of the foreign cells occupying nutrients and hindering growth within the first two hours. Because of this, the absent growth of tested staphylococci due to the unsuited cultivation conditions was tolerated.

One day after co-cultivating induced *L. curvatus* TMW 1.591 with different meat-associated species, widely different phage numbers were detected in the samples depending on the co-cultured cell type. The most significant increase in phage counts was observed after adding *L. sakei* TMW 1.2. Conversely, the addition of *Lp. plantarum* TMW 1.25 and *Lc. paracasei*

isolate 1 led to considerably less detectable phages, partly below the ~1×10^3 PFU/mL detection limit of the assay. TMW 1.2 was chosen because it lacked intact prophages that could interfere with *L. curvatus* TMW 1.591 or its cured derivative. Moreover, TMW 1.2 showed no phage-mediated lysis after contact with the combi-strain lysate (containing TMW 1.591 P1 phages). Therefore, TMW 1.591 P1 was unlikely to be propagatable in TMW 1.2, which could have explained the increased phage count. This experiment suggested that *S. carnosus* TMW 2.212, also added to meat model fermentations, did not affect TMW 1.591 P1 induction or release during fermentation. Noteworthy, the mere presence of a foreign cell type was not enough to encourage high levels of phage induction but needed a prior UV light induction treatment.

Discrete information that could explain the effect of other species on phage induction was only scarcely found. Most likely, the observed enhanced phage production upon co-culturing with *L. sakei* TMW 1.2 was caused by released bacteriocins that exert additional cell stress on *L. curvatus* TMW 1.591. *L. sakei* and *L. curvatus* are well-known bacteriocin producers [13, 198–200]. In fact, *L. sakei* TMW 1.2 = CTC 372 was described to produce sakacin T, which belongs to the class IIb bacteriocins [200] that kill cells by inducing membrane leakage [201]. In contrast to other phage-inducing genotoxic bacteriocins like colibactin [202], this mode of action first contradicts the hypothesis that *L. sakei* TMW 1.2 releases bacteriocins that could induce phages. However, a study that analysed bacteriocin-phage interaction (BaPI) in *Lactococcus* [203] found bigger plaque sizes (equivalent to a higher number of released phages) as a result of culturing sk1-infected strains with lactococcin 972 (which interacts with lipid II, the primary building block of the Gram-positive cell walls) [204]. Despite this missing implication on genotoxicity, authors have suggested BaPI as a phage/strain-overarching phenomenon and warned about bacteriocin-facilitated phage predation against dairy lactococci [203]. Analogically, sakacin T released by TMW 1.2, which also affects cell envelope construction, could cause the observed increased TMW 1.591 P1 phage release.

The reason why phage counts were reduced after co-cultivation with *Lp. plantarum* TMW 1.25 or *Lc. paracasei* isolate 1 (and *P. pentosaceus* TMW 1.1974 to a lesser extent) remains unknown. Inactivation of released phages by the added cells before phage harvest (after app. one day), e.g. by proteolytic digestion, cannot be excluded.

In summary, the microbiota present during meat fermentation can affect the number of free phages. This can be caused by additional cell stress on induced lysogens (e.g., through BaPI) or presumably by proteolytic digestion of phages decreasing their number.

5.12 Phage Induction Maintenance During Cryopreservation

Janßen demonstrated for the temperate prophage φ-DJ1812, which is harboured by the strain *L. sakei* TMW 1.1398, that an induced prophage status within the bacterial cell after UV light irradiation can be maintained during cryopreservation [59]. Analogically, TMW 1.591 P1 lysed its host after reconstitution of ideal growth conditions and storage for up to ten weeks at -80°C when induced cells were cryopreserved directly after induction. This was also achieved for other tested lysogenic *Latilactobacillus* strains (e.g., *L. sakei* TMW 1.1290 and *L. curvatus* TMW 1.2272; Chapter 4.2.1). Therefore, this phenomenon can likely be applied to a broader host and phage spectrum. The induced cell samples lysed after cryopreservation to a similar extent as their unpreserved control, yet they released far fewer phages. This was most likely due to the freezing procedure, which led to fewer viable cells capable of producing new phages. The cryopreserved samples also appeared to lyse earlier than unpreserved controls. It was demonstrated for coliphage λ that the lysis time affects burst size [205]. The longer the time until host lysis after infection, the more phages are produced. This is due to the linear production rate of phages within the cell after the eclipse period (the time between phage adsorption and release of new phage particles) [205]. Thus, the shorter lysis time of TMW 1.591 after cryopreservation could also contribute to the release of fewer phage particles.

Besides phage induction, phage infection during the eclipse period can also be maintained during cryopreservation [206]. Storing induced lysogenic cells can significantly streamline experiments despite the reduction of expected phage counts. It can save time during curing processes (Chapter 4.2.1), as it allows using the same induced bacterial suspension for multiple screening rounds without repeating the induction treatment. Furthermore, it also provides quick access to fresh phage progeny for further propagation or analysis [206]. Besides these positive aspects, maintained phage induction during cryopreservation also affects starter strain preparation for food fermentations. If cells are induced before preservation, phages could be introduced early into food fermentation, lowering starter fitness due to phage-mediated lysis.

6 OUTLOOK

This work focused on the biology of prophages in the meat starter organisms *L. sakei* and *L. curvatus*. The prophage distribution, inducibility, phage morphotypes, resistance to and requirements for infection, and maintenance of phage induction during cryopreservation were investigated. This research laid the groundwork to assess if an intact temperate phage capable of traversing both life cycles can influence meat fermentation. However, phage research obviously can be a bottomless swamp, considering researchers started investigating this topic over 100 years ago, and there is still no end in sight. Many questions remain unanswered, and some of the following issues should be addressed to gain further insights into temperate *Latilactobacillus* phages:

- Are other cultivation conditions influencing phage induction?
- Is there a temperate phage that can infect multiple *Latilactobacillus* species?
- What are the domains *Latilactobacillus* phages recognise for infection, and are these conserved? Can these be exploited to confer "universal" phage resistance to a strain?
- Can other prophages influence their host during fermentation?
- Are *L. sakei* and *L. curvatus* prophages different from those of their closest relatives, *L. fuchuensis*, *L. graminis*, and *L. fragifolii*, of which some occupy different ecological niches?
- Is siphovirus the only morphotype amongst temperate *Latilactobacillus* phages?
- The 78 analysed *Latilactobacillus* phages used 13 loci for integration, but do other integration loci exist for *Latilactobacillus* phages? If not, is this exploitable in a PCR-based high-throughput prophage screening approach?
- This thesis focused on intact prophages. Do incomplete prophages affect the fitness of their hosts?

7 REFERENCES

1. Zheng J, Wittouck S, Salvetti E, Franz CMAP, Harris HMB, Mattarelli P, et al. A taxonomic note on the genus Lactobacillus: Description of 23 novel genera, emended description of the genus Lactobacillus Beijerinck 1901, and union of Lactobacillaceae and Leuconostocaceae. Int J Syst Evol Microbiol. 2020;70:2782–858. doi:10.1099/ijsem.0.004107.
2. Legein M, Wittouck S, Lebeer S. Latilactobacillus fragifolii sp. nov., isolated from leaves of a strawberry plant (Fragaria x ananassa). Int J Syst Evol Microbiol 2022. doi:10.1099/ijsem.0.005193.
3. Ibrahim SA. Lactic Acid Bacteria: Lactobacillus spp.: Other Species. In: Reference Module in Food Science: Elsevier; 2016. doi:10.1016/B978-0-08-100596-5.00857-X.
4. Beck R, Weiss N, Winter J. Lactobacillus graminis sp. nov., a New Species of Facultatively Heterofermentative Lactobacilli Surviving at Low pH in Grass Silage. Systematic and Applied Microbiology. 1988;10:279–83. doi:10.1016/S0723-2020(88)80013-4.
5. Lorenzo JM, Munekata PE, Dominguez R, Pateiro M, Saraiva JA, Franco D. Main Groups of Microorganisms of Relevance for Food Safety and Stability. In: Innovative Technologies for Food Preservation: Elsevier; 2018. p. 53–107. doi:10.1016/B978-0-12-811031-7.00003-0.
6. Leroy F, Verluyten J, Vuyst L de. Functional meat starter cultures for improved sausage fermentation. Int J Food Microbiol. 2006;106:270–85. doi:10.1016/j.ijfoodmicro.2005.06.027.
7. Katagiri H, Kitahara K, Fukami K. The Characteristics of the Lactic Acid Bacteria Isolated from Moto, Yeast Mashes for Saké Manufacture. Bulletin of the Agricultural Chemical Society of Japan. 1934;10:156–7. doi:10.1271/bbb1924.10.156.
8. Torriani S, van Reenen GA, Klein G, Reuter G, Dellaglio F, Dicks LM. Lactobacillus curvatus subsp. curvatus subsp. nov. and Lactobacillus curvatus subsp. melibiosus subsp. nov. and Lactobacillus sake subsp. sake subsp. nov. and Lactobacillus sake subsp. carnosus subsp. nov., new subspecies of Lactobacillus curvatus Abo-Elnaga and Kandler 1965 and Lactobacillus sake Katagiri, Kitahara, and Fukami 1934 (Klein et al. 1996, emended descriptions), respectively. Int J Syst Bacteriol. 1996;46:1158–63. doi:10.1099/00207713-46-4-1158.

9. Montanari C, Barbieri F, Magnani M, Grazia L, Gardini F, Tabanelli G. Phenotypic Diversity of Lactobacillus sakei Strains. Front Microbiol. 2018;9:2003. doi:10.3389/fmicb.2018.02003.
10. Eisenbach L, Geissler AJ, Ehrmann MA, Vogel RF. Comparative genomics of Lactobacillus sakei supports the development of starter strain combinations. Microbiological Research. 2019;221:1–9. doi:10.1016/j.micres.2019.01.001.
11. Nyquist OL, McLeod A, Brede DA, Snipen L, Aakra Å, Nes IF. Comparative genomics of Lactobacillus sakei with emphasis on strains from meat. Mol Genet Genomics. 2011;285:297–311. doi:10.1007/s00438-011-0608-1.
12. Champomier Vergès MC, Zuñiga M, Morel-Deville F, Pérez-Martínez G, Zagorec M, Ehrlich SD. Relationships between arginine degradation, pH and survival in Lactobacillus sakei. FEMS Microbiol Lett. 1999;180:297–304. doi:10.1111/j.1574-6968.1999.tb08809.x.
13. Eisenbach L, Janßen D, Ehrmann MA, Vogel RF. Comparative genomics of Lactobacillus curvatus enables prediction of traits relating to adaptation and strategies of assertiveness in sausage fermentation. Int J Food Microbiol. 2018;286:37–47. doi:10.1016/j.ijfoodmicro.2018.06.025.
14. Bulgasem BY, Lani MN, Hassan Z, Wan Yusoff WM, Fnaish SG. Antifungal Activity of Lactic Acid Bacteria Strains Isolated from Natural Honey against Pathogenic Candida Species. Mycobiology. 2016;44:302–9. doi:10.5941/MYCO.2016.44.4.302.
15. Baek H-W, Bae J-H, Lee Y-G, Kim S-A, Min W, Shim S, et al. Dynamic interactions of lactic acid bacteria in Korean sourdough during back-slopping process. J Appl Microbiol. 2021;131:2325–35. doi:10.1111/jam.15097.
16. Sánchez I, Seseña S, Poveda JM, Cabezas L, Palop L. Phenotypic and genotypic characterization of lactobacilli isolated from Spanish goat cheeses. Int J Food Microbiol. 2005;102:355–62. doi:10.1016/j.ijfoodmicro.2004.11.041.
17. Jo S-G, Noh E-J, Lee J-Y, Kim G, Choi J-H, Lee M-E, et al. Lactobacillus curvatus WiKim38 isolated from kimchi induces IL-10 production in dendritic cells and alleviates DSS-induced colitis in mice. J Microbiol. 2016;54:503–9. doi:10.1007/s12275-016-6160-2.
18. Mo S-J, Lee K, Hong H-J, Hong D-K, Jung S-H, Park S-D, et al. Effects of Lactobacillus curvatus HY7601 and Lactobacillus plantarum KY1032 on Overweight and the Gut Microbiota in Humans: Randomized, Double-Blinded, Placebo-Controlled Clinical Trial. Nutrients 2022. doi:10.3390/nu14122484.

19. Zhang Y, Liang S, Di Zhao M, Yang X, Choi SH, Li GY. Screening and Identification of Latilactobacillus curvatus Z12 From Rumen Fluid of an Adult Female Sika Deer as a Potential Probiotic for Feed Additives. Front Vet Sci. 2021;8:753527. doi:10.3389/fvets.2021.753527.
20. Chen Y, Yu L, Qiao N, Xiao Y, Tian F, Zhao J, et al. Latilactobacillus curvatus: A Candidate Probiotic with Excellent Fermentation Properties and Health Benefits. Foods 2020. doi:10.3390/foods9101366.
21. Cousin FJ, Lynch SM, Harris HMB, McCann A, Lynch DB, Neville BA, et al. Detection and genomic characterization of motility in Lactobacillus curvatus: confirmation of motility in a species outside the Lactobacillus salivarius clade. Appl Environ Microbiol. 2015;81:1297–308. doi:10.1128/AEM.03594-14.
22. Federici S, Nobs SP, Elinav E. Phages and their potential to modulate the microbiome and immunity. Cell Mol Immunol. 2021;18:889–904. doi:10.1038/s41423-020-00532-4.
23. Twort FW. An Investigation on the Nature of Ultra-Microscopic Viruses. The Lancet. 1915;186:1241–3. doi:10.1016/S0140-6736(01)20383-3.
24. D'Herelle F. On an invisible microbe antagonistic toward dysenteric bacilli: brief note by Mr. F. D'Herelle, presented by Mr. Roux. 1917. Res Microbiol. 2007;158:553–4. doi:10.1016/j.resmic.2007.07.005.
25. Hendrix RW, Smith MC, Burns RN, Ford ME, Hatfull GF. Evolutionary relationships among diverse bacteriophages and prophages: all the world's a phage. Proc Natl Acad Sci U S A. 1999;96:2192–7. doi:10.1073/pnas.96.5.2192.
26. Mushegian AR. Are There 1031 Virus Particles on Earth, or More, or Fewer? J Bacteriol 2020. doi:10.1128/JB.00052-20.
27. Bar-On YM, Phillips R, Milo R. The biomass distribution on Earth. Proc Natl Acad Sci U S A. 2018;115:6506–11. doi:10.1073/pnas.1711842115.
28. d'Herelle F. Bacteriophage as a Treatment in Acute Medical and Surgical Infections. Bull N Y Acad Med. 1931;7:329–48.
29. Fleming A. On the Antibacterial Action of Cultures of a Penicillium, with Special Reference to their Use in the Isolation of B. influenzæ. Br J Exp Pathol. 1929;10:226–36.
30. Loc-Carrillo C, Abedon ST. Pros and cons of phage therapy. Bacteriophage. 2011;1:111–4. doi:10.4161/bact.1.2.14590.
31. Summers WC. The strange history of phage therapy. Bacteriophage. 2012;2:130–3. doi:10.4161/bact.20757.

32. Brives C, Pourraz J. Phage therapy as a potential solution in the fight against AMR: obstacles and possible futures. Palgrave Commun 2020. doi:10.1057/s41599-020-0478-4.
33. Nikaido H. Multidrug resistance in bacteria. Annu Rev Biochem. 2009;78:119–46. doi:10.1146/annurev.biochem.78.082907.145923.
34. Global burden of bacterial antimicrobial resistance in 2019: a systematic analysis. Lancet. 2022;399:629–55. doi:10.1016/S0140-6736(21)02724-0.
35. Kahn LH, Bergeron G, Bourassa MW, Vegt B de, Gill J, Gomes F, et al. From farm management to bacteriophage therapy: strategies to reduce antibiotic use in animal agriculture. Ann N Y Acad Sci. 2019;1441:31–9. doi:10.1111/nyas.14034.
36. Brüssow H. Phage therapy: the Escherichia coli experience. Microbiology. 2005;151:2133–40. doi:10.1099/mic.0.27849-0.
37. Monteiro R, Pires DP, Costa AR, Azeredo J. Phage Therapy: Going Temperate? Trends Microbiol. 2019;27:368–78. doi:10.1016/j.tim.2018.10.008.
38. Yosef I, Manor M, Kiro R, Qimron U. Temperate and lytic bacteriophages programmed to sensitize and kill antibiotic-resistant bacteria. Proc Natl Acad Sci U S A. 2015;112:7267–72. doi:10.1073/pnas.1500107112.
39. Reinhard RG, Kalinowski RM, Bodnaruk PW, Eifert JD, Boyer RR, Duncan SE, Bailey RH. Practical application of bacteriophage in food manufacturing facilities for the control of Listeria sp. Journal of Food Safety 2023. doi:10.1111/jfs.12871.
40. Yeh Y, Moura FH de, van den Broek K, Mello AS de. Effect of ultraviolet light, organic acids, and bacteriophage on Salmonella populations in ground beef. Meat Sci. 2018;139:44–8. doi:10.1016/j.meatsci.2018.01.007.
41. Chibeu A, Agius L, Gao A, Sabour PM, Kropinski AM, Balamurugan S. Efficacy of bacteriophage LISTEX™P100 combined with chemical antimicrobials in reducing Listeria monocytogenes in cooked turkey and roast beef. Int J Food Microbiol. 2013;167:208–14. doi:10.1016/j.ijfoodmicro.2013.08.018.
42. Hagens S, Loessner MJ. Bacteriophage for biocontrol of foodborne pathogens: calculations and considerations. Curr Pharm Biotechnol. 2010;11:58–68. doi:10.2174/138920110790725429.
43. Gutiérrez D, Rodríguez-Rubio L, Martínez B, Rodríguez A, García P. Bacteriophages as Weapons Against Bacterial Biofilms in the Food Industry. Front Microbiol. 2016;7:825. doi:10.3389/fmicb.2016.00825.

44. Cronan JE. Cosmid-based system for transient expression and absolute off-to-on transcriptional control of Escherichia coli genes. J Bacteriol. 2003;185:6522–9. doi:10.1128/JB.185.22.6522–6529.2003.
45. Yang F, Liu L, Neuenschwander PF, Idell S, Vankayalapati R, Jain KG, et al. Phage Display-Derived Peptide for the Specific Binding of SARS-CoV-2. ACS Omega. 2022;7:3203–11. doi:10.1021/acsomega.1c04873.
46. Henrici RC, Pecen TJ, Johnston JL, Tan S. The pPSU Plasmids for Generating DNA Molecular Weight Markers. Sci Rep. 2017;7:2438. doi:10.1038/s41598-017-02693-1.
47. Mertens N, Remaut E, Fiers W. Tight transcriptional control mechanism ensures stable high-level expression from T7 promoter-based expression plasmids. Biotechnology (N Y). 1995;13:175–9. doi:10.1038/nbt0295-175.
48. Jechlinger W. Altered temperature induction sensitivity of the lambda pR/cI857 system for controlled gene E expression in Escherichia coli. FEMS Microbiol Lett. 1999;173:347–52. doi:10.1016/S0378-1097(99)00094-4.
49. Studier FW, Moffatt BA. Use of bacteriophage T7 RNA polymerase to direct selective high-level expression of cloned genes. J Mol Biol. 1986;189:113–30. doi:10.1016/0022-2836(86)90385-2.
50. Garneau JE, Moineau S. Bacteriophages of lactic acid bacteria and their impact on milk fermentations. Microb Cell Fact. 2011;10 Suppl 1:S20. doi:10.1186/1475-2859-10-S1-S20.
51. He J, Wong CWY, Schultze DM, Wang S. Inactivation of Salmonella enteritidis in liquid egg yolk and egg white using bacteriophage cocktails. Curr Res Food Sci. 2024;8:100703. doi:10.1016/j.crfs.2024.100703.
52. Guenther S, Herzig O, Fieseler L, Klumpp J, Loessner MJ. Biocontrol of Salmonella Typhimurium in RTE foods with the virulent bacteriophage FO1-E2. Int J Food Microbiol. 2012;154:66–72. doi:10.1016/j.ijfoodmicro.2011.12.023.
53. Nes IF, Sørheim O. Effect of Infection of a Bacteriophage in a Starter Culture during the Production of Salami Dry Sausage; A Model Study. J Food Sci. 1984;49:337–40. doi:10.1111/j.1365-2621.1984.tb12416.x.
54. White K, Yu J-H, Eraclio G, Dal Bello F, Nauta A, Mahony J, van Sinderen D. Bacteriophage-host interactions as a platform to establish the role of phages in modulating the microbial composition of fermented foods. Microbiome Res Rep. 2022;1:3. doi:10.20517/mrr.2021.04.

55. Decadt H, Weckx S, Vuyst L de. The rotation of primary starter culture mixtures results in batch-to-batch variations during Gouda cheese production. Front Microbiol. 2023;14:1128394. doi:10.3389/fmicb.2023.1128394.
56. Xu M, Ma R, Zhang C, Huang X, Gao X, Lv R, Chen X. Inactivation of Lactobacillus Bacteriophages by Dual Chemical Treatments. Pol J Microbiol. 2023;72:21–8. doi:10.33073/pjm-2023-004.
57. Taylor VL, Fitzpatrick AD, Islam Z, Maxwell KL. The Diverse Impacts of Phage Morons on Bacterial Fitness and Virulence. Adv Virus Res. 2019;103:1–31. doi:10.1016/bs.aivir.2018.08.001.
58. Bobay L-M, Touchon M, Rocha EPC. Pervasive domestication of defective prophages by bacteria. Proc Natl Acad Sci U S A. 2014;111:12127–32. doi:10.1073/pnas.1405336111.
59. Janßen D. Assertiveness of Lactobacillus sakei and Lactobacillus curvatus in raw sausage fermentations: Technical University of Munich; 2019.
60. Ramisetty BCM, Sudhakari PA. Bacterial 'Grounded' Prophages: Hotspots for Genetic Renovation and Innovation. Front Genet. 2019;10:65. doi:10.3389/fgene.2019.00065.
61. Visweswaran GRR, Kurek D, Szeliga M, Pastrana FR, Kuipers OP, Kok J, Buist G. Expression of prophage-encoded endolysins contributes to autolysis of Lactococcus lactis. Appl Microbiol Biotechnol. 2017;101:1099–110. doi:10.1007/s00253-016-7822-z.
62. Rice KC, Bayles KW. Molecular control of bacterial death and lysis. Microbiol Mol Biol Rev. 2008;72:85-109, table of contents. doi:10.1128/MMBR.00030-07.
63. Uehara T, Bernhardt TG. More than just lysins: peptidoglycan hydrolases tailor the cell wall. Curr Opin Microbiol. 2011;14:698–703. doi:10.1016/j.mib.2011.10.003.
64. Juhala RJ, Ford ME, Duda RL, Youlton A, Hatfull GF, Hendrix RW. Genomic sequences of bacteriophages HK97 and HK022: pervasive genetic mosaicism in the lambdoid bacteriophages. J Mol Biol. 2000;299:27–51. doi:10.1006/jmbi.2000.3729.
65. Dragoš A, Andersen AJC, Lozano-Andrade CN, Kempen PJ, Kovács ÁT, Strube ML. Phages carry interbacterial weapons encoded by biosynthetic gene clusters. Curr Biol. 2021;31:3479-3489.e5. doi:10.1016/j.cub.2021.05.046.
66. Mahony J, van Sinderen D. Current taxonomy of phages infecting lactic acid bacteria. Front Microbiol. 2014;5:7. doi:10.3389/fmicb.2014.00007.
67. Ackermann HW. Tailed bacteriophages: the order caudovirales. Adv Virus Res. 1998;51:135–201. doi:10.1016/s0065-3527(08)60785-x.
68. Turner D, Shkoporov AN, Lood C, Millard AD, Dutilh BE, Alfenas-Zerbini P, et al. Abolishment of morphology-based taxa and change to binomial species names: 2022

taxonomy update of the ICTV bacterial viruses subcommittee. Arch Virol. 2023;168:74. doi:10.1007/s00705-022-05694-2.

69. Canchaya C, Proux C, Fournous G, Bruttin A, Brüssow H. Prophage genomics. Microbiol Mol Biol Rev. 2003;67:238-76, table of contents. doi:10.1128/MMBR.67.2.238–276.2003.
70. Murphy J, Mahony J, Fitzgerald GF, van Sinderen D. Bacteriophages Infecting Lactic Acid Bacteria. In: Cheese: Elsevier; 2017. p. 249–272. doi:10.1016/B978-0-12-417012-4.00010-7.
71. Pei Z, Sadiq FA, Han X, Zhao J, Zhang H, Ross RP, et al. Comprehensive Scanning of Prophages in Lactobacillus: Distribution, Diversity, Antibiotic Resistance Genes, and Linkages with CRISPR-Cas Systems. mSystems. 2021;6:e0121120. doi:10.1128/mSystems.01211-20.
72. Ackermann H-W. Phage classification and characterization. Methods Mol Biol. 2009;501:127–40. doi:10.1007/978-1-60327-164-6_13.
73. Weinbauer MG. Ecology of prokaryotic viruses. FEMS Microbiol Rev. 2004;28:127–81. doi:10.1016/j.femsre.2003.08.001.
74. Mahony J, Ainsworth S, Stockdale S, van Sinderen D. Phages of lactic acid bacteria: the role of genetics in understanding phage-host interactions and their co-evolutionary processes. Virology. 2012;434:143–50. doi:10.1016/j.virol.2012.10.008.
75. Villion M, Moineau S. Bacteriophages of lactobacillus. Front Biosci (Landmark Ed). 2009;14:1661–83. doi:10.2741/3332.
76. Paul JH, Jiang SC. Lysogeny and transduction. In: Marine Microbiology: Elsevier; 2001. p. 105–125. doi:10.1016/S0580-9517(01)30042-9.
77. Goerke C, Köller J, Wolz C. Ciprofloxacin and trimethoprim cause phage induction and virulence modulation in Staphylococcus aureus. Antimicrob Agents Chemother. 2006;50:171–7. doi:10.1128/AAC.50.1.171-177.2006.
78. Kenyon CJ, Walker GC. DNA-damaging agents stimulate gene expression at specific loci in Escherichia coli. Proc Natl Acad Sci U S A. 1980;77:2819–23. doi:10.1073/pnas.77.5.2819.
79. Rastogi RP, Richa, Kumar A, Tyagi MB, Sinha RP. Molecular mechanisms of ultraviolet radiation-induced DNA damage and repair. J Nucleic Acids. 2010;2010:592980. doi:10.4061/2010/592980.

80. Galkin VE, Yu X, Bielnicki J, Ndjonka D, Bell CE, Egelman EH. Cleavage of bacteriophage lambda cI repressor involves the RecA C-terminal domain. J Mol Biol. 2009;385:779–87. doi:10.1016/j.jmb.2008.10.081.
81. Little JW. Autodigestion of lexA and phage lambda repressors. Proc Natl Acad Sci U S A. 1984;81:1375–9. doi:10.1073/pnas.81.5.1375.
82. Tomasz M. Mitomycin C: small, fast and deadly (but very selective). Chemistry & Biology. 1995;2:575–9. doi:10.1016/1074-5521(95)90120-5.
83. Bearson BL, Brunelle BW. Fluoroquinolone induction of phage-mediated gene transfer in multidrug-resistant Salmonella. Int J Antimicrob Agents. 2015;46:201–4. doi:10.1016/j.ijantimicag.2015.04.008.
84. Revitt-Mills SA, Wright EK, Vereker M, O'Flaherty C, McPherson F, Dawson C, et al. Defects in DNA double-strand break repair resensitize antibiotic-resistant Escherichia coli to multiple bactericidal antibiotics. Microbiologyopen. 2022;11:e1316. doi:10.1002/mbo3.1316.
85. Lunde M, Aastveit AH, Blatny JM, Nes IF. Effects of diverse environmental conditions on {phi}LC3 prophage stability in Lactococcus lactis. Appl Environ Microbiol. 2005;71:721–7. doi:10.1128/AEM.71.2.721–727.2005.
86. Kourilsky P. Lysogenization by bacteriophage lambda. I. Multiple infection and the lysogenic response. Mol Gen Genet. 1973;122:183–95. doi:10.1007/BF00435190.
87. Wegrzyn G, Wegrzyn A. Genetic switches during bacteriophage lambda development. Prog Nucleic Acid Res Mol Biol. 2005;79:1–48. doi:10.1016/S0079-6603(04)79001-7.
88. Zhang M, Zhang T, Yu M, Chen Y-L, Jin M. The Life Cycle Transitions of Temperate Phages: Regulating Factors and Potential Ecological Implications. Viruses 2022. doi:10.3390/v14091904.
89. Alexeeva S, Guerra Martínez JA, Spus M, Smid EJ. Spontaneously induced prophages are abundant in a naturally evolved bacterial starter culture and deliver competitive advantage to the host. BMC Microbiol. 2018;18:120. doi:10.1186/s12866-018-1229-1.
90. Mahony J, Martel B, Tremblay DM, Neve H, Heller KJ, Moineau S, van Sinderen D. Identification of a new P335 subgroup through molecular analysis of lactococcal phages Q33 and BM13. Appl Environ Microbiol. 2013;79:4401–9. doi:10.1128/AEM.00832-13.
91. Aucouturier A, Chain F, Langella P, Bidnenko E. Characterization of a Prophage-Free Derivative Strain of Lactococcus lactis ssp. lactis IL1403 Reveals the Importance of Prophages for Phenotypic Plasticity of the Host. Front Microbiol. 2018;9:2032. doi:10.3389/fmicb.2018.02032.

92. Sun S, Zhang X. Genetic characteristics and integration specificity of Salmonella enterica temperate phages. Front Microbiol. 2023;14:1199843. doi:10.3389/fmicb.2023.1199843.
93. Suzuki S, Yoshikawa M, Imamura D, Abe K, Eichenberger P, Sato T. Compatibility of Site-Specific Recombination Units between Mobile Genetic Elements. iScience. 2020;23:100805. doi:10.1016/j.isci.2019.100805.
94. Ruiz-Cruz S, Parlindungan E, Erazo Garzon A, Alqarni M, Lugli GA, Ventura M, et al. Lysogenization of a Lactococcal Host with Three Distinct Temperate Phages Provides Homologous and Heterologous Phage Resistance. Microorganisms 2020. doi:10.3390/microorganisms8111685.
95. Bobay L-M, Rocha EPC, Touchon M. The adaptation of temperate bacteriophages to their host genomes. Mol Biol Evol. 2013;30:737–51. doi:10.1093/molbev/mss279.
96. Desiere F, Lucchini S, Bruttin A, Zwahlen MC, Brüssow H. A highly conserved DNA replication module from Streptococcus thermophilus phages is similar in sequence and topology to a module from Lactococcus lactis phages. Virology. 1997;234:372–82. doi:10.1006/viro.1997.8643.
97. Arai K, Low RL, Kornberg A. Movement and site selection for priming by the primosome in phage phi X174 DNA replication. Proc Natl Acad Sci U S A. 1981;78:707–11. doi:10.1073/pnas.78.2.707.
98. Feyereisen M, Mahony J, Neve H, Franz CMAP, Noben J-P, O'Sullivan T, et al. Biodiversity and Classification of Phages Infecting Lactobacillus brevis. Front Microbiol. 2019;10:2396. doi:10.3389/fmicb.2019.02396.
99. Aksyuk AA, Rossmann MG. Bacteriophage assembly. Viruses. 2011;3:172–203. doi:10.3390/v3030172.
100. Mahony J, Alqarni M, Stockdale S, Spinelli S, Feyereisen M, Cambillau C, van Sinderen D. Functional and structural dissection of the tape measure protein of lactococcal phage TP901-1. Sci Rep. 2016;6:36667. doi:10.1038/srep36667.
101. Mahony J, Oliveira J, Collins B, Hanemaaijer L, Lugli GA, Neve H, et al. Genetic and functional characterisation of the lactococcal P335 phage-host interactions. BMC Genomics. 2017;18:146. doi:10.1186/s12864-017-3537-5.
102. Mahony J, Cambillau C, van Sinderen D. Host recognition by lactic acid bacterial phages. FEMS Microbiol Rev. 2017;41:S16-S26. doi:10.1093/femsre/fux019.
103. Legrand P, Collins B, Blangy S, Murphy J, Spinelli S, Gutierrez C, et al. The Atomic Structure of the Phage Tuc2009 Baseplate Tripod Suggests that Host Recognition

Involves Two Different Carbohydrate Binding Modules. mBio. 2016;7:e01781-15. doi:10.1128/mBio.01781-15.

104. Leroy F, Charmpi C, Vuyst L de. Meat fermentation at a crossroads: where the age-old interplay of human, animal, and microbial diversity and contemporary markets meet. FEMS Microbiol Rev 2023. doi:10.1093/femsre/fuad016.

105. Jensen LB, Paddock LS. Sausage treatment with lactobacilli; April 7, 1939.

106. DSMZ. MRS medium.doc. 2007. https://www.dsmz.de/microorganisms/medium/pdf/DSMZ_Medium11.pdf. Accessed 7 May 2024.

107. DSMZ. Tryptone soya broth (TSB). 2022. https://www.dsmz.de/microorganisms/medium/pdf/DSMZ_Medium545.pdf. Accessed 7 May 2024.

108. SM buffer. Cold Spring Harb Protoc. 2006;2006:pdb.rec8111. doi:10.1101/pdb.rec8111.

109. Cold Spring Harbor Protocols. SM buffer with gelatin. Cold Spring Harb Protoc. 2006;2006:pdb.rec466. doi:10.1101/pdb.rec466.

110. Wick RR, Judd LM, Gorrie CL, Holt KE. Unicycler: resolving bacterial genome assemblies from short and long sequencing reads 2016. doi:10.1371/journal.pcbi.1005595.

111. Li W, O'Neill KR, Haft DH, DiCuccio M, Chetvernin V, Badretdin A, et al. RefSeq: expanding the Prokaryotic Genome Annotation Pipeline reach with protein family model curation. Nucleic Acids Res. 2021;49:D1020-D1028. doi:10.1093/nar/gkaa1105.

112. Tatusova T, DiCuccio M, Badretdin A, Chetvernin V, Nawrocki EP, Zaslavsky L, et al. NCBI prokaryotic genome annotation pipeline. Nucleic Acids Res. 2016;44:6614–24. doi:10.1093/nar/gkw569.

113. Haft DH, DiCuccio M, Badretdin A, Brover V, Chetvernin V, O'Neill K, et al. RefSeq: an update on prokaryotic genome annotation and curation. Nucleic Acids Res. 2018;46:D851-D860. doi:10.1093/nar/gkx1068.

114. Kaletta J, Pickl C, Griebler C, Klingl A, Kurmayer R, Deng L. A rigorous assessment and comparison of enumeration methods for environmental viruses. Sci Rep. 2020;10:18625. doi:10.1038/s41598-020-75490-y.

115. Richter M, Rosselló-Móra R, Oliver Glöckner F, Peplies J. JSpeciesWS: a web server for prokaryotic species circumscription based on pairwise genome comparison. Bioinformatics. 2016;32:929–31. doi:10.1093/bioinformatics/btv681.

116. Arndt D, Grant JR, Marcu A, Sajed T, Pon A, Liang Y, Wishart DS. PHASTER: a better, faster version of the PHAST phage search tool. Nucleic Acids Res. 2016;44:W16-21. doi:10.1093/nar/gkw387.

117. Zhou Y, Liang Y, Lynch KH, Dennis JJ, Wishart DS. PHAST: a fast phage search tool. Nucleic Acids Res. 2011;39:W347-52. doi:10.1093/nar/gkr485.

118. Wishart DS, Han S, Saha S, Oler E, Peters H, Grant JR, et al. PHASTEST: faster than PHASTER, better than PHAST. Nucleic Acids Res. 2023;51:W443-W450. doi:10.1093/nar/gkad382.

119. ICTV. 28.07.2023. https://talk.ictvonline.org/information/w/faq/386/how-to-write-virus-species-and-other-taxa-names. Accessed 28 Jul 2023.

120. Sullivan MJ, Petty NK, Beatson SA. Easyfig: a genome comparison visualizer. Bioinformatics. 2011;27:1009–10. doi:10.1093/bioinformatics/btr039.

121. Kumar S, Stecher G, Li M, Knyaz C, Tamura K. MEGA X: Molecular Evolutionary Genetics Analysis across Computing Platforms. Mol Biol Evol. 2018;35:1547–9. doi:10.1093/molbev/msy096.

122. Chan PP, Lin BY, Mak AJ, Lowe TM. tRNAscan-SE 2.0: improved detection and functional classification of transfer RNA genes. Nucleic Acids Res. 2021;49:9077–96. doi:10.1093/nar/gkab688.

123. Lowe TM, Chan PP. tRNAscan-SE On-line: integrating search and context for analysis of transfer RNA genes. Nucleic Acids Res. 2016;44:W54-7. doi:10.1093/nar/gkw413.

124. Roberts RJ, Vincze T, Posfai J, Macelis D. REBASE: a database for DNA restriction and modification: enzymes, genes and genomes. Nucleic Acids Res. 2023;51:D629-D630. doi:10.1093/nar/gkac975.

125. Alcock BP, Huynh W, Chalil R, Smith KW, Raphenya AR, Wlodarski MA, et al. CARD 2023: expanded curation, support for machine learning, and resistome prediction at the Comprehensive Antibiotic Resistance Database. Nucleic Acids Res. 2023;51:D690-D699. doi:10.1093/nar/gkac920.

126. Janßen D, Ehrmann MA, Vogel RF. Monitoring of assertive Lactobacillus sakei and Lactobacillus curvatus strains using an industrial ring trial experiment. J Appl Microbiol. 2019;126:545–54. doi:10.1111/jam.14144.

127. Ambros CL, Ehrmann MA. Distribution, inducibility, and characterisation of prophages in Latilactobacillus sakei. BMC Microbiol. 2022;22:267. doi:10.1186/s12866-022-02675-y.

128. Ambros CL, Ehrmann MA. Distribution, inducibility, and characteristics of Latilactobacillus curvatus temperate phages. Microbiome Res Rep 2023. doi:10.20517/mrr.2023.18.

129. Ambros CL, Ehrmann MA. Fate, Inducibility, and Behavior of Latilactobacillus curvatus Temperate Phage TMW 1.591 P1 during Sausage Fermentation. J Appl Microbiol 2024. doi:10.1093/jambio/lxae175.

130. Lee S, Lewis DEA, Adhya S. The Developmental Switch in Bacteriophage λ: A Critical Role of the Cro Protein. J Mol Biol. 2018;430:58–68. doi:10.1016/j.jmb.2017.11.005.

131. Sigma-Aldrich Corp. Mitomycin C - Product Information Sheet.

132. Euler CW, Juncosa B, Ryan PA, Deutsch DR, McShan WM, Fischetti VA. Targeted Curing of All Lysogenic Bacteriophage from Streptococcus pyogenes Using a Novel Counter-selection Technique. PLoS One. 2016;11:e0146408. doi:10.1371/journal.pone.0146408.

133. Kiliç AO, Pavlova SI, Ma WG, Tao L. Analysis of Lactobacillus phages and bacteriocins in American dairy products and characterization of a phage isolated from yogurt. Appl Environ Microbiol. 1996;62:2111–6. doi:10.1128/AEM.62.6.2111-2116.1996.

134. Puspurs AH, Trun NJ, Reeve JN. Bacteriophage Mu DNA circularizes following infection of Escherichia coli. The EMBO Journal. 1983;2:345–52. doi:10.1002/j.1460-2075.1983.tb01429.x.

135. Mardanov AV, Ravin NV. Conversion of linear DNA with hairpin telomeres into a circular molecule in the course of phage N15 lytic replication. J Mol Biol. 2009;391:261–8. doi:10.1016/j.jmb.2009.06.021.

136. Asadulghani M, Ogura Y, Ooka T, Itoh T, Sawaguchi A, Iguchi A, et al. The defective prophage pool of Escherichia coli O157: prophage-prophage interactions potentiate horizontal transfer of virulence determinants. PLoS Pathog. 2009;5:e1000408. doi:10.1371/journal.ppat.1000408.

137. Casjens SR, Gilcrease EB. Determining DNA packaging strategy by analysis of the termini of the chromosomes in tailed-bacteriophage virions. Methods Mol Biol. 2009;502:91–111. doi:10.1007/978-1-60327-565-1_7.

138. Turner D, Adriaenssens EM, Tolstoy I, Kropinski AM. Phage Annotation Guide: Guidelines for Assembly and High-Quality Annotation. Phage (New Rochelle). 2021;2:170–82. doi:10.1089/phage.2021.0013.

139. Bradley DE. Ultrastructure of bacteriophage and bacteriocins. Bacteriol Rev. 1967;31:230–314. doi:10.1128/br.31.4.230-314.1967.

140. Adriaenssens EM, Sullivan MB, Knezevic P, van Zyl LJ, Sarkar BL, Dutilh BE, et al. Taxonomy of prokaryotic viruses: 2018-2019 update from the ICTV Bacterial and Archaeal Viruses Subcommittee. Arch Virol. 2020;165:1253–60. doi:10.1007/s00705-020-04577-8.

141. Beniac DR, Siemens CG, Wright CJ, Booth TF. A filtration based technique for simultaneous SEM and TEM sample preparation for the rapid detection of pathogens. Viruses. 2014;6:3458–71. doi:10.3390/v6093458.

142. Chen F, Wang K, Stewart J, Belas R. Induction of multiple prophages from a marine bacterium: a genomic approach. Appl Environ Microbiol. 2006;72:4995–5001. doi:10.1128/AEM.00056-06.

143. Bassi D, Milani G, Belloso Daza MV, Barbieri F, Montanari C, Lorenzini S, et al. Taxonomical Identification and Safety Characterization of Lactobacillaceae from Mediterranean Natural Fermented Sausages. Foods 2022. doi:10.3390/foods11182776.

144. Hoess RH, Landy A. Structure of the lambda att sites generated by int-dependent deletions. Proc Natl Acad Sci U S A. 1978;75:5437–41. doi:10.1073/pnas.75.11.5437.

145. Craig NL, editor. Mobile DNA II. Washington, DC: ASM Press; 2002.

146. Williams KP. Integration sites for genetic elements in prokaryotic tRNA and tmRNA genes: sublocation preference of integrase subfamilies. Nucleic Acids Res. 2002;30:866–75. doi:10.1093/nar/30.4.866.

147. Castillo A, Tello M, Ringwald K, Acuña LG, Quatrini R, Orellana O. A DNA segment encoding the anticodon stem/loop of tRNA determines the specific recombination of integrative-conjugative elements in Acidithiobacillus species. RNA Biol. 2018;15:492–9. doi:10.1080/15476286.2017.1408765.

148. Qin Y, Polacek N, Vesper O, Staub E, Einfeldt E, Wilson DN, Nierhaus KH. The highly conserved LepA is a ribosomal elongation factor that back-translocates the ribosome. Cell. 2006;127:721–33. doi:10.1016/j.cell.2006.09.037.

149. Vinopal RT, Hillman JD, Schulman H, Reznikoff WS, Fraenkel DG. New phosphoglucose isomerase mutants of Escherichia coli. J Bacteriol. 1975;122:1172–4. doi:10.1128/jb.122.3.1172-1174.1975.

150. Outten FW, Wood MJ, Munoz FM, Storz G. The SufE protein and the SufBCD complex enhance SufS cysteine desulfurase activity as part of a sulfur transfer pathway

for Fe-S cluster assembly in Escherichia coli. J Biol Chem. 2003;278:45713–9. doi:10.1074/jbc.M308004200.

151. Zheng M, Wang X, Templeton LJ, Smulski DR, LaRossa RA, Storz G. DNA microarray-mediated transcriptional profiling of the Escherichia coli response to hydrogen peroxide. J Bacteriol. 2001;183:4562–70. doi:10.1128/JB.183.15.4562–4570.2001.

152. Loś JM, Loś M, Wegrzyn A, Wegrzyn G. Hydrogen peroxide-mediated induction of the Shiga toxin-converting lambdoid prophage ST2-8624 in Escherichia coli O157:H7. FEMS Immunol Med Microbiol. 2010;58:322–9. doi:10.1111/j.1574-695X.2009.00644.x.

153. Maynard ND, Macklin DN, Kirkegaard K, Covert MW. Competing pathways control host resistance to virus via tRNA modification and programmed ribosomal frameshifting. Mol Syst Biol. 2012;8:567. doi:10.1038/msb.2011.101.

154. Casjens SR, Gilcrease EB, Huang WM, Bunny KL, Pedulla ML, Ford ME, et al. The pKO2 linear plasmid prophage of Klebsiella oxytoca. J Bacteriol. 2004;186:1818–32. doi:10.1128/JB.186.6.1818-1832.2004.

155. Rajagopala SV, Casjens S, Uetz P. The protein interaction map of bacteriophage lambda. BMC Microbiol. 2011;11:213. doi:10.1186/1471-2180-11-213.

156. Wendling CC, Refardt D, Hall AR. Fitness benefits to bacteria of carrying prophages and prophage-encoded antibiotic-resistance genes peak in different environments. Evolution. 2021;75:515–28. doi:10.1111/evo.14153.

157. Hickman AB, Dyda F. Mechanisms of DNA Transposition. Microbiol Spectr. 2015;3:MDNA3-0034-2014. doi:10.1128/microbiolspec.MDNA3-0034-2014.

158. Moura de Sousa JA, Pfeifer E, Touchon M, Rocha EPC. Causes and Consequences of Bacteriophage Diversification via Genetic Exchanges across Lifestyles and Bacterial Taxa. Mol Biol Evol. 2021;38:2497–512. doi:10.1093/molbev/msab044.

159. Hotopp JCD, Grifantini R, Kumar N, Tzeng YL, Fouts D, Frigimelica E, et al. Comparative genomics of Neisseria meningitidis: core genome, islands of horizontal transfer and pathogen-specific genes. Microbiology. 2006;152:3733–49. doi:10.1099/mic.0.29261-0.

160. O'Donoghue P, Ling J, Söll D. Transfer RNA function and evolution. RNA Biol. 2018;15:423–6. doi:10.1080/15476286.2018.1478942.

161. Yang JY, Fang W, Miranda-Sanchez F, Brown JM, Kauffman KM, Acevero CM, et al. Degradation of host translational machinery drives tRNA acquisition in viruses. Cell Syst. 2021;12:771-779.e5. doi:10.1016/j.cels.2021.05.019.

162. Bailly-Bechet M, Vergassola M, Rocha E. Causes for the intriguing presence of tRNAs in phages. Genome Res. 2007;17:1486–95. doi:10.1101/gr.6649807.

163. Yoshikawa G, Askora A, Blanc-Mathieu R, Kawasaki T, Li Y, Nakano M, et al. Xanthomonas citri jumbo phage XacN1 exhibits a wide host range and high complement of tRNA genes. Sci Rep. 2018;8:4486. doi:10.1038/s41598-018-22239-3.

164. McDonald MJ, Chou C-H, Swamy KBS, Huang H-D, Leu J-Y. The evolutionary dynamics of tRNA-gene copy number and codon-use in E. coli. BMC Evol Biol. 2015;15:163. doi:10.1186/s12862-015-0441-y.

165. Tomikawa C, Auxilien S, Guérineau V, Yoshioka Y, Miyoshi K, Hori H, et al. Characterization of redundant tRNAIles with CAU and UAU anticodons in Lactobacillus plantarum. J Biochem. 2018;163:233–41. doi:10.1093/jb/mvx075.

166. Gavini N, Pulakat L. The tRNA species for redundant genetic codons NNU and NNC. A thought on the absence of phenylalanine tRNA with AAA anticodon in Escherichia coli. J Biol Chem. 1992;267:2240–3.

167. Murphy J, Mahony J, Ainsworth S, Nauta A, van Sinderen D. Bacteriophage orphan DNA methyltransferases: insights from their bacterial origin, function, and occurrence. Appl Environ Microbiol. 2013;79:7547–55. doi:10.1128/AEM.02229-13.

168. Pingoud A, Fuxreiter M, Pingoud V, Wende W. Type II restriction endonucleases: structure and mechanism. Cell Mol Life Sci. 2005;62:685–707. doi:10.1007/s00018-004-4513-1.

169. Marinus MG, Morris NR. Biological function for 6-methyladenine residues in the DNA of Escherichia coli K12. J Mol Biol. 1974;85:309–22. doi:10.1016/0022-2836(74)90366-0.

170. Lahue RS, Au KG, Modrich P. DNA mismatch correction in a defined system. Science. 1989;245:160–4. doi:10.1126/science.2665076.

171. Bickle TA, Krüger DH. Biology of DNA restriction. Microbiol Rev. 1993;57:434–50. doi:10.1128/mr.57.2.434-450.1993.

172. Sternberg N, Coulby J. Cleavage of the bacteriophage P1 packaging site (pac) is regulated by adenine methylation. Proc Natl Acad Sci U S A. 1990;87:8070–4. doi:10.1073/pnas.87.20.8070.

173. Smith MJ, Jeddeloh JA. DNA methylation in lysogens of pathogenic Burkholderia spp. requires prophage induction and is restricted to excised phage DNA. J Bacteriol. 2005;187:1196–200. doi:10.1128/JB.187.3.1196–1200.2005.

174. Singer M, Boffelli D, Dhahbi J, Schönhuth A, Schroth GP, Martin DIK, Pachter L. MetMap enables genome-scale Methyltyping for determining methylation states in populations. PLoS Comput Biol. 2010;6:e1000888. doi:10.1371/journal.pcbi.1000888.

175. Johnston CD, Cotton SL, Rittling SR, Starr JR, Borisy GG, Dewhirst FE, Lemon KP. Systematic evasion of the restriction-modification barrier in bacteria. Proc Natl Acad Sci U S A. 2019;116:11454–9. doi:10.1073/pnas.1820256116.

176. Gasson MJ, Davies FL. Prophage-Cured Derivatives of Streptococcus lactis and Streptococcus cremoris. Appl Environ Microbiol. 1980;40:964–6. doi:10.1128/aem.40.5.964-966.1980.

177. Shmidov E, Zander I, Lebenthal-Loinger I, Karako-Lampert S, Shoshani S, Banin E. An Efficient, Counter-Selection-Based Method for Prophage Curing in Pseudomonas aeruginosa Strains. Viruses 2021. doi:10.3390/v13020336.

178. Cornuault JK, Moineau S. Induction and Elimination of Prophages Using CRISPR Interference. CRISPR J. 2021;4:549–57. doi:10.1089/crispr.2021.0026.

179. Davies EV, Winstanley C, Fothergill JL, James CE. The role of temperate bacteriophages in bacterial infection. FEMS Microbiol Lett. 2016;363:fnw015. doi:10.1093/femsle/fnw015.

180. Li X, Chen Y, Wang S, Duan X, Zhang F, Guo A, et al. Exploring the Benefits of Metal Ions in Phage Cocktail for the Treatment of Methicillin-Resistant Staphylococcus aureus (MRSA) Infection. Infect Drug Resist. 2022;15:2689–702. doi:10.2147/IDR.S362743.

181. Sciara G, Bebeacua C, Bron P, Tremblay D, Ortiz-Lombardia M, Lichière J, et al. Structure of lactococcal phage p2 baseplate and its mechanism of activation. Proc Natl Acad Sci U S A. 2010;107:6852–7. doi:10.1073/pnas.1000232107.

182. Veesler D, Spinelli S, Mahony J, Lichière J, Blangy S, Bricogne G, et al. Structure of the phage TP901-1 1.8 MDa baseplate suggests an alternative host adhesion mechanism. Proc Natl Acad Sci U S A. 2012;109:8954–8. doi:10.1073/pnas.1200966109.

183. Luque A, Silveira CB. Quantification of Lysogeny Caused by Phage Coinfections in Microbial Communities from Biophysical Principles. mSystems 2020. doi:10.1128/mSystems.00353-20.

184. Shao Q, Trinh JT, Zeng L. High-resolution studies of lysis-lysogeny decision-making in bacteriophage lambda. J Biol Chem. 2019;294:3343–9. doi:10.1074/jbc.TM118.003209.

185. Erez Z, Steinberger-Levy I, Shamir M, Doron S, Stokar-Avihail A, Peleg Y, et al. Communication between viruses guides lysis-lysogeny decisions. Nature. 2017;541:488–93. doi:10.1038/nature21049.

186. Lunde M, Blatny JM, Lillehaug D, Aastveit AH, Nes IF. Use of real-time quantitative PCR for the analysis of phiLC3 prophage stability in lactococci. Appl Environ Microbiol. 2003;69:41–8. doi:10.1128/AEM.69.1.41–48.2003.

187. Kaur L, Hui SX, Morton JD, Kaur R, Chian FM, Boland M. Endogenous Proteolytic Systems and Meat Tenderness: Influence of Post-Mortem Storage and Processing. Food Sci Anim Resour. 2021;41:589–607. doi:10.5851/kosfa.2021.e27.

188. Northrop JH. The Effect of Proteolytic Enzymes on E. coli Phages and on Native Proteins. J Gen Physiol. 1964;48:73–8. doi:10.1085/jgp.48.1.73.

189. Dos Santos BA, Campagnol PCB, da Cruz AG, Morgano MA, Wagner R, Pollonio MAR. Is there a potential consumer market for low-sodium fermented sausages? J Food Sci. 2015;80:S1093-9. doi:10.1111/1750-3841.12847.

190. Flores M, Nieto P, Ferrer JM, Flores J. Effect of calcium chloride on the volatile pattern and sensory acceptance of dry-fermented sausages. Eur Food Res Technol. 2005;221:624–30. doi:10.1007/s00217-005-0062-6.

191. Nurmahmudi, Veeramuthu GJ, Sams AR. Tenderizing spent fowl meat with calcium chloride. 2. The role of delayed application and ionic strength. Poult Sci. 1997;76:538–42. doi:10.1093/ps/76.3.538.

192. FoodData Central. 12.01.2024. https://fdc.nal.usda.gov/fdc-app.html#/food-details/174603/nutrients. Accessed 19 Jan 2024.

193. Lieb M. Studies of heat-inducible lambda bacteriophage. I. Order of genetic sites and properties of mutant prophages. J Mol Biol. 1966;16:149–63. doi:10.1016/S0022-2836(66)80269-3.

194. Tokman JI, Kent DJ, Wiedmann M, Denes T. Temperature Significantly Affects the Plaquing and Adsorption Efficiencies of Listeria Phages. Front Microbiol. 2016;7:631. doi:10.3389/fmicb.2016.00631.

195. Bell CE, Frescura P, Hochschild A, Lewis M. Crystal structure of the lambda repressor C-terminal domain provides a model for cooperative operator binding. Cell. 2000;101:801–11. doi:10.1016/s0092-8674(00)80891-0.

196. Senear DF, Laue TM, Ross JB, Waxman E, Eaton S, Rusinova E. The primary self-assembly reaction of bacteriophage lambda cI repressor dimers is to octamer. Biochemistry. 1993;32:6179–89. doi:10.1021/bi00075a010.

197. Sousa FJR, Lima LMTR, Pacheco ABF, Oliveira CLP, Torriani I, Almeida DF, et al. Tetramerization of the LexA repressor in solution: implications for gene regulation of the E.coli SOS system at acidic pH. J Mol Biol. 2006;359:1059–74. doi:10.1016/j.jmb.2006.03.069.

198. Tichaczek PS, Nissen-Meyer J, Nes IF, Vogel RF, Hammes WP. Characterization of the Bacteriocins Curvacin A from Lactobacillus curvatus LTH1174 and Sakacin P from L. sake LTH673. Systematic and Applied Microbiology. 1992;15:460–8. doi:10.1016/S0723-2020(11)80223-7.

199. Djenane D, Martínez L, Sánchez-Escalante A, Montañés L, Blanco D, Yangüela J, et al. Effect of Lactic Acid Bacteria on Beef Steak Microbial Flora Stored Under Modified Atmosphere and on Listeria Monocytogenes in Broth Cultures. Food sci. technol. int. 2006;12:287–95. doi:10.1177/1082013206067788.

200. Vaughan A, Eijsink VGH, van Sinderen D. Functional characterization of a composite bacteriocin locus from malt isolate Lactobacillus sakei 5. Appl Environ Microbiol. 2003;69:7194–203. doi:10.1128/AEM.69.12.7194–7203.2003.

201. Nissen-Meyer J, Oppegård C, Rogne P, Haugen HS, Kristiansen PE. The Two-Peptide (Class-IIb) Bacteriocins: Genetics, Biosynthesis, Structure, and Mode of Action. In: Drider D, Rebuffat S, editors. Prokaryotic Antimicrobial Peptides. New York, NY: Springer New York; 2011. p. 197–212. doi:10.1007/978-1-4419-7692-5_11.

202. Silpe JE, Wong JWH, Owen SV, Baym M, Balskus EP. The bacterial toxin colibactin triggers prophage induction. Nature. 2022;603:315–20. doi:10.1038/s41586-022-04444-3.

203. Rendueles C, Escobedo S, Rodríguez A, Martínez B. Bacteriocin-phage interaction (BaPI): Phage predation of Lactococcus in the presence of bacteriocins. Microbiologyopen. 2022;11:e1308. doi:10.1002/mbo3.1308.

204. Martínez B, Böttiger T, Schneider T, Rodríguez A, Sahl H-G, Wiedemann I. Specific interaction of the unmodified bacteriocin Lactococcin 972 with the cell wall precursor lipid II. Appl Environ Microbiol. 2008;74:4666–70. doi:10.1128/AEM.00092-08.

205. Wang I-N. Lysis timing and bacteriophage fitness. Genetics. 2006;172:17–26. doi:10.1534/genetics.105.045922.

206. Golec P, Dąbrowski K, Hejnowicz MS, Gozdek A, Loś JM, Węgrzyn G, et al. A reliable method for storage of tailed phages. J Microbiol Methods. 2011;84:486–9. doi:10.1016/j.mimet.2011.01.007.

8 APPENDIX

8.1 Data Availability

The forty *L. sakei* genomes (assembly levels "chromosome" and "complete"; last download: 6th May 2022) and fifty-six *L. curvatus* genomes (assembly levels: "complete", "genome", "scaffold", "contig"; last download: 10th August 2022) listed below were downloaded from the NCBI website for prophage mining.

L. sakei: 23K (NC_007576), C21B (NZ_CP043730), C22G (NZ_CP043729), CBA3614 (NZ_CP046037), CBA3635 (NZ_CP059697), DS4 (NZ_CP025839), DSM 20017^T (CP017271), E23B (NZ_CP043731), E28G (NZ_CP043728), FAM18311 (NZ_CP020459), FLEC01 (NZ_LT960777), J112 (NZ_LT907933), J156 (NZ_LT907929), J160x1 (NZ_LT907931), J18 (NZ_LT907930), J54 (NZ_LT960790), J64 (NZ_LT960781), LK-145 (NZ_AP017931), LZ217 (NZ_CP032652), MBEL1397 (NZ_CP048116), MFPB16A1401 (NZ_LT960788), MFPB19 (NZ_LT960784), ob4.1 (NZ_CP075489), Probio65 (NZ_CP020806), TMW 1.3 (CP016465), TMW 1.46 (CP015487), TMW 1.114 (CP017566), TMW 1.411 (QOSE01000001.1), TMW 1.417 (CP017568), TMW 1.578 (NZ_CP017570) TMW 1.1239 (CP017272), TMW 1.1396 (CP017273), TMW 1.1398 (CP017275), WiKim0063 (NZ_CP022709), WiKim0072 (NZ_CP025136), WiKim0073 (NZ_CP025203), WiKim0074 (NZ_CP025206), ZFM220 (NZ_CP032633), ZFM225 (NZ_CP032635), ZFM229 (NZ_CP032640).

L. curvatus: CBA3617 (NZ_CP042389), CRL 705 (NZ_AGBU01000145), DRD-164 (JAMRWB000000000), DRD-170 (JAMRWA010000000), DRD-171 (JAMRVZ010000000), ELA204023 (NZ_JAJJOM010000000), ELA204029 (NZ_JAJJON010000000), ELA204033 (NZ_JAJJOO010000000), ELA204092 (NZ_JAJJOT010000000), ELA204093 (NZ_JAIULW010000000), ELA204096 (NZ_JAJJOU010000000), ELA204098 (NZ_JAJJOV010000000), ELA204100 (NZ_JAIULV010000000), ELA214002 (NZ_JAJJOL010000000), ELA214059 (NZ_JAJJOP010000000), ELA214060 (NZ_JAJJOQ010000000), ELA214061 (NZ_JAJJOR010000000), ELA214062 (NZ_JAJJOS010000000), ELA214117 (NZ_JAJJOK010000000), ELA214388 (NZ_JAIULU010000000), FAM25164 (NZ_JAFJMA010000001), FBA2 (NZ_CP016028), IRG2 (NZ_CP025476), isolate FLEC03 chromosome LCUFL03 (NZ_LT841333), HFS9 (NZ_JAMOHH010000001), JCM 1096 = DSM 20019T (NZ_CP026116), KG6 (NZ_CP022475), MGYG-HGUT-00020 (NZ_CABIVZ010000001), MRS6 (NZ_CP022474),

NBRC 15884 (NZ_BJOQ01000001), NFH-Km12 (AP018699), NRIC0822 (NZ_JTJV01000001), RI-124 (NZ_MKDR01000001), RI-193 (NZ_MKGD01000001), RI-198 (NZ_MKGC01000001), RI-406 (NZ_MKDG01000001), S46 (NZ_SUMW01000010), SRCM103465 (NZ_CP035110), TMW 1.27 (CP016467), TMW 1.167 (CP016472), TMW 1.401 (CP016216), TMW 1.407 (CP016218), TMW 1.421 (CP016221), TMW 1.439 (CP015489), TMW 1.595 (CP016470), TMW 1.624 (CP015490), TMW 1.1381 (CP015493), TMW 1.1390 (CP015494), TMW 1.1408 (JAHIAF000000000), TMW 1.1928 (NZ_CP031003), TMW 1.2270 (JAHIAD000000000), VRA_2sq_f (NZ_WKLA01000324), VRA_2sq_n (NZ_WKKT01000028), WDN19 (NZ_AP024685), WiKim38 (NZ_CP017124), ZJUNIT8 (NZ_CP029966).

The following lactobacilli phage genomes were used for phylogenetic analyses: *Levilactobacillus brevis*: 3-521 (MK504444.1), 3-SAC12 (MK504442.1), 521B (MK504443.1), ATCCB (MK504445.1), JNU_P2 (MN830254), JNU_P4 (MN830255), Lb (MG020111.1), LBR48 (GU967410.1), SA-C12 (KU052488.1), SAC12B (MK504446.1). *Lacticaseibacillus casei*: A2 (NC_004112.1), J-1 (KC171646.1), LJ (MF999224.1), phiAT3 (NC_005893.1), PL-1 (KC171647.1), PLE2 (KU848187.1), PLE3 (KU848186.1). *Lactobacillus delbrueckii*: c5 (EU340421.2), JCL1032 (EU409559.1), Ld17 (KJ564037.1), Ld25A (KJ564036.1), Ld3 (KJ564038.1), Ldl1 (KM514685.1), LL-H (EF455602.1), LL-Ku (AY739900.2), P1174 (MG913376.1), phiJB (KF188409.1), phiLdb (KF188410.1). *Limosilactobacillus fermentum*: JNU_P1 (MN830252), JNU_P5 (MN830253), LF1 (HQ141410.1), LfeInf (KP054477.1), LfeSau (KP027015.1), phiPYB5 (GU323708.1). *Lactobacillus gasseri*: JNU_P11 (MN830257), JNU_P7 (MN830256), KC5a (DQ320509.1), phi jlb1 (KF767351.1), phiadh (AJ131519.1). *Lactobacillus helveticus*: phiAQ113 (HE956704.1). *Lactobacillus jensenii*: Lv-1 (EU871039.1). *Ligilactobacillus murinus*: phiEF-1.1 (MF041990.1). *Lacticaseibacillus paracasei*: CL1 (KR905066.1), CL2 (KR905067.1), iLp1308 (KR905070.1), iLp84 (KR905069.1), JNU_P10 (MN830259), JNU_P9 (MN830258), T25 (AP018361.1). *Lactiplantibacillus pentosus* & *Lactiplantibacillus plantarum*: LpeD (MF787246.1). *Lactiplantibacillus plantarum*: ATCC8014-B1 (JX486087.1), ATCC8014-B2 (JX486088.1), Bacchae (MG765277.2), Bassarid (MG765275.2), Bromius (MH809531.1), Dionysus (MH809530.1), Iacchus (MH809529.1), LP65 (NC_006565.1), Lpa804 (MG557979.1), Maenad (MG765274.1), Nyseid (MG765276.1), P1 (KX223815.1), P2 (KY381600.1), phig1e (NC_004305.1), phiJL-1 (NC_006936.1), PM411 (MG788324.1), Sabazios (MH809528.1), Satyr (MG744354.1), Semele (MG765279.2), Sha1 (HQ141411.1), Silenus (MG765278.2). *Limosilactobacillus reuteri*: LR1 (MH837542.1), LR2 (MH837543.1).

Lacticaseibacillus rhamnosus: BH1 (MH983004.1), Lc-Nu (NC_007501.1), Lrm1 (EU246945.1). *Fructilactobacillus sanfranciscensis*: EV3 (LN885237.1).

Furthermore, the genomes of seven *L. sakei* and five *L. curvatus* screened strains, most of them (with the exception of TMW 1.2 and TMW 1.1500) with lytic behaviour after induction (compare Chapter 4.1.1), were sequenced and provided (NCBI) under the accession numbers listed below:

L. sakei: TMW 1.2 (JAMOWF000000000), TMW 1.23 (JAHIAK000000000), TMW 1.1290 (JAHIAJ000000000), TMW 1.1386 (JAHIAI000000000), TMW 1.1393 (JAHIAH000000000), TMW 1.1397 (JAMOWE000000000), TMW 1.1500 (JAMOWD000000000). *L. curvatus*: TMW 1.591 (JAHIAT000000000), TMW 1.706 (JAHIAS000000000), TMW 1.1365 (JAHIAR000000000), TMW 1.1447 (JAHIAQ000000000), TMW 1.2272 (JAHIAP000000000).

The sequenced genomes of five *L. sakei* and nine *L. curvatus* phages from purified phage particles are provided under the following accession numbers (NCBI):

L. sakei phages: TMW 1.46 P1 (OP455939), TMW 1.46 P2 (OP455940), TMW 1.1386 P1 (OP455936), TMW 1.1393 P1 (OP455937), TMW 1.1397 P1 (OP455938). *L. curvatus* phages: TMW 1.591 P1 (OQ240252), TMW 1.706 P1 (OQ240253), TMW 1.706 P2 (OQ240254), TMW 1.1365 P1 (OQ240255), TMW 1.1365 P2 (OQ240256), TMW 1.1365 P3 (OQ240257), TMW 1.1381 P1 (OQ240258), TMW 1.1447 P1 (OQ240259), TMW 1.2272 P1 (OQ240260).

8.2 Excluded, Non-Sequenced, or Non-Inducible Strains During the Lysogen Screening

8.2.1 Lysis Monitoring After Ultraviolet Light Treatment

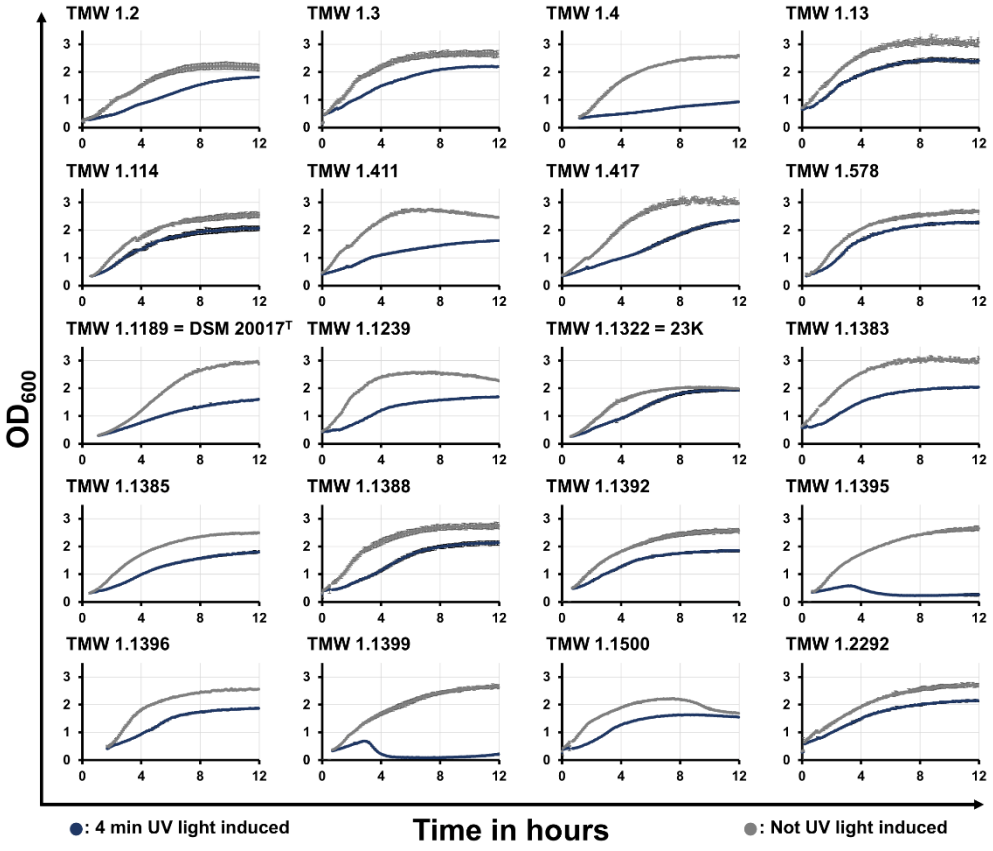

Figure 35. Growth of excluded, non-sequenced, or non-UV-light-inducible *L. sakei* strains. The growth was monitored after a 4-minute UV light treatment (blue data points). Untreated samples (grey data points) served as controls. *L. sakei* TMW 1.1399 was excluded due to high genome similarities with *L. sakei* TMW 1.1386. *L. sakei* TMW 1.1395 was excluded because of high similarities to TMW 1.1399 according to unshown randomly amplified polymorphic DNA PCR data.

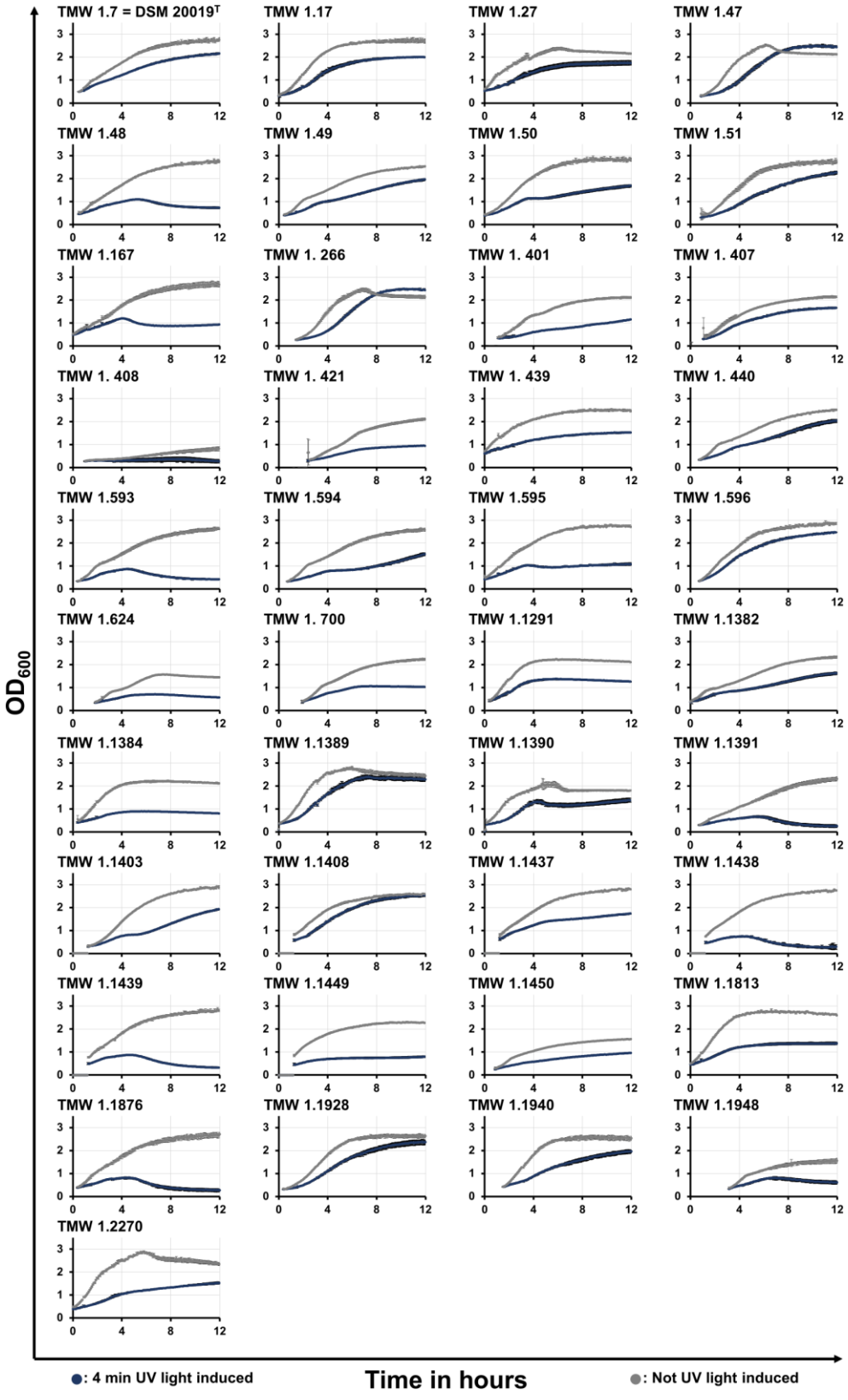

Figure 36. Growth of excluded, non-sequenced, or non-UV-light-inducible *L. curvatus* strains. The growth was monitored after a 4-minute UV light treatment (blue data points). Untreated samples (grey data points) served as controls.

8.2.2 Lysis Monitoring After Mitomycin C Treatment

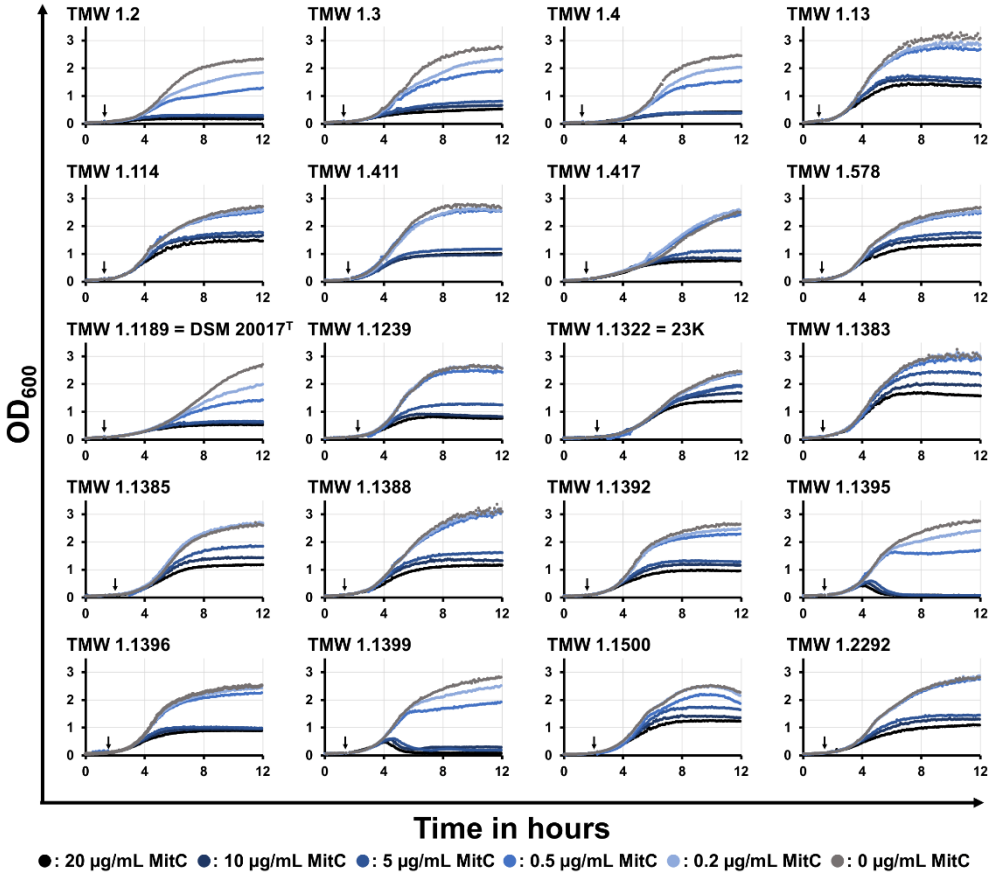

Figure 37. Growth of excluded, non-sequenced, or non-MitC-inducible *L. sakei* strains. Black arrows indicate time of MitC addition in concentrations ranging from 0.2-20 µg/mL. *L. sakei* TMW 1.1399 was excluded due to high genome similarities with *L. sakei* TMW 1.1386. *L. sakei* TMW 1.1395 was excluded because of high similarities to TMW 1.1399 according to unshown randomly amplified polymorphic DNA PCR data. Adapted from [127], modified.

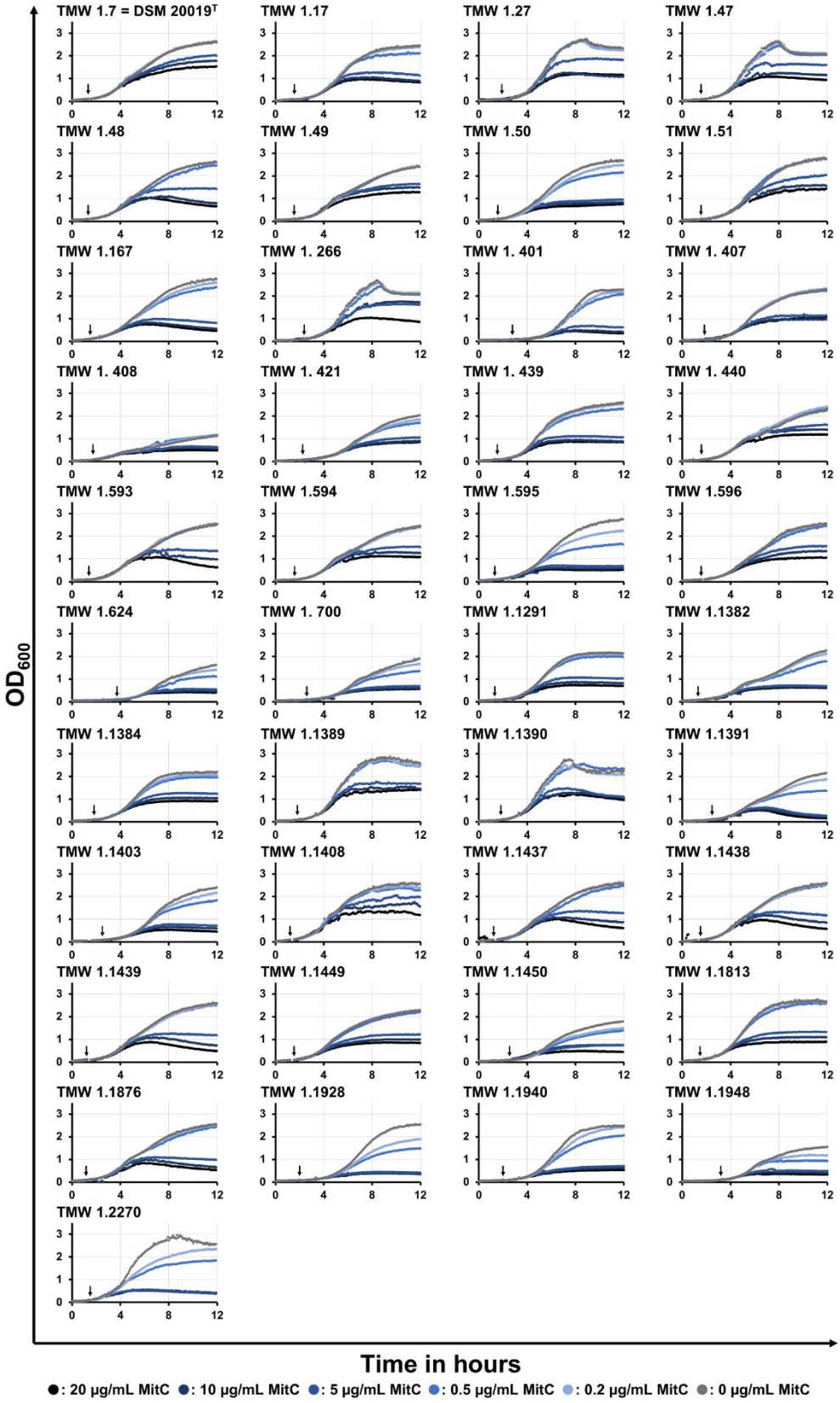

Figure 38. Growth of excluded, non-sequenced, or non-MitC-inducible *L. curvatus* strains. Black arrows indicate time of MitC addition in concentrations ranging from 0.2-20 µg/mL.

8.3 Induction Verification via Prophage-Virion DNA Alignments

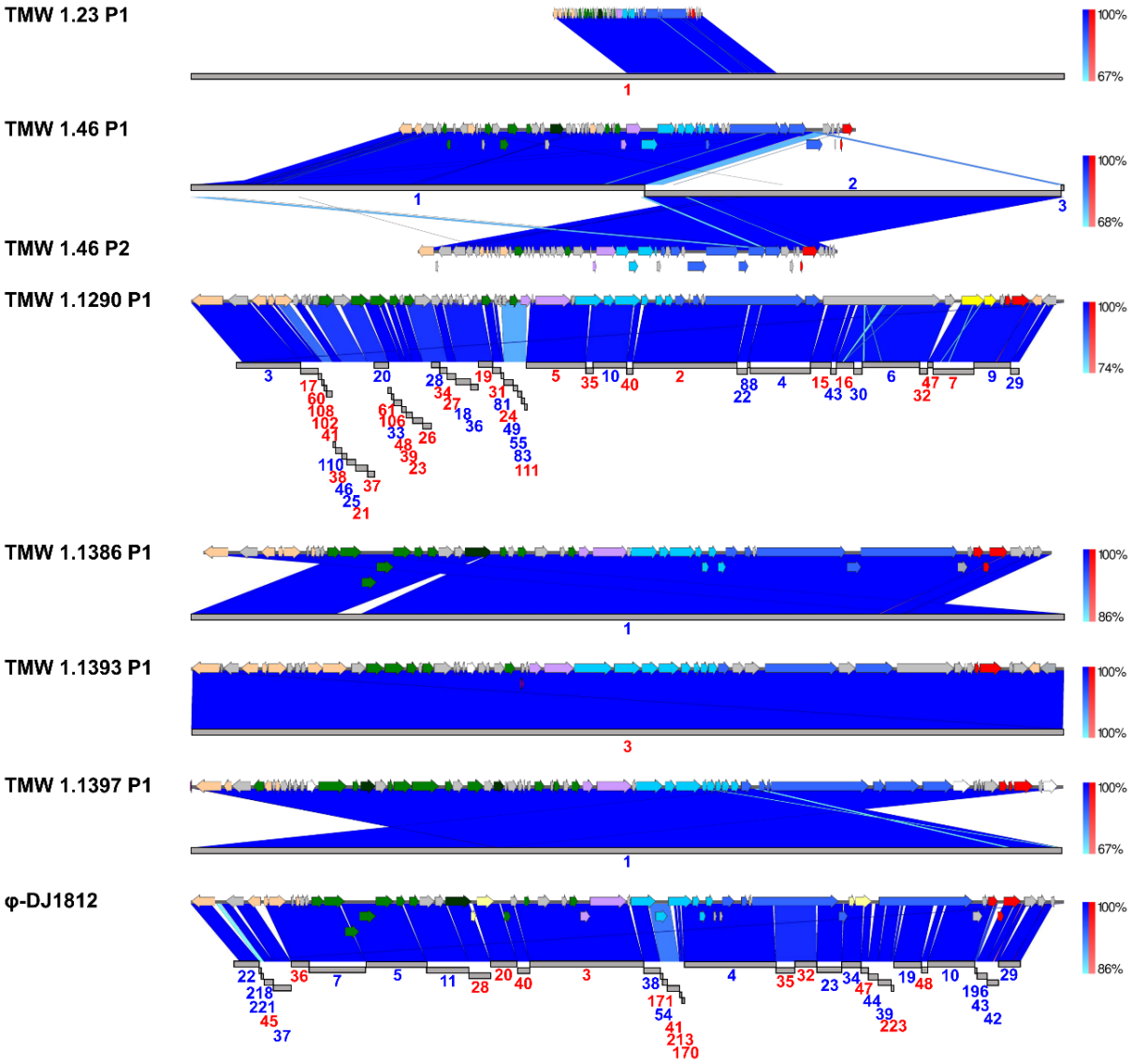

Figure 39. Induction verification via sequence alignments between *L. sakei* prophages and isolated phage DNA. If required, phage-related contigs (grey bars) were sorted, oriented, and concatenated before the alignment. The contig identifiers are depicted below respective contigs in blue (sequence was not oriented) or red (reverse complement was used). BLAST legends are shown on the right side of each alignment. Darker bars between sequences indicate higher similarity. Prophage genes are colourised after their predicted task: Lysogeny (ochre), replication (green), packaging (lilac), head (light blue), tail (dark blue), fibre (yellow), lysis (red), hypothetical protein (grey), transposase (light yellow), unknown task (white), MTase (dark green), and tRNA (pink). Sequences were joined for the analysis of TMW 1.1386 P1.

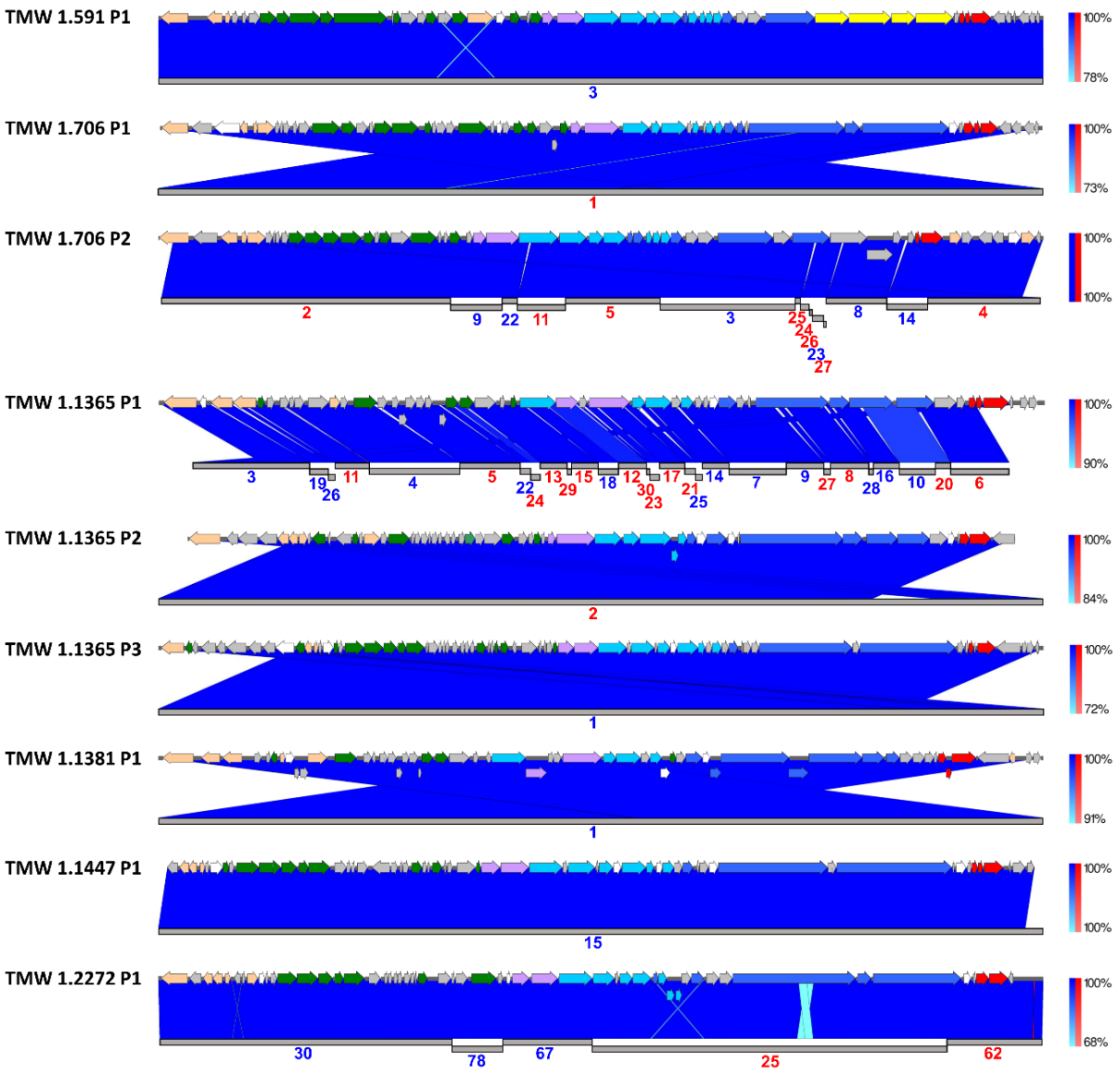

Figure 40. Induction verification via sequence alignments between *L. curvatus* prophages and isolated phage DNA. If required, phage-related contigs (grey bars) were sorted, oriented, and concatenated before the alignment. The contig identifiers are depicted below respective contigs in blue (sequence was not oriented) or red (reverse complement was used). BLAST legends are shown on the right side of each alignment. Darker bars between sequences indicate higher similarity. Prophage genes are colourised after their predicted task: Lysogeny (ochre), replication (green), packaging (lilac), head (light blue), tail (dark blue), fibre (yellow), lysis (red), hypothetical protein (grey), transposase (light yellow), unknown task (white), MTase (dark green), and tRNA (pink).

8.4 Prophage Distribution and Inducibility

Four *L. sakei* genomes (TMW 1.578 excluded to high similarity to TMW 1.114; ZFM220, ZFM225, and ZFM229 excluded to high similarity to LZ217) and 16 *L. curvatus* genomes (DRD-170, DRD-171 similar to DRD-164; ELA204023, ELA204033, ELA204093, ELA204096 similar to ELA204092; ELA204029, ELA204098, ELA204100 similar to ELA214002; ELA214059 similar to ELA214060; NBRC 15884 similar to TMW 1.706; RI-193, RI-198, TMW 1.167, TMW 1.439 similar to TMW 1.1381; VRA_2sq_n similar to VRA_2sq_f) were excluded. TMW 1.1386 and TMW 1.1398 were included despite TMW 1.1398 sharing 99.7% ANIb over 95.11% of aligned nucleotides. This was done because strains displayed different phage-mediated host lysis responses after induction. The *L. curvatus* strains TMW 1.706 and JCM 1096 = DSM 20019^T = TMW 1.7 were included for the same reason despite 100.00% ANIb over 99.95% AP. *L. curvatus* DRD-164 was included as it differed in its prophages from *L. curvatus* TMW 1.1447 P1 despite the overall close relationship between the strains (99.52% ANIb over 95.39% AP). The genome of *L. sakei* TMW 1.1399 was excluded after sequencing (unpublished data) due to high similarity to the genome of *L. sakei* TMW 1.1386 (*L. sakei* TMW 1.1399 shares 99.65% ANIb over 97.40% AP with strain TMW 1.1386).

Table 9. Prophage distribution and inducibility in *L. sakei*. The number and completeness evaluation ("i", intact; "q", questionable; "inc", incomplete) of prophages as predicted via PHASTER are listed. Moreover, the isolation source of analysed *L. sakei* strains (accession numbers: Appendix; Chapter 8.1) and the lysis response of accessible strains after phage induction with UV light or MitC ("+", strong lysis; "(+)", weak lysis; "-", no visible lysis) are included. "nd," no genome/strain was available. "Ex", excluded due to high genome similarity with other strains. Adapted from [127], modified.

***L. sakei* strain**	**Isolation source (Origin)**	**Prophages**			**Inducibility**	
		i	**q**	**inc**	**UV**	**MitC**
23K	Meat	0	0	2	-	-
C21B	Artisanal dry-fermented salami (Italy)	1	0	1	nd	nd
C22G	Artisanal dry-fermented salami (Italy)	0	0	1	nd	nd
CBA3614	Kimchi (South Korea)	0	0	2	nd	nd
CBA3635	Fermented vegetables (South Korea)	2	0	1	nd	nd
DS4	Korean kimchi (South Korea)	1	0	0	nd	nd
DSM 20017T = TMW 1.1189	Moto	0	1	2	-	-
E23B	Artisanal dry-fermented salami (Italy)	0	0	1	nd	nd
E28G	Artisanal dry-fermented salami (Italy)	1	0	1	nd	nd
FAM18311	Food (Switzerland)	1	0	0	nd	nd
FLEC01	Human faeces	0	0	1	nd	nd
J112	French dry-type pork sausage	0	1	1	nd	nd

L. sakei strain	Isolation source (Origin)	Prophages			Inducibility	
		i	q	inc	UV	MitC
J156	French dry-type pork sausage	0	0	2	nd	nd
J160x1	Horse meat	0	0	1	nd	nd
J18	French dry-type pork sausage	0	0	2	nd	nd
J54	French dry-type pork sausage	0	1	1	nd	nd
J64	French dry-type pork sausage	3	0	1	nd	nd
LK-145	Japanese sake cellar (Japan)	0	1	3	nd	nd
LZ217	Fermented vegetables (China)	1	0	0	nd	nd
MBEL1397	Kimchi (South Korea)	0	0	2	nd	nd
MFPB16A1401	Beef carpaccio	1	0	1	nd	nd
MFPB19	Beef carpaccio	1	0	0	nd	nd
ob4.1	Human faeces (South Korea)	1	1	2	nd	nd
Probio65	Kimchi	2	0	1	nd	nd
TMW 1.2	Fermented sausage (Spain)	0	0	1	-	-
TMW 1.3	Fermented sausage (Spain)	0	0	2	-	-
TMW 1.4	Fermented sausage (Spain)	nd	nd	nd	-	-
TMW 1.13	Starter culture (Germany)	nd	nd	nd	-	-
TMW 1.23	Fermented sausage (Germany)	1	0	0	(+)	+
TMW 1.46	Starter culture (Germany)	2	1	0	+	+
TMW 1.114	Starter culture (Germany)	0	1	3	-	-
TMW 1.411	Sauerkraut (Germany)	1	0	0	-	-
TMW 1.417	Starter culture (Germany)	0	1	2	-	-
TMW 1.578	Unknown	ex	ex	ex	-	-
TMW 1.1239	Wheat sourdough (France)	0	1	0	-	-
TMW 1.1290	Fermented sausage (Germany)	1	0	0	+	+
TMW 1.1383	Salami starter culture (Germany)	nd	nd	nd	-	-
TMW 1.1385	Salami starter culture (Germany)	nd	nd	nd	-	-
TMW 1.1386	Salami starter culture (Germany)	1	0	1	+	+
TMW 1.1388	Salami starter culture (Germany)	nd	nd	nd	-	-
TMW 1.1392	Salami starter culture (Germany)	nd	nd	nd	-	-
TMW 1.1393	Salami starter culture (Germany)	1	0	0	+	+
TMW 1.1395	Salami starter culture (Germany)	ex	ex	ex	+	+
TMW 1.1396	Salami starter culture (Germany)	0	1	2	-	-
TMW 1.1397	Salami starter culture (Germany)	1	0	1	(+)	+
TMW 1.1398	Salami starter culture (Germany)	1	0	4	+	+
TMW 1.1399	Salami starter culture (Germany)	ex	ex	ex	+	+
TMW 1.1500	Fermented sausage (Germany)	0	0	1	-	-
TMW 1.2292	Prophage free derivative of TMW 1.1398 [59]	nd	nd	nd	-	-
WiKim0063	Water (South Korea)	1	0	0	nd	nd
WiKim0072	Kimchi (South Korea)	1	0	0	nd	nd
WiKim0073	Kimchi (South Korea)	0	0	3	nd	nd
WiKim0074	Kimchi (South Korea)	0	1	3	nd	nd

Table 10. Prophage distribution and inducibility in *L. curvatus*. The number and completeness evaluation ("i", intact; "q", questionable; "inc", incomplete) of prophages as predicted via PHASTER are listed. Moreover, the isolation source of analysed *L. curvatus* strains (accession numbers: Appendix; Chapter 8.1) and the lysis response of accessible strains after phage induction with UV light or MitC ("+", strong lysis; "(+)", weak lysis; "-", no visible lysis) are included. "nd," no genome/strain was available. "Ex", excluded due to high similarity with other strain. Adapted from [128], modified.

***L. curvatus* strain**	**Isolation source (Origin)**	**Prophages**			**Inducibility**	
		i	**q**	**inc**	**UV**	**MitC**
CBA3617	Kimchi (South Korea)	3	1	6	nd	nd
CRL 705	Argentinian dry fermented sausage (Argentina)	0	0	2	nd	nd
DRD-164	Artisanal Greek feta cheese (Greece)	3	1	0	nd	nd
ELA204092	Atlantic salmon (Norway)	0	0	2	nd	nd
ELA214002	Atlantic salmon (USA)	0	0	1	nd	nd
ELA214060	Atlantic salmon (USA)	0	0	1	nd	nd
ELA214061	Atlantic salmon (USA)	0	1	1	nd	nd
ELA214062	Atlantic salmon (USA)	0	0	2	nd	nd
ELA214117	Atlantic salmon (USA)	2	0	1	nd	nd
ELA214388	Atlantic salmon (USA)	2	0	11	nd	nd
FAM25164	Cheese (Switzerland)	1	0	1	nd	nd
FBA2	Radish and carrot pickled with rice bran and salt (Japan)	0	0	6	nd	nd
FLEC03	Beef carpaccio	1	0	1	nd	nd
LCUFL03						
HFS9	Human faeces (China)	0	1	1	nd	nd
IRG2	Human faeces (South Korea)	1	4	1	nd	nd
JCM 1096 = DSM 20019^{T} = TMW 1.7	Milk (Germany)	3	0	4	(+)	-
KG6	Salami (Switzerland)	1	3	2	nd	nd
MGYG-HGUT-00020	Human gut	0	0	2	nd	nd
MRS6	Fermented sausage salsiz (Switzerland)	1	0	0	nd	nd
NFH-Km12	Kabura-zushi (Japan)	0	1	8	nd	nd
NRIC0822	Kabura-zushi (Japan)	1	0	2	nd	nd
RI-124	Food	0	0	1	nd	nd
RI-406	Food	1	0	0	nd	nd
S46	Cattle (Canada)	0	0	2	nd	nd
SRCM103465	Food (South Korea)	1	0	1	nd	nd
TMW 1.17	Raw sausage	nd	nd	nd	-	-
TMW 1.27	Unknown	0	1	2	-	-
TMW 1.47	Unknown	nd	nd	nd	-	-
TMW 1.48	Unknown	nd	nd	nd	+	+
TMW 1.49	Unknown	nd	nd	nd	(+)	-
TMW 1.50	Unknown	nd	nd	nd	(+)	-
TMW 1.51	Unknown	nd	nd	nd	-	-
TMW 1.167	Unknown	ex	ex	ex	+	(+)
TMW 1.266	Palm wine	nd	nd	nd	-	(+)
TMW 1.401	Sauerkraut (Germany)	0	1	4	-	-
TMW 1.407	Sauerkraut (Germany)	1	2	3	-	-
TMW 1.408	Sauerkraut (Germany)	nd	nd	nd	-	-
TMW 1.421	Unknown	1	1	10	-	-
TMW 1.439	Unknown	ex	ex	ex	-	-
TMW 1.440	Unknown	nd	nd	nd	-	-

***L. curvatus* strain**	**Isolation source (Origin)**	**Prophages**			**Inducibility**	
		i	**q**	**inc**	**UV**	**MitC**
TMW 1.591	Unknown	1	0	0	+	+
TMW 1.593	Unknown	nd	nd	nd	+	+
TMW 1.594	Unknown	nd	nd	nd	(+)	-
TMW 1.595	Unknown	1	2	4	(+)	-
TMW 1.596	Unknown	nd	nd	nd	-	-
TMW 1.624	Italian raw sausage (Germany)	3	4	1	-	-
TMW 1.700	Italian raw sausage (Germany), TMW 1.624 with deleted dextran sucrose (knockout mutant)	nd	nd	nd	-	-
TMW 1.706	Sourdough (Germany)	2	0	4	+	+
TMW 1.1291	Raw sausage	nd	nd	nd	-	-
TMW 1.1365	Unknown	2	0	4	+	+
TMW 1.1381	Salami starter culture (Germany)	0	6	3	+	(+)
TMW 1.1382	Salami starter culture (Germany)	nd	nd	nd	(+)	-
TMW 1.1384	Salami starter culture (Germany)	nd	nd	nd	-	-
TMW 1.1389	Salami starter culture (Germany)	nd	nd	nd	-	-
TMW 1.1390	Salami starter culture (Germany)	2	1	1	(+)	-
TMW 1.1391	Salami starter culture (Germany)	nd	nd	nd	+	+
TMW 1.1403	Unknown	nd	nd	nd	(+)	-
TMW 1.1408	Fermented freshwater fish (Norway)	1	0	1	-	-
TMW 1.1437	Lc2-c: pNZ12 (Cmr, Kmr, Neor, *E. coli-Streptococcus* shuttle vector, 4.3 kbp)	nd	nd	nd	-	+
TMW 1.1438	Lc2-c: pLipPS1 (Cmr, lip gene from *S. hyicus* under control of an *S. carnosus* promoter, 5.4 kbp)	nd	nd	nd	+	+
TMW 1.1439	Unknown	nd	nd	nd	+	+
TMW 1.1447	Pecorino cheese (Sardinia)	1	0	0	+	(+)
TMW 1.1449	Italian brenta cheese	nd	nd	nd	-	-
TMW 1.1450	Italian brenta cheese	nd	nd	nd	-	-
TMW 1.1813	Belladonna/honey ferment	nd	nd	nd	-	-
TMW 1.1876	Raw sausage starter culture	nd	nd	nd	+	(+)
TMW 1.1928	Italian raw sausage (Italy)	2	2	10	-	-
TMW 1.1940	Italian raw sausage	nd	nd	nd	-	-
TMW 1.1948	Hungarian salami	nd	nd	nd	(+)	-
TMW 1.2270	Rye sourdough (Germany)	1	1	2	-	-
TMW 1.2272	Mealworm (Germany)	1	0	1	+	+
VRA_2sq_f	Pheasant (Russia)	3	0	0	nd	nd
WDN19	Japanese pickle (Japan)	2	3	5	nd	nd
WiKim38	Baechu-Kimchi (South Korea)	2	1	5	nd	nd
ZJUNIT8	Chinese pickle (China)	0	1	9	nd	nd

8.5 General Features and Integration Sites of *Latilactobacillus* Prophages

Table 11. Features of intact *L. sakei* prophages. Length, GC-content, number of coding sequences (CDS), tRNA genes with used anticodon (tRNA-other ≙ undeterminable type; Anticodon = ? ≙ undeterminable anticodon), and integration sites (region, *attL* and *attR* sites, gene/gene product, and integration site locus tag) are listed. "-RC" (reverse complement) was listed, so prophages start with an integrase gene and end with host lysis genes. "*1", the genome of *L. sakei* strain Probio65 featured two identical prophage sequences (Probio65 P1 and Probio65 P2) at its proximal ends. Probio65 P2 sequence parts are located on each proximal end of the chromosome. Probio65 P2 was listed and counted as a complete prophage despite being most likely the result of an erroneous genome assembly. "*2", TMW 1.1386 P1 was encoded on two genomic contigs due to non-sequenced transposases. Its sequence information was completed using viral DNA sequencing data. Adapted from [127], modified.

Phage	Length [kb]	GC-content [%]	CDS	tRNA genes	Region	*attL* (integrase site)	*attR* (lysin site)	Integration site gene product	Integration site locus tag
C21B P1	40.6	39.7	56	Ile(?)	NZ_CP043730.1, 350959-391601	TATGCGCCACCCGGGA	TATGCGCCACCCGGGA	tRNA-Arg	FXV74_RS02010
CBA3635 P1-RC	45.6	39.2	72	Ile(CAU)	NZ_CP059697, complement(237535-283167	TCTATTCCCATTCCACTGTT	TCTATTCCCATTCAATTGTT	Glutamine-hydrolysing GMP synthase	H3M14_RS01450
CBA3635 P2-RC	36.5	39.5	52	0	NZ_CP059697, complement(1682420-1718886)	TCCCGGGTGGCGCATA	TCCCGGGTGGCGCATA	tRNA-Arg	H3M14_RS08475
DS4 P1	37.0	39.4	56	0	NZ_CP025839.1, 650105-687150	TATATGCGCCACCCGGGA	TATATGCGCCACCCGGGA	tRNA-Arg	C0213_RS03410
E28G P1	37.7	39.6	48	Phe(GAA)	NZ_CP043728.1, 388921-426644	TAAAATGTCACAGGCG	TAAAATGTCACAGGCG	tRNA-Arg	FX990_RS02215
FAM18311 P1-RC	39.2	40.1	50	0	NZ_CP020459, complement(1283867-1323068)	AATGGAGCCGGCG	AATGGAGCCGGCG	ssrA (transfer-messenger RNA)	B4V05_RS06785
J54 P1	33.2	42.0	50	0	NZ_LT960790, 614556-647724	ATGCGCCACCCGGGAGT	ATGCGCCACCCGGGAGT	tRNA-Arg	LSAJ54_RS03305
J64 P1	38.6	39.6	54	Val(AAC)	NZ_LT960781, 649891-688477	ATTATGCGCCACCCGGGA	ATTATGCGCCACCCGGGA	tRNA-Arg	LSAJ64_RS03525

Phage	Length [kb]	GC-content [%]	CDS	tRNA genes	Region	*attL* (integrase site)	*attR* (lysin site)	Integration site gene product	Integration site locus tag
J64 P2	36.1	40.5	53	Phe(GAA)	NZ_LT960781, 891083-927162	AATTTGACCATAATTAATTACC	AATTTGACCATAATTTAAAACC	Hypothetical protein	LSAJ64_RS04570
J64 P3-RC	42.2	39.5	59	0	NZ_LT960781, complement(1294967-1337175)	TTATAGGCGTTCGTTTAATT	TTATAGACGTTCATTTAATT	Glucose-6-phosphate isomerase	LSAJ64_RS06935
J112 P1	41.1	39.7	58	Phe(GAA)	NZ_LT907933, 785036-826095	AATTTGACCATAATTAATTACC	AATTTGACCATAATTTAAAACC	Hypothetical protein	LSAJ112_RS03875
LK-145 P1	39.1	39.5	58	0	NZ_AP017931, 457907-497042	CCTGCCACGGGCAT	CCTGCCACGGGCAT	tRNA-Leu	CCX78_RS02335
LZ217 P1-RC	38.7	40.3	59	tRNA-other(?)	NZ_CP032652, complement(941732-980453)	AATTATGGTCAAATT	AATTATGGTCAAATT	Hypothetical protein	CFK76_RS05020
MFPB16A1401 P1	37.1	40.4	52	0	NZ_LT960788, 654201-691327	TATGCGCCACCCGGGAGT	TATGCGCCACCCGGGAGT	tRNA-Arg	MFPB16_RS03465
MFPB19 P1	37.7	39.6	50	Phe(GAA)	NZ_LT960784, 670158-707882	TAAAATGTCACAGGCG	TAAAATGTCACAGGCG	tRNA-Arg	MFPB19_RS03605
ob4.1 P1	44.7	39.1	63	0	NZ_CP075489.1, 129837-174491	AACAGTGGAATGGGAATAGA	AACAATTGAATGGGAATAGA	Glutamine-hydrolysing GMP synthase	KIK01_RS00640
ob4.1 P2-RC	40.7	40.1	55	0	NZ_CP075489.1, complement(1509133-1549819)	ATGCCCGTGGCAGG	ATGCCCGTGGCAGG	tRNA-Leu	KIK01_RS07950
Probio65 P1 *1	36.1	40.7	55	0	NZ_CP020806, 1999018-2035120	AATTTGACCATAATT	AATTTGACCATAATT	Hypothetical protein	LP065_RS09960
Probio65 P2 *1									
TMW 1.23 P1-RC	39.3	39.9	52	Ile(CAU)	JAHIAK000000000, contig 17: complement(1888-39112)	AATGGAGCCGGCG	AATGGAGCCGGCG	ssrA (transfer-messenger RNA)	KNO63_02330
TMW 1.46 P1	39.6	40.8	57	Phe(GAA)	CP015487, 852024-891679	AATTTGACCATAATTAATTACC	AATTTGACCATAATTTAAAACC	Hypothetical protein	A4W82_04310
TMW 1.46 P2-RC	36.4	40.1	51	0	CP015487, complement(1197847-1227163)	TATCCGACGGAGCCTTCCA	TAGCCCACGGACCCTTCCA	Fe-S cluster assembly protein SufB	A4W82_06315

Phage	Length [kb]	GC-content [%]	CDS	tRNA genes	Region	*attL* (integrase site)	*attR* (lysin site)	Integration site gene product	Integration site locus tag
TMW 1.1290 P1	38.0	40.2	54	0	JAHIAJ000000000, contig 1: 45015-93497	TACCCTACGGACCCTTCCA	TATCCTACAGACCCTTCCA	Fe-S cluster assembly protein SufB	KNO49_00270
TMW 1.1386 P1[*2]	39.4	39.3	51	0	JAHIAI000000000, contig15: 32892-45859, contig18: 1-25303	AATTTGACCATAATTAATTACC	AATTTGACCATAATTTAAAACC	Hypothetical protein	KNO52_05825
TMW 1.1393 P1	34.7	40.6	54	Ile(TAT), Ile(GAT)	JAHIAH000000000, contig 5: 69791-108578	AATTTGACCATAATTAATTACC	AATTTGACCATAATTTAAAACC	Hypothetical protein	KNO57_04740
TMW 1.1397 P1-RC	38.4	39.0	62	0	JAMOWE000000000, contig 1: complement(442601-480500)	ATGCCCGTGGCAGG	ATGCCCGTGGCAGG	tRNA-Leu	NCX38_RS02535
φ-DJ1812 (strain TMW 1.1398)	40.6	39.3	54	0	CP017275, 789443-830015	AATTTGACCATAATTAATTACC	AATTTGACCATAATTTAAAACC	Hypothetical protein	A4W88_04025
WiKim0063 P1	35.2	40.0	51	0	NZ_CP022709, 359788-394976	AATTTGACCATAATTAATTACC	AATTTGACCATAATTTAAAACC	Hypothetical protein	LBS_RS02005
WiKim0072 P1	37.9	40.5	59	0	NZ_CP025136, 1663827-1701767	AATTTGACCATAATTAATTACC	AATTTGACCATAATTTAAAACC	Hypothetical protein	CW750_RS08280

Table 12. Features of intact *L. curvatus* prophages. Length, GC-content, number of coding sequences (CDS), tRNA genes with used anticodon (tRNA-other ≙ undeterminable type; Anticodon = ? ≙ undeterminable anticodon), and integration sites (region, *attL* and *attR* sites, gene/gene product, and integration site locus tag) are listed. "-RC" (reverse complement) was listed, so prophages start with an integrase gene and end with host lysis genes. "Joined sequences" indicate that the prophages contain missing sequence data or that the prophages are located on multiple contigs. "*", DRD-164 P1 and DRD-164 P2 both harboured assembly gaps in their tail gene module. This most likely led to phage DRD-164 P2 "lacking" its lysis genes. While DRD-164 P2 could be incomplete, it was still counted as intact and was included in most analyses except for prophage feature statistics. "nd", information is undeterminable due to missing sequencing data. Adapted from [128], modified.

Phage	Length [kb]	GC-content [%]	CDS	tRNA genes	Region	*attL* (integrase site)	*attR* (lysin site)	Integration site gene product	Integration site locus tag
CBA3617 P1	35.3	39.9	55	0	NZ_CP042389, complement(join(1896984-1915352, 1-16913))	AATATTTTTAAAA	TTTTAAAAATATT	Non-coding region	Non-coding region
CBA3617 P2-RC	39.1	39.6	56	Ile(AAT), tRNA-other(?)	NZ_CP042389, complement(1731973-1771119)	ATTGGGTATATAGG	ATTGGGTATATAGG	tRNA-Gln	FGL79_RS09100
DRD-164 P1*	34.1	39.5	47	Phe(GAA)	NZ_JAMRWB010000001, 1167675-1201761	ATTGGGTATATAGG, alternatively: TATTCGTTGATGATATT	ATTGGGTATATAGG alternatively: TATTCGTTGATCATTTT	tRNA-Gln alternatively: FtsX-like permease family protein	NE283_RS06015 alternatively: NE283_RS06260
DRD-164 P2-RC*	29.1	40.2	49	0	NZ_JAMRWB010000001, complement(1628643-1657701)	AGTAAGGAGAGTACAGGATT	AGTAAGGAGAGTACAGGATT	tRNA-Ser	NE283_RS08625
DSM 20019 P1	35.6	40.2	53	Phe(GAA)	NZ_CP026116, 424333-459926	AAAAGTTACCACATAAATTACCACA	AAAACTTACCACATAATTTACCACA	Non-coding region	Non-coding region
DSM 20019 P2-RC	40.9	39.2	55	0	NZ_CP026116, complement(702468-743345)	ATTGGGTATATAGG	ATTGGGTATATAGG	tRNA-Gln	LCU_RS03995

Phage	Length [kb]	GC-content [%]	CDS	tRNA genes	Region	*attL* (integrase site)	*attR* (lysin site)	Integration site gene product	Integration site locus tag
ELA214061 P1-RC	40.3	40.1	59	Ile(CAT), Phe(GAA)	NZ_JAJJOR010000001, complement(26454-66791)	AGTAAGGAGAGTACAGG	AGTAAGGAGAGTACAGG	tRNA-Ser	LOX59_RS00460
ELA214117 P1-RC	39.9	39.6	55	Phe(GAA)	NZ_JAJJOK010000001, complement(26487-66435)	AGGAGAGTACAGG	AGTAAGGAGAGTACAGG	tRNA-Ser	LOX61_RS00435
ELA214117 P2	38.3	41.9	62	0	NZ_JAJJOK010000002, 52155-90428	TGTTTTAAATATCACCCGTACGG	TGTTTTAAATATCACCCGTACGG	tRNA-Glu	LOX61_RS01630
ELA214388 P1	36.6	40.6	49	0	NZ_JAIULU010000001, 485049-521609	TATGAAAAAATG	CATTTTTTCATA	*sufB* product: Fe-S cluster assembly protein SufB and bacteriophage abortive infection AbiH family protein	LBW12_RS02485 and LBW12_RS02730
ELA214388 P2-RC	37.7	38.9	53	0	NZ_JAIULU010000001, complement(1023191-1060868)	CCCGGGTGACGCATATATA	CCCGGGTGACGCATATATA	tRNA-Arg	LBW12_RS05205
FAM25164 P1	37.9	40.4	56	0	NZ_JAFJMA010000002, 84044-121969	CCTGTACTCTCCTTACT	CCTGTACTCTCCTTACT	tRNA-Ser	JYG89_RS00990
FLEC03 P1-RC	37.2	39.7	49	Phe(GAA)	NZ_LT841333, complement(1344331-1381522)	ATGCCCGTGGCAGG	ATGCCCGTGGCAGG	tRNA-Leu	LCUFL03_RS07095
HFS9 P1-RC	39.9	40.6	57	0	NZ_JAMOHH010000002, complement(602-40455)	TAAGGAGAGTACAGG	TAAGGAGAGTACAGG	tRNA-Ser	NB814_RS01100
IRG2 P1	42.0	39.8	58	tRNA-other(?)	NZ_CP025476, 693056-735063	CCTGTACTCTCCTTACT	CCTGTACTCTCCTTACT	tRNA-Ser	CYK59_RS03750

Phage	Length [kb]	GC-content [%]	CDS	tRNA genes	Region	*attL* (integrase site)	*attR* (lysin site)	Integration site gene product	Integration site locus tag
KG6 P1-RC	29.4	39.4	40	tRNA-other(?)	NZ_CP022475, complement(1152128-1181547)	ATTGGGTATATAGG	ATTGGGTATATAGG	tRNA-Gln	CGZ47_RS06095
MRS6 P1	51.2	38.3	71	Ile(CAT), Ile(CAT)	NZ_CP022474, 740806-792042	AGAAGCCTTCATGTCCATT	AGAAGCCTTCATGTCCATT	*lepA* product: translation elongation factor 4	CG419_RS03715
NFH-Km12 P1-RC	36.1	38.2	53	0	AP018699, complement(1508477-1544557)	ATTATACCGGTGATCGG	ATTATACCGGTGATCGG	tRNA-Leu	NFHkm12_t00360
NRIC0822 P1 joined sequences	43.8	39.3	58	Ile(CAT)	P1.1: NZ_JTJV01000015, 33699-47934; P1.2: NZ_JTJV01000021, 1-29607	AACAGTGGAATGGGAATAGA	nd	*guaA* product: glutamine-hydrolysing GMP synthase	OA78_RS02880
RI-406 P1-RC	44.6	39.3	68	Ile(CAT)	NZ_MKDG01000003, complement(5063-49709)	ATTCTATTCCCATTCCACTGTT	ATTTTATTCCCATTCAATTGTT	*guaA* product: glutamine-hydrolysing GMP synthase	B0D99_RS01070
SRCM103465 P1	40.6	40.0	61	Ile(CAT)	NZ_CP035110, 763448-804071	AGAAGCCTTCATGTCCATT	AGAAGCCTTCATGTCCATT	*lepA* product: translation elongation factor 4	EQK21_RS03855
TMW 1.27 P1	44.8	39.2	63	0	CP016467, complement(905943-950773)	AAACGTTGAATTATA	AAACGTTGAATTATA	*pgi* product: glucose-6-phosphate isomerase	A4W75_04750
TMW 1.27 P2	35.6	41.1	47	0	CP016467, complement(1053370-1088969)	AATGGAGCCGGCG	AATGGAGCCGGCG	*ssrA* (tmRNA-gene)	A4W75_05470
TMW 1.591 P1	38.2	41.0	52	Phe(GAA)	JAHIAT000000000, 1, complement(115313-153539)	ATTGGGTATATAGG	ATTGGGTATATAGG	tRNA-Gln	KNP41_00865

Phage	Length [kb]	GC-content [%]	CDS	tRNA genes	Region	*attL* (integrase site)	*attR* (lysin site)	Integration site gene product	Integration site locus tag
TMW 1.595 P1	34.1	39.8	40	Phe(GAA)	CP016470, 913930-948049	CCTATATACCCAAT	CCTATATACCCAAT	tRNA-Gln	A4W80_04695
TMW 1.624 P1	36.9	42.3	59	0	CP015490, 578300-615242	CGCCTGTGACATTCAA	CGCCTGTGACATTCAA	tRNA-Arg	A4W72_02985
TMW 1.624 P2	36.4	39.8	49	Phe(GAA)	CP015490, complement(1134239-1170622)	ATTGGGTATATAGG	ATTGGGTATATAGG	tRNA-Gln	A4W72_06160
TMW 1.706 P1 joined sequences	39.9	39.1	55	0	JAHIAS000000000, P1.1: 8, complement(146-17188); P1.2: 11, complement (42792-65657)	ATTGGGTATATAGG	ATTGGGTATATAGG	tRNA-Gln	KNP59_03170
TMW 1.706 P2 joined sequences	34.8	40.2	52	0	JAHIAS000000000, P2.1: 15, 45596-57594; P2.2: 16, complement (32242-55012)	AAAAGTTACCACATAAATTACCACA	AAAACTTACCACATAATTTACCACA	Non-coding region	Non-coding region
TMW 1.1365 P1	30.5	43.5	51	0	JAHIAR000000000, 1, 11430-41929	ATGCGTCACCCGGGAGT	ATGCGTCACCCGGGAGT	tRNA-Arg	KNP66_00315
TMW 1.1365 P2	35.4	40.4	54	0	JAHIAR000000000, 5, complement(1-35394)	TATCCTACAGACCCTTCCA	nd	*sufB* product: Fe-S cluster assembly protein SufB	KNP66_03450
TMW 1.1365 P3	45.8	39.1	71	Ile(CAT)	JAHIAR000000000, 9, complement(5148-50903)	TTATTTACCGGCTTTATCTTCATCATTCATTTTAAGAATGGACATGAACGCCTCT	TTATTTACCTTTGGTATCTTCATCATTCATCTTCAAAATGGACATGAACGCCTCT	*lepA* product: translation elongation factor 4	KNP66_05290
TMW 1.1381 P1	32.3	42.2	55	0	CP015493, complement(1350810-1383146)	TTGAATGTCACAGGCG	TTGAATGTCACAGGCG	tRNA-Arg	A4W73_07170
TMW 1.1390 P1	36.7	40.5	54	Met= Ile(CAT), Ile(TAT)	CP015494, complement(1276640-1313353)	AGTAAGGAGAGTACAGG	AGTAAGGAGAGTACAGG	tRNA-Ser	A4W74_06765

Phage	Length [kb]	GC-content [%]	CDS	tRNA genes	Region	*attL* (integrase site)	*attR* (lysin site)	Integration site gene product	Integration site locus tag
TMW 1.1390 P2	36.8	39.6	51	0	CP015494, complement(1385297-1422129)	CGCCTGTGACATT	CGCCTGTGACATT	tRNA-Arg	A4W74_07405
TMW 1.1408 P1	33.6	42.0	55	0	JAHIAF000000000, 4, 7850-41447	ATGCGTCACCCGGGAGT	ATGCGTCACCCGGGAGT	tRNA-Arg	KNO77_02635
TMW 1.1447 P1	38.1	40.0	58	0	JAHIAQ000000000, 15, 1-38073	nd	nd	nd	nd
TMW 1.1928 P1	36.2	39.3	48	0	NZ_CP031003, 605975-642218	CCTGCCACGGGCAT	CCTGCCACGGGCAT	tRNA-Leu	DT351_RS03180
TMW 1.1928 P2-RC	33.1	41.6	55	0	NZ_CP031003, complement(1401111-1434248)	AATGTCACAGGCG	AATGTCACAGGCG	tRNA-Arg	DT351_RS07515
TMW 1.2270 P1	38.2	38.7	51	0	JAHIAD000000000, 2, 109923-148085	AATCCTGTACTCTCCTT	AAGCCTGTACTCTCCTT	tRNA-Ser	KNO48_01595
TMW 1.2272 P1	41.1	40.3	53	0	JAHIAP000000000, 9, 36126-77250	AACAGTGGAGTGGGAATA	AACAATTGAGTGGGAATA	*guaA* product: glutamine-hydrolysing GMP synthase	KNP65_06740
VRA_2sq_f P1 = P3-RC	38.2	39.3	58	Ile(CAT)	NZ_WKLA01000001, complement(589070-627248)	TAAGGAGAGTACAGG	TAAGGAGAGTACAGG	nd (potentially in serine tRNA gene)	nd
VRA_2sq_f P2	44.0	37.9	61	0	NZ_WKLA01000001, 108148-152172	ATTAAACGAACGCCTATAA	ACTAAACGAACGCCTATAA	glucose-6-phosphate isomerase	GKC32_RS00475
WDN19 P1	38.8	39.8	62	His(GTG)	NZ_AP024685, 39849-78625	CCTATATACCCAAT	CCTATATACCCAAT	tRNA-Gln	LTWDN19_RS00245
WDN19 P2	35.4	40.0	54	Phe(GAA)	NZ_AP024685, 1804328-1839767	AATGGTCGTACATAAATATTTTTAAAA	TTTTAAAAATATTAGTGAACTGCCATT	Non-coding region	Non-coding region
WDN19 P3	44.1	39.0	63	0	NZ_AP024685, join(1946333-1967462,1-22950)	TACAAGAAGAACATGTTTGC	TACAAGAAGAACATGTTTGC	glucose-6-phosphate isomerase	LTWDN19_RS10095
WiKim38 P1	44.1	39.3	65	0	NZ_CP017124, 658472-702547	AATATTTTTAAAA	TTTTAAAAATATT	Non-coding region	Non-coding region

Phage	Length [kb]	GC-content [%]	CDS	tRNA genes	Region	*attL* (integrase site)	*attR* (lysin site)	Integration site gene product	Integration site locus tag
WiKim38 P2-RC	29.3	38.2	43	0	NZ_CP017124, complement(1522489-1551828)	ATTATACCGGTGATCGG	ATTATACCGGTGATCGG	tRNA-Leu	LCW_RS07950
ZJUNIT8 P1	35.5	41.8	43	Phe(GAA)	NZ_CP029966, 542769-578224	CCTGCCACGGGCAT	CCTGCCACGGGCAT	tRNA-Leu	C0W45_RS02825
ZJUNIT8 P2-RC	32.8	41.9	51	0	NZ_CP029966, complement(1295227-1327980)	AATGTCACAGGCG	AATGTCACAGGCG	tRNA-Arg	C0W45_RS06965

8.6 MTases of *Latilactobacillus* Phages

Table 13. MTases encoded by *Latilactobacillus* phages. Restriction enzymes present downstream were identified via BLAST of downstream genes at uniprot.org. The predicted methylation type (according to NCBI annotation) was verified via BLAST at rebase.neb.org. "nd", non-determinable. "*", presumably truncated because of downstream overlapping transposase (as harboured by φ-DJ1812). "**", poor alignment quality. MTases encoded by *L. curvatus* prophages were adapted from [128].

Host species	Phage	Gene product	Locus tag	Present restriction enzymes (locus tag)	Methylation type according to BLAST
L. sakei	CBA3635 P2	DNA adenine methylase	H3M14_RS08665	No	nd
	φ-DJ1812*	Hypothetical protein (DNA cytosine methyltransferase)	A4W88_04130	No	C5
	DS4 P1	DNA adenine methylase	C0213_RS03215	No	nd
	FAM18311 P1	DNA cytosine methyltransferase	B4V05_RS06690	No	C5
	J64 P1	Class I SAM-dependent methyltransferase	LSAJ64_RS03360	No	nd
	J64 P1	DNA (cytosine-5-)-methyltransferase	LSAJ64_RS03365	Hypothetical protein (LSAJ64_RS03370 ≙ DNA-binding protein)	C5
	J64 P2	DNA (cytosine-5-)-methyltransferase	LSAJ64_RS04695	No	C5
	J112 P1	DNA (cytosine-5-)-methyltransferase	LSAJ112_RS04005	No	C5
	ob4.1 P2	DNA (cytosine-5-)-methyltransferase	KIK01_RS07860	No	C5
	TMW 1.23 P1	DNA cytosine methyltransferase	KNO63_08520	No	C5
	TMW 1.46 P1	DNA cytosine methyltransferase	A4W82_04430	No	C5
	TMW 1.1386 P1*	DNA cytosine methyltransferase	KNO52_05935	nd (end of contig)	C5
	TMW 1.1397 P1	ATP-binding protein (DNA adenine methyltransferase)	NCX38_02470	Hypothetical protein (NCX38_02465 ≙ single-stranded DNA-binding protein); 2nd gene downstream: helix-turn-helix domain-containing protein (NCX38_02460)	N6A**
	TMW 1.1397 P1	Phage N-6-adenine-methyltransferase	NCX38_02420	No	nd
L. curvatus	DSM20019 P1	DNA cytosine methyltransferase	LCU_RS02350	No	C5
	DSM20019 P2	DNA cytosine methyltransferase	LCU_RS03890	No	C5
	ELA214117 P1	DNA cytosine methyltransferase	LOX61_RS00330	No	C5

Host species	Phage	Gene product	Locus tag	Present restriction enzymes (locus tag)	Methylation type according to BLAST
L. curvatus	ELA214388 P1	DNA adenine methylase	LBW12_RS02565	No	nd
	FAM25164 P1	BREX-1 system adenine-specific DNA-methyltransferase PglX	JYG89_RS01120	Integrase (tyrosine recombinase) (JYG89_RS01125)	N6A
	HFS9 P1	DNA (cytosine-5-)-methyltransferase	NB814_RS00990	No	C5 **
	MRS6 P1	DNA cytosine methyltransferase	CG419_RS03870	HNH homing endonuclease (CG419_RS03875)	C5
	NRIC0822 P1	DNA (cytosine-5-)-methyltransferase	OA78_RS03005	No	C5
	TMW 1.2270 P1	DNA adenine methylase	KNO48_01670	No	nd
	TMW 1.591 P1	Phage N-6-adenine-methyltransferase	KNP41_00790	Integrase (tyrosine recombinase) (KNP41_00775)	nd
	TMW 1.591 P1	SAM-dependent DNA methyltransferase	KNP41_00780	No	N6A**
	TMW 1.706 P1	DNA adenine methyltransferase	KNP59_03110	No	N6A**
	TMW 1.706 P1	Cytosine-specific methyltransferase	KNP59_03060	No	C5
	TMW 1.706 P2	Cytosine-specific methyltransferase	KNP59_05685	No	C5
	VRA_2sq_f P2	DNA modification methylase	GKC32_RS00630	No	nd
	WiKim38 P1	Class I SAM-dependent methyltransferase	LCW_RS03455	No	nd
	TMW 1.595 P1	Phage N-6-adenine-methyltransferase	A4W80_04775	No	nd
	TMW 1.1390 P2	Site-specific DNA-methyltransferase (adenine-specific)	A4W74_07330	No	nd

8.7 Prophage Curing Data

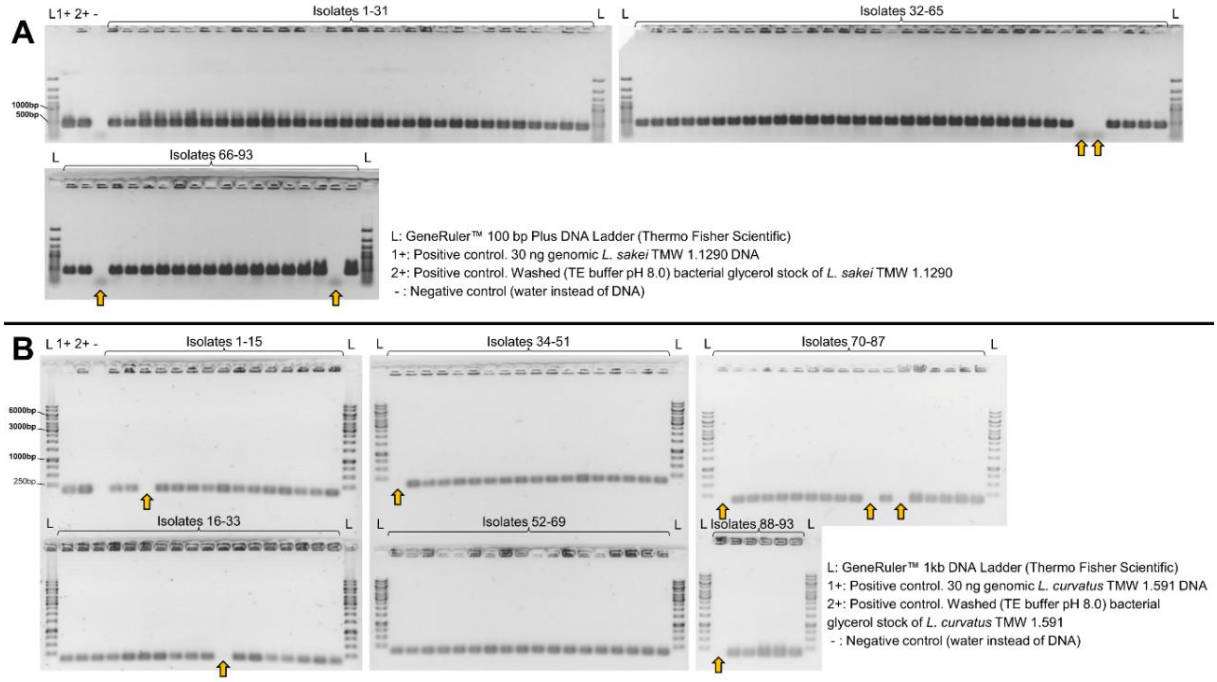

Figure 41. Identification of prophage-free *Latilactobacillus* isolates during prophage curing. The screening for cured isolates was performed via phage-specific colony PCR. For (A) *L. sakei* TMW 1.1290, the primer set 1.1290_ INT_FWD/1.1290_ INT_REV was used expecting a 431 bp long amplicon in the presence of prophage TMW 1.1290 P1. For (B) *L. curvatus* TMW 1.591, the primer set 1.591_ INT_FWD/1.591_ INT_REV was used, expecting a 112 bp long amplicon in the presence of prophage TMW 1.591 P1. Primer sequences are listed in Table 4. A negative PCR result indicates a missing prophage and successful curing. Four of 93 *L. sakei* TMW 1.1290 and seven of 93 *L. curvatus* TMW 1.591 isolates were prophage-negative (yellow arrow). B was adapted from [129], modified.

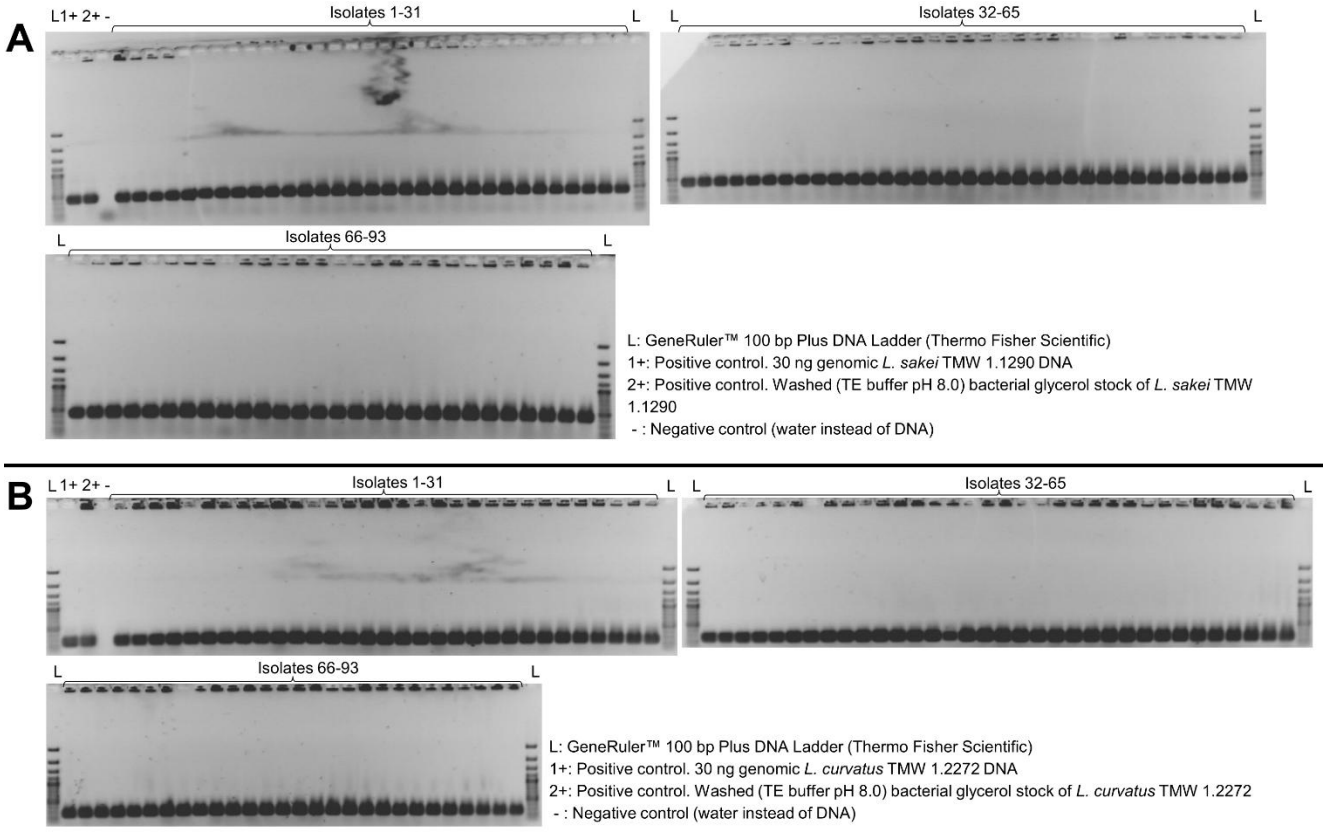

Figure 42. Unsuccessful prophage curing attempts. Displayed are the results of the prophage-specific PCR during the curing of (A) *L. sakei* TMW 1.1290 and (B) *L. curvatus* TMW 1.2272. In the presence of the prophage, a 431 bp long amplicon was expected for TMW 1.1290 P1 and a 238 bp long amplicon for TMW 1.2272 P1. Negative PCR results would have indicated successfully cured candidates.

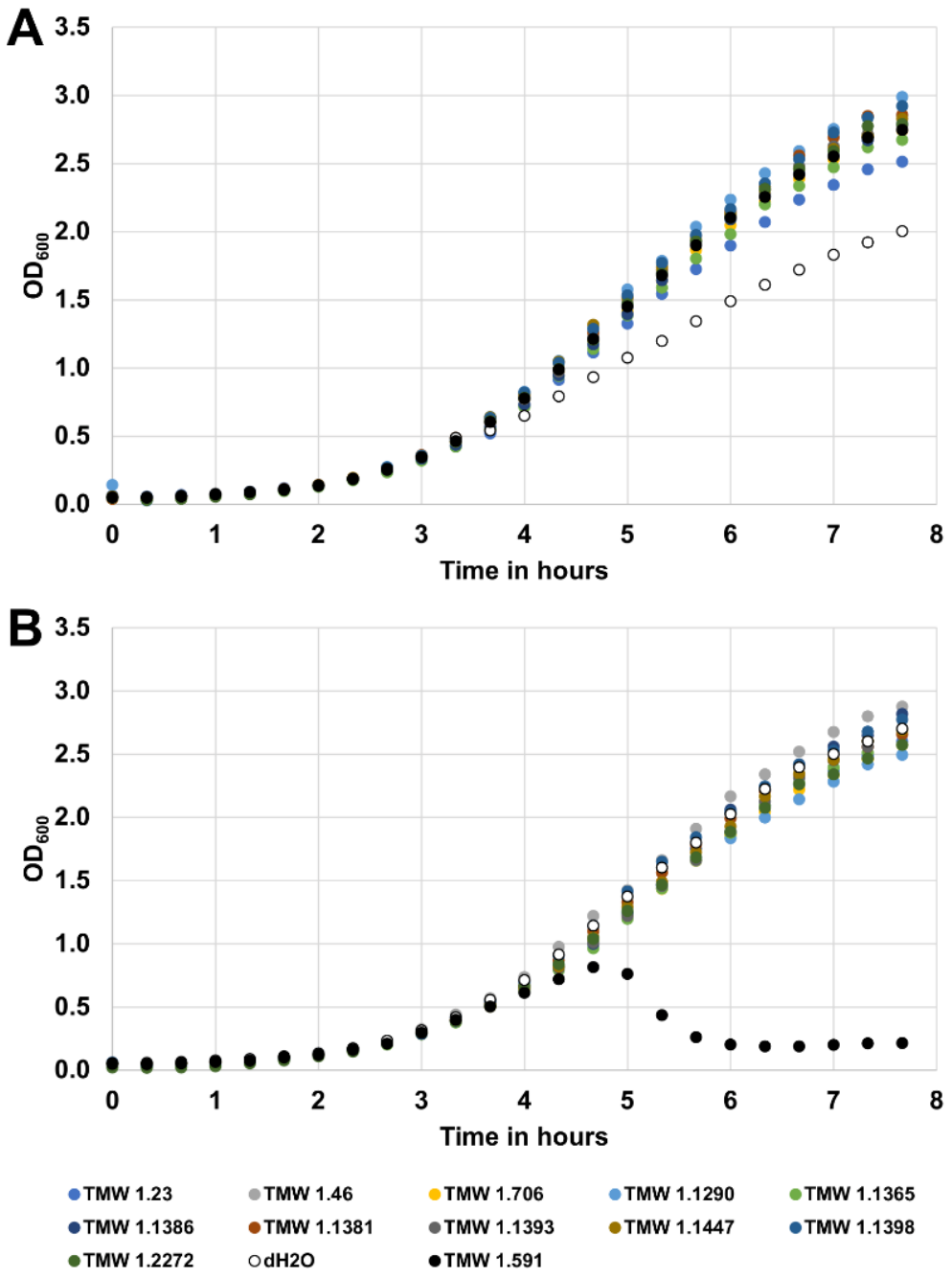

Figure 43. Resistance of WT and cured *L. curvatus* TMW 1.591 to single-strain lysates. The growth of (A) WT *L. curvatus* TMW 1.591 and (B) cured *L. curvatus* TMW 1.591 isolate 6 after treatment with phage-containing post-induction single-strain lysates is displayed. Only administration of TMW 1.591 lysate (black data points) led to the lysis of cured isolate. Sterile water served as the negative control (empty data points). Both strain derivatives were resistant to phages of other lysogenic *L. sakei* and *L. curvatus* strains, indicated by absent lysis.

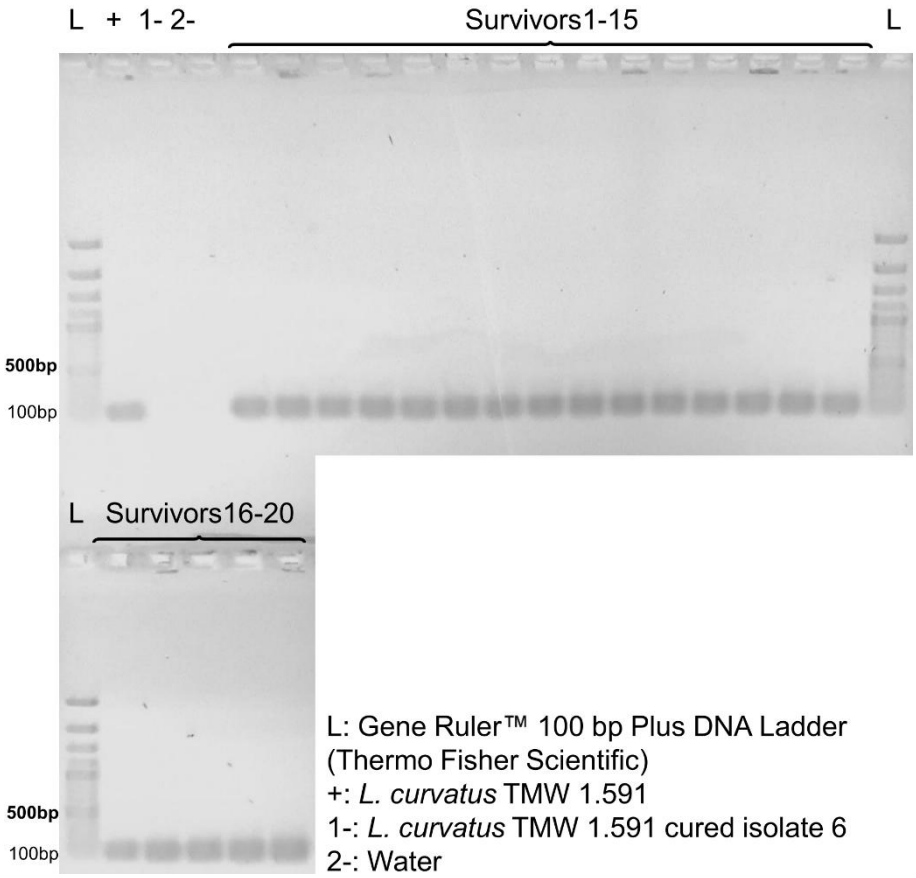

Figure 44. Verification of relysogenisation of cured *L. curvatus* TMW 1.591 isolate 6 with phage TMW 1.591 P1. Twenty survivors were tested for the presence of the prophage via colony PCR using the primer set 1.591_ INT_FWD/1.591_ INT_REV (Table 4). The 112 bp amplicon indicates the presence of the prophage. WT *L. curvatus* TMW 1.591 cells were used as the positive control (+). Cured *L. curvatus* TMW 1.591 isolate 6 cells (1-) and water (2-) served as negative controls.

8.8 TMW 1.591 P1 Occurrence in Fermented Salamis

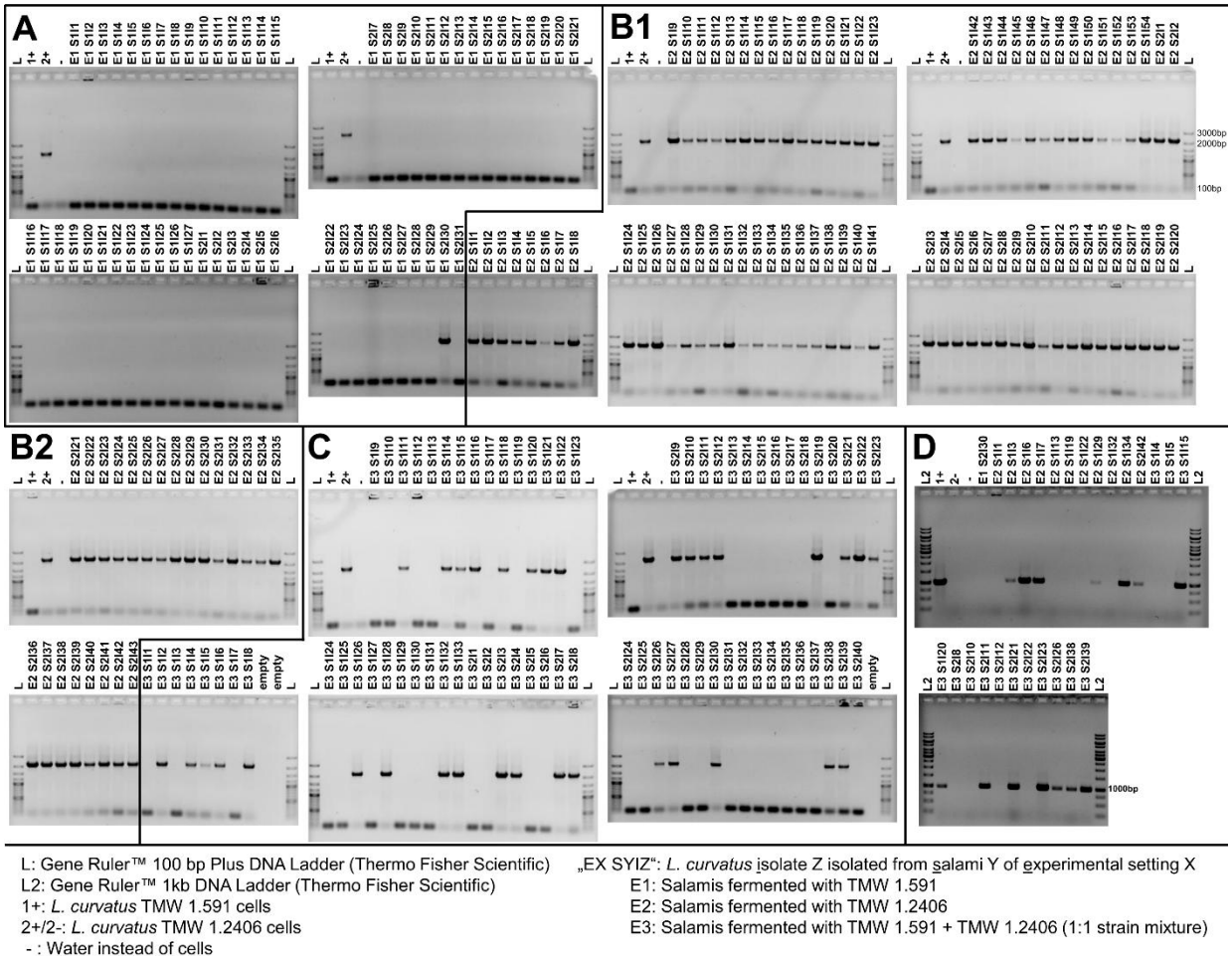

Figure 45. TMW 1.591 P1 occurrence in fermented salamis. The via MALDI-TOF MS identified *L. curvatus* isolates were tested for the presence of TMW 1.591 P1 or an empty integration site. For the TMW-1.591-P1-specific colony PCR, a four-primer-multiplex-approach was utilised (Primers: 1.591_INT_FWD/1.591_INT_REV/1.591_PC_INT-site_FWD/1.591_PC_LYS-site_REV; Table 4) that produces a 112 bp amplicon if the TMW 1.591 P1 phage-integrase is detected, or a 2.2 kbp amplicon if an empty chromosomal integration site is detected. For this, (A) 58 isolates of TMW 1.591-fermented salamis (single-strain), (B1-2) 97 isolates of TMW 1.2406-fermented salamis, and (C) 73 isolates of salamis fermented with a 1:1 strain mixture of both strains were tested. Prophage-positive excision-negative results indicate the phage-harbouring WT strain TMW 1.591. Prophage-negative excision-positive results indicate the cured strain derivative TMW 1.2406. Prophage-positive but also excision-positive isolates were retested (D) using the phage-integrase-specific primer set TMW_1.591_P1_INT_FWD_NEW/ TMW_1.591_P1_INT_REV_NEW. A 983 bp long amplicon is produced if the TMW 1.591 P1 integrase is detected.

8.9 Influence of Prolonged Carbon Source Deficiency on TMW 1.591 P1 Induction

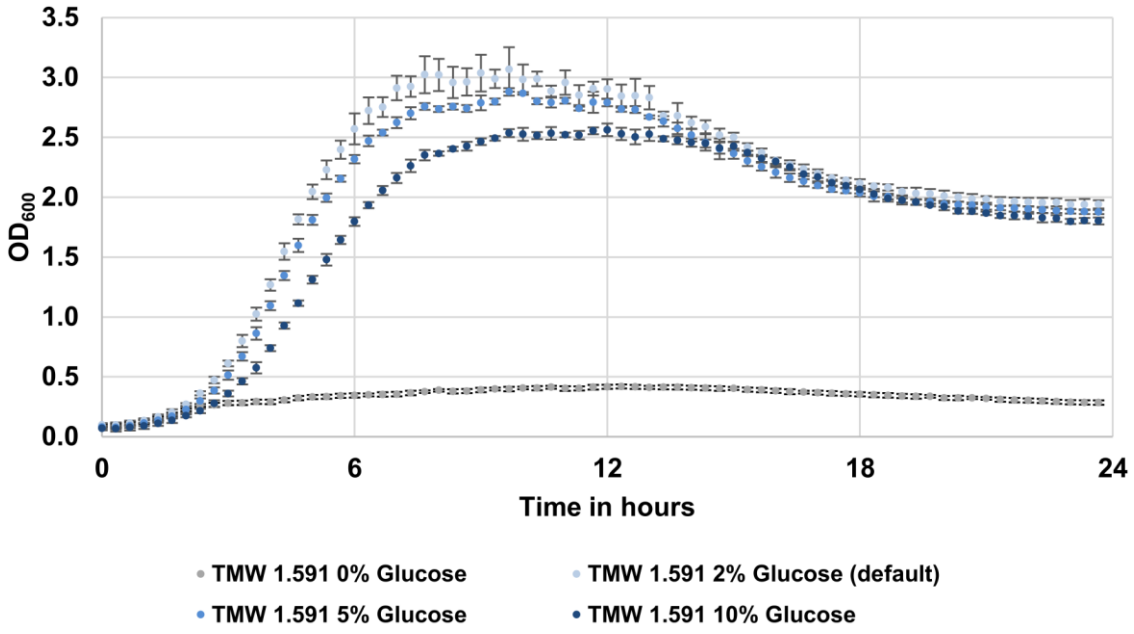

Figure 46. Influence of prolonged carbon source deficiency on TMW 1.591 P1 induction. The growth of *L. curvatus* TMW 1.591 in mMRS medium containing different glucose concentrations is displayed.